INFORMATION TO USERS

This manuscript has been reproduced from the microfilm master. UMI films the text directly from the original or copy submitted. Thus, some thesis and dissertation copies are in typewriter face, while others may be from any type of computer printer.

The quality of this reproduction is dependent upon the quality of the copy submitted. Broken or indistinct print, colored or poor quality illustrations and photographs, print bleedthrough, substandard margins, and improper alignment can adversely affect reproduction.

In the unlikely event that the author did not send UMI a complete manuscript and there are missing pages, these will be noted. Also, if unauthorized copyright material had to be removed, a note will indicate the deletion.

Oversize materials (e.g., maps, drawings, charts) are reproduced by sectioning the original, beginning at the upper left-hand corner and continuing from left to right in equal sections with small overlaps.

Photographs included in the original manuscript have been reproduced xerographically in this copy. Higher quality 6" x 9" black and white photographic prints are available for any photographs or illustrations appearing in this copy for an additional charge. Contact UMI directly to order.

Bell & Howell Information and Learning
300 North Zeeb Road, Ann Arbor, MI 48106-1346 USA

UMI®
800-521-0600

HUMAN LEAD METABOLISM:
CHRONIC EXPOSURE, BONE LEAD
AND PHYSIOLOGICAL MODELS

By

DAVID E.B. FLEMING, B.Sc., M.Sc.

A Thesis

Submitted to the School of Graduate Studies

in Partial Fulfilment of the Requirements

for the Degree

Doctor of Philosophy

McMaster University

HUMAN LEAD METABOLISM

DOCTOR OF PHILOSOPHY (1998) McMaster University

(Physics & Astronomy) Hamilton, Ontario

TITLE: Human Lead Metabolism: Chronic Exposure, Bone Lead and Physiological Models

AUTHOR: David E.B. Fleming, B.Sc.(Mount Allison University), M.Sc.(McMaster University)

SUPERVISORS: Dr. Colin E. Webber and Dr. David R. Chettle

NUMBER OF PAGES: xiv; 269

Abstract

Exposure to lead is associated with a variety of detrimental health effects. After ingestion or inhalation, lead may be taken up from the bloodstream and retained by bone tissue. X-ray fluorescence was used to make *in vivo* measurements of bone lead concentration at the tibia and calcaneus for 367 active and 14 retired lead smelter workers. Blood lead levels following a labour disruption were used in conjunction with bone lead readings to examine the endogenous release of lead from bone. Relations between bone lead and a cumulative blood lead index differed depending on time of hiring. This suggests that the transfer of lead from blood to bone has changed over time, possibly as a result of varying exposure conditions. A common polymorphism in the δ-aminolevulinate dehydratase (ALAD) enzyme may influence the distribution of lead in humans. Blood lead levels were higher for smelter workers expressing the more rare $ALAD^2$ allele. Bone lead concentrations, however, were not significantly different. This implies that a smaller proportion of lead in blood is distributed to tissue for individuals expressing the $ALAD^2$ allele.

The O'Flaherty physiological model of lead metabolism was modified slightly and tested with input from the personal exposure histories of smelter workers. The model results were

consistent with observation in terms of endogenous exposure to lead and accumulation of lead in cortical bone. Modelling the calcaneus as a trabecular bone site did not reproduce observed trends. Variations in lead metabolism between different trabecular sites may therefore be significant. The model does not incorporate a genetic component, and its output did not reflect observed differences in this respect. This result provides further support for the influence of the ALAD polymorphism on lead metabolism. Experimental trials with a digital spectrometer revealed superior energy resolution and count throughput relative to the conventional X-ray fluorescence system. The associated reduction in the uncertainty of lead measurement has the potential to benefit future surveys and modelling efforts.

Acknowledgements

Sincere thanks go out to Dr. Colin Webber and Dr. David Chettle for their guidance and patience during the completion of this project. It has been an entirely pleasurable experience. I have also appreciated the committee work and continual help of Dr. Fiona McNeill. Essential contributions have come from Dr. Ellen O'Flaherty, Dr. James Wetmur, Dr. Robert Desnick, Dr. Jean-Paul Robin, Ms. Denise Boulay, Dr. Norbert Richard, Dr. Din Lal, and Dr. Chris Gordon. My contribution to this endeavour would not have been possible without the support and encouragement of Christiana. Thank you. Bailey Elizabeth has been a wonderful source of inspiration and happiness over the last two years. Thanks are also due to my family for helping me along throughout, and to various relatives in the area for the well-appreciated invitations. Finally, I have been lucky to share offices with a vast array of friendly people over the last four years: Marcel, George, Chris, Pat, Lesley, Norma, Monique, Quan, and Jimmy.

Table of Contents

List of Figures

List of Tables

Chapter 1

Introduction

Lead is a toxicant that has found widespread application in our society. In terms of worldwide metal use, lead ranks behind only iron, copper, zinc, and aluminum. The utility of lead is derived from its low melting point (327 degrees Celsius), overall malleability, high density, and resistance to corrosion. About one-half of Canada's lead consumption is accounted for by automotive batteries. The other principal applications of lead include its use in solders, paint pigments, glazes, ship sheeting, cabling, plastics, and radiation shielding. In some countries, lead is still used as an additive to automotive gasoline. Lead has a significant presence in modern life, and the legacy of its earlier, more uninhibited use, remains.

The most sensitive populations in regard to background or "environmental" lead exposure include children, infants, and fetuses *in utero*. Although lead exposure in North America has declined substantially over the last thirty years, lead toxicity remains a high profile public health issue. A recent example of note was the widespread concern generated over quantities of lead found in some plastic blinds (The Globe &

Mail; June 26, 27, 28, 1996). A gradual realization has emerged that the effects of lead are not limited to circumstances of acute, heavy exposure, but rather may be quite significant with chronic, lower-level exposures.

A population of particular concern consists of individuals exposed to lead occupationally. Exposures in certain industries are dramatically higher than typical environmental levels. Considerable effort has therefore been invested in reducing exposure levels for lead workers, and in studying health outcomes. As adults, exposed individuals generally display more subtle end effects, which complicate understanding of the overall dose-response relationship. In terms of magnitude of uptake, however, lead industry workers are clearly the population most suited for investigation.

To further the understanding of human lead metabolism, therefore, a group of lead smelter workers will be studied in detail. Records of these workers' blood lead concentrations over time were made available by their employer, Brunswick Mining and Smelting Corporation Limited. The measurement of blood lead is the most common means of monitoring an individual's recent absorption of lead.

Blood lead concentration is often reported in micrograms of lead per decilitre of whole blood. For perspective, blood lead levels in Canada and the United States are now typically

less than 5 μg/dl for all age groups (Pirkle *et al.*, 1994; Koren *et al.*, 1990). Since 1991, the United States' Centers for Disease Control have identified a blood lead concentration of 10 μg/dl in children as a level for concern. This may be compared with the 1978 level of 30 μg/dl. The worker relocation level at Brunswick Mining and Smelting is currently 40 μg/dl, considerably less than the 90 μg/dl limit set in the late 1960's. These figures may be kept in mind when considering health outcomes associated with various levels of lead exposure.

1.1 Health Effects of Lead

In humans, lead has been implicated as an adverse influence on the nervous system, kidney function, and the biosynthesis of heme. In these respects, lead is recognized as a subclinical toxin. Symptoms such as "wrist drop", kidney failure, and anemia result under only severe exposure. Subclinical analogues such as slowed nerve conduction, altered uric acid excretion, and impaired heme synthesis may nonetheless signal consequences for long-term health. Lead has also been linked with elevated blood pressure, effects on the reproductive system, and as a possible carcinogen.

1.1.1 Nervous system

Lead exerts effects on the central and peripheral nervous

systems. Under extreme circumstances, acute lead exposure can produce encephalopathy (blood lead concentrations in excess of 120 µg/dl are required in adults). A classic example of lead poisoning involves polyneuritis of sensory and motor nerves. Subsequent loss of motor function may result in wrist drop (Baker *et al.*, 1979), although this symptom is rarely observed in contemporary times. At lower levels of exposure, reduced nerve conduction velocities have been observed in workers with blood lead concentrations above 40 µg/dl (Jeyaratnam *et al.*, 1985). Substantial recent concern has focused on lower-level effects of lead on the central nervous system of children and newborns. For example, an association has been drawn between umbilical cord blood lead levels over 10 µg/dl and subsequent low scores on the Mental Development Index of Bayley, administered over the first two years of life (Bellinger *et al.*, 1987).

1.1.2 Kidneys

Chronic lead nephropathy, which may proceed to renal failure, has been observed in workers demonstrating blood lead levels in excess of 60 µg/dl (Wedeen *et al.*, 1975). Lead acts upon the cells which line the proximal tubules (where substances such as water and nitrogenous waste are processed). Early damage often remains undetected due to a substantial renal reserve capacity. In addition, reliable subclinical indices of kidney malfunction are generally lacking.

Measurement of creatinine clearance has, however, shown an inverse correlation with blood lead concentration in the general population (Staessen *et al.*, 1992). Other subclinical indices potentially associated with lead exposure include uric acid excretion, and blood urea nitrogen (Smith *et al.*, 1995). In children, moderate lead exposure may interfere with Vitamin D metabolism proceeding through the kidney (Rosen *et al.*, 1980; Mahaffey *et al.*, 1982). This effect was not observed in a population of occupationally exposed adults (Mason *et al.*, 1990).

1.1.3 Heme synthesis

The inhibition of heme production by lead proceeds through the impairment of enzymes such as δ-aminolevulinate dehydratase and ferrochelatase. Under extreme exposure, the associated reduction in hemoglobin results in anemia (Baker *et al.*, 1979). Decreases in hemoglobin levels are first noted at blood lead concentrations of about 50 μg/dl in adults, and 25 μg/dl in children (Schwartz *et al.*, 1990). Inhibition of δ-aminolevulinate dehydratase begins at blood lead levels under 10 μg/dl (Hernberg and Nikkanen, 1970). This effect is one of the most sensitive indicators of lead exposure. Human δ-aminolevulinate dehydratase has been shown to be a polymorphic enzyme, leading to speculation about its possible role in mediating differential effects of lead on human health (Wetmur, 1994).

1.1.4 Blood pressure

An association between lead exposure and elevated blood pressure has generated substantial recent concern. The overall effect appears to be subtle, but has been observed at low exposure levels consistent with blood lead concentrations under 10 μg/dl (Schwartz, 1988). In general, the increase in systolic blood pressure associated with an increase in blood lead concentration from 5 μg/dl to 10 μg/dl has been found to be less than 2 mm Hg, with slightly smaller elevations in diastolic blood pressure. The association between lead exposure and hypertension has also been noted in controlled animal studies (Nakhoul *et al.*, 1992). One potential mechanism of effect relates to lead's interference with calcium homeostasis in smooth muscle cells. It is still uncertain, however, whether lead exerts its effects on blood pressure through the cardiovascular system or through the renal system.

1.1.5 Reproductive system

A number of reproductive issues, distinct from the previously discussed concern over fetal neurodevelopment, have been associated with lead exposure . At umbilical cord blood lead concentrations over 15 μg/dl, modest reductions in fetal growth were reported in one recent study (Bellinger *et al.*, 1991). This result, however, was not consistent with a larger

study comparing blood and cord blood lead concentrations with birth weight (Factor-Litvak *et al.*, 1991). Male populations with mean blood lead concentrations over 60 µg/dl have demonstrated reduced sperm counts (Assennato *et al.*, 1986) and altered testicular function (Rodamilans *et al.*, 1988).

1.1.6 Carcinogenesis

The evidence implicating lead in the induction of cancer is limited. Animal studies involving high doses of lead acetate are suggestive of lead as a renal carcinogen and a promoter of renal cancer caused by other organic compounds (Shirai *et al.*, 1984; Tanner and Lipsky, 1984). Studies of lead industry workers are not conclusive; some have noted increased incidence of kidney cancer (Cantor *et al.*, 1986), while others have not (Cooper *et al.*, 1985).

1.2 Environmental exposure to lead

Historically, human use of lead dates from at least 6500 BC (National Research Council, 1993). The direct production of lead via cupellation began approximately 5000 years ago. Lead was incorporated into the aqueducts of the Roman Empire, an application from which the word plumbing is derived. The addition of leaded syrups to wine may have contributed to widespread lead poisoning among the Roman aristocracy, and the overall decline of Roman influence (Nriagu, 1983). The

production of lead during Roman times would not be equalled until the onset of the Industrial Revolution. Over the millennia, the removal of lead from the earth has introduced humans to greater levels of exposure. Notably, studies of ancient native North American bodies have revealed that modern lead body burdens are one to two orders of magnitude higher than those of pre-Columbian time (Ericson *et al.*, 1991).

Unless directly transported by humans, lead has a rather limited environmental mobility (NRC, 1993). This implies relatively greater exposures in urban, industrial areas. The surface water lead concentration in Hamilton Harbour, for example, is almost 50 times higher than some offshore waters of Lake Ontario (Flegal *et al.*, 1989). The past and present use of lead in soldering, plumbing, paint, and gasoline has nonetheless ensured the ubiquity of lead in air, soil and dust, water, and food.

Lead concentrations in air have been contributed mainly by industrial emissions and leaded gasoline combustion. Leaded antiknock compounds were first introduced to gasoline in the 1920's (Royal Society of Canada, 1986). The addition of lead to gasoline in Ontario was regulated out of existence in 1990, contributing largely to the 96% decrease in air lead concentrations observed between 1984 and 1993 (Ontario Ministry of Environment and Energy, 1994). Approximately 80% of the province's lead emissions currently result from mining

and metal smelting. Environmental air lead concentrations are presently of limited concern for the vast majority of Canadians, but have likely figured prominently in earlier buildups of body burdens.

Quantities of lead found in soil and dust are derived mainly from leaded paint or lead which has fallen out from the air. The intake pathway through soil or dust is significant for young children, who may ingest lead as a result of normal mouthing activity. Children engaging in pica, the indiscriminate eating of non-nutritious substances, are at particular risk from direct ingestion of paint chips and lead-containing soil or dust. Not surprisingly, lead contamination of soil and dust has been associated with older housing units (Chisolm *et al.*, 1985), and proximity to lead smelters (Hertzman *et al.*, 1991; Langlois *et al.*, 1996).

Lead can enter drinking water from a number of sites within the water distribution network (NRC, 1993). Lead may be present in plumbing connectors or service pipes in houses constructed before the 1920's. Lead soldering of copper plumbing joints allows lead to leach into the supply, particularly if the water is of high acidity. Brass fixtures may also contain lead, potentially resulting in a high lead concentration in standing water. Similarly, school water fountains containing lead may accumulate very high concentrations over holiday periods. Intake of lead through

drinking water varies from household to household, and constitutes a risk to children and adults alike.

The presence of lead in food follows as a natural consequence of lead contamination of air, soil, and water. In addition, lead may enter food from the solder of canned goods, from glazed dinnerware, or from lead crystal containers. Extreme intake of lead from improperly soldered cans may have contributed to the ultimate fate of the crew of the Franklin expedition through Canada's Northwest passage (Keenleyside *et al.*, 1996). The use of lead solder for canned food or drinks has been curtailed in recent years. In the United States, the percentage of food and soft drink cans produced with lead soldering dropped from 47% in 1980 to 2.2% by 1988 (NRC, 1993). Poorly made, lead-glazed dinnerware or pottery will allow lead to leach into food (Wallace *et al.*, 1985), although commercially manufactured products are generally safe. Storage in lead-crystal has been shown to contribute to high concentrations in sherry (Graziano *et al.*, 1996). Unless an individual is exposed to lead from one or more of these point sources, however, current lead intake from the diet may generally be expected to be low.

1.3 Industrial exposure to lead: Brunswick Mining and Smelting

Exposure to lead in an industrial setting results primarily from the inhalation of lead in air. Lead may also

settle upon food, drinks, or tobacco products which are consumed on the job or at home. Disturbances of leaded dusts can allow further inhalation or ingestion of lead at work. These pathways for intake create the potential for exposures well above the background levels associated with the general population. The processes which result in the accumulation of lead on the work site will be examined for one particular industrial setting, the Brunswick primary lead smelter.

The lead smelter operated by Brunswick Mining and Smelting out of Belledune, New Brunswick represents one of Canada's two primary lead smelters (the other is located in Trail, British Columbia). The Belledune complex receives shipments of concentrated lead ore from various sources, including a local mine which operates just south of Bathurst, New Brunswick. Concentrates are initially sintered so as to remove sulphur dioxide. This byproduct is used to manufacture sulphuric acid, which is employed in an adjacent fertilizer plant. The product is then roasted with coke to form molten lead. Impurities are contained in a "slag", which is not retained for further processing. Subsequent refining separates out quantities of silver, antimony, arsenic, copper, and bismuth. The highly purified lead may then be cast into blocks, or "pigs", for shipment.

Tasks performed by Brunswick workers include the monitoring and execution of crushing, sintering, refining, and

shipping operations. To control exposure on the job, Brunswick employees are required to wear boots, coveralls, gloves, and goggles on site. These articles do not leave the smelter premises; washing of clothes is performed by plant staff. Workers wear respirators to limit their direct inhalation of lead. Smoking is not permitted anywhere on the Brunswick site, and meals are taken in a controlled clean area. Showering is mandatory following a work shift. Ventilation and dust collection has improved substantially since the plant opened in 1966.

Through these initiatives, lead exposure conditions at Brunswick are no longer as severe as those seen during the earliest years of production. The presence of lead in the homes of workers, and in the community at large, has also been limited by these actions. Changes enacted at Brunswick and other lead industry operations have reflected greater awareness of the potential effects of lead on human health. It is through the past and present medical monitoring of Brunswick workers (and specifically, their blood lead concentrations) that individual exposure histories may by recreated and the metabolism of lead investigated.

1.4 Lead in the body

One disadvantage of the blood lead measurement is that it reflects only relatively recent absorption of lead. The half-

life of lead in blood is about 35 days (Rabinowitz *et al.*, 1976), meaning that any single measurement cannot reflect long-term exposure. This drawback is not a major consideration with the Brunswick population, however, since multiple readings over time are available for all employees. More significant is the fact that blood lead concentration does not directly indicate how lead has been distributed to body tissues and target organs.

Lead concentration in tissue may be sampled by biopsy, or at autopsy. An extensive postmortem study of lead concentrations in human tissue was performed by Barry (1975). Among adults with no known occupational exposure to lead, a mean concentration (± standard deviation) was derived from various tissues of interest. Results for males included concentrations in the brain (0.10 ± 0.14 parts per million wet weight, cortex, N=58; 0.09 ± 0.04 ppm, basal ganglia, N=34), kidney (0.78 ± 0.38 ppm, cortex, N=59; 0.50 ± 0.25 ppm, medulla, N=59), testis (0.08 ± 0.04 ppm, N=43), liver (1.03 ± 0.62 ppm, N=58), and spleen (0.23 ± 0.25 ppm, N=59). These values are in very good accord with those from a similar study performed by Gross *et al.* (1975).

Significantly, over 90% of lead body burden is localized to bone tissue (Barry, 1975; Gross *et al.*, 1975). Even greater proportions, more than 95%, are found in bone for occupationally exposed males (Barry, 1975). Bone lead

concentration increases as a function of age, suggesting that lead is well-retained by bone. Therefore, bone lead is expected to reflect cumulative exposure to lead. A measure of lead in bone should correlate well with the integrated lead dose to body tissue, compiled over a lifetime.

Such investigations are useful in explorations of human lead metabolism, but the invasive nature of tissue sampling renders analyses on living humans impractical. This impediment was overcome with the development of an *in vivo* technique for sampling bone lead concentration (Ahlgren *et al.*, 1976). An application of this procedure to an occupationally exposed population (such as the Brunswick smelter workers) could greatly advance the understanding of lead metabolism. By employing the available records of blood lead absorption from individual workers, and exploiting the high accumulations of lead expected in their bone tissue, existing concepts of lead distribution within the body may be tested and refined.

1.5 Lead in bone: X-ray fluorescence

An X-ray fluorescence system, employed in the measure of bone lead, relies on the interaction of radiation with human bone. The effective radiation dose equivalent associated with a single measurement is approximately the same as that received from background radiation over a time period of 10

minutes. Bone lead systems may be easily transported; one such experimental setup, used in the Brunswick smelter survey, is illustrated in Figure 1.1.

Study participants from Brunswick had 30 minute measurements performed on both their left tibia and their right calcaneus (heel bone). The tibia consists mainly of cortical bone, while the calcaneus is predominantly trabecular. These sites were chosen to represent the two general types of bone because of their relative purity of composition, the near absence of overlying tissue, their large sampling areas, and their location remote from radiosensitive organs. The biological half-time of lead has been estimated by Gerhardsson *et al.* (1993) to be 27 years for the tibia (95% confidence interval of 16 to 98 years), and 16 years for the calcaneus (95% confidence interval of 11 to 29 years). More complete details of procedure will be provided in later chapters.

In essence, the bone lead apparatus consists of a γ-ray photon source encapsulated in a small cylinder (8 mm diameter, including tungsten shielding), and a high purity germanium detector which records the energies of radiation resulting from photon interactions in the sample. The very first *in vivo* measurements of lead in bone were performed using a ^{57}Co γ-ray source (Ahlgren *et al.*, 1976). This technique employed a different source-sample-detector geometry than displayed in

Figure 1.1

McMaster X-ray fluorescence bone lead system:

Figure 1.1. More recently, a ^{109}Cd source of γ-rays, in combination with a backscatter geometry, has gained favour (Somervaille *et al.*, 1985). The ^{109}Cd isotope is commercially produced in cyclotron labs (Amersham Ind., Amersham, UK; Cyclotron Co. Ltd., Obninsk, Russia). A fresh ^{109}Cd source typically arrives with an activity of about 1 GBq. The isotopic half-life is 463 days (Firestone, 1996). ^{109}Cd decays by electron capture (Figure 1.2), emitting γ-rays of 88 keV and silver K X-rays of 22 or 25 keV. The silver X-rays are normally undesired, and may be filtered out by a small copper screen (thickness of 0.5 mm) placed in front of the source. The active face of the ^{109}Cd source is restricted to a diameter of 1.5 mm.

Source photons may interact in the body in one of three ways. Evidence of these interactions are received by the germanium detector as radiations of various energies. Photoelectric absorption of photons is the process which allows the presence of lead in bone to be inferred. Elastic scattering, representing the coherent interaction of a photon with an atom within the sample, reflects the quantity of bone mineral interrogated by the photon fluence. Compton scattering is a consequence of inelastic collision, and is by far the most commonly detected (and least useful) result.

The measurement of lead in bone via X-ray fluorescence relies upon the photoelectric effect. Electrons bound within

Figure 1.2

Decay scheme for ^{109}Cd radioisotope (Firestone, 1996):

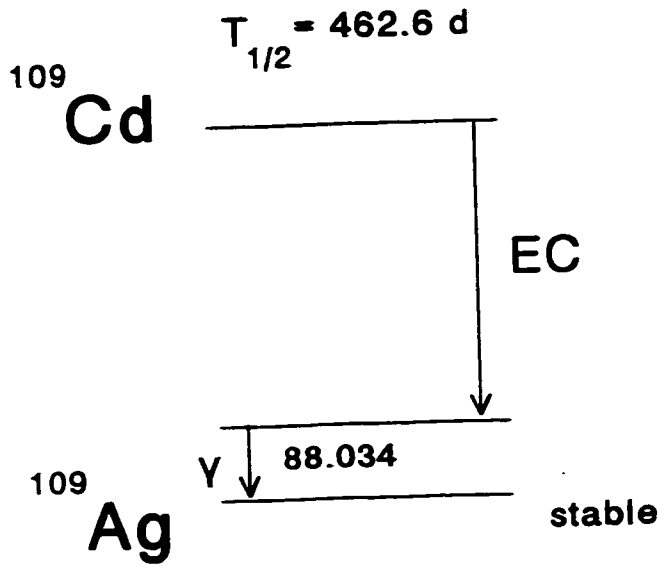

an atom reside in one of a series of orbital shells. From the nucleus outward, these shells are designated by the letters K, L, M, N, O, P, *etc.* If of sufficient energy, a photon incident on an atom may be absorbed, ejecting an electron from one of these shells (usually the K-shell; Figure 1.3). The kinetic energy of this ejected electron is equal to the energy of the original photon, minus the energy which bound the electron to the atom. The resulting shell vacancy is filled by another electron, usually from a separate orbital within the same atom. This transition may be accompanied by the emission of an X-ray (Figure 1.3) or an Auger electron. The fluorescent yield for lead is approximately 96%, so an X-ray photon will nearly always emerge. The X-ray energy is characteristic of a specific transition within a specific elemental atom, and is therefore characteristic of lead. By detecting X-rays of a certain energy "fingerprint", it is possible to determine the presence of lead in bone.

An elastic, or coherent, scatter results in the detection of a photon with an energy identical to the original photon. Coherent scattering is the net effect of a superposition of scattering contributions resulting from a photon's interaction with atomic electrons. Each electron acts as an independent scattering centre. The scattering cross section is related by

$$d\sigma=\frac{1}{2}r^2(1+\cos^2\theta)|F(K)|^2d\Omega \quad [1.1]$$

Figure 1.3

Photon absorption by the photoelectric effect, followed by emission of a characteristic X-ray (Hall, 1994):

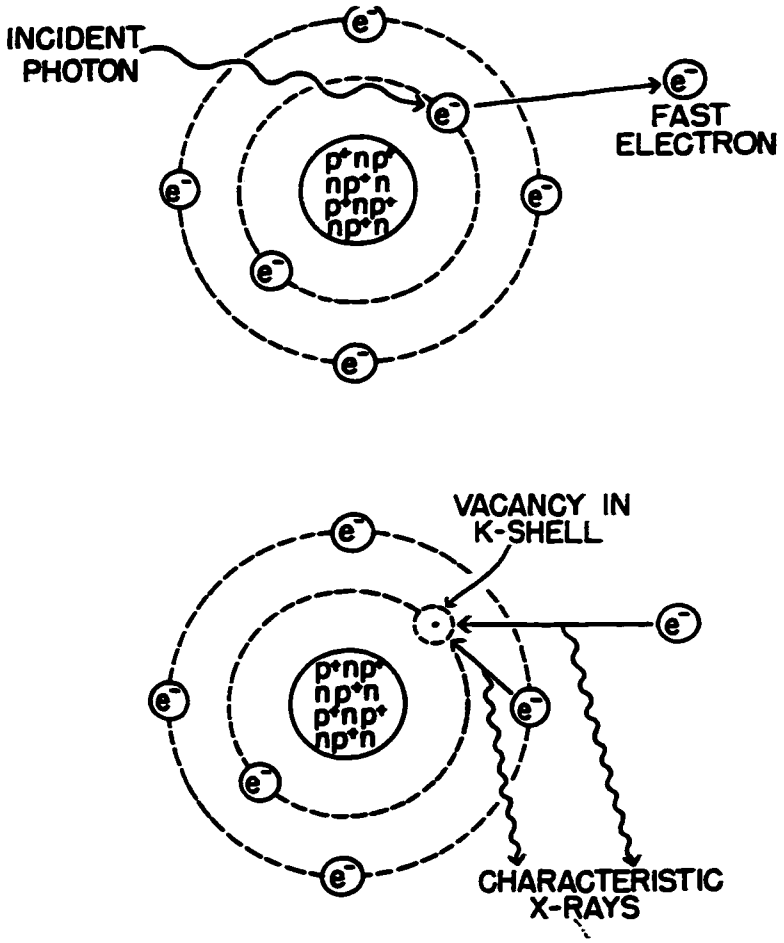

where r is the classical radius of the electron (2.8×10^{-15} m), θ is the angle of scatter, F(K) is the atomic form factor, and $d\Omega$ is an element of solid angle. The form factor is a function of atomic number, photon energy, and angle of scatter. As will be discussed below, the properties of the coherent scatter form factor lend themselves to a normalization procedure which relates the amount of lead in bone to the amount of bone mineral.

Compton scattering represents *inelastic* scattering of a photon from an atom. Detections resulting from Compton interaction dominate the spectrum at the energies associated with X-ray fluorescence analysis of lead. A Compton scattered photon will possess an energy

$$E_\gamma = \frac{E_0}{1+\alpha(1-\cos\theta)} \quad [1.2];$$

where

$$\alpha = \frac{E_0}{mc^2} \quad [1.3].$$

E_0 is the energy of the original photon, θ is the angle of scatter, and mc^2 is the rest mass energy of the electron (511 keV).

Depending on system design, bone lead may be quantified through the detection of either the L-shell or K-shell series of X-rays (Todd and Landrigan, 1993). L X-ray fluorescence

systems may employ radioisotope sources such as ^{109}Cd or ^{125}I which provide photons above the lead L-shell absorption edge of 15.87 keV (Wielopolski *et al.*, 1981). Alternatively, an X-ray generator may be used to produce a partly plane polarized irradiating source (Wielopolski *et al.*, 1989). The latter technique is preferable as it serves to reduce signal interference from Compton scattering. L-shell lead X-rays are found in the low energy range of 9-13 keV. Therefore, both the incident photons from the fluorescing source and the characteristic lead X-ray emissions are strongly attenuated by bone and overlying soft tissue. This results in a superficial measure, effectively sampling bone lead over a thickness of about 1 mm.

The K X-ray fluorescence system has a number of positive features not enjoyed by its L-shell counterparts, and is the method presently applied at McMaster University. Advantages derive mainly from the higher energy of the K-shell fluorescing source. The commonly employed ^{109}Cd source emits γ-ray photons of 88.034 keV in 3.6% of its decays (Firestone, 1996). This energy is just above the lead K-shell absorption edge at 88.005 keV, and ensures an efficient yield of characteristic lead X-rays in the 72-87 keV range. This lead signal may be conveniently normalized to the quantity of bone mineral interrogated, thanks to some important properties of elastically scattered photons. In a backscatter geometry, the probability of an elastic scatter for a photon of ~88 keV is

markedly greater from atoms of high atomic number (Ca or P) than from atoms of relatively low atomic number (H, C, N, O). This ensures that 98 to 99% of the elastic scatter events from a bone site arise from bone mineral (Chettle *et al.*, 1991), allowing a direct comparison of the amount of lead present in bone to the mass of bone mineral. Since the fluorescing source energy is so close to the K-absorption edge, the lead signal and bone mineral signal are derived from a nearly identical photon fluence. The normalization renders the measurement of lead concentration in bone insensitive to variations in source to sample distance and thickness of overlying tissue (Somervaille *et al.*, 1985). A further advantage is that K-shell fluorescence samples a thickness of bone on the order of 3 cm. This is important if an integrated average bone lead concentration is desired; the highly localized result associated with the L-shell technique may fall victim to short-range fluctuations in lead concentration (Wittmers *et al.*, 1988).

A spectrum of energies is detected during an *in vivo* bone lead measurement. An example from a K-shell X-ray fluorescence system is displayed in Figure 1.4 (Chettle *et al.*, 1991). Detections resulting from the three types of photon interactions described above are evident. Photoelectric absorption allows the emission of characteristic lead X-rays at energies of 72.8 keV (designated $K_{\alpha 2}$), 75.0 keV ($K_{\alpha 1}$), 84.5 keV ($K_{\beta 3}$) and 85.0 keV ($K_{\beta 1}$). The $K_{\beta 2}$ peak may be

Figure 1.4

Energy spectrum from an *in vivo* bone lead measurement. (a) Entire spectrum, displayed on a log-normal scale; (b) Expanded spectrum, showing K_α and K_β X-ray detections and elastic scatter detections (Chettle *et al.*, 1991):

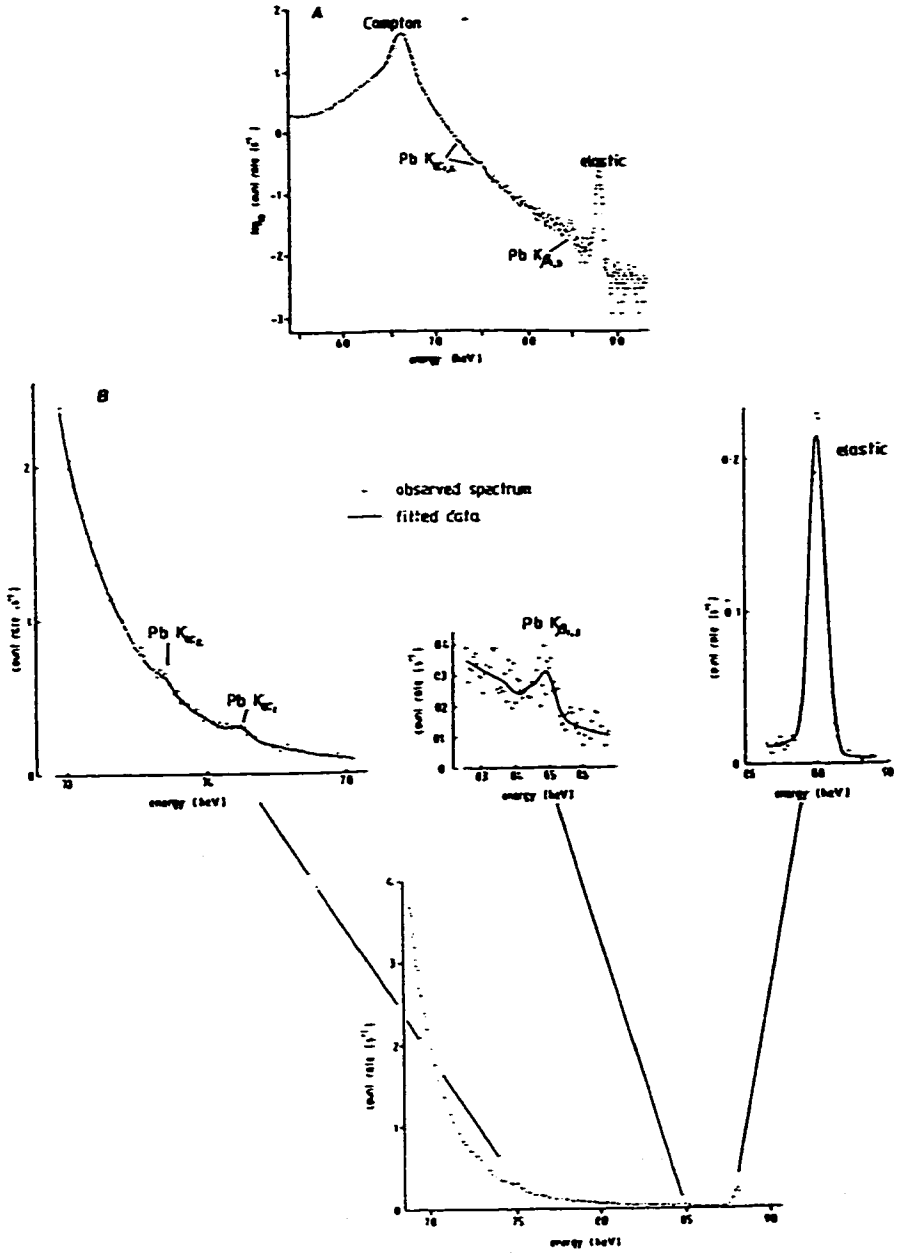

found at an energy of 87.3 keV, but this peak is normally not employed for *in vivo* analyses. A signal artifact resulting from oxygen in overlying soft tissue interferes with the $K_{\beta 2}$ peak, and is difficult to correct (Chettle *et al.*, 1991). The K_{α} events involve electron transitions from the L-shell to the K-shell, while the $K_{\beta 1}$ and $K_{\beta 3}$ events require a transition from the M-shell to the K-shell. Relative to the strongest lead X-ray peak ($K_{\alpha 1}$), the other peaks have intensities of 0.593 ($K_{\alpha 2}$), 0.228 ($K_{\beta 1}$), and 0.119 ($K_{\beta 3}$) (Chettle *et al.*, 1991). Elastic scatter from bone mineral produces a large detection peak at 88.0 keV. The detection of Compton scattered photons represents the most obvious peak, at 66.5 keV. This energy is consistent with equation [1.2] above, where θ is the mean angle of scatter from sample to detector, approximately 160 degrees. As noted, the lead X-ray signals may be normalized against the elastic scatter signal to derive the amount of lead in bone per unit bone mineral. This task is accomplished by numerically extracting peak amplitudes from the energy spectrum.

The fitting routine employed for spectral analysis is based on the Marquardt method of nonlinear least squares (Marquardt, 1963). A Gaussian function, scaled for width and height, is initially fit to the coherent scatter peak. The width of this function is retained as the function height is fit to each pair of lead X-ray peaks. The spectrum is analyzed in three segments: one containing the K_{α} peaks,

another the $K_{\beta 1}$ and $K_{\beta 3}$ peaks, and a third the $K_{\beta 2}$ and coherent peaks. In each case, consideration is given to the large Compton scatter contribution. The lead X-ray peaks and the coherent scatter peak are essentially sitting on top of a "Compton background" (Figure 1.4). This is taken into account by fitting a rapidly declining double exponential function over the K_{α} energy regions, and a single exponential over the K_{β} and coherent scatter regions. Attention is also directed toward spectral features created by an inhibition of Compton scattering which occurs when the amount of energy transferred to the electron is relatively low (Harding, 1995). For example, a small edge beginning at 84.0 keV marks a reduced probability of Compton scatter from the K-shell of calcium atoms. A final consideration is the tendency for the Gaussian peaks to exhibit a slight "step" in their low-energy tails. This feature results from incomplete charge collection within the detector, and is controlled by the inclusion of a "complementary error function" in the spectral analysis.

Once the ratio of lead signal to bone mineral signal is derived from a spectrum, it is useful to convert to the more informative measure of lead concentration per mass of bone mineral. This is accomplished through the employment of a series of calibrating phantoms. These bone phantoms, made from plaster-of-Paris, are doped with known quantities of lead. The ratio of lead signal to mineral signal from phantom measurements is strongly correlated with lead content.

Calibration lines relating the various ratios of peaks and the associated lead concentrations are then used to determine the lead concentration in the bone of a human subject. The contribution of each of the lead X-ray peaks to the final result is weighted according to the inverse of the variance. Of course, the elastic scattering properties of human bone and plaster-of-Paris (calcium sulphate) are not identical. A correction factor is therefore applied to the calculation of lead concentration in bone (Hubbell and Øverbø, 1979; Chettle *et al.*, 1991).

The accuracy of K-shell X-ray fluorescence bone lead measurements has been assessed by comparison with atomic absorption spectroscopy (AAS) results. 20 mg quantities from sections and fragments of tibia, calcaneus, and metatarsal had bone mineral removed for AAS lead quantitation. The remaining portions of each sample were analyzed for lead concentration by X-ray fluorescence. The mean difference for all samples (N=80) between the X-ray fluorescence and AAS results (± standard deviation) was 0.0 ± 14.1 μg lead / g bone mineral (Somervaille *et al.*, 1986). The mean differences for the tibia sections (N=41) and calcaneus samples (N=22) were 0.2 ± 8.8 and 2.0 ± 23.7 μg lead / g bone mineral, respectively.

The precision of an X-ray fluorescence bone lead measurement displays substantial interindividual variation. Key factors are the amount of tissue overlying the bone site

and the mass of bone sampled. The median uncertainty in bone lead observed from one population of 30 nonoccupationally exposed males was approximately 3 μg lead / g bone mineral (Gordon *et al.*, 1994). Measurement uncertainty is usually calculated from individual uncertainties in the X-ray peaks, the coherent peak, and the calibration lines. A recent study of X-ray fluorescence bone lead reproducibility indicated that the standard deviation between repeat *in vivo* measurements is in reality 20-30% greater than the calculated uncertainty (Gordon *et al.*, 1994). A more conservative figure of 4 μg lead / g bone mineral may therefore be the appropriate estimate of measurement precision in nonoccupationally exposed males. Nonoccupationally exposed females typically demonstrate slightly higher uncertainties in bone lead concentration. Occupationally exposed individuals generally display higher absolute (but lower relative) uncertainties (Gerhardsson *et al.*, 1993).

1.6 Overview of thesis

Lead toxicity is a major issue in environmental health. The effects of acute, high exposure to lead are well documented. More uncertain, and likely more significant to society, are the consequences of chronic exposure to low or moderate levels of lead. A necessary step towards a better understanding of these consequences is the development and

employment of non-invasive tools capable of more completely describing the distribution of lead in the human body. The focus of this thesis is on the application of two such tools: X-ray fluorescence measurement of the concentration of lead in bone, and computer modelling of lead metabolism within the human body.

In Chapter 2, results will be presented from a bone lead study involving nearly 400 lead smelter workers. Blood lead concentrations taken from a subset of these workers following a labour disruption allow constraints to be placed on the relation between bone lead and endogenous lead exposure. Such internal exposure can be substantial for lead industry workers. The contribution of lead from bone stores also has implications for nonoccupationally exposed individuals, particularly those experiencing the higher bone turnovers associated with pregnancy and lactation, or post-menopause. The blood lead records of the smelter workers will also be used to construct detailed lead exposure histories. A comparison of these histories to bone lead levels can provide valuable information concerning the distribution of lead to body tissue. The long-term kinetics of lead is important to occupationally and nonoccupationally exposed populations alike.

Chapter 3 describes results for the Brunswick population in regard to a polymorphism in the δ-aminolevulinate

dehydratase (ALAD) enzyme. Recently developed blood sample analyses allow an accurate determination of ALAD genotype. In a predominantly Caucasian population such as the Brunswick smelter workforce, about 20% of individuals express the more rare $ALAD^2$ allele. Previous studies have indicated that this polymorphism may be a genetic factor in the metabolism of lead. This hypothesis will be examined using measures of blood lead, serum lead, and bone lead concentration in combination with ALAD genotype analysis.

Efforts into the mathematical modelling of lead metabolism will be reviewed in Chapter 4. Special attention is directed toward bone metabolism. The recent metabolic models of Marcus, Leggett, and O'Flaherty are of particular interest, and are described in turn. The treatment of O'Flaherty is examined in detail, with reference to the modelled partitioning of lead between plasma and whole blood and the modelled kinetics of lead in bone.

The O'Flaherty model, with its careful physiological approach and consideration of bone lead metabolism, will be applied to the Brunswick data set in Chapter 5. Preliminary output from the model is introduced and used to refine various parameters governing the distribution of lead within the human body. The revised model is then applied to the complete population of Brunswick workers. Model predictions are compared with observed results concerning endogenous lead

exposure and total bone lead accumulation. The power of this technique is further highlighted by examining output from the perspective of the individual worker.

Chapter 6 is concerned with an attempt to improve the precision of the existing X-ray fluorescence bone lead system. This experimental application involves the assessment of a digital spectrometer unit which was recently introduced to market. An improvement in the precision of bone lead measurement, if achieved clinically, would impact future investigations of lead exposure and metabolism.

Conclusions and future research directions are summarized in Chapter 7.

Chapter 2

Accumulated Body Burden and Release of Lead

2.1 Introduction

The study population consisted of both active and retired workers from a lead smelter located in the province of New Brunswick, Canada. Brunswick Mining & Smelting has operated since 1966, initially as a lead-zinc smelter. In 1972, the Brunswick site was converted for exclusively lead smelting operations. Whole blood lead measurements for Brunswick workers have been compiled since 1968. Bone lead readings were performed on smelter employees during the months of May and June of 1994. Bone lead measurements were performed on smelter premises by members of the McMaster body composition research group, prior to the author's joining this team.

In previous studies of *retired* workers, a positive correlation has been observed between current whole blood lead and bone lead (Erkkilä *et al.*, 1992; Gerhardsson *et al.*, 1993). These results imply that the release of lead from bone is a dominant source of exposure for retired workers. That such a strong correlation has not been evident amongst active workers suggests that endogenous exposure, while perhaps still

present, is being overwhelmed by exogenous lead supply (inhaled or ingested lead). A ten-month strike at Brunswick smelting, lasting from July 1990 - May 1991, provided an opportunity to test this hypothesis.

Following the resumption of work duties, blood lead readings were performed on all employees. These results and the subsequent bone lead measurements of 1994 were examined to gauge the intensity of endogenous lead exposure for a typical smelter worker. The unique advantages of this survey lie in the large sample of workers involved, and the fact that these individuals would otherwise have been active smelter employees but for the disruption of labour. This point addresses the potential objection to results obtained from *retired* workers that the endogenous exposures observed were partially a consequence of age-related bone store releases, and therefore not applicable to the population in general. A smaller sample of retired Brunswick workers was also included in a similar analysis of endogenous lead contribution to total exposure.

A strong positive correlation has been noted in lead industry workers between bone lead concentrations at various bone sites (Somervaille *et al.*, 1989; , Cake *et al.*, 1996). This present analysis will examine bone lead levels for the tibia and calcaneus. The tibia is taken as representative of compact, cortical bone, which comprises approximately 80% of skeletal mass. Of five skeletal sites investigated by

Wittmers *et al.* (1988), the tibia was deemed to be most representative of total skeletal lead burden. The calcaneus is predominantly trabecular bone, and would therefore be expected to exhibit a somewhat different pattern of lead metabolism (Gerhardsson *et al.*, 1993).

Bone lead results were compared to a cumulative blood lead index in an attempt to derive a relation between these two long-term exposure markers (Christoffersson *et al.*, 1984; Somervaille *et al.*, 1988). Since past levels of exposure were higher than current levels, the slope of this relation was examined as a function of time of hiring for the worker population. A difference in slope between groups selected by time of hiring might then be indicative of a change in the transfer of lead from whole blood to tissue. As will become evident, such a variation would be consistent with existing conceptions of lead kinetics in the human body.

2.2 Methods

The worker population for which bone lead readings were performed consisted of 381 people; three were women, 378 were men. Of this total group of 381, a subset of 14 consisted of retired employees, all of whom were males of age 55-72 years. The ages of the active workers ranged from 22-63 years.

Prior to bone lead measurement, informed, written consent

was obtained from all workers participating in the study. The tibia lead measurements were made at the midpoint of the left tibial bone shaft, with a source-to-skin distance of about 2 cm. The calcaneus readings were taken from the lateral aspect of the right heel bone. Each procedure lasted approximately 30 minutes, resulting in a total effective dose of about 0.07 μSv (Todd *et al.*, 1992).

Blood samples were drawn from all workers following the strike, in most cases immediately upon an individual's return to work. The monitoring of blood lead is a routine program administered by Occupational Health Services at Brunswick. Whole blood lead concentration is analyzed by atomic absorption spectrometry, yielding a relative precision of about 5% (NRC, 1993). In order to screen out workers whose blood leads were *not* reflective of mostly endogenous and background lead exposures, it was required that a blood lead reading be carried out within five working days of the resumption of employment for inclusion in this component of the study. In total, this resulted in a sample size of 204 employees. The bone lead values of these 204 workers were derived from the X-ray fluorescence measurements of 1994. A correction to this data was implemented to account for the slight increase in bone lead which would have occurred over the three years between the return to work and the bone lead readings. The magnitude of this correction was generated from the average rates of increase of bone lead concentration per

year per unit blood lead concentration for the smelter workers. These constants for the tibia and calcaneus bone sites will be introduced below.

The time between whole blood lead measurements at Brunswick varies depending on the exposure history of each particular employee, but the sampling frequency generally ranges from once per month to once per year. A cumulative blood lead index (CBLI) was constructed for each of the workers using the blood lead data provided by the smelter. Such an index is simply an integration of blood lead levels over a worker's employment time, and therefore provides a good approximation of the total exposure to lead (Roels *et al.*, 1995).

The CBLI was calculated for each worker by integrating blood lead readings over time via the trapezoidal rule:

$$CBLI=\int BPb\ dt=\sum 0.5(BPb_i+BPb_{i+1})\Delta t \quad [2.1].$$

Here, BPb_i and BPb_{i+1} represent the i^{th} and $(i+1)^{th}$ measurements of blood lead, taken Δt years apart. A number of assumptions were necessary in order to determine realistic CBLI estimates. The starting point for integration was originally selected to be either the time of hiring, or the time of first blood lead measurement, which ever came first. If a particular individual was hired *before* the time of routine blood lead monitoring (pre-1968), the missing span was covered by

extending a linear fit to the available data backward to the time of hiring (Cake, 1994). To some extent, this technique accounts for changes in worker blood leads associated with variations in both occupational and environmental exposures (Pirkle *et al.*, 1994). In all cases, a period of adjustment was incorporated between a "background" blood lead at hiring and the first "working" blood lead (Roels *et al.*, 1995). The amount of time allocated to reach an equilibrium working value was at most 90 days; less if the worker's first blood lead measurement occurred within 90 days of hiring. The end point of integration was defined to occur at the time of an individual's bone lead measurement.

2.3 Results

2.3.1 Endogenous release of lead

The post-strike blood lead levels (BPb, given in μg/dl) are shown as a function of tibia lead concentrations (T, given in μg/g) in Figure 2.1a. In accordance with previous work in this field, simple linear regression will be employed for the analysis of x-y data. Alternate methods exist which may account for estimated uncertainties in individual measurements (Quenouille, 1952; Williamson, 1968). A simple linear fit to the data yields the following line of regression:

$$BPb=(0.136\pm0.014)\,T+(13.6\pm0.8),$$

with a coefficient of determination (r^2) of 0.31 from a sample size (N) of 204 workers. A similar fit to the post-strike blood lead (BPb) versus calcaneus lead concentration (C, given in μg/g) data is shown in Figure 2.1b. These results produced a best fit relation of

$$BPb=(0.0776\pm0.0074)C+(13.6\pm0.7)\ [N=204; r^2=0.35].$$

When the set of 14 retired Brunswick workers were analyzed in a similar fashion, the following relations provided the best fits to the data:

$$BPb=(0.162\pm0.051)T+(6.1\pm3.6)\ [N=14; r^2=0.46];$$

and

$$BPb=(0.0593\pm0.0305)C+(9.2\pm4.2)\ [N=14; r^2=0.24].$$

2.3.2 Bone lead at different sites

A linear regression was also applied to a comparison of workers' calcaneus and tibia bone lead levels. In such a relation, the tibia lead data is normally designated as the independent variable. This treatment is appropriate since the tibia lead measurements were more precise (~± 5 μg/g median) than the calcaneus readings (~± 8 μg/g). In addition, as a cortical bone site, the tibia lead concentration represents a more stable parameter over time. The complete set of results for current workers is illustrated in Figure 2.2a, with the

Figure 2.1

Blood lead level as a function of bone lead concentration for workers returning following labour disruption.

(a) Blood lead as a function of tibia lead;

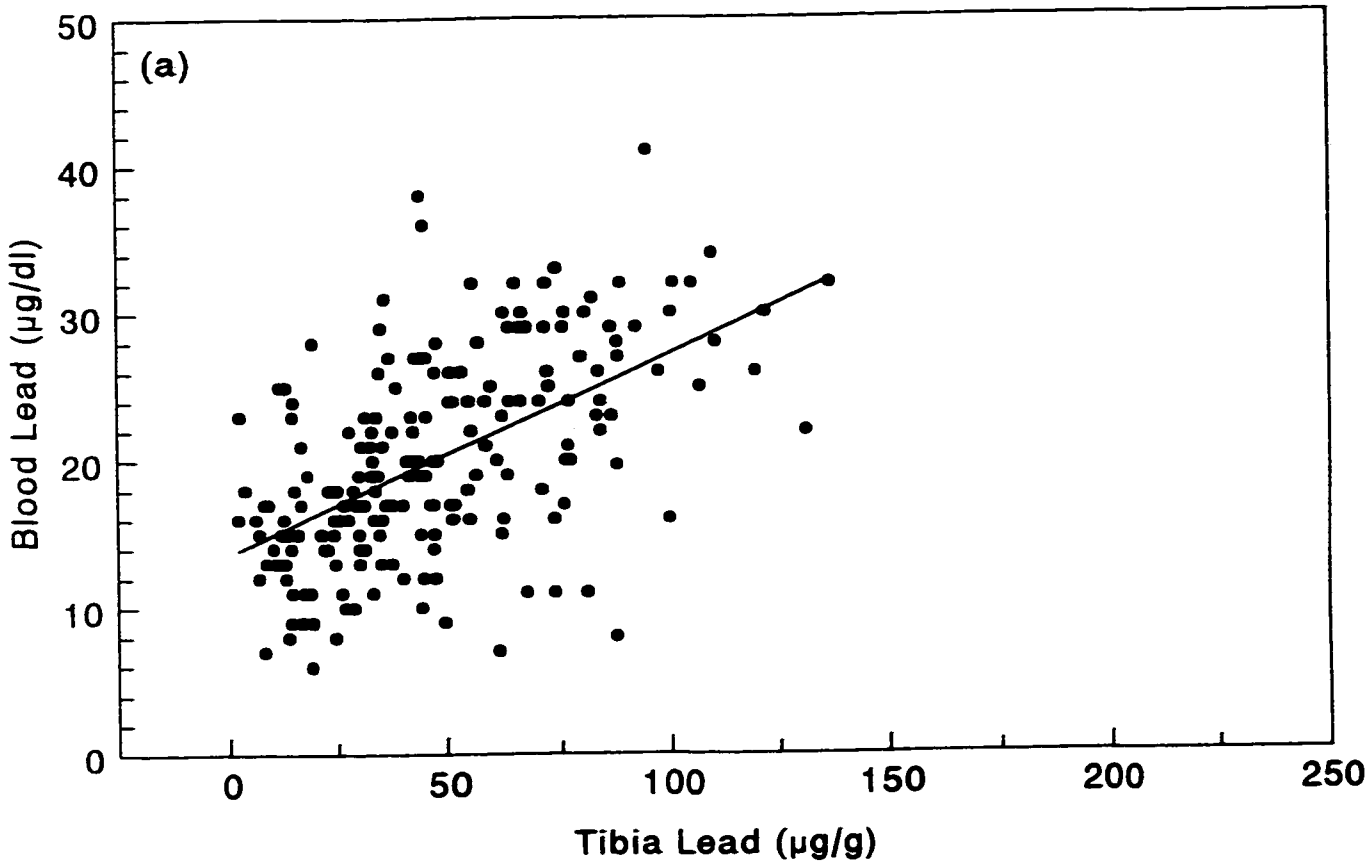

Figure 2.1

Blood lead level as a function of bone lead concentration for workers returning following labour disruption.

(b) Blood lead as a function of calcaneus lead;

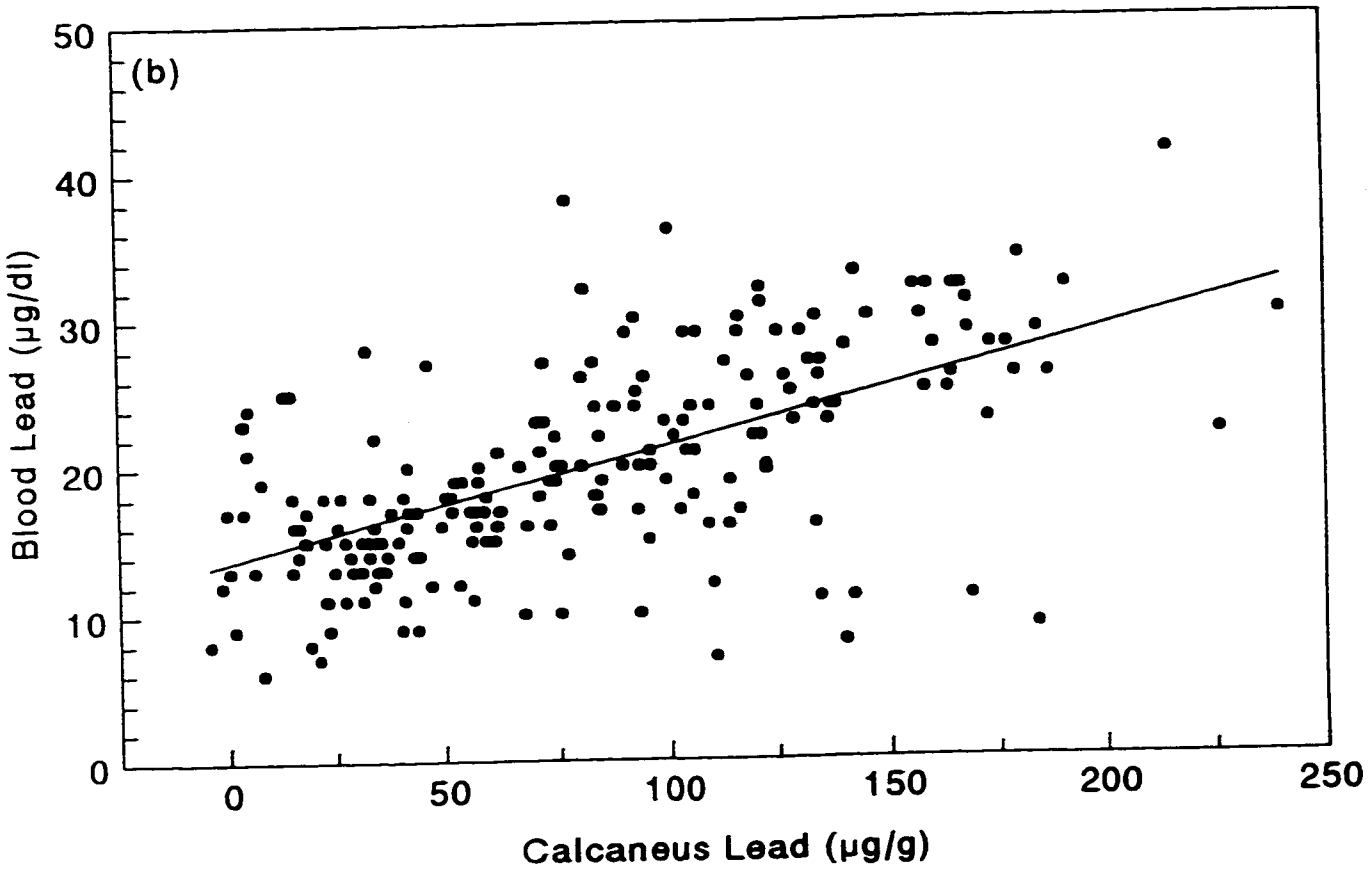

following line of best fit superimposed:

$$C=(1.70\pm0.04)\,T+(0.6\pm2.2)\;[N=367;r^2=0.81].$$

For the retired Brunswick workers (results shown in Figure 2.2b), an analysis of the bone lead relation yields a fit such that

$$C=(1.70\pm0.29)\,T+(16.7\pm20.7)\;[N=14;r^2=0.74].$$

2.3.3 Accumulated lead body burden

When tibia lead levels of occupationally exposed individuals are plotted against CBLI values, a linear relationship has been found to prevail over a variety of studies. These results, and those derived from measurements at other bone sites of interest, are summarized in Table 2.1. If one expects to derive this ideal, linear relation between the long-term indices of bone lead and CBLI, two complicating factors must be assumed negligible. The first is the common assumption that the blood lead contribution from bone is relatively small for workers subjected to heavy exogenous exposures. This assumption is a reasonable one for the smelter population, particularly given the relatively long half-life of lead in bone (Gerhardsson *et al.*, 1993). A second important point implicit in the linear approximation is that the transfer efficiency of lead from blood to bone is to be taken as constant. This ignores potential variations in

Figure 2.2

Calcaneus lead concentration as a function of tibia lead.

(a) Active workers;

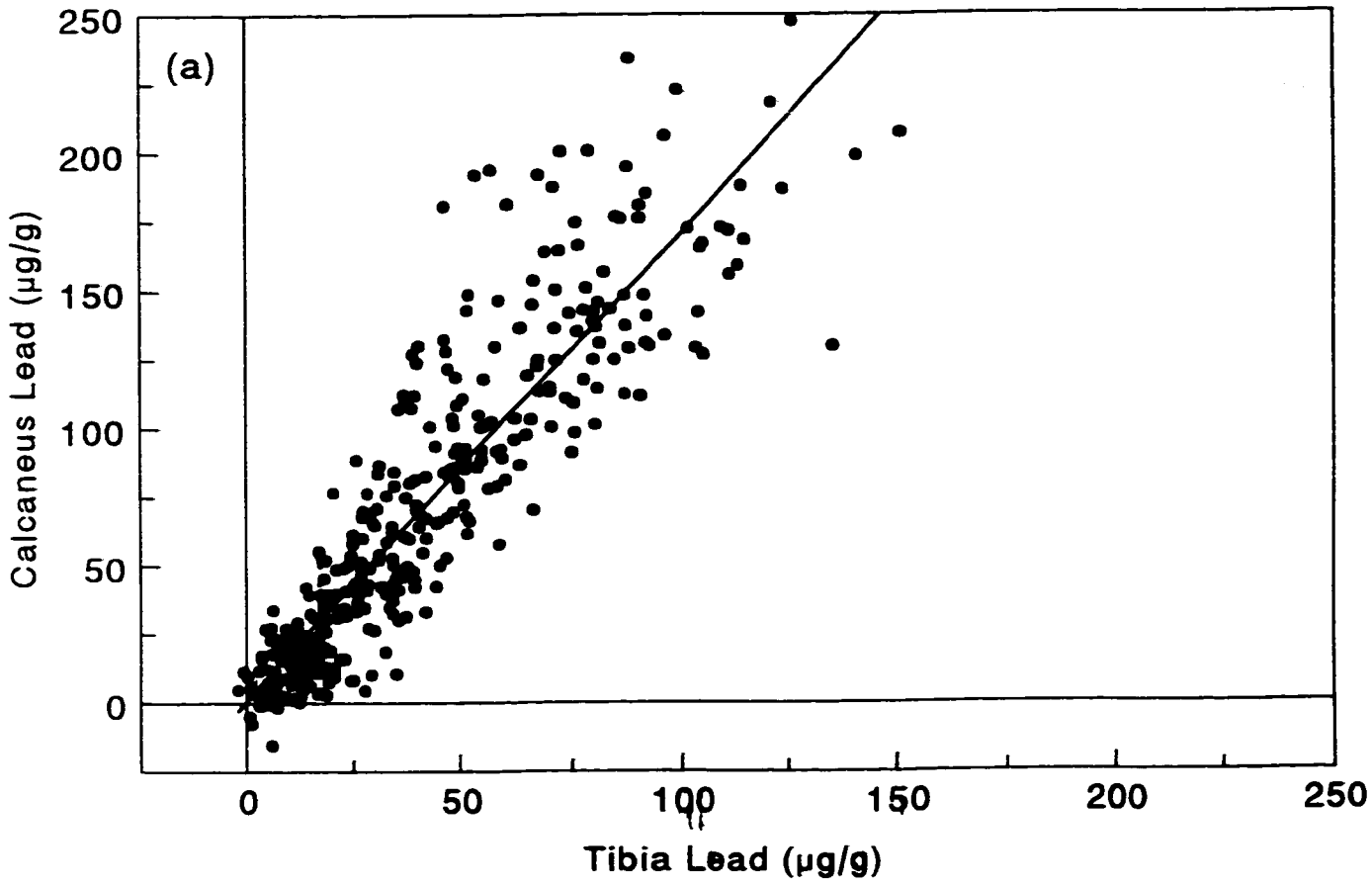

Figure 2.2

Calcaneus lead concentration as a function of tibia lead.

(b) Retired workers;

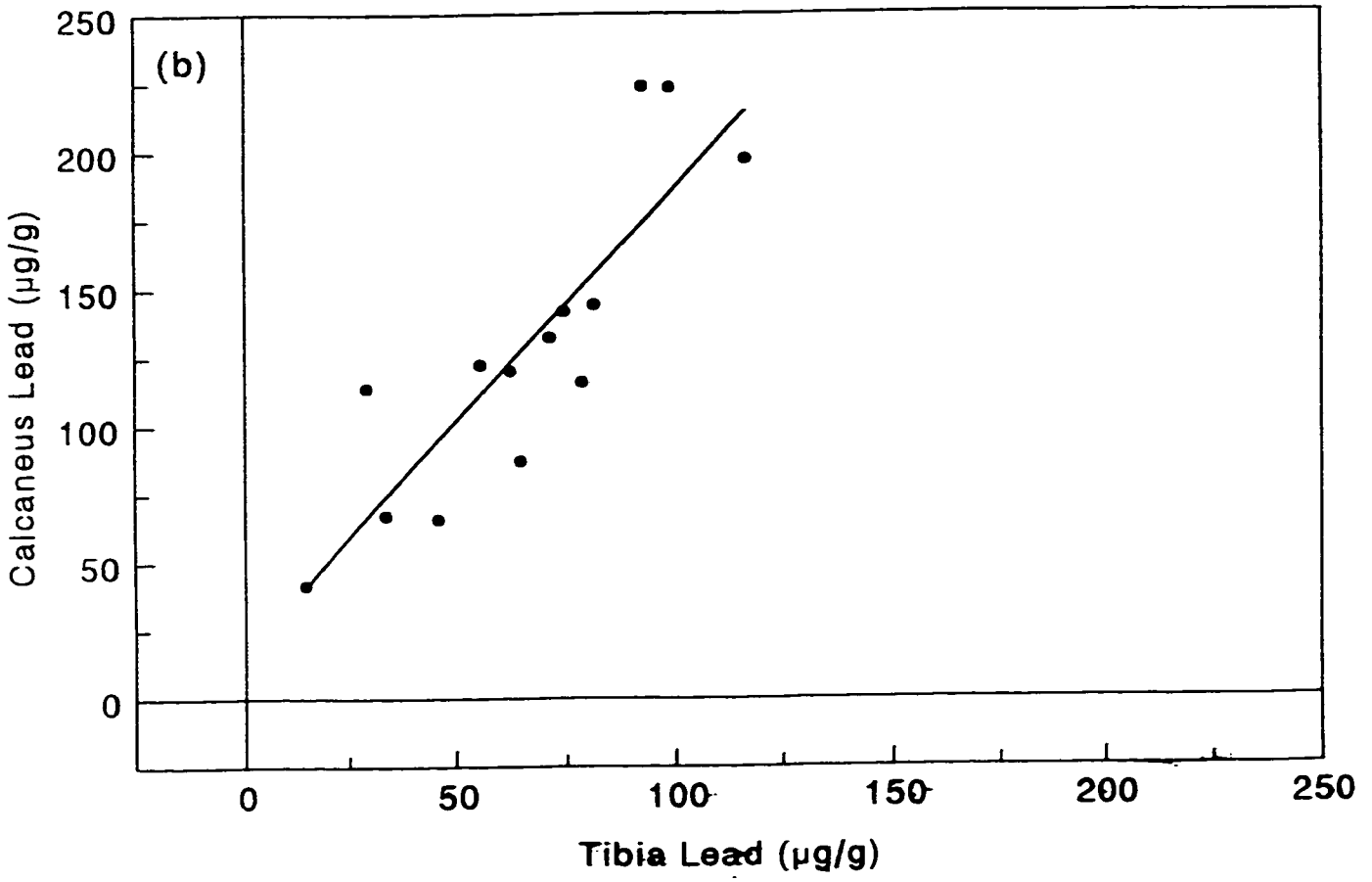

Table 2.1

Linear fits to bone lead-CBLI relations for various bone sites in occupationally exposed populations:

Reference	Industry	Bone Site	N	Slope	r
Christoffersson *et al.* (1984)	various	phalanx	43	0.17	0.41(r_s)
Somervaille *et al.* (1988)	battery	tibia	88	0.060±0.005	0.82
Somervaille *et al.* (1988)	crystal glass	tibia	79	0.050±0.003	0.86
Hu *et al.* (1991)	various	tibia	12	0.061±0.008	0.92
Hu *et al.* (1991)	"	patella	12	0.218±0.026	0.93
Armstrong *et al.* (1992)	refinery	tibia	15	0.10±0.02	0.87
Armstrong *et al.* (1992)	"	tibia	11	0.10±0.02	0.91
Armstrong *et al.* (1992)	(longitudinal)	tibia	7	0.052±0.021	-
Erkkilä *et al.* (1992)	battery	tibia	91	0.028±0.003	0.67
Erkkilä *et al.* (1992)	"	calcaneus	90	0.073±0.013	0.54
Erkkilä *et al.* (1992)	(retired)	tibia	13	0.061±0.012	0.79
Erkkilä *et al.* (1992)	"	calcaneus	13	0.105±0.018	0.87
Gerhardsson *et al.* (1993)	smelter	tibia	100	0.022	0.60
Gerhardsson *et al.* (1993)	"	calcaneus	100	0.042	0.44
Cake (1994)	recycling	tibia	53	0.059±0.009	0.70
Cake (1994)	"	calcaneus	53	0.117±0.018	0.68
Roels *et al.* (1995)	smelter	tibia	123	0.07	0.80
Bleecker *et al.* (1995)	smelter	tibia	81	0.06±0.01	0.70

transfer caused by age, blood lead concentration, or source of lead (endogenous versus exogenous).

The relations between bone lead and CBLI for the active smelter workers are illustrated in Figures 2.3a and 2.3b. Although these results suggest a certain non-linearity, a best fit linear relation has been determined between the parameters of bone lead (μg/g) and CBLI (y*μg/dl) via a least squares method. This permits a more direct comparison with results from previous studies. In addition, the linear model conveys a physically obvious meaning, with the slope coefficient representing the proportion of lead transferred from whole blood and retained by bone. For the tibia, the best fit linear equation was of the following form (Figure 2.3a):

$$T=(0.0556\pm0.0020)\,CBLI+(2\pm2)\;[N=367;r^2=0.69].$$

Entering the calcaneus lead data as a function of CBLI produced a more steeply rising slope, as shown in Figure 2.3b:

$$C=(0.111\pm0.003)\,CBLI-(9\pm3)\;[N=367;r^2=0.77].$$

These fitted slopes are similar to those obtained by Somervaille *et al.* (1988), Hu *et al.* (1991), and Cake (1994) from other occupationally exposed populations (see Table 2.1). Agreement is also evident with an earlier, smaller study of Brunswick smelter workers (Bleecker *et al.*, 1995). This previous investigation involved a subset of the Brunswick population which was largely distinct from the group described

Figure 2.3

Bone lead concentration as a function of cumulative blood lead index (CBLI) for active smelter workers.

(a) Tibia as bone site of measurement;

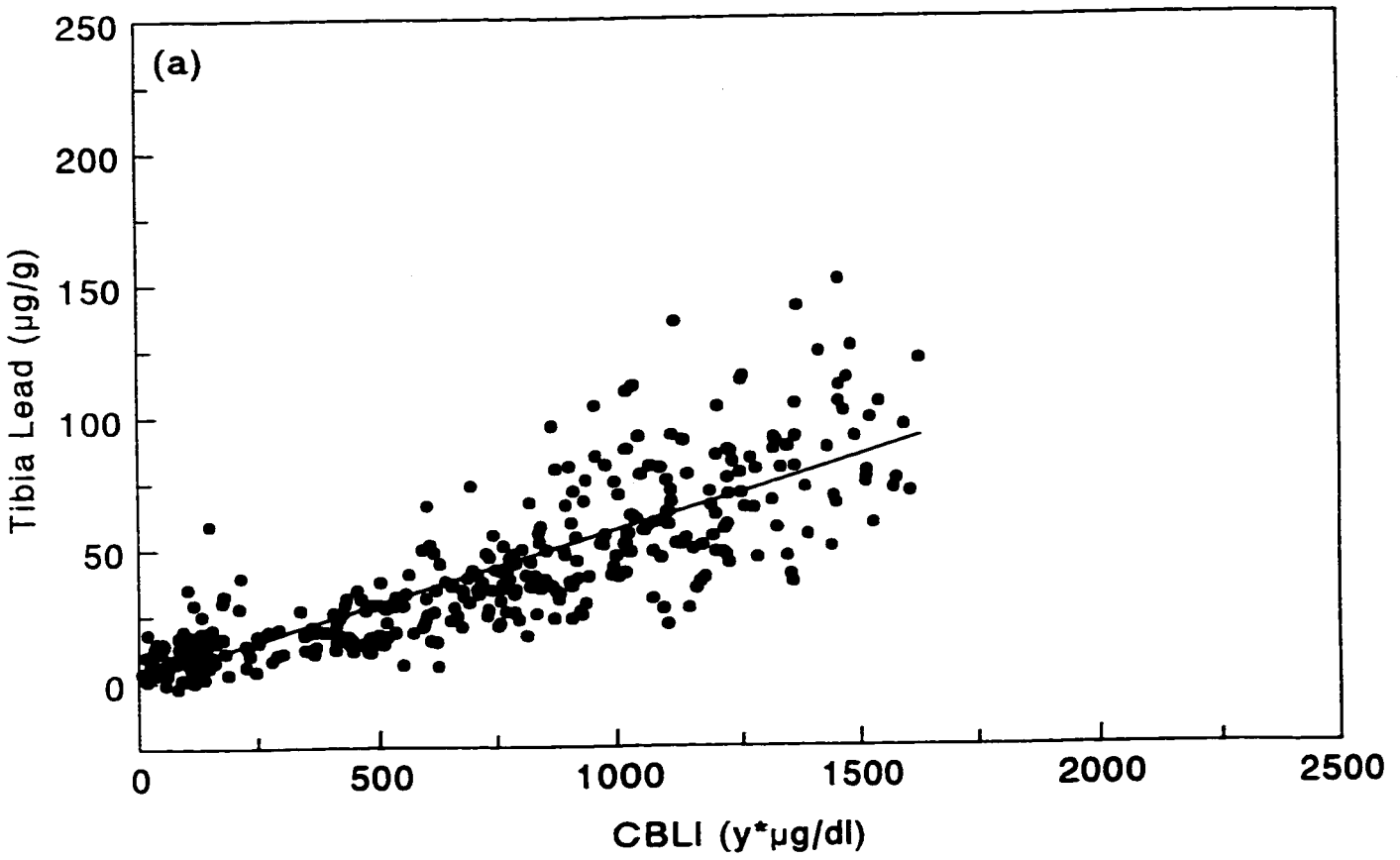

Figure 2.3

Bone lead concentration as a function of cumulative blood lead index (CBLI) for active smelter workers.

(b) Calcaneus as bone site of measurement;

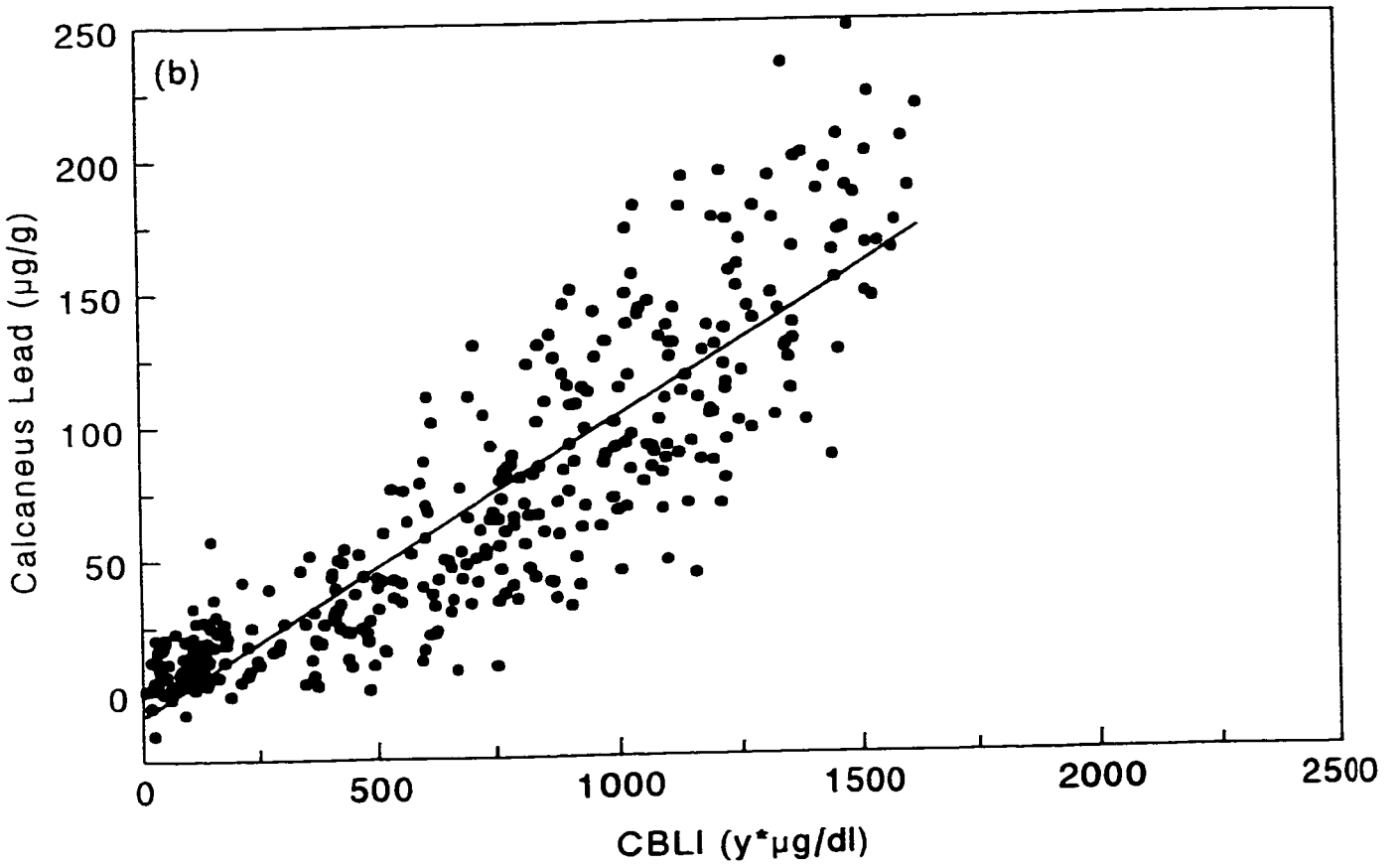

presently.

A similar analysis may be applied to the subset of retired smelter workers. For the tibia lead-CBLI comparison (Figure 2.4a), the best fit relation was determined as

$$T=(0.0700\pm0.0216)\,CBLI-(17\pm26)\,[N=14;r^2=0.47].$$

In turn, the calcaneus lead data as a function of CBLI (Figure 2.4b) was best described by the following linear equation:

$$C=(0.144\pm0.041)\,CBLI-(42\pm50)\,[N=14;r^2=0.50].$$

Although retired workers demonstrated larger bone lead-CBLI slopes than active workers, the differences between the two populations are not statistically significant. Statistical significance will be defined throughout this text to occur for p values less than 0.05 (two-tailed tests).

Figure 2.5 shows the mean blood lead levels of participating workers as a function of time from 1968 to 1995. There is a general decline in blood lead level over time, with the most marked decrease observed after about the year 1977. This decline in lead exposure was attributed to changes made at the smelter in regards to working conditions, hygiene, and safety regulations just prior to 1977. The non-linearities observed in Figure 2.3 (active workers) suggest differences in the uptake of lead amongst the smelter employees. Given the changes in working conditions noted above, it was speculated

Figure 2.4

Bone lead concentration as a function of cumulative blood lead index (CBLI) for retired smelter workers.

(a) Tibia as bone site of measurement;

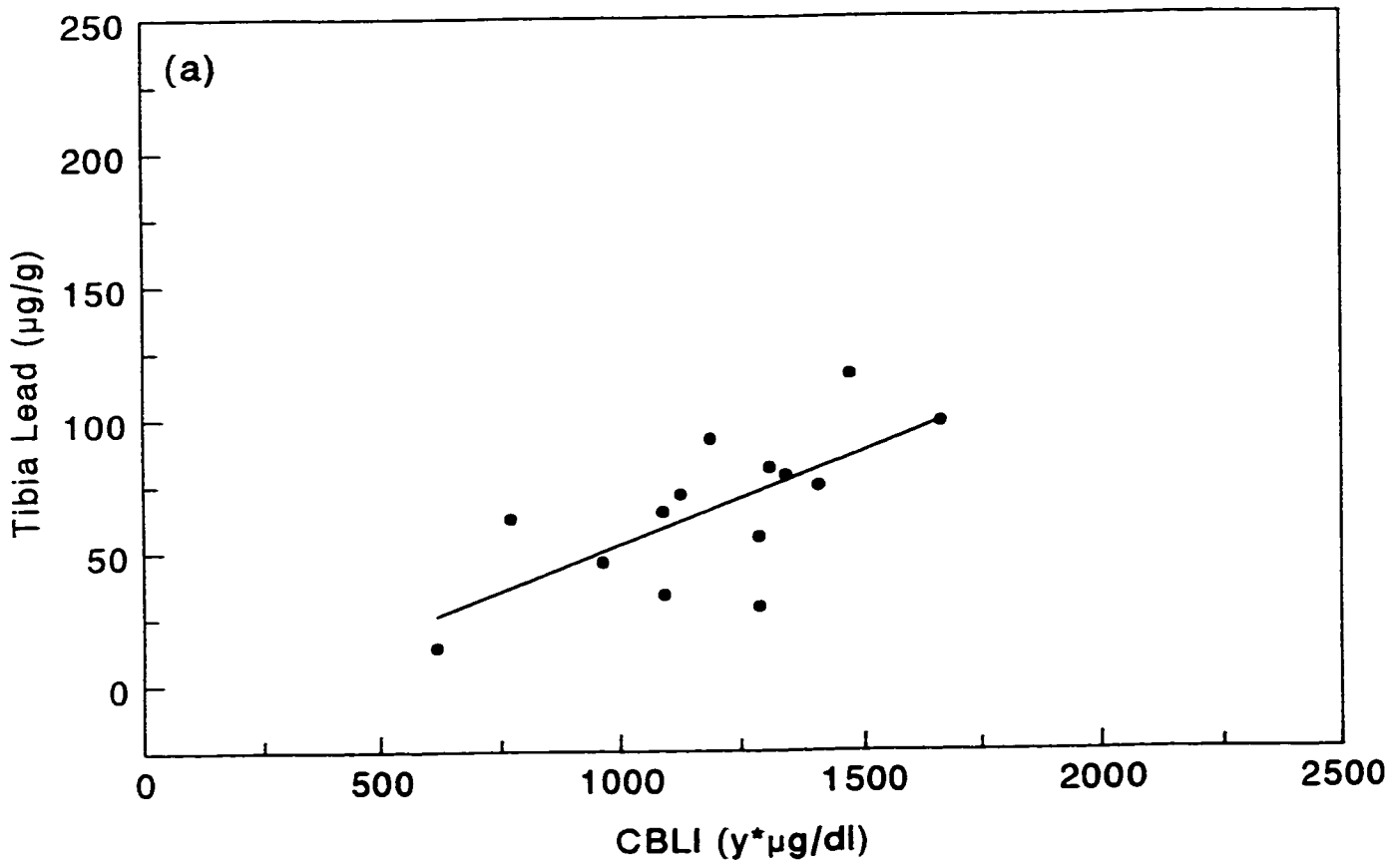

Figure 2.4

Bone lead concentration as a function of cumulative blood lead index (CBLI) for retired smelter workers.

(b) Calcaneus as bone site of measurement;

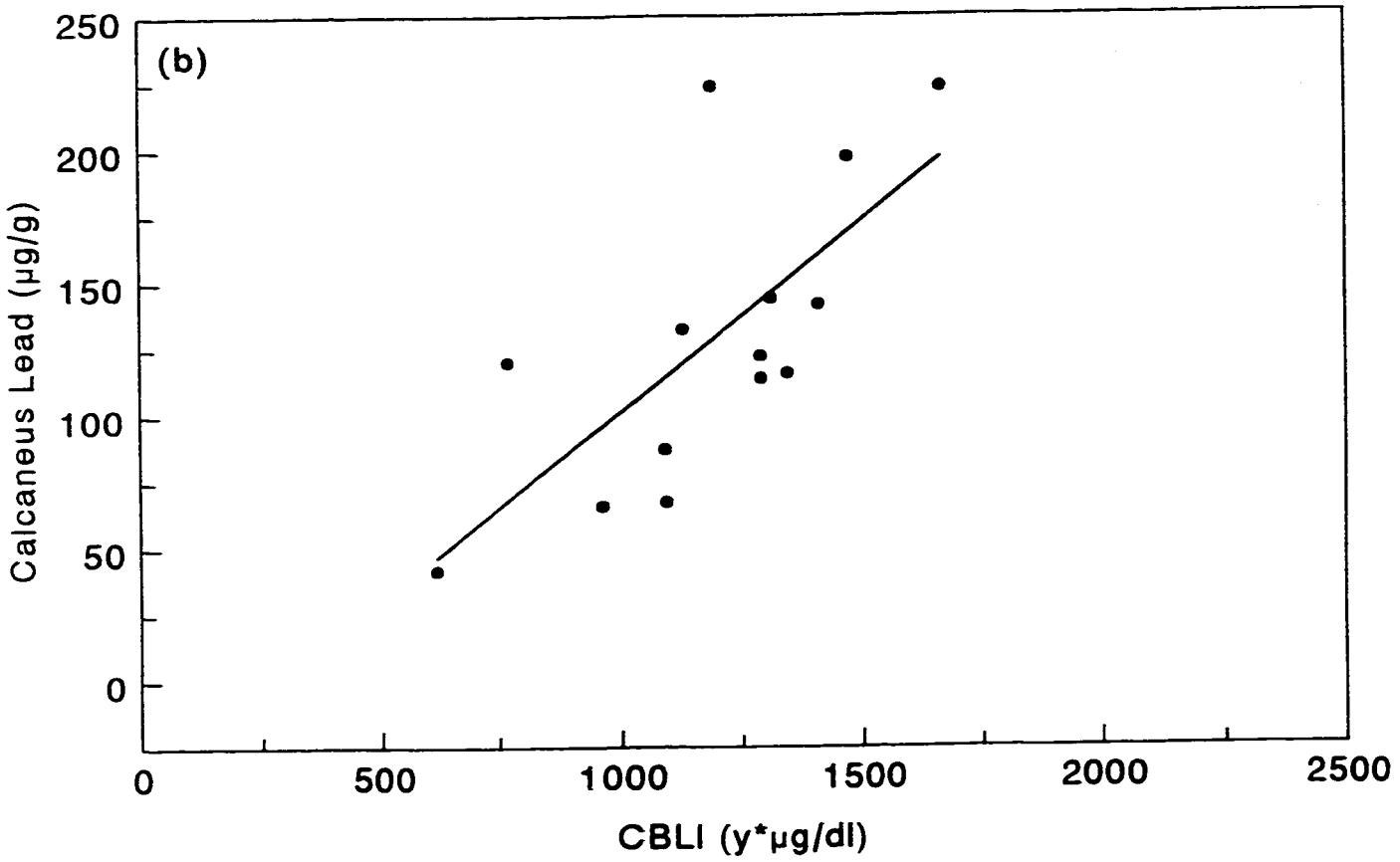

Figure 2.5

Mean blood lead of smelter workers as a function of time.

The bars represent standard errors of the mean.

The dashed line indicates a point of division by time of hire.

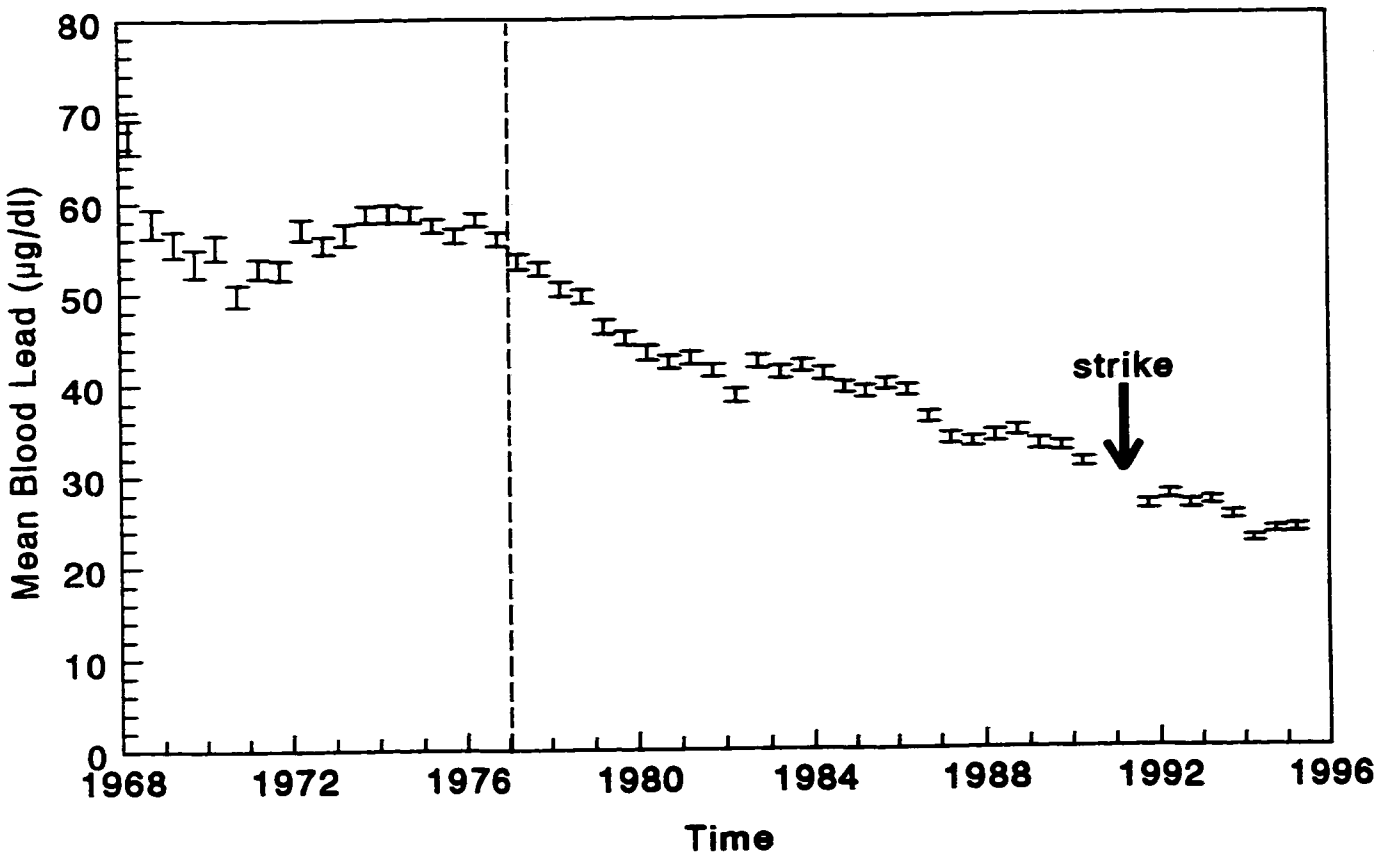

that such variations could result from employment history. With this in mind, the *active* smelter workers were divided into two categories based on time of hiring, and their results were subjected to further analysis.

One subset of active workers was composed of individuals hired before January 1, 1977, while the other consisted of those who began work after this date. The linear fits to the data for workers hired before 1977 (Figure 2.6) resulted in the following relations:

$$T=(0.0687\pm0.0049)\,CBLI-(13\pm5)\;[N=209;r^2=0.49];$$

and

$$C=(0.147\pm0.007)\,CBLI-(48\pm8)\;[N=209;r^2=0.65].$$

In contrast, the same linear fitting routine, when applied to the workers hired after 1977 (Figure 2.6), produces best fit equations of

$$T=(0.0466\pm0.0033)\,CBLI+(5\pm1)\;[N=158;r^2=0.57];$$

and

$$C=(0.101\pm0.006)\,CBLI-(1\pm2)\;[N=158;r^2=0.67].$$

The differences in slope between the two sets of workers are significant, with individuals hired more recently demonstrating more shallow bone lead-CBLI relations. The probability associated with the difference in tibia slopes is

Figure 2.6

Bone lead concentration as a function of CBLI, with data divided by time of worker's hire.

(a) Tibia as bone site of measurement;

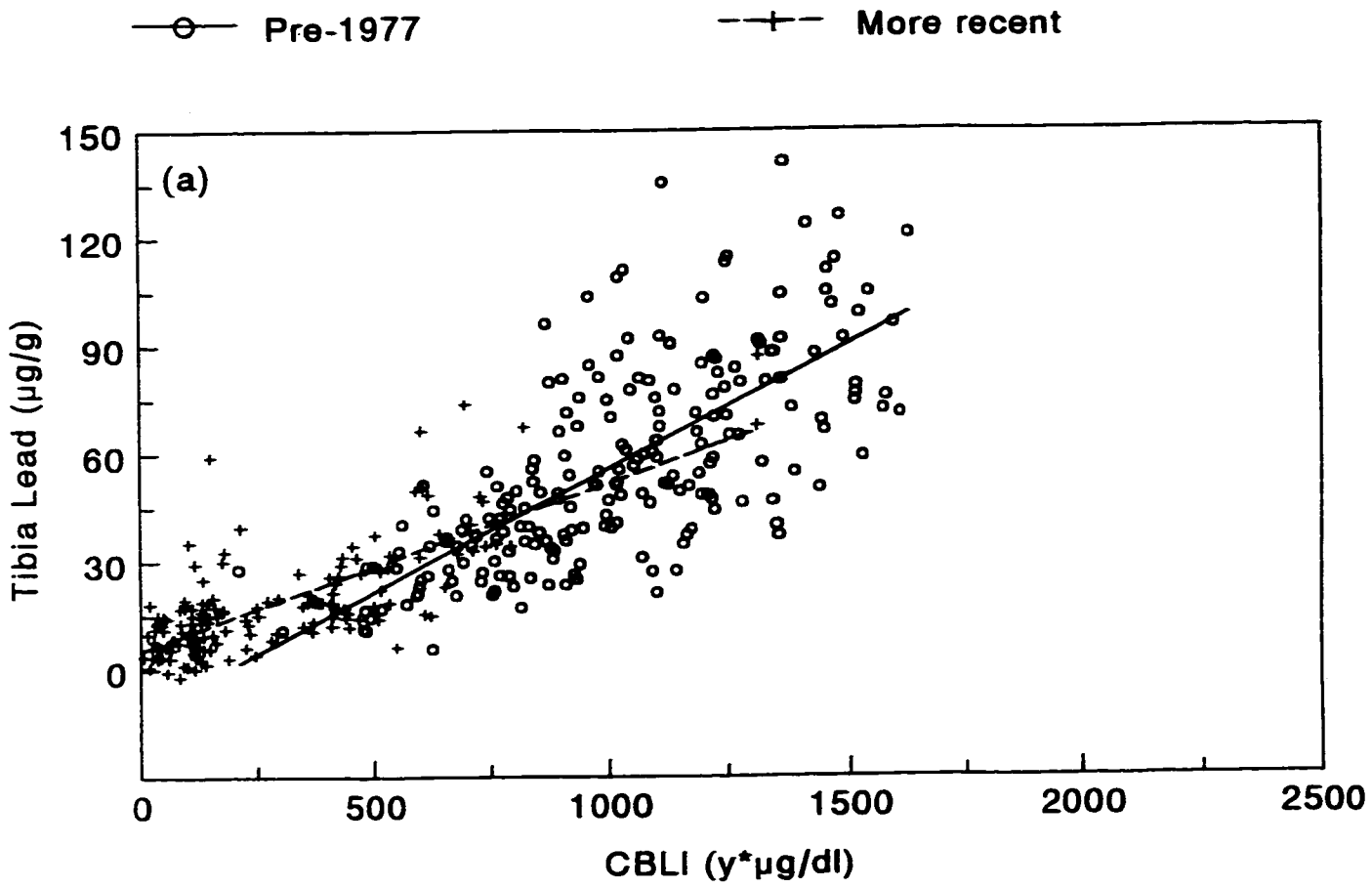

Figure 2.6

Bone lead concentration as a function of CBLI, with data divided by time of worker's hire. (b) Calcaneus as bone site of measurement;

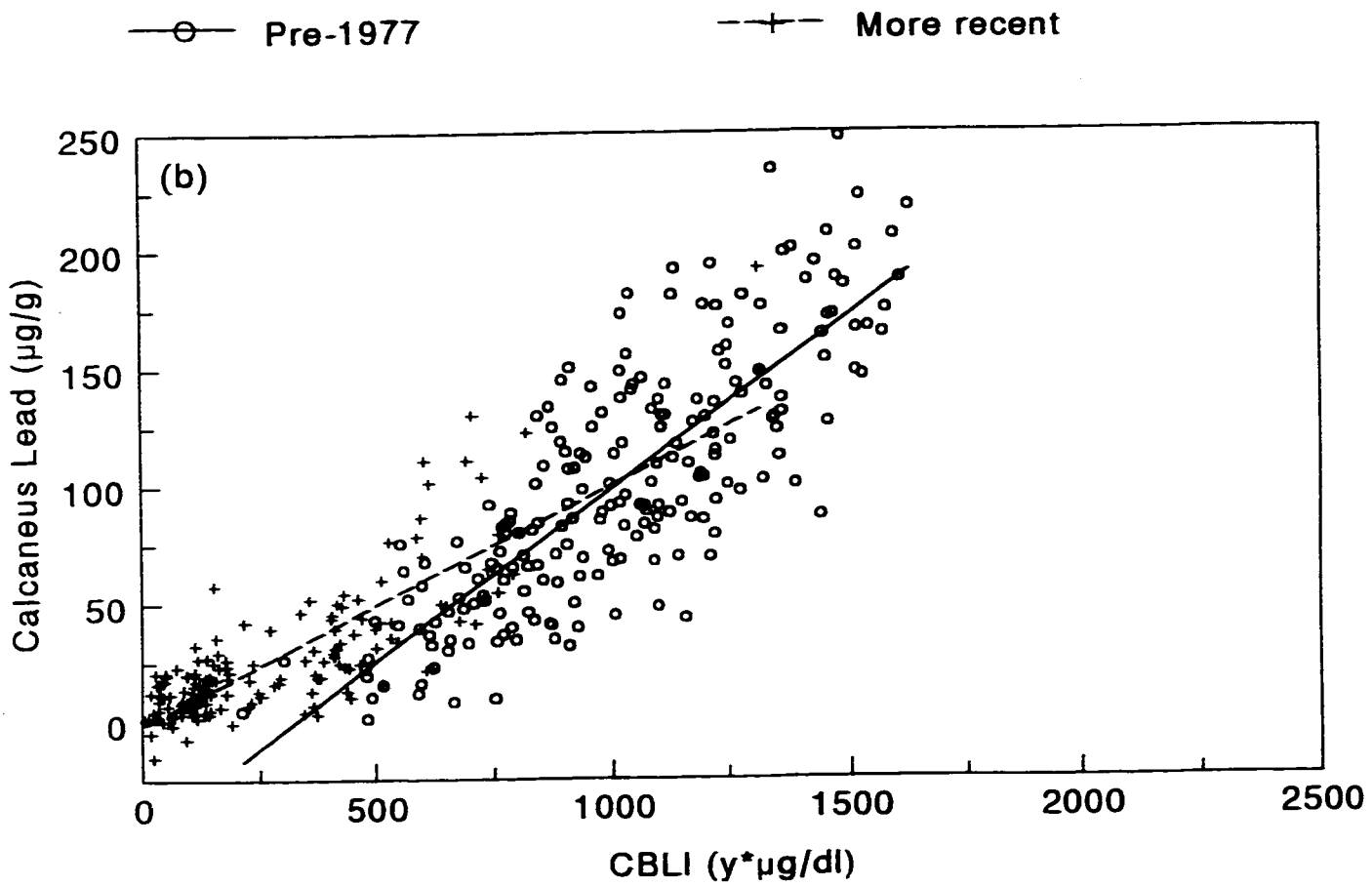

$p<0.001$, while that from the calcaneus values is $p<0.00001$. It is of interest that the bone lead-CBLI relations of retired workers match quite closely to those of active workers hired before 1977. Two explanations for these apparent variations in slope over time are immediately obvious, and will be considered below. A third hypothesis, which should at least be considered, is the possibility that blood lead values in the early years of smelter operation were erroneously underestimated. This would serve to reduce the CBLI and create inflated bone lead-CBLI slope relations for the early workers. Such an underestimation could conceivably result from early limitations in technology, or from a desire to diminish the apparent extent of worker exposure. Improvements in the accuracy of lead measurement, however, have generally revealed previous analyses of lead content as being too *high* (NRC, 1993). As well, the long-term blood lead monitoring of other exposed populations have apparently not suffered from either deficit (Gerhardsson *et al.*, 1993). The blood lead results will therefore be assumed valid.

2.3.4 Variable transfer hypothesis

The differences in slope may be a product of some variation in the workers' transfer of lead from whole blood to bone. This explanation would suggest that the workers hired before 1977 have demonstrated a more efficient transfer of lead to bone than those who have been hired more recently.

This situation is designated the variable transfer hypothesis and is illustrated in Figure 2.7. Here, the arrows represent efficiency of lead transfer from blood to bone. Potential causes of such a variation in tissue uptake per unit of blood lead will be discussed below. Note that the CBLI calculated over an individual's occupational history at the smelter is actually an underestimate of their *lifetime* CBLI. The lifetime CBLI would be a sum of the smelter CBLI and a pre-smelter CBLI. For the variable transfer explanation to be valid, therefore, one would have to demonstrate that the component of a typical individual's CBLI compiled *before* their occupational exposure to lead was not a contributing factor in producing the differences which are observed in slope.

2.3.5 Systematic bias hypothesis

Alternatively, the differences observed in slope may be mere artifacts of incomplete lifetime CBLI data. As a consequence of elevated "background" exposures to lead in the past, it seems possible that the sample of workers hired before 1977 have smelter CBLI values which grossly underestimate their true lifetime CBLI. Conceivably, this could produce artificially steep bone lead-CBLI relations, particularly if the largest underestimations occurred for those workers who have spent the greatest amount of time at Brunswick. Conditions which could give rise to such asystematic CBLI bias are illustrated in Figure 2.8. This

Figure 2.7

Variable transfer hypothesis. Under this scenario, the greater amount of bone lead per unit occupational CBLI for workers hired before 1977 results from a more efficient transfer of lead from blood to bone (represented by arrows) during the early years of smelter operation.

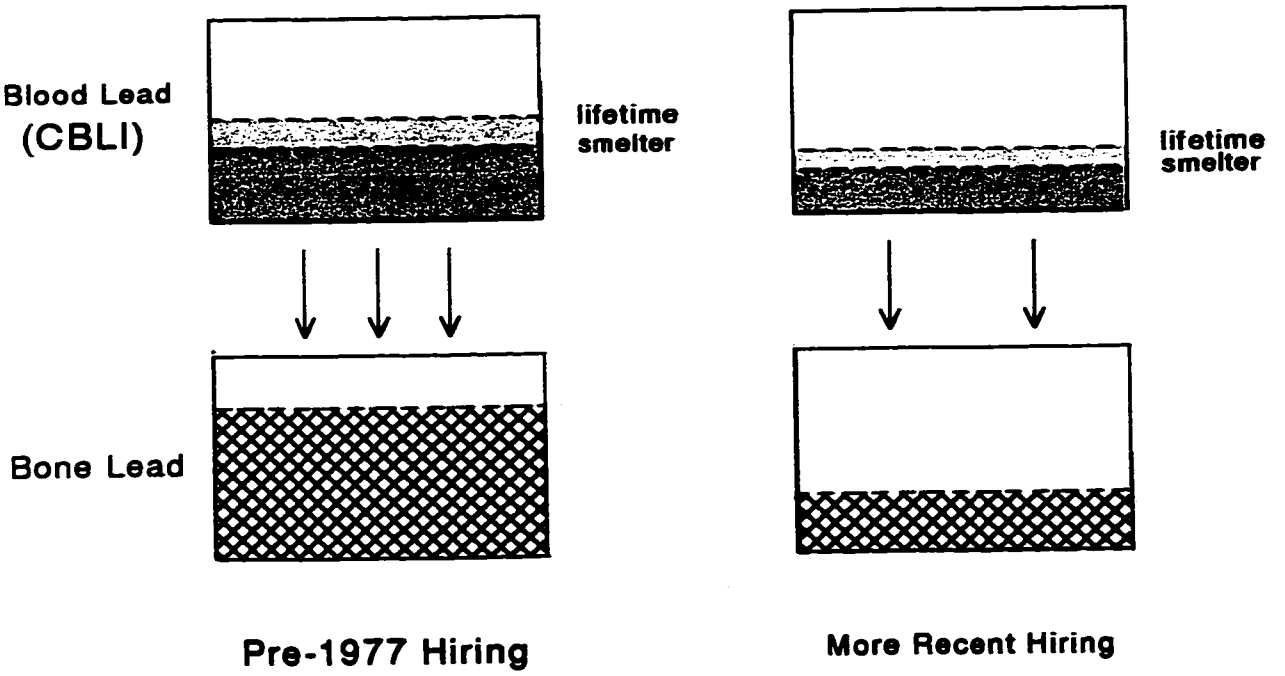

Figure 2.8

Systematic bias hypothesis. Under this scenario, the large pre-employment CBLI of workers hired before 1977 contributes substantially to their bone lead levels. The transfer of lead from blood to bone (represented by arrows) is relatively constant over time.

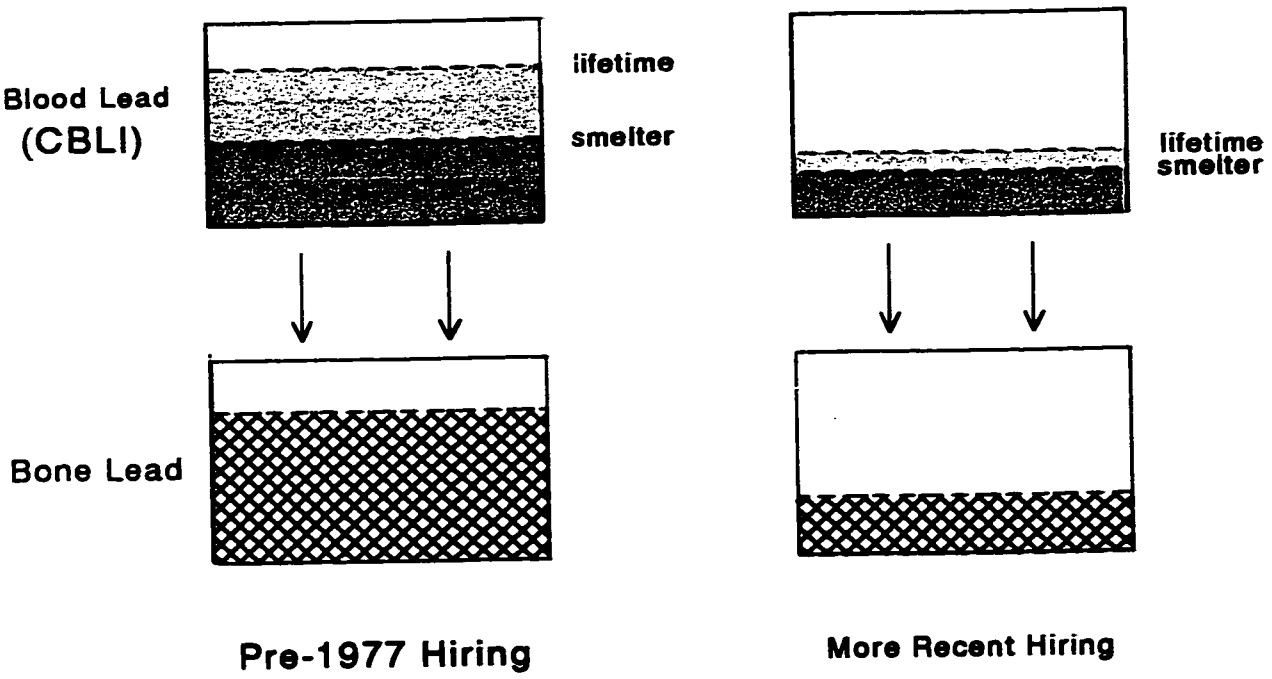

scenario seems plausible, considering that blood lead levels for the general population were measurably higher in the past (Pirkle *et al.*, 1994). The net effect of such a set of circumstances would be the illusion of a higher efficiency of transfer to bone, resulting solely from a bias in CBLI data. In other words, even if the true efficiency of uptake had been exactly the same over time (as illustrated by the arrows in Figure 2.8), a comparison of the *smelter* CBLI to bone lead would suggest a significant difference.

2.3.6 Pre-smelter CBLI

To investigate which of these two potential explanations is more likely true, it is necessary to calculate a pre-smelter CBLI component for each worker. A revised, or *lifetime*, CBLI may then be implemented to see if the differences between the two populations persist. In order to construct a worker's lifetime CBLI which includes pre-smelter contributions, certain assumptions must be introduced. The question of a starting point in time for the integration is not a trivial one. The rapid turnover in bone exhibited throughout the childhood years renders the idealized treatment of bone as a long-term storage site of lead inappropriate. In this respect, a case could be made for beginning the revised CBLI post-adolescence. This assumption is particularly appealing in regards to the calculation of a lifetime CBLI for a lead industry worker, whose exposure to lead before the age

of employment would in most cases be negligible in comparison (Roels *et al.*, 1995). Others would argue that the *entire* life history of exposure to lead must be accounted for if both the CBLI and bone lead are to be used as chronic indices. This point of view would suggest that the revised CBLI should be extended to the time of birth (Hu *et al.*, 1991).

For the present purpose, it was decided to approach this problem from an empirical perspective. A recent study of 149 individuals (90 females, 59 males) of ages 6-81 in Southern Ontario, Canada produced a detailed plot of tibia lead as a function of age for the general population (Roy *et al.*, 1997). The relation between tibia lead and age was not significantly different between men and women. Based on these results, the intercept of the temporal axis occurs at approximately five years of age, and this age was selected as a starting point for the revised CBLI integration. Inspection of similar data sets gathered for a variety of studies (Barry, 1975; Erkkilä *et al.*, 1992; Gerhardsson *et al.*, 1993; Somervaille *et al.*, 1989; Somervaille *et al.*, 1988; Kosnett *et al.*, 1994; Morgan *et al.*, 1990) generally indicate x-axis intercepts of $t>5$ years. The five year starting point therefore represents a conservative approach to the present investigation of systematic bias.

A further consideration is the need for an estimate of the "background" level of lead exposure as a function of time.

The concentration of lead in blood for a given non-occupationally exposed individual will of course depend on a variety of factors, and even producing a mean estimate over a large population is no simple matter. For guidance in this respect, one may refer to blood lead measurements from the National Health and Nutrition Examination Surveys (NHANES) performed in the United States. The median blood lead level for American males surveyed from 1988-1991 (N=6051) was 3.8 μg/dl, while the median for those examined between 1976-1980 (N=4895) was 15.0 μg/dl (Pirkle *et al.*, 1994). This significant decrease in blood lead level was partially a result of the steep reduction in lead as a gasoline additive (99.8% decrease from 1976 to 1990). Other contributing factors included drops in the production of lead-based paints and lead-soldered cans, and local reductions of lead in water supplies and industrial emissions. While the exposure to lead in rural New Brunswick might normally be expected to be less than that of the United States as a whole, the local presence of a lead smelter would likely offset any such difference. Nonetheless, it would be useful to derive a pre-employment background blood lead level for the Brunswick workers in order to make a naive comparison with the American data.

Toward this end, the blood lead data of the Brunswick employees were scanned for any measurements which occurred either on the day of hiring or up to three days *prior to* the day of hiring. These readings were then assumed to be

indicative of the background blood lead level of individuals hired for employment at the Brunswick smelter. The relevant individuals were classified by time of hiring into the following groups: 1987 to 1992 (N=17), 1975 to 1981 (N=13), and 1969 to 1974 (N=38). No workers fitting the selection criterion were available over the time intervals of 1982 to 1986 or 1993 to present.

The 1987 to 1992 subset of hirees exhibited a median blood lead level of 8.0 μg/dl. This is in contrast to the NHANES median over the 1988 to 1991 period, which was determined to be 3.8 μg/dl for the American male. The offset is statistically significant, with the elevated levels exhibited by the Brunswick hirees possibly a consequence of hiring local area residents. The relative proximity of residence to a lead smelter would presumably introduce such individuals to a slightly elevated lead exposure. This finding reflects those of the 1991 readings discussed above, which suggested background blood lead levels of 13.0±0.8 μg/dl for Brunswick workers, and levels of 6.1±3.6 μg/dl and 9.2±4.2 μg/dl for retired employees. Based on this information, a 1991 background blood lead level of 10 μg/dl was assumed to be representative for incoming personnel.

The 1975 to 1981 subset of individuals hired by Brunswick demonstrated a median blood lead level of 16.0 μg/dl. This value is consistent with that determined by the 1976 to 1980

NHANES survey: 15.0 μg/dl for the American male. The lead exposure of the two populations might be expected to match more closely over this period because the smelter's contribution would not be as dominant a source, in light of the more widespread presence of lead in North American society at this time. The background blood lead level was therefore taken as 15 μg/dl for an intermediate time in 1978.

Finally, the 1969 to 1974 group of hirees displayed even higher blood lead levels, with a median value of 22.0 μg/dl. Considering that the introduction of lead-free gasoline did not occur in Canada until 1972 and that automotive lead emissions did not begin to decline until 1973, this is not a surprising result. Even within the 1976 to 1980 NHANES data, a downward trend in blood lead as a function of time had been noted (Annest *et al.*, 1983), suggesting that levels were higher than 15 μg/dl earlier in the decade. For the purpose of CBLI extrapolation, a background level of 20 μg/dl was assumed to apply at all times before 1972.

In summary, the blood lead background for incoming workers, which was used to calculate the pre-smelter component of CBLI, was established as 10 μg/dl in 1991 and at all times that followed, 15 μg/dl in 1978, and 20 μg/dl in 1972. A linear rate of change was applied between these three points.

2.3.7 Revised CBLI

Again dividing the Brunswick workers into groups consisting of those hired before and after 1977, the lifetime (revised) CBLI data was compared with the tibia and calcaneus lead concentrations. A linear fit to the tibia lead versus revised CBLI data for those hired before 1977 (Figure 2.9a) now produces the following relation:

$$T=(0.0584\pm0.0048)\,CBLI-(24\pm7)\;[N=209;r^2=0.42].$$

Similarly, the calcaneus lead-revised CBLI data (Figure 2.9b) yields:

$$C=(0.127\pm0.008)\,CBLI-(76\pm11)\;[N=209;r^2=0.58].$$

For workers hired more recently, the best fit linear equations relating the same variables are as follows (Figures 2.9a and 2.9b):

$$T=(0.0406\pm0.0029)\,CBLI-(7\pm2)\;[N=158;r^2=0.56];$$

and

$$C=(0.0842\pm0.0054)\,CBLI-(26\pm4)\;[N=158;r^2=0.61].$$

The differences between the slopes of the relations for those hired before 1977 as opposed to those hired after this time remain clearly significant, with $p<0.01$ for the tibia and $p<0.001$ for the calcaneus. This result implies that the

Figure 2.9

Bone lead concentration as a function of revised CBLI, with data divided by time of worker's hire.

(a) Tibia as bone site of measurement;

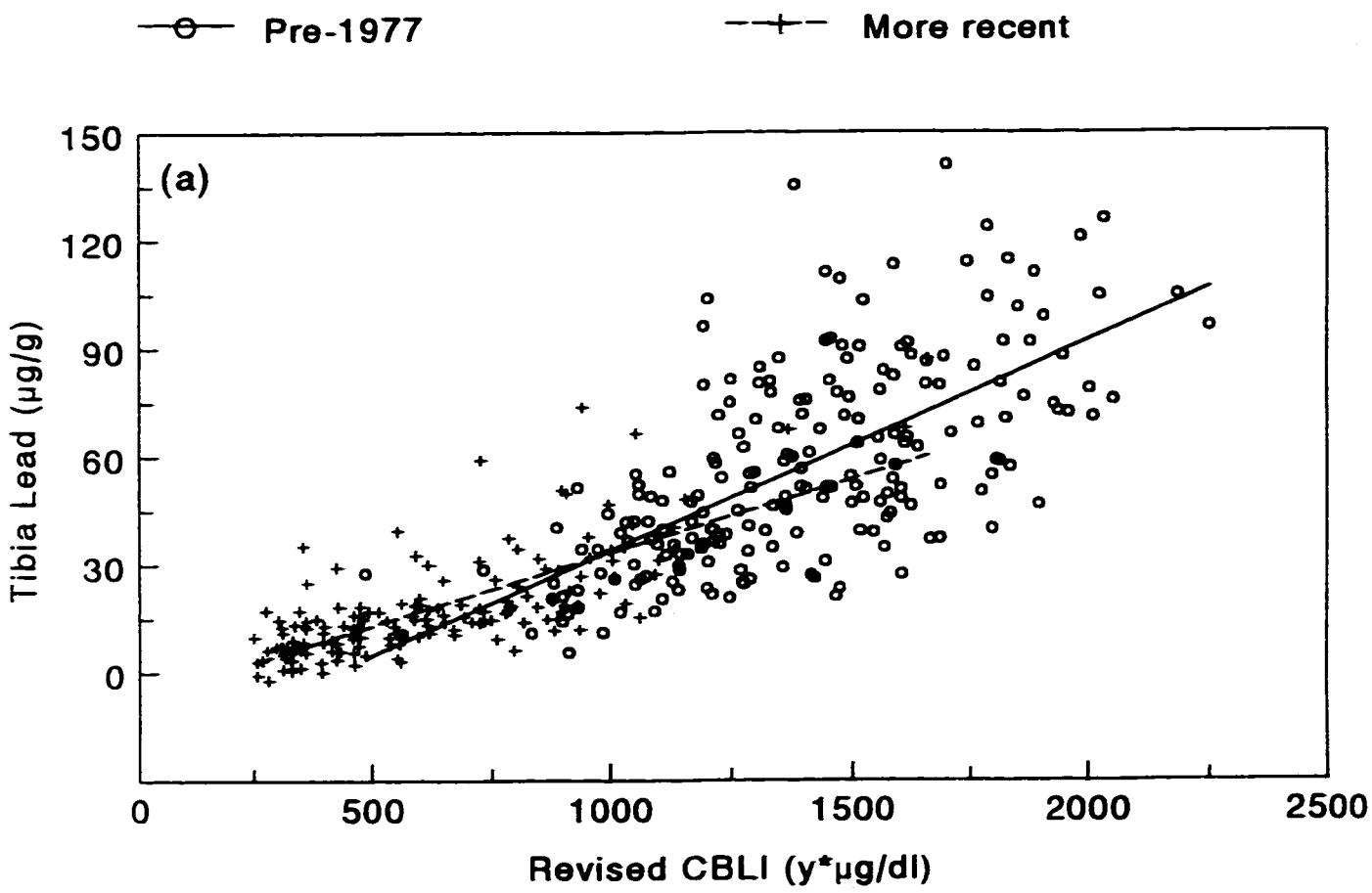

Figure 2.9

Bone lead concentration as a function of revised CBLI, with data divided by time of worker's hire.

(b) Calcaneus as bone site of measurement;

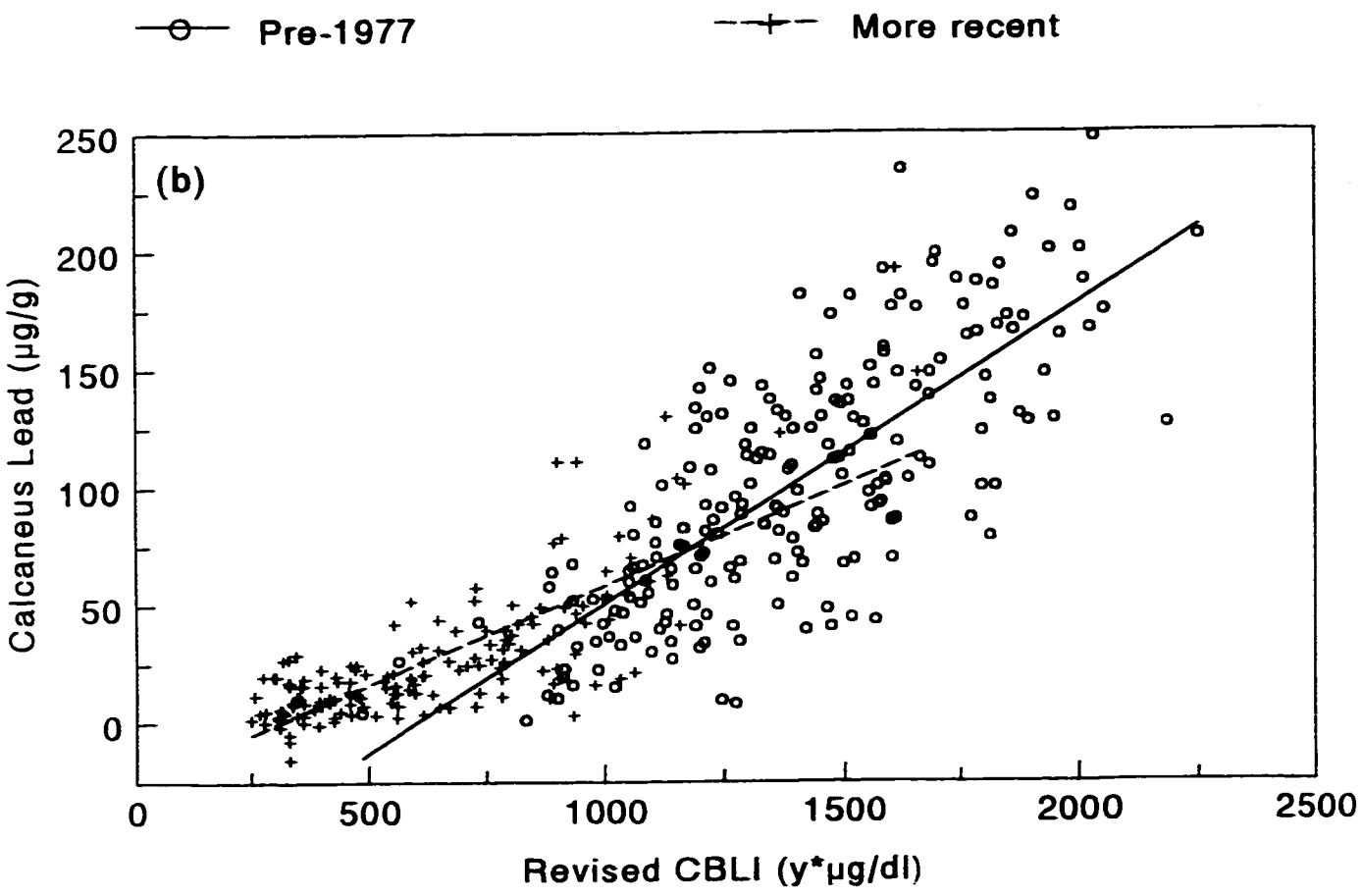

original differences observed in slope (with the CBLI integrated only over smelter employment time) were *not* artifacts of a systematic bias in CBLI calculation. Consequently, the existence of a variation in the efficiency of lead transfer from blood to bone becomes a more persuasive possibility. Potential explanations for this variation include age-related effects, changing blood lead concentrations resulting from changing exposure conditions, and whether or not the lead exposure involves a strong endogenous component.

2.4 Discussion

2.4.1 Endogenous release of lead

The relation between bone lead concentration and the resulting endogenous exposure to lead is one of great importance. Instances of acute lead poisoning may occasionally have some component originating from lead stores in bone. Knowledge of the link between bone lead and endogenous exposure to lead allows an objective assessment of this contribution to be made. This relation also provides a baseline from which to consider the effects of bone lead stores on exposure during times of elevated bone turnover such as during pregnancy and lactation (Manton, 1985), and following menopause (Silbergeld *et al.*, 1988; Webber *et al.*, 1995). Long-term workers in the lead industry often report an

inability to lower personal blood lead levels despite all manner of exposure precautions; endogenous exposure from accumulated bone stores dictates this lowest achievable level. The contribution from bone-released lead is particularly significant for retired workers of lead-related industries.

The present study indicates that the relation between blood lead and tibia lead for workers who have been removed from their occupational exposure to lead may be characterized by a linear relation of slope 0.136±0.014. This result is consistent with analogous studies involving *retired* workers from a lead smelter in Sweden and two lead acid battery factories in Finland:

$$BPb=(0.133)\,T+(5.3)\,[N=30];$$

and

$$BPb=(0.138)\,T+(7.7)\,[N=16].$$

(Gerhardsson *et al.*, 1993; Erkkilä *et al.*, 1992). This may also be compared to the result determined from a distinct subset of the Brunswick workforce, again measured after the 1990-91 strike:

$$BPb=(0.178\pm0.025)\,T+(12.8\pm1.2)\,[N=84]$$

(Bleecker *et al.*, 1995).

When the blood lead levels of returning Brunswick workers

were plotted against calcaneus lead concentrations, a more shallow slope of 0.0776±0.0074 was derived. Again, this value is much the same as those determined from the European research:

$$BPb=(0.0622)C+(4.0)\ [N=30];$$

and

$$BPb=(0.0721)C+(6.9)\ [N=16].$$

(Gerhardsson *et al.*, 1993; Erkkilä *et al.*, 1992). Calcaneus lead measurements were not performed in the study of Bleecker *et al.* (1995).

Therefore, it seems that the contribution to blood lead from bone stores at any instant in time is similar for all occupationally exposed populations, regardless of whether active or retired workers are considered. The implication is that, at least for the samples examined to date, age-related variations in bone turnover are not a dominant factor in the endogenous exposure of male lead workers. The circumstances that allowed this analysis to be performed on such a large population of active lead industry employees are not likely to prevail again in the near future. This may therefore represent the most precise currently feasible statement of the bone lead-endogenous lead exposure relation.

The y-intercept values, which essentially indicate the

expected blood lead levels in the absence of any bone lead stores, are high in the current study- at 13.6±0.8 μg/dl and 13.6±0.7 μg/dl from the tibia and calcaneus measures, respectively. These results are consistent with the other result from post-strike Brunswick workers- 12.8±1.2 μg/dl (Bleecker *et al.*, 1995). Although uncertainties in the y-intercepts are not provided in the European studies, the consistency of their results, together with the small uncertainties in the Brunswick data, suggest that the offset is significant. This may be representative of a higher background exposure to lead for the Brunswick workers relative to their Scandinavian counterparts. Alternatively, this elevation may be an artifact of the inclusion of some workers in the study whose blood lead samples were not taken *immediately* upon their return to work. However, when the current sample was limited to those workers whose blood leads were recorded on the day of their return, the results were unchanged within uncertainty limits.

As a final check for the link between bone lead and endogenous exposure, the slopes and intercepts of linear fits to plots of blood lead against bone lead were derived for the 14 participating retired workers. For the tibia as the bone site of inspection, the slope was found to be 0.162±0.051, while the y-intercept was 6.1±3.6 μg/dl. The calcaneus yielded a slope of 0.0593±0.0305, with an intercept of 9.2±4.2 μg/dl. Although the uncertainties are much larger in this

relatively small sample of retirees, it is evident that the slope results are consistent with both those of the retired European workers and those of the post-strike Brunswick employees. The y-intercepts appear to be of an intermediate magnitude. To verify these trends, a larger sample of retired workers would be desirable.

2.4.2 Bone lead at different sites

The positive correlations found between calcaneus lead and tibia lead in both active and retired smelter workers may be compared with those identified by other recent investigations. As displayed by Figure 2.2, the Brunswick results suggest a fairly tight relationship between the two variables, with a slope of 1.70±0.04 and an intercept of 0.6±2.2 μg/g describing the active workers' calcaneus lead against tibia lead regression. The small population of retired workers provided similar results; the slope was determined to be 1.70±0.29, while the y-intercept was 16.7±20.7 μg/g. The apparent invariance of this relation amongst workers with different employment histories introduces some doubt to the hypothesis that the calcaneus (as a trabecular bone) has a faster rate of bone turnover than the tibia. The fact that calcaneus lead concentrations tend to be elevated relative to those of tibia lead does indicate that accumulation is more rapid at this particular bone site. Comparisons of bone lead concentration at these two sites have

been performed for various other occupationally exposed populations in the past. Although a range of regression results are represented in the literature, the Brunswick relation is certainly consistent in suggesting by how much the calcaneus lead concentration will typically exceed that of the tibia in a given exposed worker.

2.4.3 Accumulated lead body burden

The bone lead-CBLI relations derived from a small sample of former Brunswick employees were suggestive of a different slope relative to active workers. The results from these retired individuals were similar to those from active workers hired *before* the year 1977. It is interesting to note that Erkkilä *et al.* (1992) also identified higher bone lead-CBLI slopes amongst a group of retired lead battery workers.

Workers hired during the initial years of smelter operation were found to have been exposed to higher levels of lead (Figure 2.5). It was speculated that the non-linear nature of the active worker bone lead-CBLI plots could be a consequence of employment history. The possibility that the uptake of lead per unit exposure can vary in occupationally exposed individuals was probed by dividing the Brunswick workers by time of hire.

The relation between bone lead and the cumulative blood

lead index for lead industry workers is normally assumed to be of a linear nature. The application of linear regressions to the two subsets of Brunswick workers (those hired before 1977 and those hired more recently) revealed distinctly different relations between bone lead and CBLI. This difference emerged regardless of whether the occupational CBLI was entered as the independent variable, or whether a more rigorous lifetime CBLI was introduced. Greater bone lead to CBLI ratios were identified for those workers who were hired on early in the smelter's operation. These workers were more heavily exposed during their initial years of employment, exhibited the highest instantaneous blood leads, and tended to possess the greatest CBLI values. Therefore, the present results represent the first time that distinctly non-linear components have been seen in a bone lead-CBLI comparison. The implication is that lead transfer from whole blood to bone tissue has varied in this population.

2.4.4 Explaining the variation in transfer

The mechanism by which lead has been transferred more efficiently into the bone of the early workers is uncertain. The possibility that age is a factor in lead kinetics has been suggested by at least two X-ray fluorescence studies of environmentally exposed populations (Kosnett *et al.*, 1994; Morgan *et al.*, 1990). Specifically, males of age 55 years or greater were identified as demonstrating more extreme tibia

lead-age slopes than their younger cohorts (Kosnett *et al.*, 1994). Rejecting workers older than 55 years from the Brunswick data set leaves a total of 177 individuals hired before 1977, and 157 hired since that time. Including both the revised CBLI *and* age as variables in multivariate fits to the bone lead data of these remaining workers does not change the overall nature of observed bone lead-CBLI slope differences (all results unchanged within uncertainty limits; $p<0.001$, tibia; $p<0.01$, calcaneus; results not shown). Age alone does not appear to explain the variation in slope between workers hired during the early years of smelter operation and those hired more recently. The fact that Brunswick workers hired before 1977 were likely to receive higher exposure to lead than those hired since that time implies that any difference in uptake could simply be related to exposure level. Two distinct explanations involving lead kinetics are consistent with this hypothesis and will be examined below.

2.4.5 Blood lead level and red cell binding

There has been much speculation regarding the existence of a saturation level for lead binding in red blood cells. Models of lead kinetics normally assume the transport of lead throughout the body to be governed by the plasma component of whole blood (O'Flaherty, 1993; Leggett, 1993). At elevated blood lead levels, a distinctly non-linear relation between

serum lead and blood lead has been observed (deSilva, 1981; Manton and Malloy, 1983; Manton and Cook, 1984; Schütz *et al.*, 1996), suggesting a gradual saturation of binding sites in red blood cells beyond which more lead becomes biologically available. This mechanism is consistent with the results of the present study. Early smelter workers exhibited relatively high blood lead levels and may have frequently obtained saturation concentrations. This would cause a higher proportion of the lead in whole blood to reside in the plasma component, resulting in a more efficient transfer of lead from whole blood to bone tissue. Workers hired more recently would be more likely to have spent their careers at the smelter with blood lead concentrations *below* saturation levels. The difference observed in slope between the two hiring groups would then be a consequence of the analysis of two distinct portions of a continuous, non-linear relation between bone lead uptake and cumulative lead exposure.

2.4.6 Endogenous/exogenous sources and partitioning

Recently, an alternative hypothesis regarding lead kinetics has been proposed (Cake *et al.*, 1996). Blood, serum, and bone lead measurements from a population of battery recycling workers pointed to a differential partitioning of lead between plasma and blood, depending upon whether the source of exposure was endogenous or exogenous. Endogenous

exposures appeared to favour the plasma compartment more strongly than did exogenous sources. This interpretation would also be capable of explaining the Brunswick results. Those workers who have been employed for the longest periods of time generally have higher bone leads as a result of both their time of service and their initial levels of exposure. They are therefore subject to higher endogenous exposures (lead returning to the bloodstream from bone) than those workers hired more recently. Consequently, under the differential partitioning scenario, a greater proportion of the lead in the early workers' blood would be biologically available for redistribution in the body.

In any case, the result of significance remains: bone lead-CBLI relations show a more efficient transfer of lead to bone for those workers who have experienced the most extreme cumulative exposures. With bone lead acting as an indicator of overall body burden, the apparent variation in blood-bone transfer serves to emphasize the importance of the smelter's safety initiatives of the mid-1970's.

A secondary question which arises in light of this result is why similar non-linear findings have not been apparent in previous investigations of lead industry workers. There are a number of factors which could conceivably differentiate this study from those which it has followed. Differences deal mainly with the quality of the data set available from the

Brunswick survey. A total of 280 of the 367 participating active workers had complete blood lead records, dating to within one month of their initial hiring. This represents 76% of the population, and suggests that extrapolation was not an important feature for the majority of CBLI estimations. For those workers who *did* require an extrapolation, the application of a routine taking into account the temporal trend in their personal blood lead records should have produced more accurate results than would an alternative approach. The large sample of workers involved, representing a wide distribution of CBLI and bone lead readings, is a further advantage. As a final note, the use of a revised X-ray fluorescence system (Gordon *et al.*, 1993) for these bone lead measurements resulted in the collection of a more precise data set than would previously have been possible.

Taking a broad perspective, it appears possible that at least some of the variation in bone lead-CBLI slopes exhibited between studies is a result of differences in lead exposure intensity. Referring to Table 2.1, it is interesting to note that the largest tibia lead-CBLI slope results have been derived from those populations who have displayed the *highest* blood leads and CBLIs: smelter workers in Belgium (Roels *et al.*, 1995) and retired Finnish battery plant employees (Erkkilä *et al.*, 1992). The lowest slopes have been observed from those workers with more moderate exposures: smelter workers in Sweden (Gerhardsson *et al.*, 1993) and active

Finnish battery plant workers (Erkkilä *et al.*, 1992).

As a gauge of long-term body burden, elevated bone lead readings are a cause for some concern. It will be of considerable interest to see if a similar non-linear relation is evident in future bone lead-CBLI results. Regardless of the mechanism, it remains significant that as a consequence of changing exposure conditions, individuals who have been working for the longest periods of time have also experienced an accelerated accumulation of lead body burden.

Chapter 3

The δ-Aminolevulinate Dehydratase Polymorphism

3.1 Introduction

δ-aminolevulinate dehydratase (ALAD, also known as porphobilinogen synthase, EC 4.2.1.24) is the second enzyme in the heme biosynthetic pathway. ALAD catalyzes the condensation of two molecules of 5-aminolevulinate (ALA) to form porphobilinogen (Figure 3.1). Porphobilinogen is a precursor of heme, cytochromes and other hemoproteins. ALAD is expressed in all tissues, but occurs at elevated levels in the liver, and in the highest levels in erythrocytes and their precursors.

Inhibition of erythrocyte ALAD through replacement of zinc by lead is one of the most sensitive diagnostic indicators of blood lead accumulation and a useful measure of recent lead exposure (Jaffe *et al.*, 1991). Because of its disruptive effect on heme synthesis, high exposure to lead can contribute to anaemia (Schwartz *et al.*, 1990). In addition, the resultant accumulation of ALA in itself appears to contribute to adverse effects of lead on the body (Cutler *et al.*, 1985; Solliway *et al.*, 1994). Human ALAD has been shown

Figure 3.1

Heme biosynthesis pathway. A common polymorphism exists for the δ-aminolevulinate dehydratase (ALAD) enzyme.

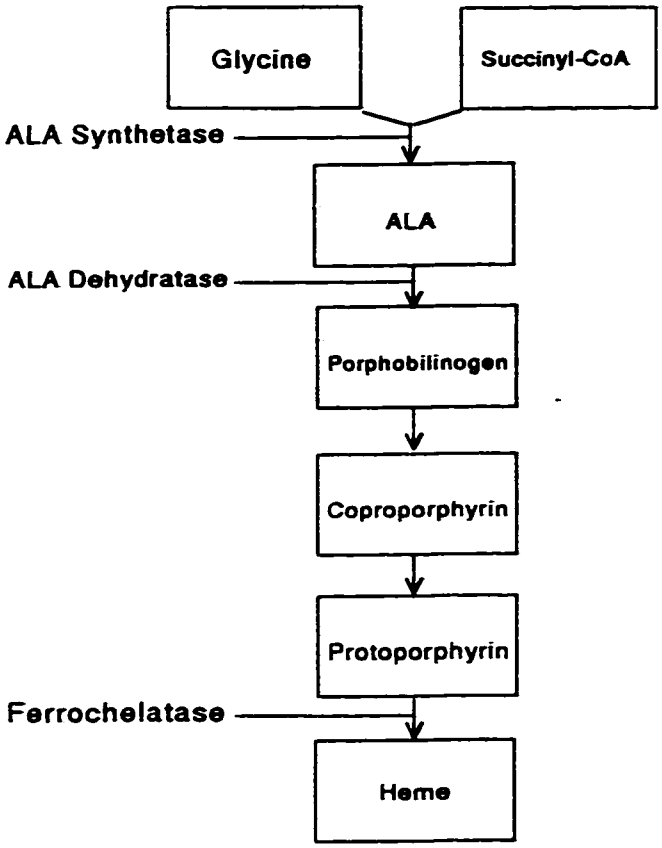

to be a polymorphic enzyme (Battistuzzi *et al.*, 1981), with two alleles, (ALAD1 and ALAD2) responsible for three distinct charge isozyme phenotypes: ALAD 1-1, ALAD 1-2, and ALAD 2-2. A single base substitution in the $ALAD^2$ allele allowed development of the now standard ALAD genotyping system (Wetmur *et al.*, 1991a). Essentially, the addition of a "restriction enzyme" (an enzyme that cuts DNA into small segments) produces DNA fragments of a characteristic length which may be used to classify individuals for ALAD genotype.

A previous study involving 202 lead industry workers from a German factory (Ziemsen *et al.*, 1986) allowed an association to be drawn between average blood lead level and ALAD genotype, where individuals of phenotype 1-2 or the rarer 2-2 were grouped together for comparison with those homozygous for the ALAD1 allele (Wetmur *et al.*, 1991b). The mean blood leads for these workers were 38.4 (SEM 1.3) μg/dl and 47.0 (SEM 2.8) μg/dl for workers homozygous for the ALAD1 allele and workers with the ALAD2 allele, respectively. Similarly, in an investigation involving 1278 New York City schoolchildren screened for elevated environmental lead exposure by free erythrocyte protoporphyrin level, the mean blood leads were 19.5 (SEM 0.3) μg/dl and 27.1 (SEM 2.8) μg/dl for children homozygous for the ALAD1 allele and children with the ALAD2 allele, respectively.

On the other hand, a small study involving three lead

smelters in Korea with a total of 21 individuals with the ALAD2 allele found no difference in blood lead levels, but the frequency of the ALAD2 allele was higher among workers with high blood lead concentrations (Schwartz *et al.*, 1995). More recently, blood lead values and ALAD genotypes for 691 construction trade union members were determined and compared (Smith *et al.*, 1995). These workers, having received only modest exposures to lead, did not show any significant variation in blood lead between the two genetic subgroups. A suggestion of differential lead metabolism was nonetheless apparent from a review of kidney function indices and from a comparison of lead readings at two bone sites. Thus these studies, and particularly those of the two larger lead-exposed populations, suggest that lead metabolism is at least partially dependent on the ALAD polymorphism.

An investigation into the possible influence of the ALAD polymorphism on blood lead level and lead body burden would be particularly instructive for the large Brunswick population. Blood samples of Brunswick workers were stored for this purpose and classified for ALAD genotype by the lab of Drs. James Wetmur and Robert Desnick of the Departments of Human Genetics and Microbiology at the Mount Sinai School of Medicine in New York City.

3.2 Methods

3.2.1 ALAD genotyping

The ALAD genotyping procedure employs a polymerase chain reaction (PCR) assay within whole blood. Briefly, the PCR technique produces a number of copies of a particular portion of an organism's deoxyribonucleic acid (DNA) sequence. In this case, the region of interest is localized to a single gene, flanked by a known sequence of nucleotides (consisting of adenine, guanine, thymine, and cytosine). Appropriate flanking sequences, or primers, are added, which combine with denatured strands of DNA and facilitate the replication process. Specifically, nested primers are used, first with 5'-CACCAGCCTCCCAGGAGTGG-3' and 5'-GGCAAAGACCACGTCCATTC-3' to give a 1 kb (1 x 10^3 base pairs) product and then 5'-GGAGAGAT-TCCACAGGTG-3' and 5'-GTCAGTGTGGACCCTCAG-3' to give a 0.9 kb product for subsequent analysis. A DNA polymerase (*Taq* polymerase) extends the sequence by synthesizing the remaining series of nucleotides. The complete process doubles the number of DNA sequences available, and may be repeated as many times as deemed necessary.

The two ALAD alleles may then be differentiated by the addition of a restriction enzyme (*Msp*I endonuclease) which produces DNA fragments of a characteristic length. Under an

electric field, fragments of different length will migrate different distances. This is the basis of agarose gel electrophoresis. Following fragment separation by electrophoresis, the gel is immersed in ethidium bromide. Under ultraviolet light, the DNA fragments will then fluoresce, revealing band patterns characteristic of an individual homozygous for the $ALAD^1$ allele, heterozygous for the $ALAD^1$ and $ALAD^2$ alleles, or homozygous for the $ALAD^2$ allele (Figure 3.2).

3.2.2 Blood lead

As described in Chapter 2, blood samples were drawn in accordance with Brunswick smelter lead monitoring procedures. This enabled the isolation of blood lead values for individual workers at the approximate time of their bone lead measurement (May-June 1994), and at the time of their return from an extended labour disruption (May 1991).

3.2.3 Serum lead

Serum lead quantification was performed by Drs. Robert Bowins and Robert McNutt of the Department of Geology, McMaster University. The method used relies on sample volatization, followed by introduction to an inductively coupled mass spectrometer (Bowins and McNutt, 1994). The original serum sample is spiked with a known amount of ^{204}Pb

Figure 3.2

Ethidium bromide staining reveals DNA from ALAD 1-1 (lane 3; 582 bp), ALAD 1-2 (lane 4; 582 bp and 511 bp), and ALAD 2-2 (lane 5; 511 bp) individuals (from Wetmur *et al.*, 1991a).

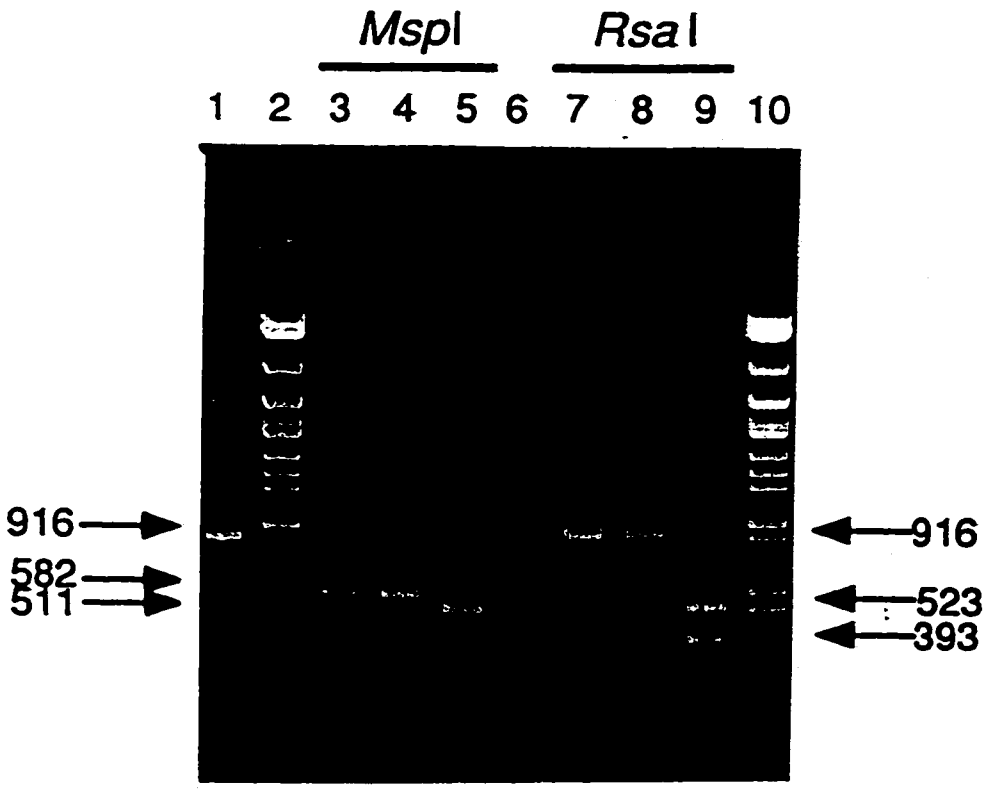

(the least abundant of the four isotopes in common lead). Following acidification, samples are subjected to heating by a graphite furnace. Contact with a highly ionized gas ensues, after which the various isotopes of the sample ions are separated by their different mass:charge ratios via standard mass spectrometry techniques. The ^{204}Pb result is then used as a relative standard against which total lead content may be calculated. At a serum lead concentration of 0.3 μg/l (lower than that typically observed in the Brunswick population), the procedure yields a coefficient of variation of ±20% (Cake *et al.*, 1996).

3.2.4 Bone lead

Bone lead concentration was measured at the tibia and calcaneus sites via X-ray fluorescence, as detailed in Chapters 1 and 2. The influence of ALAD genotype on lead accumulation at these two sites was examined. Analysis of the Brunswick smelter bone lead data indicated that the ratio of calcaneus to tibia lead concentrations was similar to that observed in other lead industry populations. This relation was reviewed in light of the genotyping information. The possibility of a genetic difference in the division of lead between cortical and trabecular bone was further examined by subtracting tibia lead results from those of calcaneus lead (Smith *et al.*, 1995).

3.2.5 Endogenous exposure

An investigation of blood lead levels from smelter employees who have been removed from the working environment will provide insight into the release of lead from bone. As discussed in Chapter 2, 204 Brunswick workers returning from a ten-month strike had blood lead measurements performed. The group of 14 former Brunswick workers, retired from the site for at least six months, were included with this larger data set for the purpose of analyzing the influence of ALAD genotype on endogenous lead exposure. Bone lead concentrations were compared with either blood lead level following the strike (returning workers), or with blood lead level in 1994 (retired), depending on the employment status of the individual.

3.2.6 Revised CBLI

The CBLI of a lead worker, as an approximation of cumulative exposure, is generally an excellent predictor of bone lead. The exact relation between these two indices, however, appears to be influenced by exposure condition (Chapter 2). The possibility that the ALAD polymorphism might introduce a genetic consideration concerning lead uptake from blood to tissue was examined in the Brunswick population. Bone lead concentration was again used as a marker of body burden. Time of hiring was also considered. The more

moderate exposure conditions experienced by workers hired during the last twenty years (generally resulting in blood lead concentrations of 25-50 μg/dl) are characteristic of contemporary lead industry populations. Although retired workers were isolated as displaying bone lead-CBLI slopes which were somewhat distinct from active workers as a whole, their results were very similar to the pool of active workers hired early in the history of the smelter. For this reason, retired workers were included in the overall analysis.

3.3 Results

3.3.1 ALAD genotypes

Of the 382 lead smelter employees tested for ALAD genotype, 312 were ALAD1-1, 67 were ALAD1-2 and three were ALAD2-2. The ALAD2 allele frequency was thus 0.096, quite consistent with that found to prevail among other Caucasian populations (Battistuzzi *et al.*, 1981; Petrucci *et al.*, 1982; Benkmann *et al.*, 1983). Due to the scarcity of individuals homozygous for the ALAD2 allele, this population was divided into two genetic subgroups for subsequent analyses, one subgroup of employees homozygous for the ALAD1 allele (ALAD 1-1), and the other subgroup expressing one or two ALAD2 alleles (ALAD 1-2/2-2).

Because mean blood lead levels of the lead smelter workers were constant until 1977 and have fallen continuously since that date due to introduction of new safety initiatives, the same population of 382 workers was divided into two hiring subgroups. Of the subgroup of 223 who were hired prior to 1977, 43 expressed an ALAD2 allele, including the three ALAD2-2 workers. The ALAD2 allele frequency was 0.103. Of the subgroup of 159 smelter employees hired since 1977, 27 expressed an ALAD2 allele. The ALAD2 allele frequency was 0.085.

3.3.2 Blood lead

The average blood lead of the 303 ALAD 1-1 active workers was 22.85±0.43 μg/dl while that of the 65 ALAD 1-2/2-2 active workers was 25.18±1.04 μg/dl. The difference of means, 2.3 μg/dl or 10%, was of statistical significance with $p<0.04$. Furthermore, the corresponding median blood lead levels were 23 and 27, differing by 4 μg/dl or 17%. While these differences are not as substantial as those observed with the cohorts of German lead workers or New York schoolchildren (Wetmur *et al.*, 1991b), higher blood lead levels for ALAD 1-2/2-2 individuals are confirmed.

Moreover, a review of blood lead records from the Brunswick smelter revealed that this was not an isolated finding; workers in the ALAD 1-2/2-2 subgroup consistently

exhibited higher lead levels since the initial years of plant operation. In Figure 3.3, the average blood leads of Brunswick workers over various six-month intervals are displayed. These data are subdivided by ALAD genotype. It is clear that workers displaying at least one ALAD2 allele tended to record higher blood leads. The magnitude of the difference between the ALAD subgroups was fairly constant over time. On average, the smelter records indicated that the elevation was 1.6 μg/dl, or 5.3% above the levels of the 1-1 population, including data from the initial few years of employment when the differences in blood lead levels appeared to be less pronounced. The difference of means over the six-month intervals was significant with $p < 0.0001$. Notably, the ALAD 1-2/2-2 subgroup mean blood lead was the higher of the two subgroups for each and every six-month interval over the last ten years. The difference of means over this time was highly significant with $p < 0.000001$.

3.3.3 Serum lead

The serum lead measurements provided additional insight into the lead kinetics for workers with different ALAD genotypes. Figure 3.4 depicts a cumulative distribution of serum lead levels subdivided by ALAD genotype. The average serum lead concentration for the 302 active smelter employees in the ALAD 1-1 subgroup was 2.848±0.086 μg/l. The mean serum lead level of the 65 active workers in the ALAD 1-2/2-2

Figure 3.3

Mean blood lead of smelter workers as a function of time and ALAD genotype.

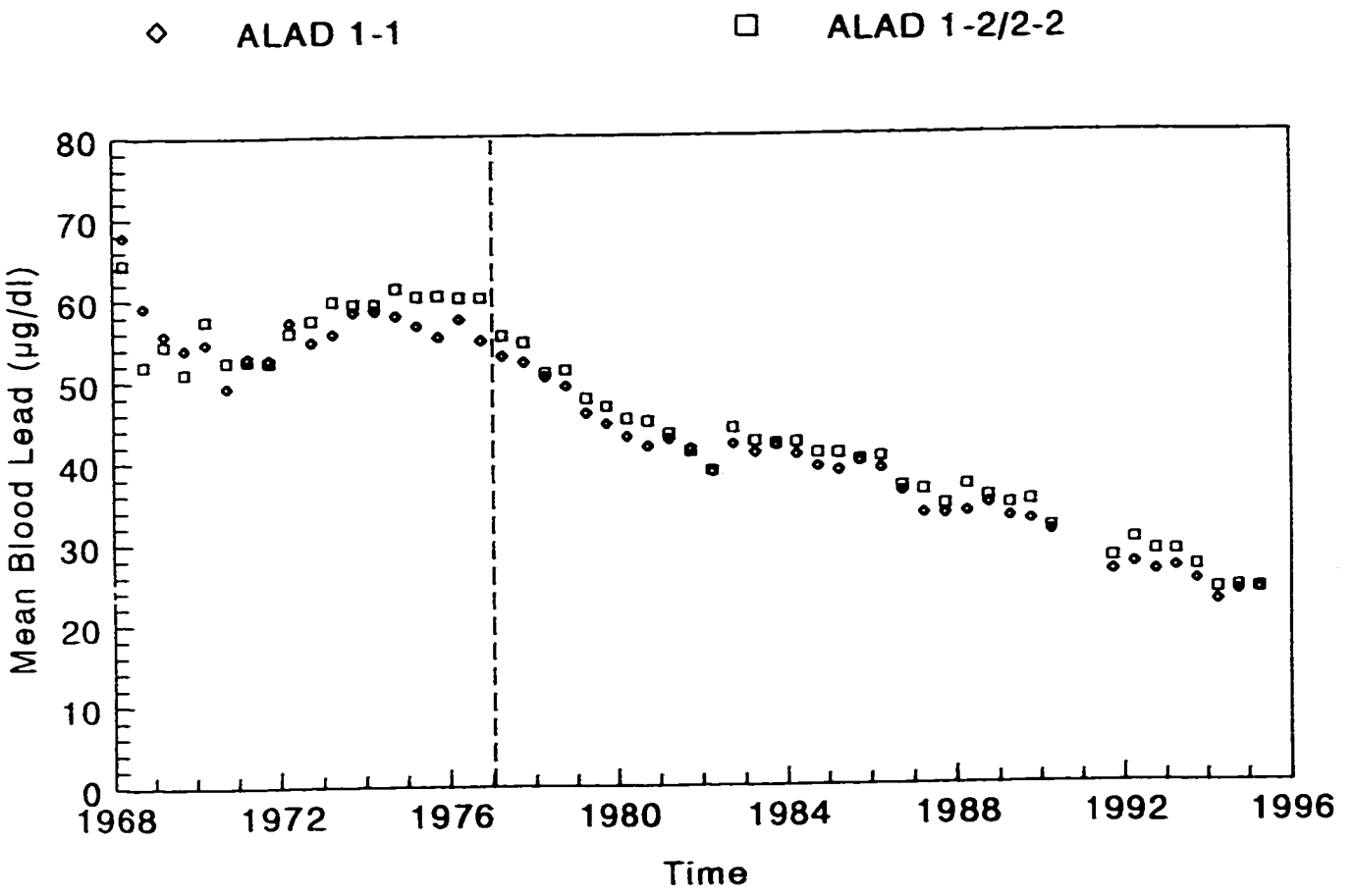

Figure 3.4

Serum lead concentration as a function of cumulative percent of sample for smelter workers. Note the general elevation for workers of genotype 1-2/2-2.

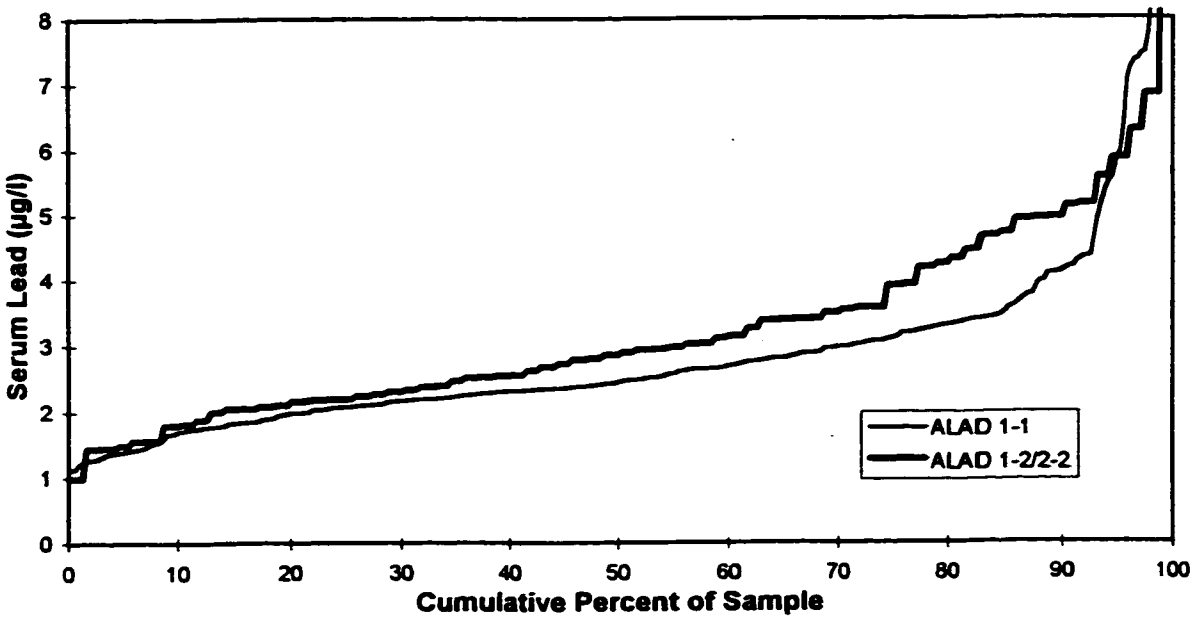

subgroup was 3.350±0.253 μg/l. The difference of means, 0.5 μg/l or 18%, was of borderline statistical significance with $p<0.06$. The corresponding median serum lead levels were 2.44 and 2.89 μg/l, differing by 0.45 μg/l or 19%. Thus the elevated mean and median serum lead levels affirmed the elevated mean and median blood lead levels for workers in the ALAD 1-2/2-2 subgroup.

3.3.4 Bone lead

Bone lead concentrations did not, however, appear to be associated with ALAD genotype. Mean tibia lead levels were 41.19±1.76 μg/g and 42.66±3.37 μg/g for the ALAD 1-1 and ALAD 1-2/2-2 subgroups, respectively. The average calcaneus lead concentration for ALAD 1-1 workers was 71.57±3.38 μg/g, while individuals in the ALAD 1-2/2-2 subgroup displayed a mean of 72.32±6.15 μg/g. Similarly, the differences between calcaneus and tibia lead, 30.38±1.93 versus 29.66±3.75 μg/g, and the differences after weighting for the 1.7-fold higher magnitude of the calcaneus lead values, 1.54±1.42 and -0.20±3.30 μg/g, were not associated with ALAD genotype. The distribution of lead between tibia and calcaneus did not therefore appear to be strongly associated with ALAD genotype.

As a further illustration, plots of calcaneus lead (C) relative to tibia lead (T) for the two ALAD subgroups are displayed in Figures 3.5a and 3.5b. Linear regressions were

Figure 3.5

Calcaneus lead concentration as a function of tibia lead.

(a) Workers of genotype 1-1;

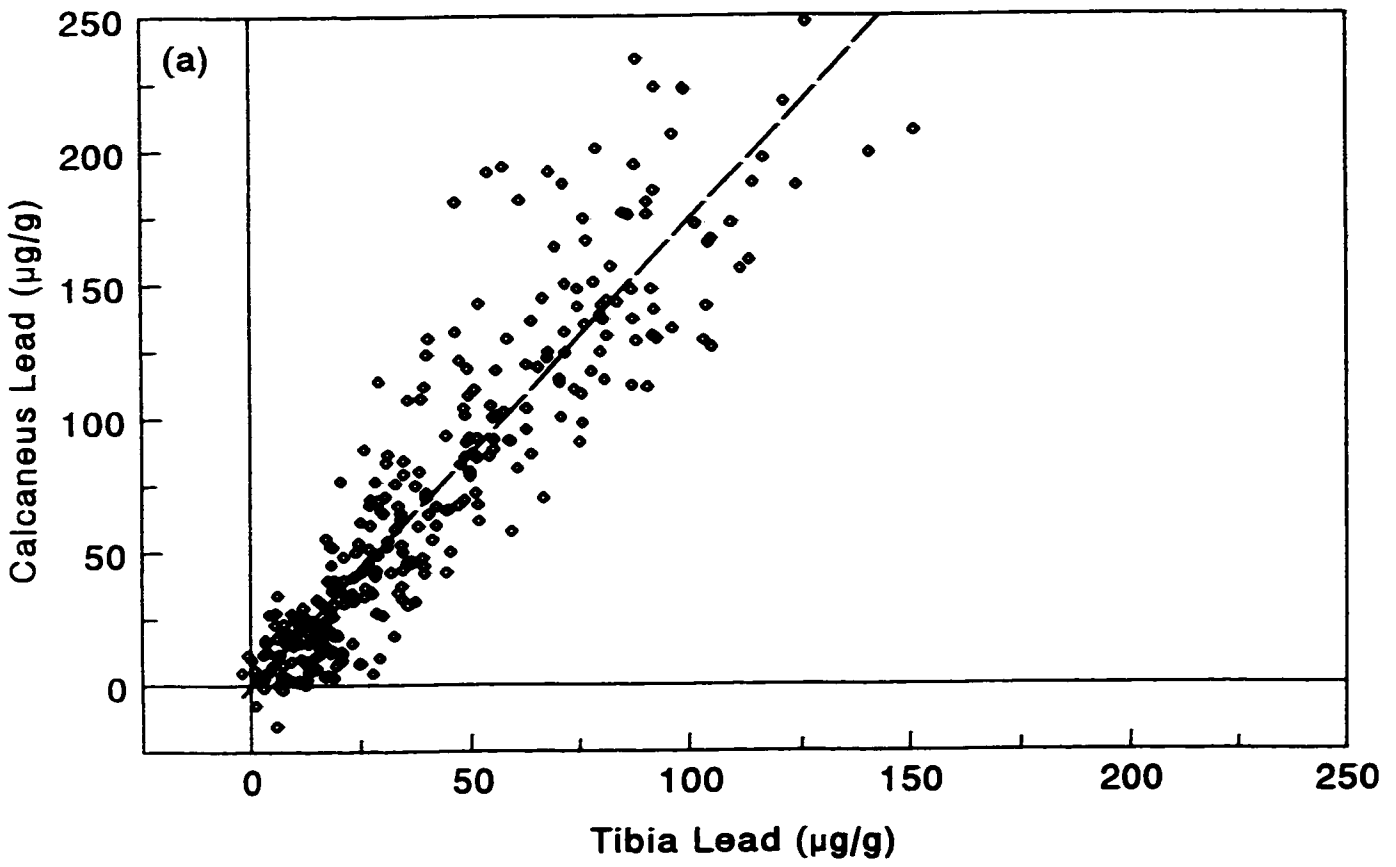

Figure 3.5

Calcaneus lead concentration as a function of tibia lead.

(b) Workers of genotype 1-2/2-2.

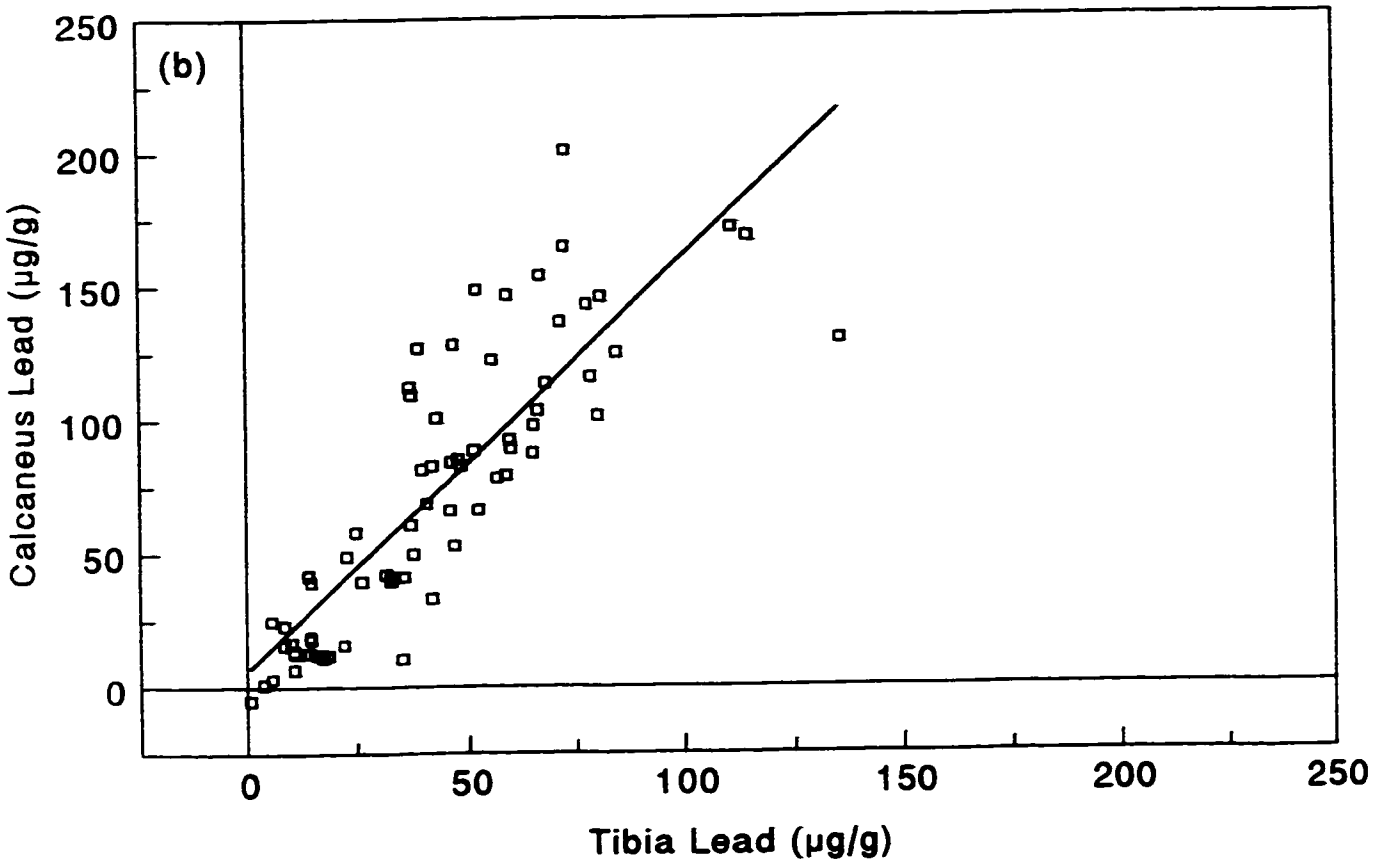

applied to the data, treating tibia lead concentration as the independent variable. The equation of best fit for ALAD 1-1 subgroup smelter workers was

$$C=(1.75\pm0.05)T-(0.4\pm2.4)\ [N=312;r^2=0.83];$$

while that for ALAD 1-2/2-2 subgroup workers was

$$C=(1.55\pm0.12)T+(6.3\pm6.0)\ [N=70;r^2=0.72].$$

When the intercepts were set equal to zero, the slopes were 1.74 ± 0.03 ($r^2=0.83$) and 1.65 ± 0.06 ($r^2=0.71$) for the ALAD 1-1 and ALAD 1-2/2-2 subgroups, respectively. Although there was a slight suggestion of a variation in slopes between the two subgroups, the difference was not of statistical significance ($p < 0.18$).

3.3.5 Endogenous exposure

Blood lead measurements taken after prolonged removal from lead exposure should reflect endogenous exposure due to release of lead from tissue lead stores, especially from bone. Blood lead levels (BPb), taken either after an extended strike at the smelter or following worker retirement, were compared with tibia lead concentration (T) for the two ALAD subgroups (Figure 3.6a). The best fit equation for the linear regression of BPb versus T for workers in the ALAD 1-1 subgroup yielded the following relation:

Figure 3.6

Blood lead level as function of bone lead concentration following removal from workplace.

(a) Blood lead as a function of tibia lead, workers subdivided by genotype;

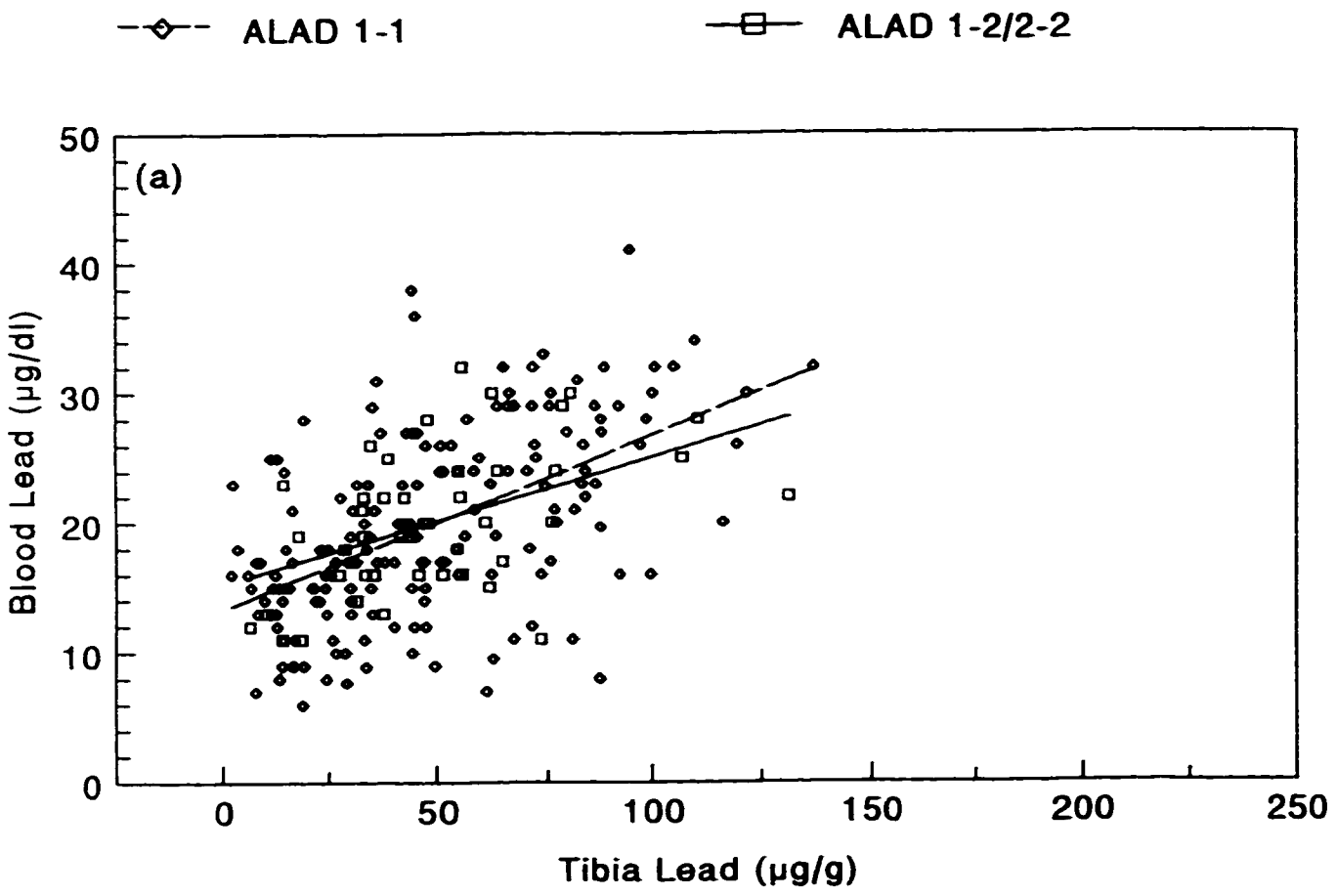

Figure 3.6

Blood lead level as function of bone lead concentration following removal from workplace.

(b) Blood lead as a function of calcaneus lead, workers subdivided by ALAD genotype.

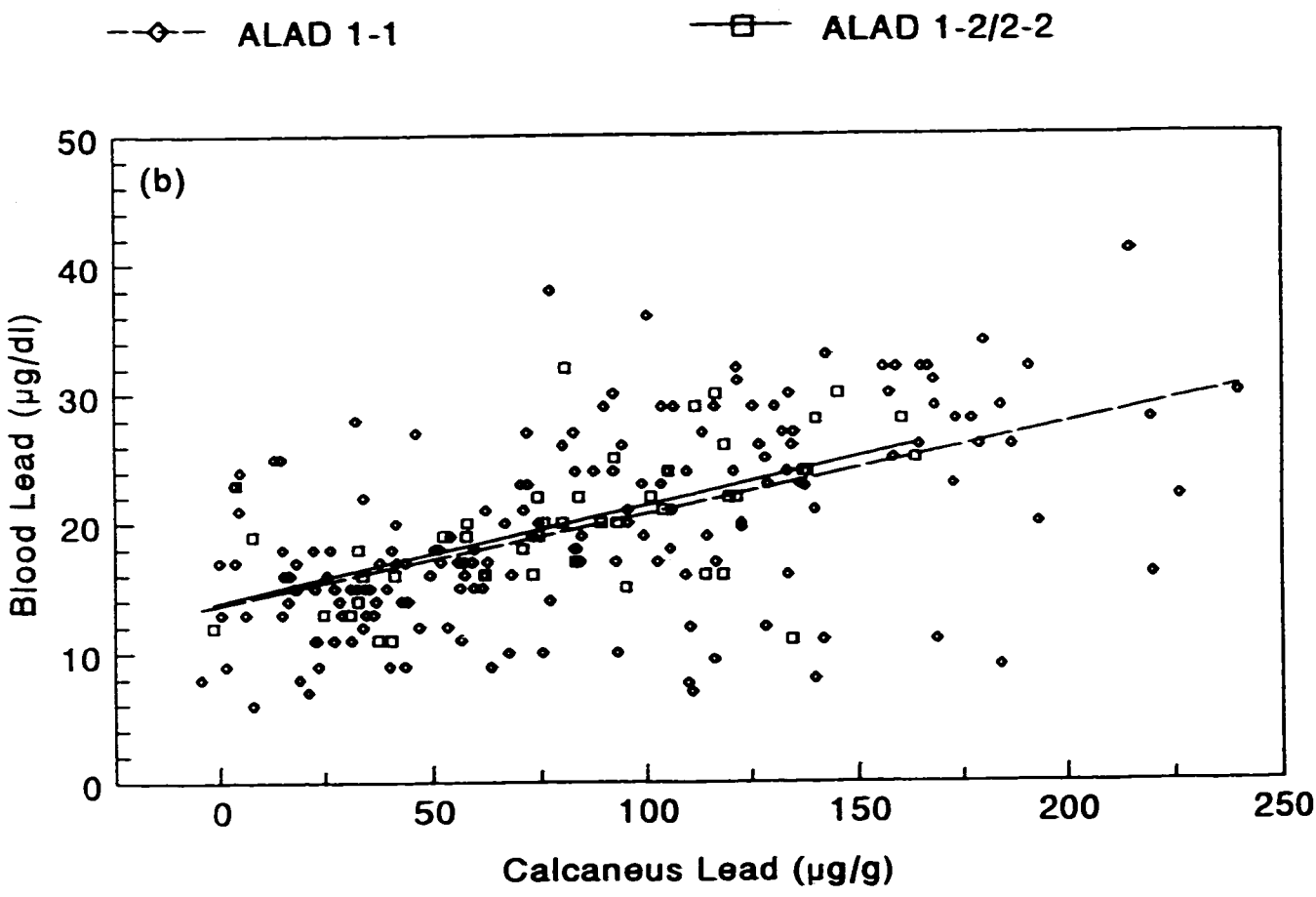

$$BPb=(0.136\pm0.016)T+(13.2\pm0.9)\ [N=173;r^2=0.30];$$

while for the workers in the ALAD 1-2/2-2 subgroup, the relation was

$$BPb=(0.0986\pm0.0281)T+(15.2\pm1.6)\ [N=45;r^2=0.22].$$

Similar comparisons of blood lead (BPb) against calcaneus lead (C) are displayed in Figures 3.6b. The best fit equation for BPb versus C for workers in the ALAD 1-1 subgroup was determined to be

$$BPb=(0.0701\pm0.0082)C+(13.7\pm0.8)\ [N=173;r^2=0.30];$$

and for the workers in the ALAD 1-2/2-2 subgroup,

$$BPb=(0.0744\pm0.0159)C+(13.9\pm1.5)\ [N=45;r^2=0.34].$$

For the two ALAD subgroups, then, neither the blood lead-calcaneus lead nor the blood lead-tibia lead relation showed any difference approaching significance.

3.3.6 Revised CBLI

Blood lead measurements taken during employment were used to calculate the revised cumulative blood lead index (CBLI). Because the historic blood leads were higher for the ALAD 1-2/2-2 subgroup, the revised CBLI was also elevated. The cumulative distribution of revised CBLI for the ALAD subgroups is depicted in Figure 3.7.

Figure 3.7

Revised cumulative blood lead index (CBLI) as a function of cumulative percent of sample for smelter workers. Note the elevation in CBLI for workers of genotype 1-2/2-2.

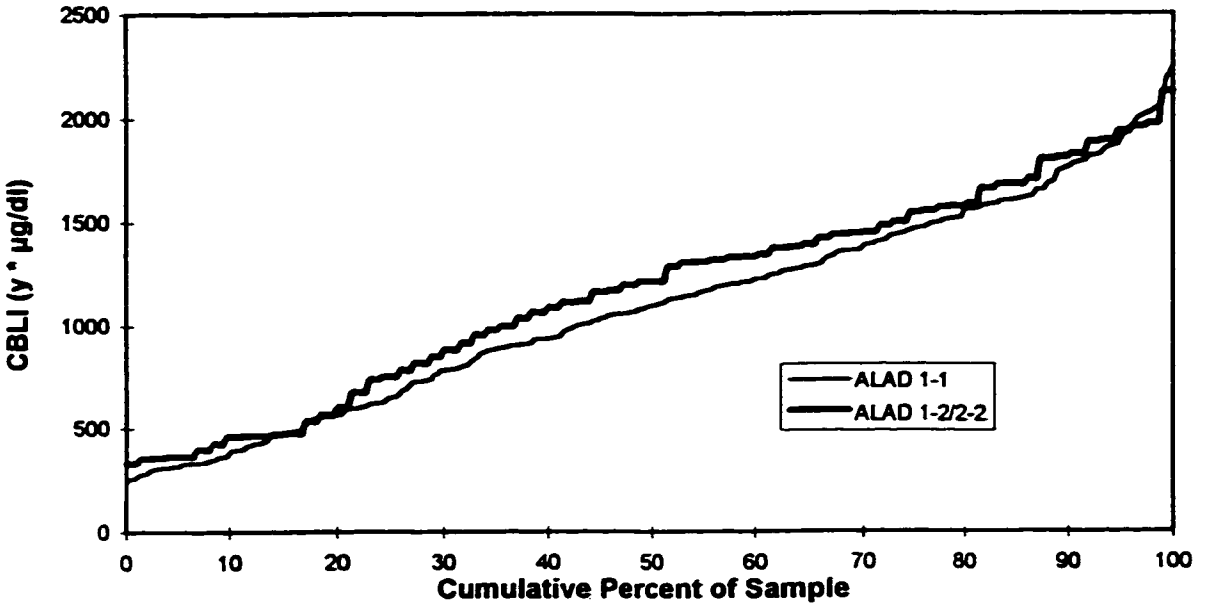

With the tibia as the bone site of inspection and the revised CBLI as the independent variable (Figure 3.8a), the best fit equation for workers of the ALAD 1-1 subgroup was

$$T=(0.0513\pm0.0020)\,CBLI-(14.3\pm2.4)\;[N=311;r^2=0.67].$$

For workers of the ALAD 1-2/2-2 subgroup (Figure 3.8a), the variables yielded the following result:

$$T=(0.0427\pm0.0045)\,CBLI-(6.9\pm5.7)\;[N=70;r^2=0.57].$$

The linear regression of the calcaneus lead-CBLI data for the ALAD 1-1 subgroup (Figure 3.8b) was

$$C=(0.103\pm0.004)\,CBLI-(40.0\pm4.2)\;[N=311;r^2=0.73].$$

Workers in the ALAD 1-2/2-2 subgroup (Figure 3.8b) displayed a best fit linear relation of

$$C=(0.0909\pm0.0060)\,CBLI-(33.1\pm7.6)\;[N=70;r^2=0.77].$$

The y-intercepts for the two ALAD subgroups were indistinguishable within uncertainty limits. There were borderline indications of difference in slope ($p < 0.09$ for tibia; $p < 0.09$ for calcaneus).

Because there exists no reason to suspect an offset between the true intercepts, the linear fit was repeated with a zero-intercept constraint to allow a more direct comparison of slope values. For the tibia lead-CBLI data, the best fit

Figure 3.8

Bone lead concentration as a function of revised CBLI.

(a) Tibia as bone site, workers subdivided by ALAD genotype;

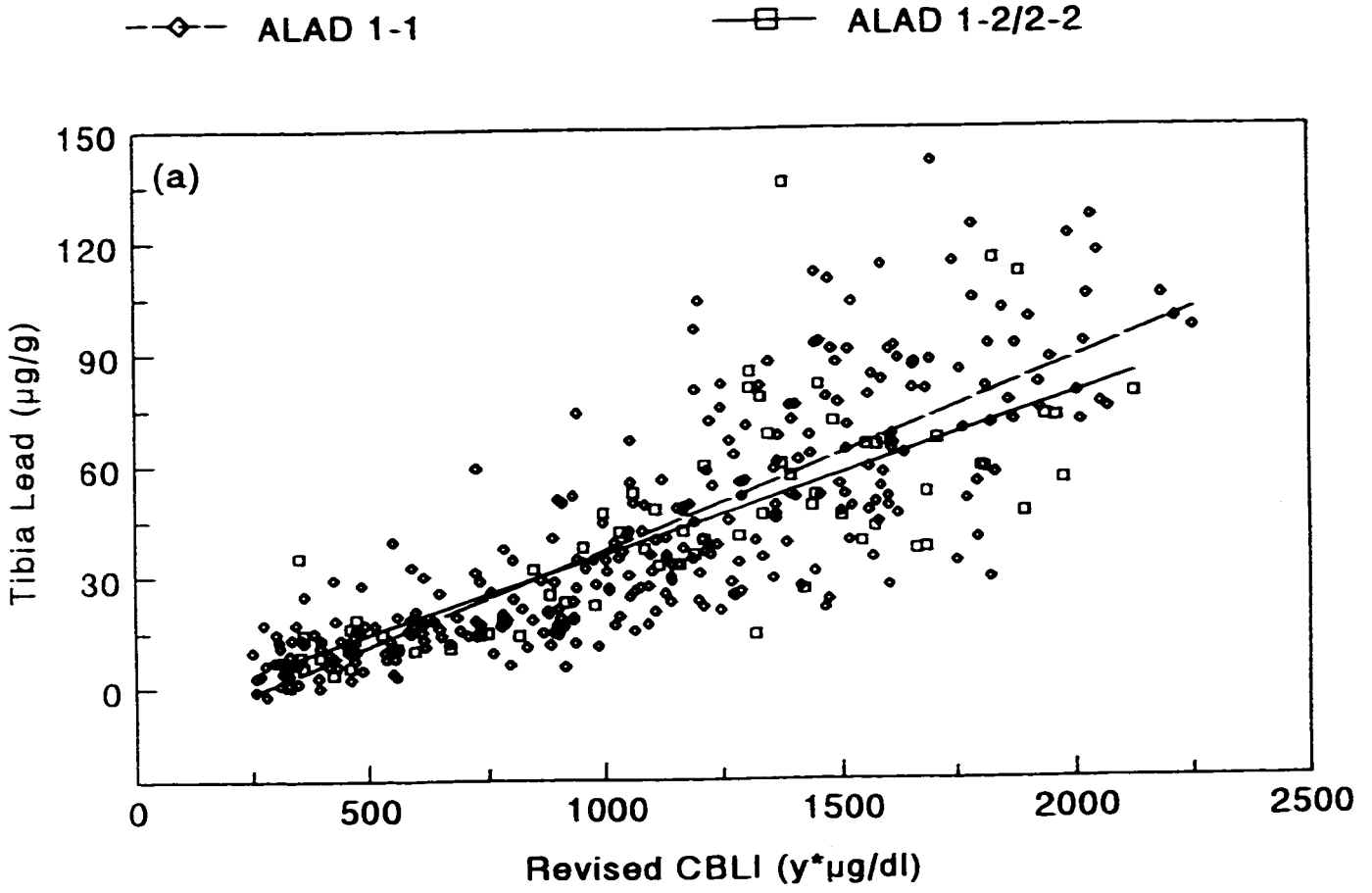

Figure 3.8

Bone lead concentration as a function of revised CBLI. (b) Calcaneus as bone site, workers subdivided by ALAD genotype.

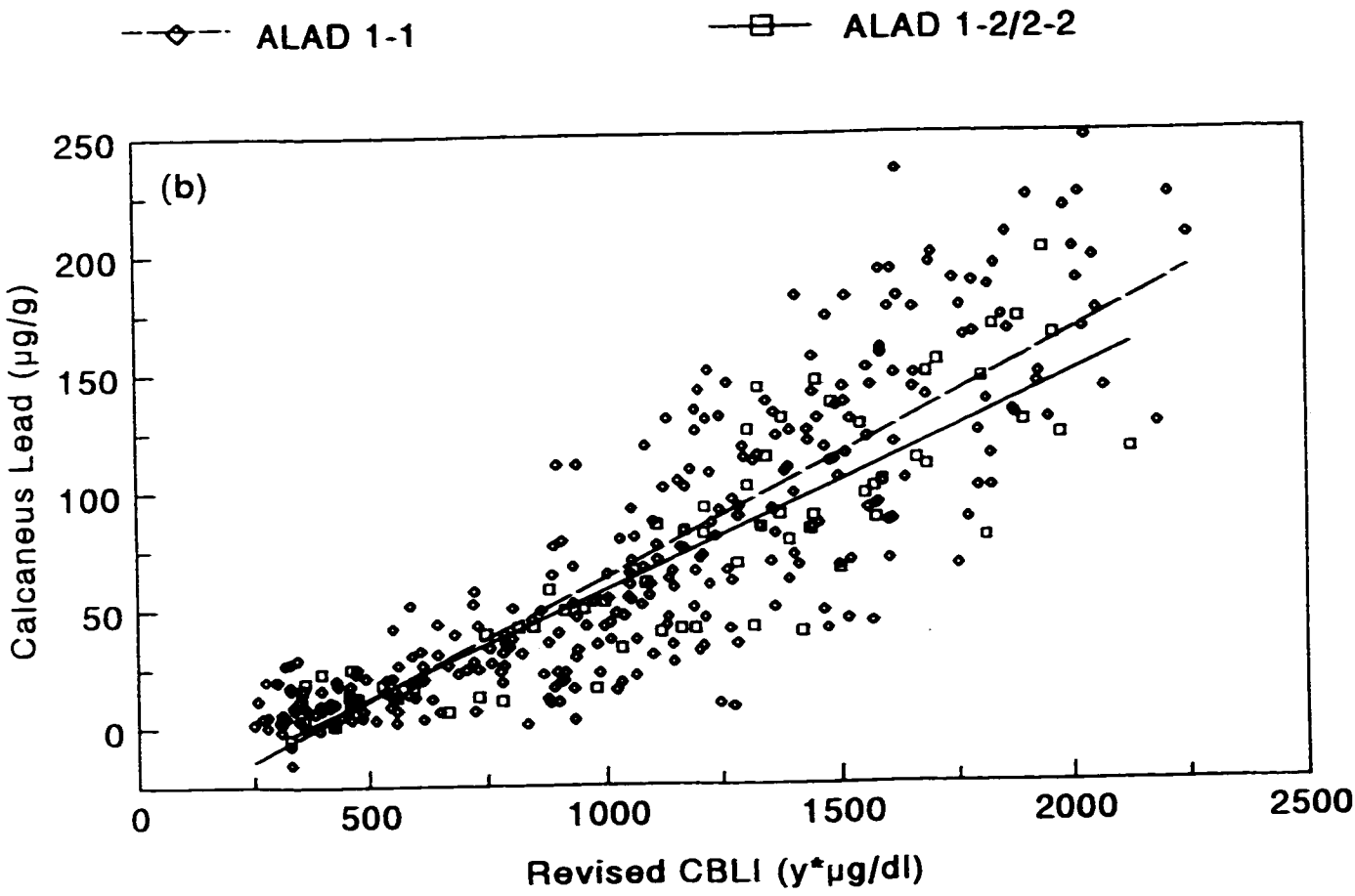

equation for workers of the ALAD 1-1 subgroup yielded a slope of 0.0404±0.0009 (N=311; r^2=0.63). For workers of the ALAD 1-2/2-2 subgroup, the slope was 0.0377±0.0018 (N=70; r^2=0.56). For the calcaneus lead-CBLI data, the best fit equation for workers of the ALAD 1-1 yielded a slope of 0.0726±0.0017 (N=311; r^2=0.66). For workers in the ALAD 1-2/2-2 subgroup, the slope was 0.0667±0.0026 (N=70; r^2=0.71). ALAD 1-1 workers displayed steeper slopes with either tibia lead or calcaneus lead as the dependent variable. The slopes were higher for the ALAD 1-1 subgroup by 7.2% for tibia and 8.9% for calcaneus. The probabilities associated with these differences were $p < 0.18$ for the tibia and $p < 0.07$ for calcaneus.

3.3.7 Division by time of hire

Since the blood lead levels of the smelter workers have decreased consistently since about 1977, workers were divided by time of hire (before or after January 1, 1977) for further analysis. The total worker population was divided into both two ALAD subgroups and two hiring subgroups for a four-way comparison of bone lead-CBLI relations. A summary of the CBLI, tibia lead, and calcaneus lead results for each of the four worker subgroups is provided in Tables 3.1-3.3.

Table 3.1

Summary of revised Cumulative Blood Lead Index (CBLI in y*μg/dl) results for Brunswick workers by ALAD status, time of hiring:

	1-1, <1977	1-2/2-2, <1977	1-1, >1977	1-2/2-2, >1977
N	179	43	132	27
Mean±SEM	1410±25	1481±45	638±25	649±53
Range	486-2251	881-2126	249-1659	330-1319
Median	1393	1446	594	561
20 %ile	1123	1213	345	362
40 %ile	1283	1375	516	471
60 %ile	1480	1545	671	672
80 %ile	1693	1709	890	913

Table 3.2

Summary of tibia lead concentrations (μg/g bone mineral) for Brunswick workers by ALAD status, time of hiring:

	1-1, <1977	1-2/2-2, <1977	1-1, >1977	1-2/2-2, >1977
N	179	43	132	27
Mean±SEM	57.61±2.19	58.82±3.53	19.04±1.38	16.92±2.16
Range	5.64 -151.13	25.01-135.42	-2.08-87.07	0.67-46.85
Median	51.59	55.58	15.22	14.34
20 %ile	29.25	39.70	7.16	8.49
40 %ile	45.27	47.82	13.15	13.33
60 %ile	61.05	59.54	17.57	14.65
80 %ile	83.78	72.31	28.47	22.93

Table 3.3

Summary of calcaneus lead concentrations (μg/g bone mineral) for Brunswick workers by ALAD status, time of hiring:

	1-1, <1977	1-2/2-2, <1977	1-1, >1977	1-2/2-2, >1977
N	179	43	132	27
Mean±SEM	103.09±4.17	103.88±5.99	29.06±2.80	22.06±3.15
Range	1.20-247.84	33.09-200.55	-15.30-192.10	-4.88-52.85
Median	95.84	100.63	19.73	15.93
20 %ile	50.04	68.62	6.94	10.57
40 %ile	83.57	87.24	16.06	12.85
60 %ile	114.34	112.24	23.39	18.00
80 %ile	148.30	136.21	43.86	41.68

For a zero-intercept, linear model, a tendency was observed in the Brunswick population of ALAD 1-2/2-2 workers to produce more shallow bone lead-CBLI relations than their ALAD 1-1 cohorts (Table 3.4). In particular, significant differences in slope were determined with either tibia or calcaneus lead as the dependent variable for the most recently hired workers. Specifically, the slopes for the ALAD 1-1 subgroup exceeded the slopes for the ALAD 1-2/2-2 subgroup by 25% for the tibia and 49% for the calcaneus. These offsets were significant at the $p < 0.04$ level for the tibia and at $p < 0.001$ for the calcaneus. Furthermore, for each of the four analyses in Table 3.4, removal of the zero-intercept constraint would result in the differences in slope becoming *more* significant (Figures 3.9a, 3.9b, 3.10a, 3.10b).

Application of a polynomial function produced slightly stronger fits to the bone lead-CBLI data than a simple linear regression. The linear model conveys a physically obvious meaning, with the slope coefficient representing the proportion of lead transferred from whole blood and retained by bone. Non-linear models do not confer this advantage and linear relations were therefore retained. Furthermore, the difference in fitting between the linear and polynomial models was found to be statistically significant for only the recently hired ALAD 1-1 subgroup of workers. The results of the polynomial fitting for these workers will be detailed

Table 3.4

Comparison of bone lead-CBLI slopes (zero-intercept constraint) between ALAD status of Brunswick workers:

Hiring Date	Bone Site	1-1 Slope	1-2/2-2 Slope	p
< 1977	tibia	0.0419±0.0012 (N=179;r^2=0.42)	0.0393±0.0022 (N=43;r^2=0.12)	< 0.32
< 1977	calcaneus	0.0760±0.0021 (N=179;r^2=0.49)	0.0710±0.0029 (N=43;r^2=0.45)	< 0.17
> 1977	tibia	0.0319±0.0013 (N=132;r^2=0.54)	0.0256±0.0026 (N=27;r^2=0.31)	< 0.04
> 1977	calcaneus	0.0528±0.0028 (N=132;r^2=0.51)	0.0355±0.0031 (N=27;r^2=0.52)	< 0.001

Figure 3.9

Bone lead concentration as a function of revised CBLI for workers hired before 1977.

(a) Tibia as bone site, workers subdivided by ALAD genotype;

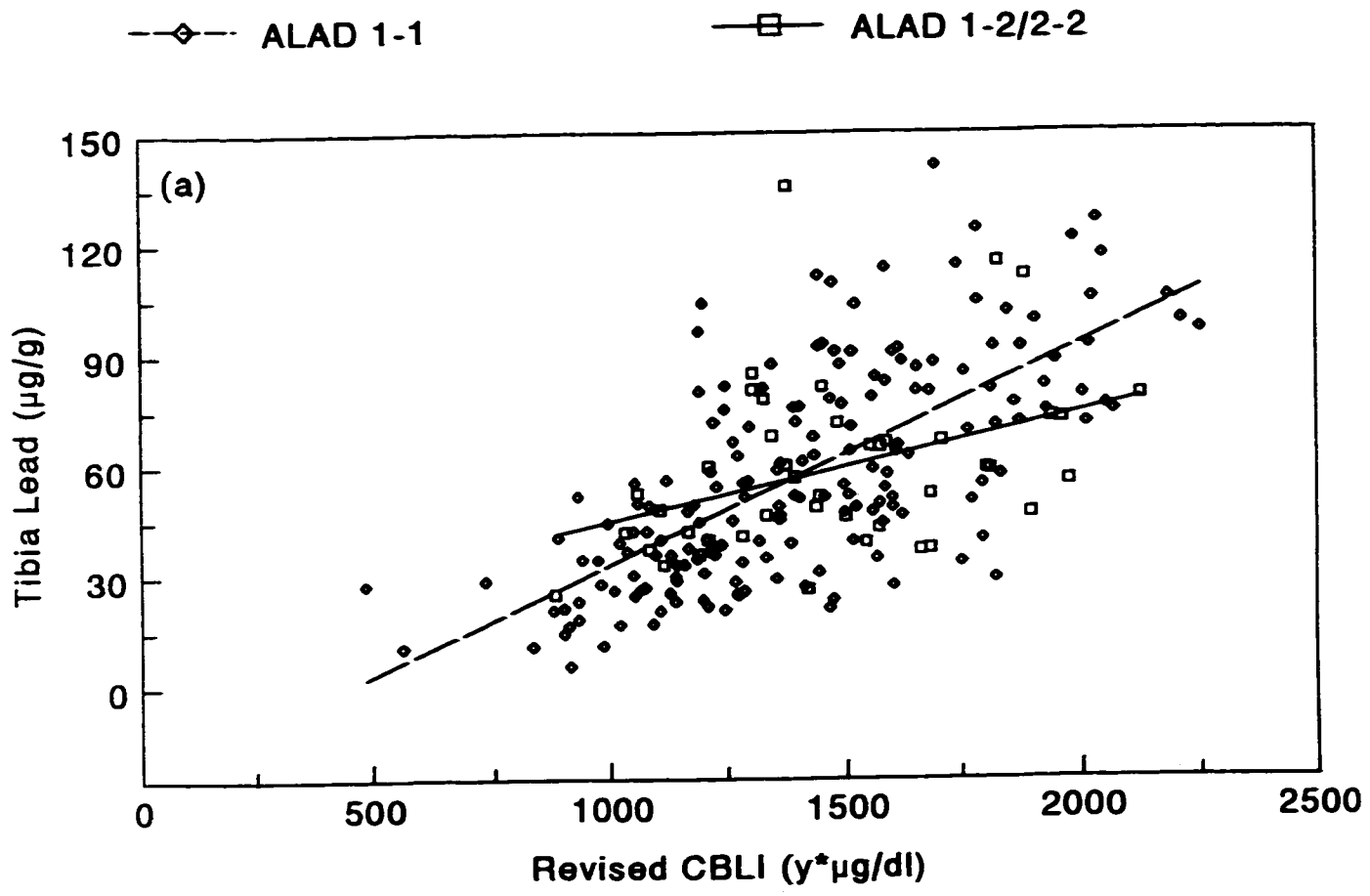

Figure 3.9

Bone lead concentration as a function of revised CBLI for workers hired before 1977.

(b) Calcaneus as bone site, workers subdivided by ALAD genotype.

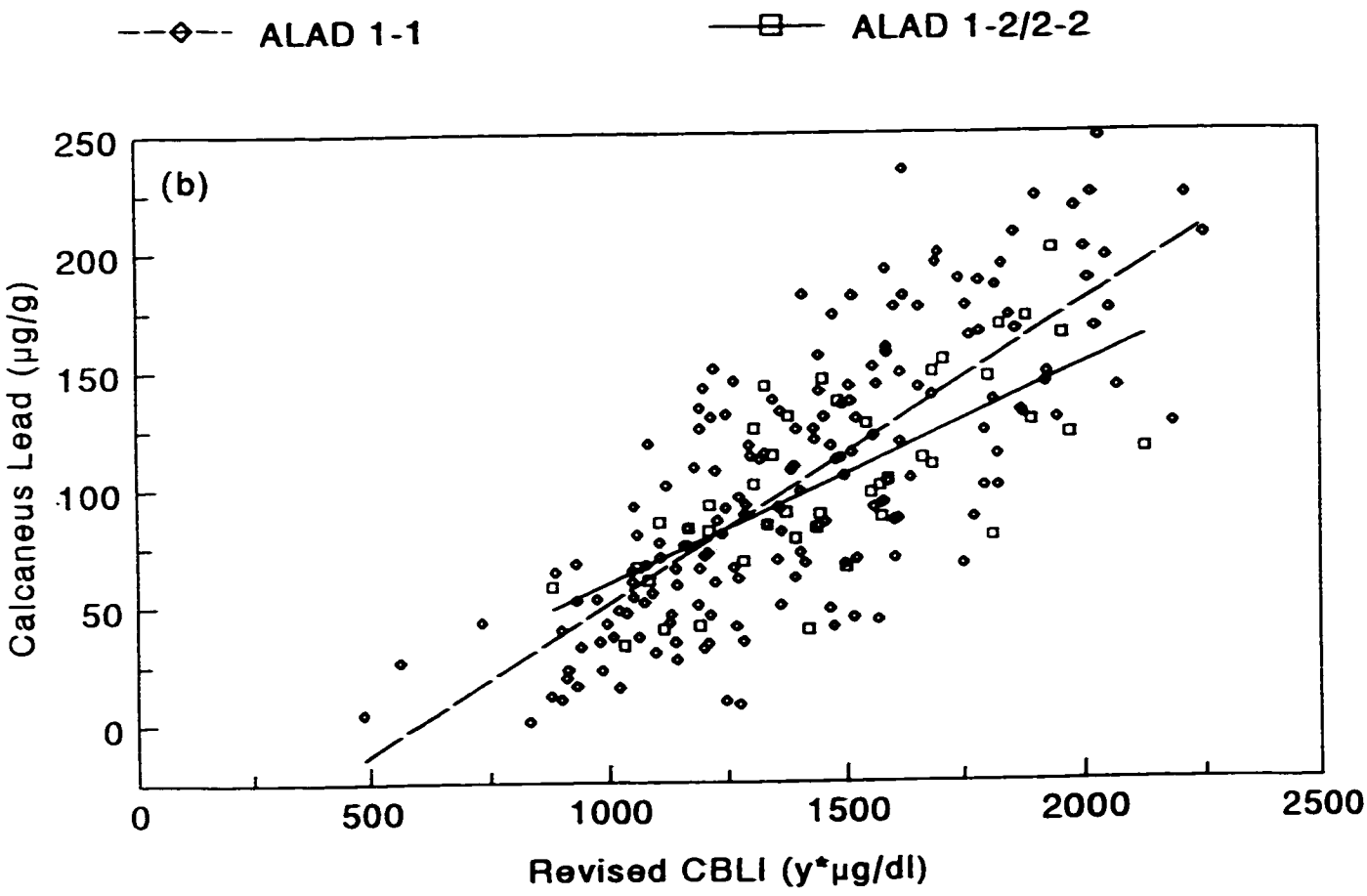

Figure 3.10

Bone lead concentration as a function of revised CBLI for workers hired recently. Linear and polynomial fits are included for workers of ALAD genotype 1-1.

(a) Tibia as bone site, workers subdivided by ALAD genotype;

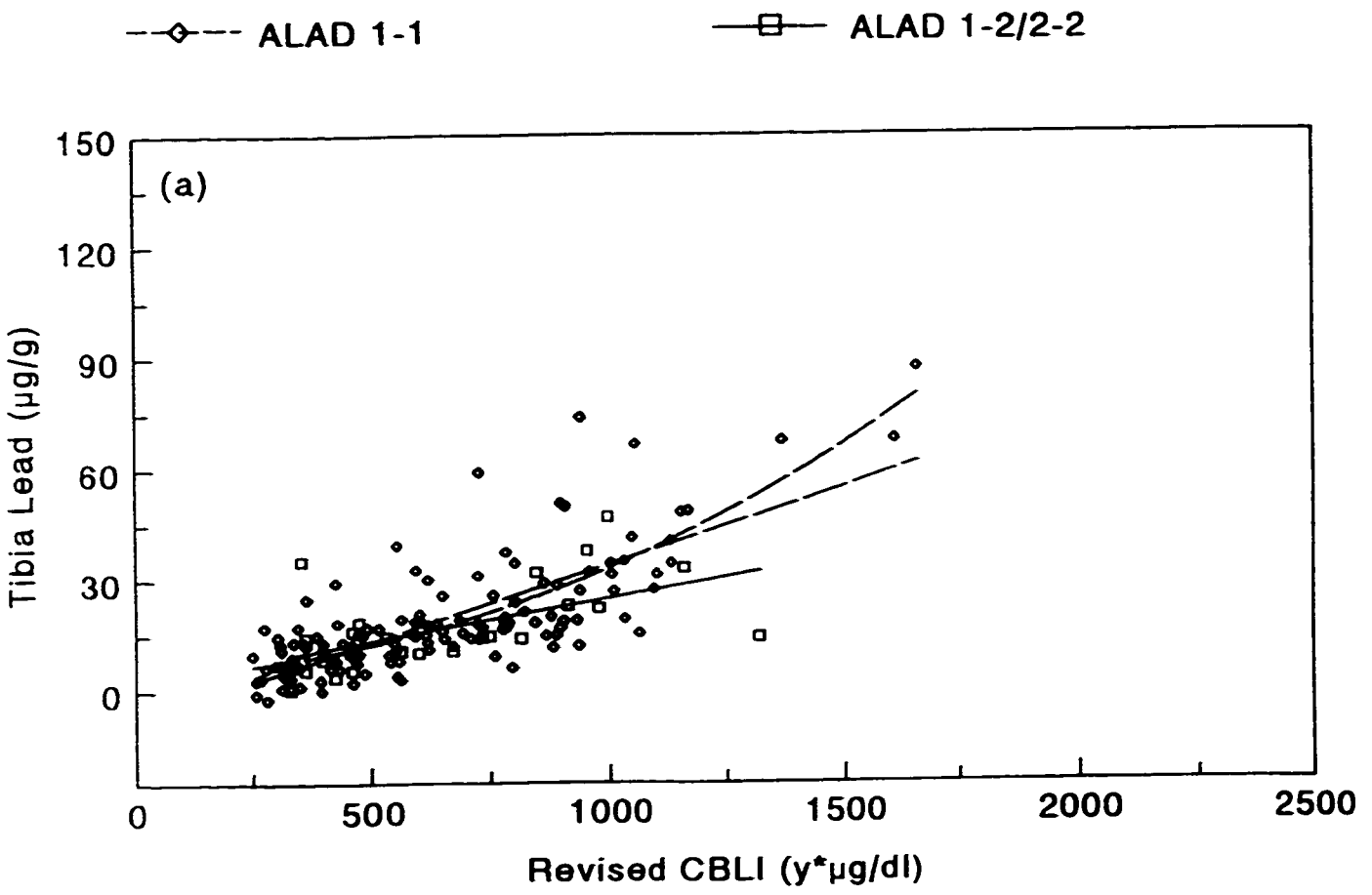

Figure 3.10

Bone lead concentration as a function of revised CBLI for workers hired recently. Linear and polynomial fits are included for workers of ALAD genotype 1-1.

(b) Calcaneus as bone site, workers subdivided by ALAD genotype.

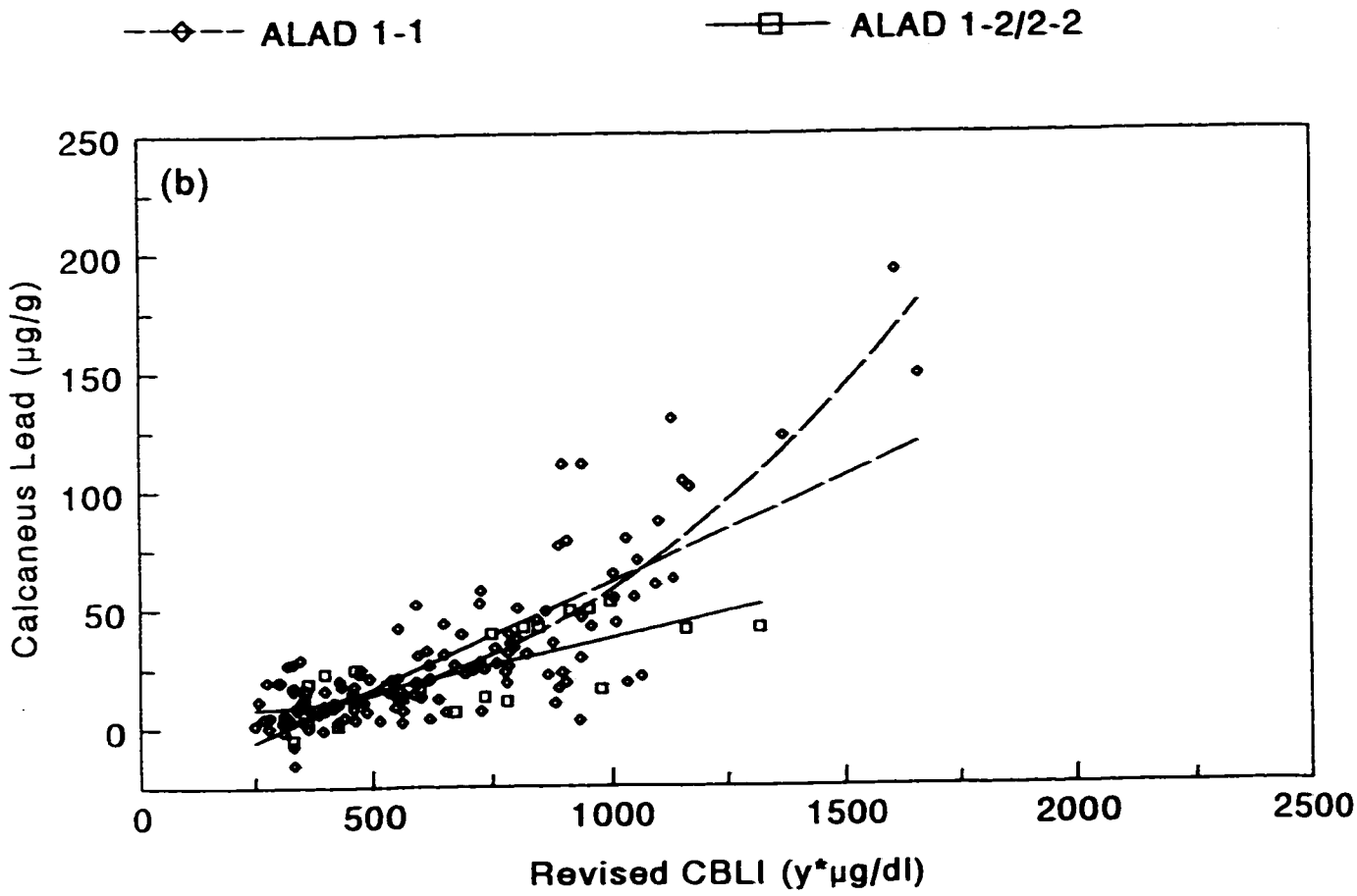

below, and compared with the appropriate linear models.

The best fit linear relation to the tibia lead-CBLI data for recently hired ALAD 1-1 workers had a slope of 0.0419±0.0031 (N=132; r^2=0.58). The associated polynomial equation for this subgroup displayed a linear coefficient of 0.0356±0.0035 and a quadratic coefficient of (2.56±0.75)x10^{-5} (N=132; r^2=0.62). These results compare with the linear fit to the recently hired ALAD 1-2/2-2 workers, which produced a slope of 0.0229±0.0068 (N=32; r^2=0.31). Notably, despite a significant positive quadratic term, the linear coefficient of the ALAD 1-1 polynomial expression remains greater than the slope of the ALAD 1-2/2-2 expression. All three equations of fit are displayed in Figure 3.10a.

Similarly, the linear equation of best fit for the calcaneus lead-CBLI data of recently hired ALAD 1-1 workers had a slope of 0.0888±0.0059 (N=132; r^2=0.63). The associated polynomial equation had a linear coefficient of 0.0683±0.0060 and a quadratic coefficient of (8.37±1.29)x10^{-5} (N=132; r^2=0.72). These results are to be compared with the linear fit for the ALAD 1-2/2-2 subgroup, which displayed a slope of 0.0442±0.0081 (N=32; r^2=0.55). Again, despite a significant quadratic term, the linear coefficient of the ALAD 1-1 polynomial expression is greater than the slope of the ALAD 1-2/2-2 relation. These three equations of fit are displayed in Figure 3.10b.

3.4 Discussion

The primary motivation for this chapter has been to investigate the possibility that a common polymorphism in the δ-aminolevulinate dehydratase (ALAD) enzyme has an effect on lead body burden in humans. Recent studies have demonstrated elevated blood lead levels for individuals expressing the $ALAD^2$ allele who have been occupationally or environmentally exposed to high amounts of lead (Wetmur *et al.*, 1991b). This elevation has been confirmed for the population of Brunswick lead smelter workers. An offset of 2.3 μg/dl or 10% was demonstrated among active workers, which was of statistical significance with $p < 0.04$. Median blood lead levels differed by 4 μg/dl or 17%. Similarly, the offset in serum lead was 0.5 μg/l or 18%, which was of borderline statistical significance with $p < 0.06$. Median serum lead levels differed by 0.45 μg/l or 19%. Furthermore, the smelter records indicated an elevation of blood lead in the ALAD 1-2/2-2 subgroup in blood lead records dating back over a period of more than 20 years. This difference, while smaller in magnitude than those identified in populations of German lead workers and environmentally exposed New York schoolchildren, corresponds to a >5% elevation in the blood lead level.

It has been hypothesized that such a genetically influenced variation in blood lead could result in one of two scenarios for the ultimate distribution of lead in the body

(Wetmur, 1994). One consequence would see the enhanced binding of lead in blood successfully competing with similar processes in other tissues. ALAD 1-2/2-2 individuals would have a beneficial, protective mechanism against the toxic effects of lead. Alternatively, the raised affinity of blood for lead of those homozygous or heterozygous for the $ALAD^2$ allele could imply an altogether more efficient uptake of lead into all tissues. Increased inhibition of heme synthesis would result, bringing about more biological damage. Bone lead concentrations may be used as an analogue of body burden to further probe the effect of the ALAD polymorphism on lead toxicity.

The division of lead between the calcaneus (representing trabecular bone) and the tibia (cortical bone) was uniform amongst the two ALAD subgroups. Plots of calcaneus lead against tibia lead revealed an insignificant difference in slope. The mean subtracted difference between calcaneus and tibia lead concentrations also showed no association with ALAD status. Relative to the calcaneus, tibia lead levels were slightly, but not significantly, higher in ALAD 1-2/2-2 workers. This contrasts with a recent study which found systematically lower tibia lead levels relative to those found at a trabecular site for construction workers of type 1-2/2-2 (Smith *et al.*, 1995). The implication of the current data is that the distribution of lead between cortical bone and the trabecular calcaneus site is not influenced by ALAD

genotype.

The blood lead levels of individuals removed from the smelter working environment for more than six months were strongly associated with bone lead concentration. The endogenous exposure to lead from bone dominated in these circumstances (Erkkilä *et al.*, 1992). The apparent contribution of bone lead to blood lead levels was not significantly different between the two ALAD subgroups. The slopes and intercepts of both the blood lead-tibia lead and blood lead-calcaneus lead relations were similar, regardless of isozyme phenotype. The retention of lead therefore seems to be unaffected by ALAD status, at least as it pertains to bone stores. Thus, ALAD-specific differences in blood lead levels of active workers must reflect recent exposure.

Significant differences between the genetic subgroups were evident in comparisons of bone lead to a cumulative blood lead index (CBLI). This measure of long-term exposure indicated the total amount of lead which had been eligible for uptake into bone stores. Non-uniformities in the slope of bone lead-CBLI relations would therefore indicate differences in the net transfer of lead from the bloodstream to bone tissue. A suggestion of a difference in the coefficient of net transfer was evident when the working population was divided by ALAD genotype. The variation only became

significant when workers were isolated by time of hiring. Brunswick employees in the ALAD 1-2/2-2 subgroup who had begun work since 1977 demonstrated reduced coefficients of net transfer relative to those in the ALAD 1-1 subgroup. This effect was most clearly noted when the calcaneus was introduced as the bone site of inspection. The magnitudes of the difference in net transfer were substantial: the ALAD 1-1 individuals displayed a 25% elevation for the tibia, with a nearly 50% elevation for the calcaneus. These values were greater than the ~10% mean blood lead elevation, or even the 17% median blood lead elevation, observed for the ALAD 1-2/2-2 workers. All else being equal, this would suggest a greater body burden for those homozygous for the $ALAD^1$ allele.

The differences in transfer between the genetic subgroups, however, were only significant for the more moderately exposed workers of recent hire. For the population as a whole, the blood to bone transfer for workers of type 1-1 was only raised sufficiently to compensate their lower blood lead concentrations. Assuming equal circumstance of exposure, the net accumulation of lead in bone tissue was therefore comparable between the ALAD subgroups. This partially explains the absence of difference in mean bone lead level between the genetic subgroups, despite the elevated blood to bone transfer in workers of type 1-1. Another factor contributing to this result was the tendency for ALAD 1-2/2-2

workers to have been employed for greater periods of time at the smelter than their ALAD 1-1 counterparts.

The mechanism of a genetically dependent binding of lead is uncertain. At the 25 µg/dl blood lead concentration typical of contemporary Brunswick workers, >10 µg/dl can be bound to the enzymatically active ALAD, with additional potential binding capacity in inactive enzyme (Wetmur, 1994). This suggests a differential ALAD-1 versus ALAD-2 subunit binding as a possible explanation for the observed results. It is conceivable that workers of ALAD type 1-2/2-2 retain lead in blood with a longer half-life than their type 1-1 counterparts. Whole blood lead concentrations from workers of type 1-2/2-2 would then reflect slightly longer periods of exposure. Other blood proteins, perhaps including hemoglobin, also demonstrate an affinity for lead (Lolin and O'Gorman, 1988) and may bind varying proportions of the lead in blood.

A polymorphism in the δ-aminolevulinate dehydratase gene exerts some influence over the kinetics of lead in the human body. The raised blood lead levels of ALAD 1-2/2-2 smelter workers are consistent with the concept of genetically different lead-binding enzyme properties (Wetmur, 1994). The difference in lead transfer from blood to tissue, inferred from the bone lead-CBLI results, suggests that the ALAD-2 subunit of the protein is also less likely to surrender lead

to the skeletal system.

One observation of this study has been the increased likelihood that Brunswick workers with the longest record of employment are of ALAD status 1-2 or 2-2. A highly speculative inference is that individuals of these phenotypes are less susceptible to any adverse health effects associated with labour in a lead-related industry. A potential benefit regarding the neurotoxic effects of lead for individuals of type 1-2/2-2 has been proposed (Smith *et al.*, 1995; Bellinger *et al.*, 1994). The investigation of 72 young adults by Bellinger *et al.* noted lower lead levels in the deciduous teeth and tibia of the five ALAD 1-2 subjects, along with higher neuropsychological test scores relative to those homozygous for the $ALAD^1$ allele. The net effect of the polymorphism, however, is unlikely to be uniform over the entire body. The elevated levels of lead present in the whole blood (and perhaps serum) of ALAD 1-2/2-2 individuals may have negative effects on particularly well-perfused tissue. For example, a potential link has recently been suggested between the ALAD-2 variation and subclinical indices of renal malfunction (elevated blood urea nitrogen, uric acid, and creatinine; Smith *et al.*, 1995). The ultimate influence of the ALAD polymorphism on lead toxicity is not obvious at this point in time. No definitive statement in this regard may be made based on the analysis of blood lead, serum lead, and bone

lead concentrations in the Brunswick workers.

Future work in this area involving either occupational or more moderately exposed environmental populations would be of certain interest. The application of neuropsychological testing or measurement of markers of kidney function, in conjunction with isozyme and lead exposure analyses, would provide valuable information. The common ALAD polymorphism, as inferred from the Brunswick data, modifies lead kinetics within the human body.

Chapter 4

Lead Metabolism

4.1 Introduction

In order to understand more completely the deleterious effects of lead on the human body, it is necessary to develop a reliable understanding of its metabolism. These efforts have been hampered in the past by the rather limited temporal data on lead concentration in the body. Blood lead, urine lead, or hair lead concentrations may be readily available, but can only relate a small portion of the story. For example, blood lead concentration, as a primarily acute index of exposure, does not necessarily reflect long-term distribution of lead to critical target organs such as the brain or kidney. Tissue concentrations at autopsy represent only an endpoint, and can provide little information on variations over time or general metabolic features (Marcus, 1985a). The goal of a lead metabolic model is to incorporate available lead concentration data into a physiologically realistic model. A successful model can then be used to infer information that would not otherwise be possible to measure in a non-invasive manner. In addition to blood lead concentration, routine measurements of serum lead and bone

lead are now becoming feasible, and should enhance the predictive powers of lead metabolic models.

Many models of lead metabolism have appeared in the literature which have employed some kind of compartmental analysis (Abdelnour *et al.*, 1974; Rabinowitz *et al.*, 1976; Batschelet *et al.*, 1979). Compartmental analysis operates on the assumption that metabolism of a substance in the human body can be approximated by transfer amongst a series of compartments representing anatomical sites. A single compartment is taken to have an homogeneous and well-mixed concentration of the substance in question (Marcus, 1985a). Transport from one compartment to another is governed by a rate constant (Leggett, 1993). The rate constant multiplied by the amount of substance present in the original compartment produces the transfer rate to the new compartment. If all inflow could be halted and outflow to one new compartment was modelled, the concentration of the substance in the original compartment would follow the relation

$$C(t) = C_0 e^{-\lambda t} \quad [4.1].$$

Here, C_0 represents the original concentration, λ the rate constant, and t the time interval. Often, however, a given compartment is linked in both directions to more than one other compartment, so that continuous inflows and outflows to multiple sites must be considered. Models of lead metabolism

typically specify compartments such as whole blood, plasma, kidneys, brain, liver, cortical bone, and trabecular bone. Of particular concern is the kinetics of lead with respect to bone. Bone modelling, remodelling, formation, and resorption must be described as a function of age. The diffusion of lead within quiescent bone must also be considered. A general description of these processes, which any model of lead metabolism should address, will be provided. The sections which follow the initial description of bone metabolism summarize three of the most recent models of lead metabolism.

4.2 Bone Metabolism

Bone modelling is associated with the shaping of the skeleton during growth in childhood and adolescence. Remodelling, on the other hand, is characteristic of bone tissue in adults. The transition from modelling-dominated youth to remodelling-exclusive adult processes is a gradual one. The rate of bone formation is highest after birth and at the onset of puberty. Formation settles to a near-uniform rate in mature adults. The rate of bone resorption rises following birth and peaks during puberty. Unlike bone formation, bone resorption increases toward the later stages of life, leading to such effects as osteoporosis.

During bone modelling, an entire bone surface is the site

of either formation or resorption. These concerted, segregated, efforts by osteoblasts (bone-forming cells) and osteoclasts (bone-resorbing cells) serve to sculpt and enlarge bone mass. With remodelling, however, only a very localized portion of bone tissue is involved at any one time (Parfitt, 1976). Osteoclasts begin their activity near the centre point of the future bone unit. Osteoblasts then work to fill the resulting "hole" (cortical bone) or "trench" (trabecular bone) from the outside-inward. This cyclical process provides a constant renewal of bone tissue. A further distinction between modelling and remodelling may be drawn in regards to the associated rates of action during bone formation or resorption (Parfitt, 1976). Whereas in modelling, the resorptive and formative velocities are similar in magnitude, the resorptive rate of action is about five times greater than that of formation during remodelling. This is a consequence of the slower appositional (formative) rate of action in adults. Note that overall bone mass still remains roughly constant in the adult for it is only the relative *velocity* of formative action that is reduced.

The constituents of bone mineral (notably calcium, phosphorus, and carbon; but also lead) may enter or leave bone tissue through two key mechanisms. The preceding paragraph examined the more widely-appreciated method of transfer: bone formation/resorption. The other important effect involves the

diffusion of mineral from the bloodstream into bone, and *vice versa*. In other words, consideration must be given to ions which perform a type of "swap" between blood and bone (Frost, 1966). The distinction between these processes is also drawn by Parfitt (1976) in a description of the flux of calcium inward to bone tissue. The total flux consists of both new bone formation *and* long-term exchange processes.

4.3 Marcus Models

Using lead retention data from dogs and human subjects, Marcus examined a series of multicompartment kinetic models for lead (Marcus, 1985a; 1985b; 1985c). The first publication in this series deals with models for the diffusion of lead within bone (Marcus, 1985a), a topic of particular importance to X-ray fluorescence studies. The second paper considers the application of multicompartment linear kinetic models to four human subjects (Marcus, 1985b). The final publication in the series investigates the apparently nonlinear relation between plasma lead and blood lead concentrations in exposed humans (Marcus, 1985c). While addressing each of these issues somewhat distinctly, the Marcus models highlight some of the major points of interest facing current efforts in modelling lead metabolism.

The lead diffusion concept was built upon the work of

Marshall and Onckelinx (1968), and assumes that lead can reach the bone volume by travelling from blood vessels in the Haversian canals (central passages of ~50 μm diameter which run through compact bone). From the Haversian canals, lead passes to canalculi, minute channels of order of 0.1 μm diameter which run into the bone volume. It is from these canaliculi that lead ions diffuse into the surrounding bone volume. Essentially, a given ion then performs a "random walk" within a cylindrical bone volume. The ion might return to its canalicule of origin immediately, or to an altogether separate canalicule after a prolonged residence. Bone turnover is also incorporated into the models.

Several compartmental models were tested by Marcus (1985b) in an attempt to describe the results of a series of well-controlled lead exposure studies involving human subjects (Rabinowitz *et al.*, 1976). The bone lead diffusion concept was deemed unnecessary in these analyses, given the relatively short span of time (106 to 407 days) over which the subjects were monitored (Marcus, 1985b). One particular model, comprising blood, cortical bone, trabecular bone, soft tissue, and hair compartments (Figure 4.1), was selected for detailed description. The kinetics of transfer in all instances was linear; twice the lead concentration in a given compartment implied twice the transfer rate to an adjoining compartment. A model employing linear kinetics proved sufficient for blood

Figure 4.1

Compartmental model of lead metabolism (Marcus, 1985b):

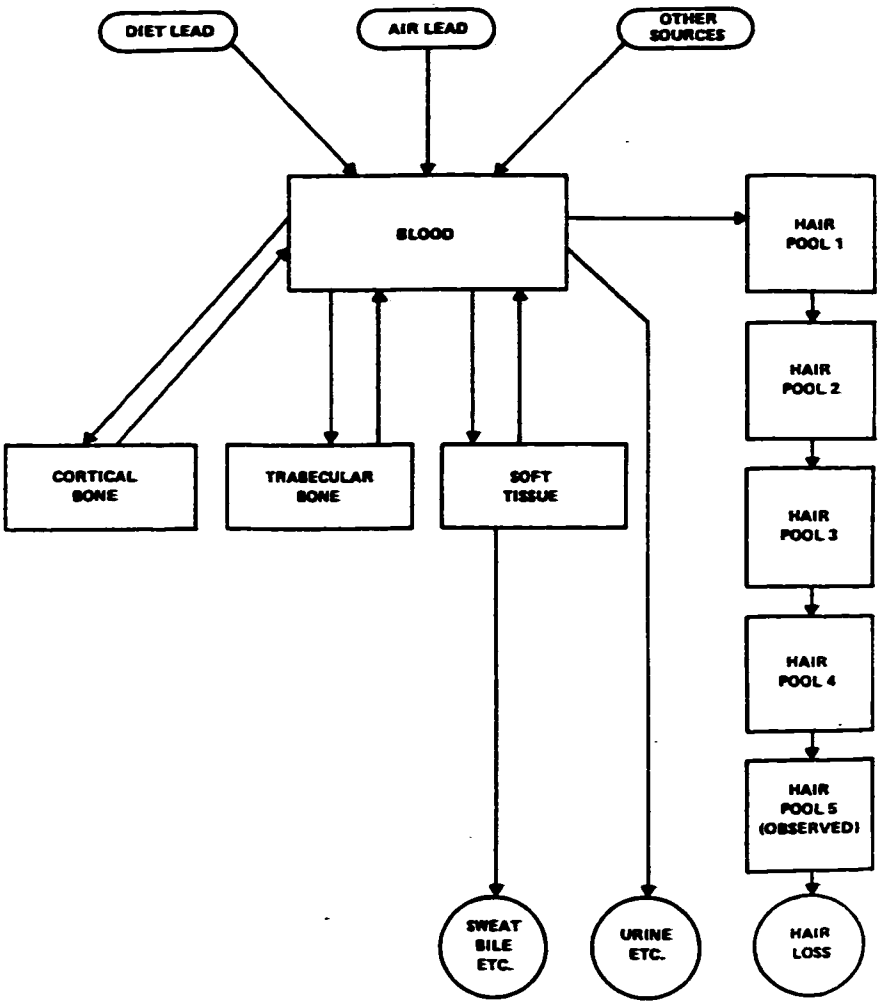

lead concentrations up to at least 30 μg/dl. A significant indication of change in gut absorption of lead over time was noted for three of the subjects, possibly as a consequence of the sudden change in diet caused by introduction to the controlled ward environment (Marcus, 1985b).

The nature of any nonlinear relation between plasma lead and blood lead was examined in the final paper of the series (Marcus, 1985c). At relatively high blood lead levels, evidence suggests that a disproportionately large amount of lead will reside in the plasma component of whole blood (deSilva, 1981; Manton and Malloy, 1983; Manton and Cook, 1984). Lead contained in the erythrocyte (red blood cell) will bind with blood proteins, including δ-aminolevulinate dehydratase (Wetmur, 1994). At high blood concentrations, some proportion of lead may be bound to a lead-induced cell protein (Raghavan *et al.*, 1980). Lead remaining in the plasma may bind with proteins such as albumin (Simons, 1986) and α-globulin (Griffin and Matson, 1972). The distribution rate of lead from the bloodstream to various body compartments is assumed to be governed by the concentration in plasma. Therefore, understanding how lead divides between blood components is of great importance. The difficulty in measuring plasma lead or serum lead has at times clouded this issue (Marcus, 1985c). Marcus employed statistical tests to compare results predicted from a variety of biologically

plausible models of blood lead partition with observational results from over 100 lead workers (deSilva, 1981). The successful models stipulated that as lead concentration increases, the rate of flow from erythrocytes to plasma accelerates (or alternatively, a limited or decreased rate of flow from plasma to erythrocytes occurs). Intercept terms provided significantly improved fits to the data, perhaps suggesting a departure from equilibrium conditions. In all cases, the nonlinear models provided significantly better results than a linear mechanism. The elimination of data from workers with blood lead > 80 μg/dl was required to enable an adequate fit from a linear model.

4.4 Leggett Model

Following the 1986 Chernobyl nuclear accident, the International Commission on Radiological Protection (ICRP) initiated the construction of a series of biokinetic models. These efforts were geared toward the calculation of dose resulting from the intake of nuclides with potential radiological significance, including some isotopes of lead. In general, the metabolism of lead in the human body is similar to that of other "bone volume-seeking" elements, such as calcium, barium, radium, and strontium. The age-specific kinetic model described by Leggett (1993) was originally developed in this context, but was expanded for a more

complete consideration of lead, and its role as a chemical toxicant.

The Leggett model provides a very detailed compartmental scheme for lead metabolism (Figure 4.2). Distribution of lead throughout the body is dependent on the concentration in a diffusible plasma compartment. Lead kinetics are assumed linear as long as the concentration in erythrocytes stays below a threshold value of 60 μg/dl. Transfer rates between the various compartments are provided for each of six age groups: 0-100 days, 1 year, 5 years, 10 years, 15 years, and ≥ 25 years. These rates were inferred from a variety of studies involving experimental animals and human subjects. Intermediate age values are calculated by linear interpolation. For example, a 12 year-old's rate would be determined as 0.6 times the transfer rate for a 10 year-old plus 0.4 times the rate for a 15 year-old.

The treatment of bone in the Leggett model is generally in accord with the alkaline earth model detailed in ICRP Publication 20 (1973). Both cortical and trabecular bone are divided into surface and volume compartments (Figure 4.2). Bone surfaces include endosteal and periosteal surfaces of cortical bone, Haversian canal surfaces, resorption cavity surfaces, and surfaces of trabecular bone. Lead in bone which is retained over long time scales is assumed to reside in the bone volume component. A further distinction is drawn between

Figure 4.2

Leggett compartmental model of lead metabolism (Leggett, 1993):

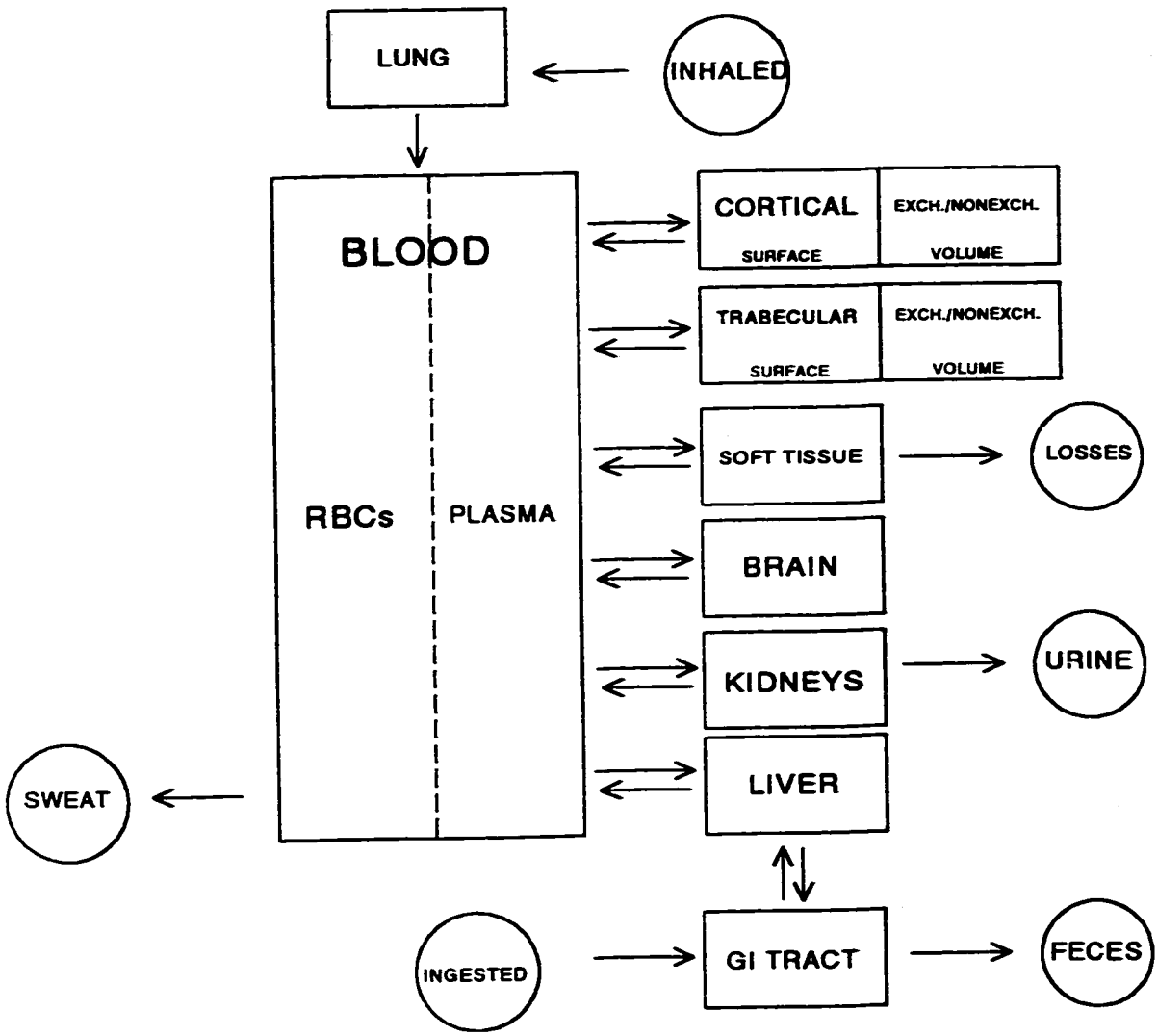

exchangeable and non-exchangeable bone volume, so that both cortical and trabecular bone are divided into three subcompartments.

Lead exchange between plasma and bone occurs first at the surface layer of bone. One half of this lead will make the transfer to the exchangeable bone volume, from where 20% of the amount will eventually move to the non-exchangeable volume. As the name implies, lead which reaches this subcompartment cannot transfer out of bone in the same fashion, but rather must wait for wholesale bone resorption in order to return to plasma. This trilayered approach will have an overall effect on lead kinetics similar to the diffusion model noted above (Marcus, 1985b).

The Leggett model relies on a two-compartment makeup for plasma in order to describe the gradual affiliation of plasma lead with plasma proteins, notably α-globulin (Griffin and Matson, 1972). The portion of lead in plasma bound to such proteins makes up the nondiffusible plasma lead compartment, and eventually contains the majority of lead in plasma. As noted, it is the diffusible plasma compartment which governs the transfer of lead to various tissues of interest. The fraction of whole blood lead residing in plasma increases at elevated blood lead levels, just as it did in the Marcus models.

This nonlinear relation between plasma lead and whole blood lead is modelled by Leggett as resulting from a reduced rate of flow from diffusible plasma to erythrocytes as red blood cell binding sites become saturated. Transfer rates from diffusible plasma to tissue increase with the somewhat reduced competition from erythrocytes. The threshold lead concentration for the commencement of nonlinear effects is 60 μg/dl red blood cell (about 150000 lead atoms per cell), which translates to a whole blood lead concentration of ~25 μg/dl for adults.

4.5 O'Flaherty Model

With the vast majority of retained lead accumulating in bone, it is apparent that the kinetics of lead in the human body will be largely influenced by its behaviour with respect to bone tissue. The long time scales associated with bone metabolism therefore necessitate a model of lead kinetics which considers physiologic variations over a human lifetime. The O'Flaherty model of lead metabolism provides a continuous approach to human growth and development, with a detailed examination of age-dependent bone processes (O'Flaherty, 1993). The model originated from analyses of the growth of, and lead distribution in, experimental rats (O'Flaherty, 1991a; 1991b); and from a detailed consideration of human development (O'Flaherty, 1991c). This attention to time-dependent processes, in particular with regard to bone lead

metabolism, makes the O'Flaherty model appealing for comparison with X-ray fluorescence results. On this basis, the model was adopted for a detailed comparison of its predictions with the observed bone lead concentrations of the Brunswick smelter workers. This project represents the first application of the model to a data set comprised of both bone lead *and* long-term blood lead results. The O'Flaherty model of lead metabolism will be described in some detail.

4.5.1 General Considerations

The version of the O'Flaherty model employed explicitly considered the following biocomponents: blood, plasma, liver, kidney, other well-perfused tissue, cortical bone (metabolically active and diffusion regions), trabecular bone, and other poorly-perfused tissue (see Figure 4.3). Transfer of lead from the bloodstream was again assumed to be regulated through the plasma. The relative absorption of lead from the gastrointestinal tract was modelled by a rapid decline from 58% at birth to 8% by the age of ten. The relative lead absorption from the lungs was 50%. Lead was eliminated from the system with 70% passing through the kidneys and 30% through the liver. Parameters such as cardiac output, body clearance rates, bone volume, and other tissue and organ volumes were dependent on body weight and age. Body weight was described by a five-parameter fit with adjustable end-point. In practice, since no smelter worker body masses were

Figure 4.3

O'Flaherty physiological model of lead metabolism (O'Flaherty, 1993):

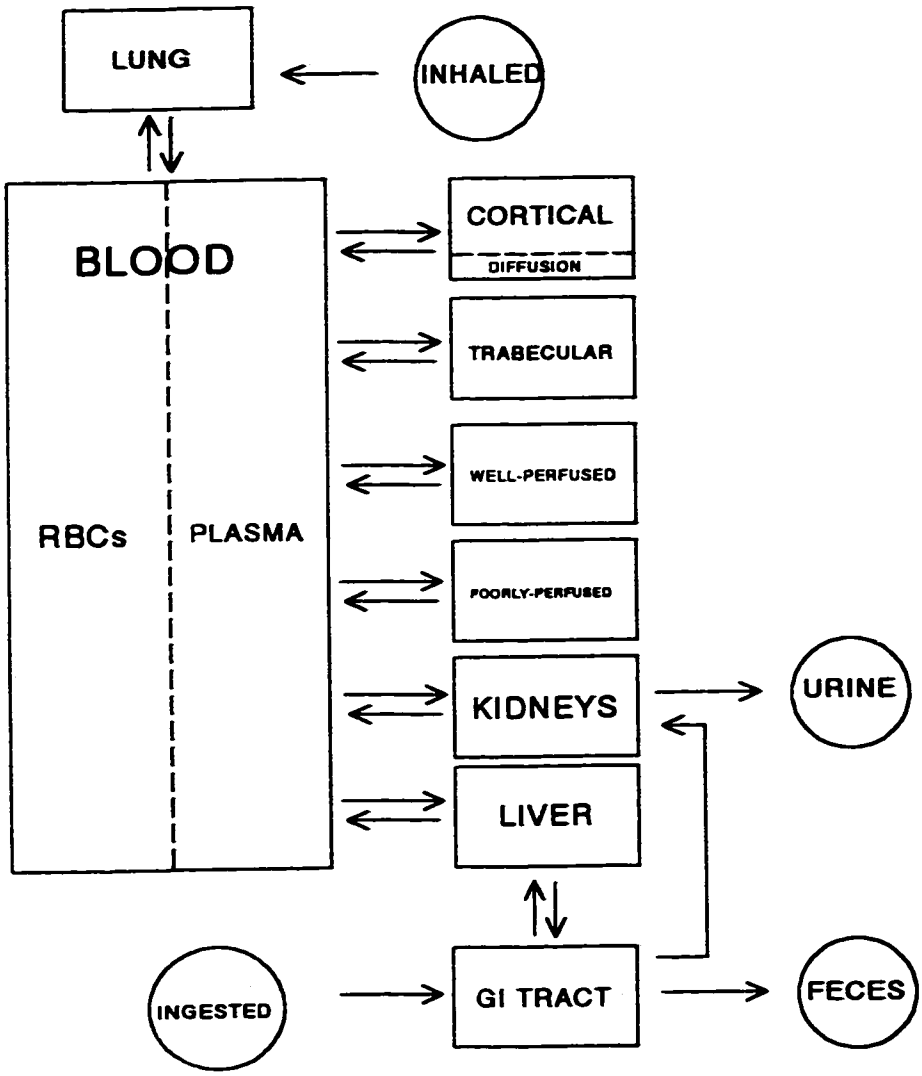

recorded initially, a generic adult weight was assumed. Adult body weight was divided between well-perfused (10%) and poorly-perfused tissues (90%). From the heart, 25% of the output was modelled to the liver, 17% to the kidneys, 44% to other well-perfused tissue, 5% to bone, and 9% to other poorly-perfused tissue. Total blood volume was 0.067 L/kg body mass.

4.5.2 Blood Lead Partitioning

The nonlinear relation between plasma lead and blood lead is considered to result from a capacity-limited binding of lead by erythrocytes. At higher levels of whole blood lead concentration, a greater portion of the lead in blood will therefore reside in the plasma component. Since the transfer rates of lead from blood to body tissue are regulated by plasma lead concentration, this effectively increases the rate of distribution to compartments such as bone, kidney, and liver. The mathematical relation between concentration of lead in whole blood (CB) and concentration in plasma (CPLASMA) is as follows

$$CB = PLASMA * CPLASMA + (HCT * CPLASMA) * \left(G + \frac{BIND}{KBIND + CPLASMA}\right) \quad [4.2].$$

where PLASMA is the plasma fraction of whole blood by volume (PLASMA=1-HCT), HCT is the hematocrit, G is the ratio of unbound red cell lead to plasma lead, BIND is the maximum binding capacity for lead in erythrocytes (mg / l of red blood

cell), and KBIND is the half-saturation concentration (mg / l of red blood cell). This relation is very similar to the zero-intercept plasma lead-blood lead relation derived by Marcus (1985c), which pertained at increased erythrocyte lead concentrations (Figure 4.4).

4.5.3 Lead Kinetics in Bone

Lead metabolism in cortical bone is described by two distinct processes: one pertaining to "metabolically active" cortical bone, another to "quiescent" cortical bone. Recall that remodelling affects kinetics within mature cortical bone, and modelling affects kinetics within juvenile cortical bone. These features are associated with "metabolically active" cortical bone. A second process is the slow exchange of lead and calcium ions within bone and between bone and blood. This kinetic process is only considered for mature cortical bone since metabolically active processes dominate juvenile kinetics.

The metabolism of lead within trabecular bone is modeled in the same fashion as lead in metabolically active cortical bone. There is no consideration of exchange for trabecular bone. Model equations describing metabolically active cortical bone and trabecular bone follow identical algorithms, regardless of whether mature or juvenile bone is considered. The description of kinetics in the diffusion region of

Figure 4.4

Plasma lead concentration against blood lead concentration (data from deSilva, 1981; plot from O'Flaherty, 1993).
A) Original relation from O'Flaherty model (O'Flaherty, 1993),
B) No-intercept relation derived by Marcus (Marcus, 1985c):

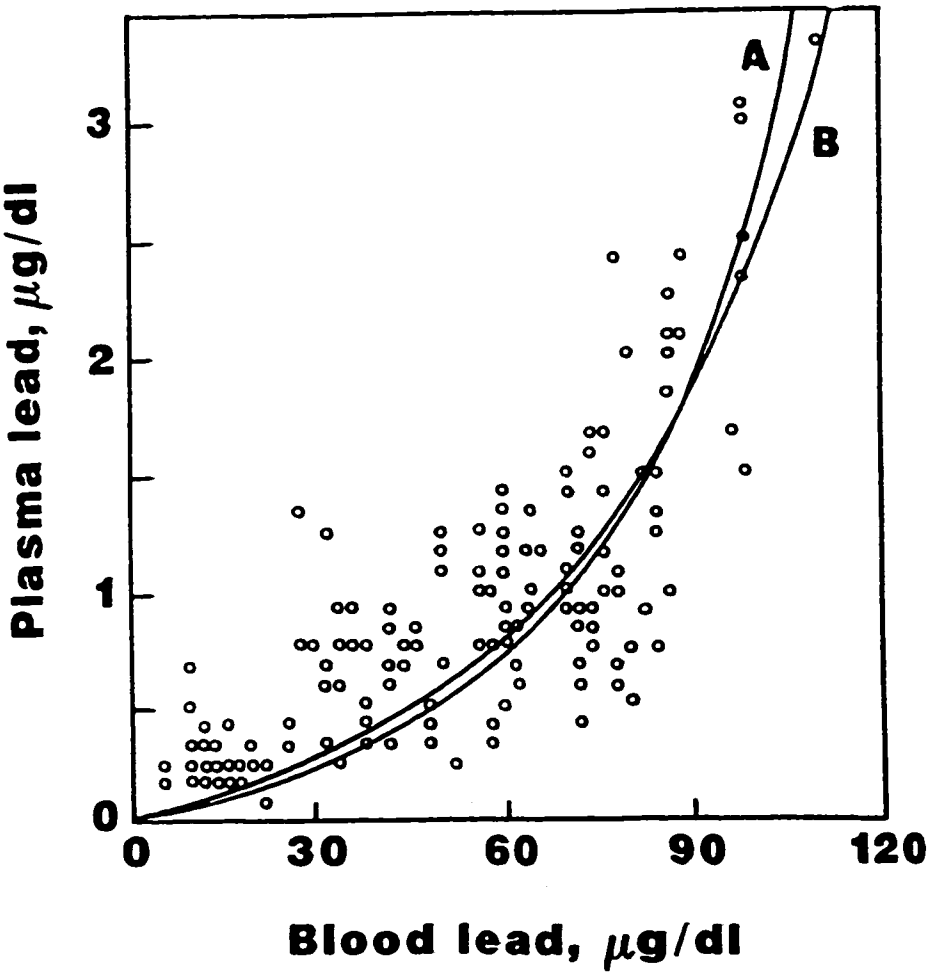

cortical bone, on the other hand, is unique to mature bone.

Metabolically active regions in cortical bone include endosteal and periosteal bone surfaces, and haversian canals. In general, the transfer of lead from blood to bone is governed by the clearance of lead from plasma to bone, and the rate of cortical bone formation. For example, in the specific case of lead transfer to newly-appositioned juvenile cortical bone, the following equation applies:

$$CRVAFC=LEAD*CBFRC \quad [4.3].$$

CRVAFC is the clearance of lead from blood during mineralization of newly-appositioned cortical bone (units: volume / year), LEAD corresponds to the clearance from plasma to forming bone (volume plasma cleared / volume bone formed), and CBFRC is the cortical bone formation rate (volume bone / year). It is worth noting that in all kinetic descriptions, lead is assumed to move in tandem with much greater quantities of calcium. The actual rate of lead deposition in cortical bone during modelling (CRAFBC) is then

$$CRAFBC=CRVAFC*CPLASMA \quad [4.4].$$

This uptake is balanced by a return of lead to blood with resorption of cortical bone (CRARBC), such that

$$CRARBC=CBRRC*CCMC \quad [4.5].$$

Here, CBRRC represents cortical bone resorption rate (volume

bone / year) and CCMC the concentration of lead in cortical bone (mg / volume bone). The total amount of lead in cortical bone engaged in modelling during growth (CAMC) is then

$$CAMC=\int (CRAFBC-CRARBC-(CRFBON*CAMC))\,dt \quad [4.6].$$

An important parameter in this expression is CRFBON, an age-dependent rate describing the transformation of bone involved in modelling during growth (juvenile bone) to bone involved in adult-type remodelling (mature bone). By the mid-twenties, all bone is assumed to be of the mature type.

The exchange of lead within mature bulk bone is modeled as a diffusion process. Upon entering the tiny canalicules which are distributed throughout the bone volume, lead has the potential to exchange from plasma to a superficial layer of bone. Lead in this first layer, or "shell", may then migrate deeper into the bone volume to a second shell, or return to the canalicule from where it originated. The O'Flaherty model considers a total of eight such shells, arranged concentrically about each canalicule, producing a cylindrical diffusion region (Figure 4.5). The distance between shell walls is 0.5 μm. The exchange of lead between shells effectively approximates the more continuous lead diffusion theory of Marcus (1985a). The whole bulk of mature cortical bone is represented as a vast collection of these tiny eight-shelled diffusion regions.

Figure 4.5

Diffusion region of mature cortical bone (O'Flaherty, 1993):

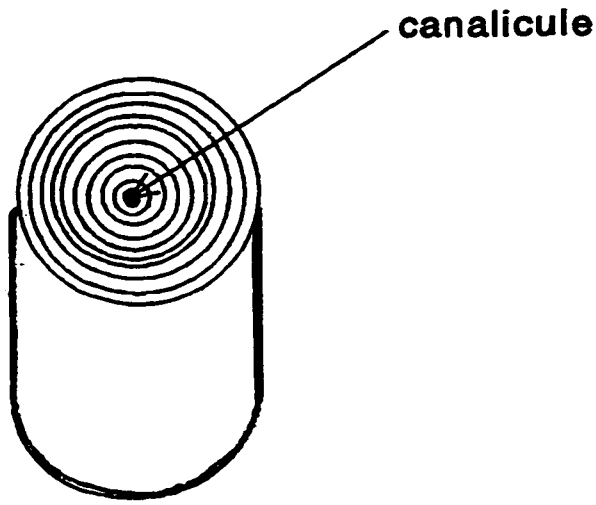

The rate of change of lead in shell 1 of mature cortical bone (RAB1) is given by the expression

$$RAB1=\frac{S*L*CVBONEA}{1000}*(P*CCBPHA-R*CB1)-\frac{D*CVBONEA*S1*L}{1000}*(CB1-CB2)+$$

$$F1*(CRAFBA-CRARBA+CRFBON*CAMC) \quad [4.7].$$

Here, the notation represents the following terms:
S...surface area of canalicule (cm^2) per unit length;
L...canalicule length per liter of bone (cm / L);
CVBONEA...cortical bone volume participating in adult remodelling (L);
P...constant for diffusion from canalicule to bone;
CCBPHA...concentration of lead in plasma leaving metabolically active region of mature cortical bone engaged in remodelling (mg / L);
R...constant for diffusion from bone to canalicule;
CB1...concentration of lead in shell 1 (mg / L);
D...constant for diffusion within bone volume;
S1...surface area of shell 1 (cm^2);
F1...fraction of diffusion region bone volume in shell 1;
CRAFBA...rate of lead deposition in cortical bone due to the formation phase of adult-type remodelling (mg / year);
CRARBA...rate of lead removal from cortical bone due to the resorption phase of adult-type remodelling (mg / year).
This rather complicated expression may be described more succinctly. Simply put, the rate of change of lead in shell 1

(mg / year) is equal to:
(the rate of diffusion from the canalicule to the shell)
- (the rate of diffusion from the shell to the canalicule)
- (the net rate of loss resulting from diffusion from shell 1 to shell 2)
+ (the net rate of deposition resulting from adult-type remodelling).
The amount of lead in shell 1 of cortical bone is

$$AB1=\int RAB1\ dt \quad [4.8],$$

from which the concentration of lead in shell 1 is derived. Similar expressions are constructed for each of the eight shells composing the diffusion region.

As noted above, the kinetics of lead in trabecular bone is modeled as being similar to that in the metabolically active cortical regions. Following the same prescription, lead transfer to newly-appositioned trabecular bone involved in modelling during growth (TRVAFC) is:

$$TRVAFC=LEAD*TBFRC \quad [4.9].$$

TBFRC represents trabecular bone formation rate (volume bone / year). The rate of lead deposition (TRAFBC) is

$$TRAFBC=TRVAFC*CPLASMA \quad [4.10].$$

This uptake is countered by a return of lead to blood with

resorption of trabecular bone (TRARBC);

$$TRARBC=TBRRC*TCMC \quad [4.11].$$

TBRRC corresponds to the trabecular bone resorption rate (volume bone / year) and TCMC the concentration of lead in trabecular bone (mg / volume). The total amount of lead in trabecular bone engaged in modelling during growth (TAMC) is

$$TAMC=\int (TRAFBC-TRARBC-(TRFBON*TAMC))\,dt \quad [4.12].$$

TRFBON is the rate of transformation of trabecular bone involved in modelling during growth to bone presently involved in adult-type remodelling.

The quantities of importance which may be derived from such analyses are the total amounts of lead in cortical bone (CAB) and trabecular bone (TAB). The total for cortical bone will consist of the amount of lead in each of the eight diffusion region shells, in addition to the amount in cortical stores which are engaged in modelling:

$$CAB=AB1+AB2+AB3+AB4+AB5+AB6+AB7+AB8+CAMC \quad [4.13].$$

Each of the diffusion shells involve only mature components of bone, so the growth-associated modelling component (CAMC) is required for completeness. All terms have undergone integration with respect to time. The total amount of lead in trabecular bone does not involve any diffusion shell

contributions:

$$TAB=\int (TRAFBA+TRAFBC-TRARBA-TRARBC)\,dt \quad [4.14].$$

Here, TRAFBA designates the rate of deposition of lead in mature trabecular bone engaged in remodelling (mg / year) and TRARBA the rate of resorption of mature trabecular bone engaged in remodelling (mg / year).

4.5.4 Conversion Factors

For the sake of comparison with X-ray fluorescence bone lead measurements, two results of particular importance emerge from the Brunswick smelter workers' model simulations. From personal blood lead records, the concentration of lead in marrow-free dry cortical bone (CCMFDB, in units of mg / kg) and concentration of lead in marrow-free dry trabecular bone (TCMFDB, mg / kg), may be predicted for any individual worker. These quantities are derived in the following manner:

$$CCMFDB=\frac{CAB}{0.8*WMFDB}; \quad [4.15]$$

and

$$TCMFDB=\frac{TAB}{0.2*WMFDB}; \quad [4.16]$$

where WMFDB is the weight of marrow-free dry bone in kg. Note that the modelled bone lead concentration is described as a mass of lead per mass of marrow-free dry bone. Marrow-free dry bone consists of bone mineral (bone ash) *and* protein. As

described in Chapter 1, however, the X-ray fluorescence measurement yields the amount of lead present per unit of bone mineral alone. Therefore, in order to make a direct comparison between the theoretical model concentrations and the observed results from X-ray fluorescence analysis, it was necessary to introduce conversion factors.

These conversion factors may be inferred from empirical evidence gathered from amputated limbs or autopsies. In a review of the literature pertaining to healthy adults, the ratio of (mean bone ash plus protein weight) to (mean bone ash weight) was determined to be 1.42 for cortical bone (Woodard and White, 1986). Similarly, the Report of the Task Group on Reference Man (ICRP, 1975) reports ratios of 1.51 and 1.50 for two male tibia samples (Forbes *et al.*, 1953; Mitchell *et al.*, 1945). Based on these considerations, the multiplication factor selected to convert from model output to experimental concentration was 1.5 for the tibia. The Report of the Task Group on Reference Man (ICRP, 1975) does not comment directly on the ratio of bone ash plus protein to bone ash in the human calcaneus. For trabecular bone in general, however, 50% of bone mass is reported to be associated with ash weight, and 24% with protein. Following this prescription, the ratio is 1.48. A conversion factor of 1.5 was therefore also applied for the calcaneus.

4.5.5 Computation

The version of the O'Flaherty code which was used in the present analysis employs the Advanced Continuous Simulation Langauge (ACSL) Model software (available from MGA Software; Concord, MA). Version 10, designed for use with Microsoft Windows 3.1 and Microsoft Fortran 5.1, was utilized throughout. ACSL was designed specifically for the modelling of systems which are described by time dependent differential equations or transfer functions (ACSL Reference Manual).

A complete ACSL project consists of a variety of components. The most critical portion of any project is the simulation code itself. The original O'Flaherty model for lead metabolism was contained in the file HUMAN10.CSL (Appendix A). It is apparent that the simulation language itself is very similar in structure to Fortran. The first step in running a project is the translation of the ACSL code into a file which may be directly compiled by Fortran, HUMAN10.FOR. This file is passed through the compiler to produce HUMAN10.PRX, which in turn is linked with the ACSL runtime library. The final step before executing the code is to read in the command file, HUMAN10.CMD, which contains initial conditions and trial information specific to a particular simulation run.

Chapter 5

Lead Metabolism Results

5.1 Application of Model

Two versions of the model were originally supplied by Dr. Ellen O'Flaherty. The first was roughly similar to the model which produced the results reported in O'Flaherty (1993). The second version was identical in structure, but included a series of parameter changes. These variations involved the diffusion and partitioning of lead in the body and served to reduce the amount of lead released from bone. These two versions were tested independently, and will be described herein as models 96A and 96B.

Rather than perform preliminary simulations on each of the nearly 400 workers involved in the Brunswick survey, a subset with well-documented blood lead histories were chosen for initial trials. A total of 20 workers were examined (ten hired before 1977, ten hired more recently). This subset was selected to be similar to the larger working population with respect to the following relations:

(1) blood lead immediately following the strike as a function of tibia lead and calcaneus lead concentration,

(2) tibia lead and calcaneus lead as a function of revised

cumulative blood lead index for workers hired before 1977, (3) tibia lead and calcaneus lead as a function of revised cumulative blood lead index for workers hired more recently, (4) calcaneus lead as a function of tibia lead concentration. An examination of the results from the 20 simulations provided an indication of potential model refinements without an overexpenditure of computing time.

As input, the model requires a description of lead exposure as a function of time. For the Brunswick workers, the dominant source of life exposure has been lead inhaled from the work environment. Nonetheless, an accurate assessment of "background" lead sources would obviously help in making the simulations more reliable. The recommended parameters (supplied for an American subject) were as follows:

lead in food (pre-1970)..... 200 μg/day
lead in food (contemporary)..... 30 μg/day
lead in air (pre-1975)..... 2 $\mu g/m^3$
lead in air (contemporary)..... 0.15 $\mu g/m^3$
lead in water..... 5 μg/l
lead in dust and soil..... 40 μg/g

The values adopted for the Brunswick workers were similar, but not identical to those given above. The contemporary concentration of lead in food was elevated to 50 μg/day to account for the local environment (in close

proximity to a smelter). The initial air lead level was revised downward to 1 $\mu g/m^3$ for consistency with the Canadian report, Air Quality in Ontario 1993. The contemporary air lead exposure, however, was hypothesized to be somewhat higher for the smelter workers (0.5 $\mu g/m^3$) than the present-day U.S. value. A slightly lower concentration of lead in water was adopted, 2 $\mu g/l$ (Méranger *et al.*, 1981). The values for lead in dust and soil were retained, although one Canadian estimate places the levels as high as 200 $\mu g/g$ (Royal Society of Canada, 1986). By necessity, the selection of background estimates for the Brunswick workers involved a degree of uncertainty. The model predictions were found to be insensitive to reasonable variations in background parameters, other than those made for lead in air or food.

5.2 Brunswick Air Lead Exposure

The question of air lead exposure on the job is a crucial one for the modelling procedure. Extensive documentation of blood lead measurements exist for the Brunswick workers, dating from 1968. The air lead exposure of individual workers at specific times must be inferred from these numbers in order to proceed with the simulations. A relation between worker blood lead and air lead exposure must therefore be constructed. A number of air lead surveys have been performed at Brunswick which could help in this task. These surveys

have included static samplings at various job sites and personal monitorings of various workers. The personal samplings are more useful, since they can be directly compared with blood lead measurements from the specific workers involved. The most complete survey of this kind is documented in the summary of personal air lead sampling, 1990 (obtained with permission from Julie Walton, Industrial Hygiene at Brunswick).

The date of sampling and personal air lead value were recorded for 41 workers during 1990. The blood lead histories for these employees were examined, and the blood lead concentration for the sample most closely matching the date of the air lead survey was extracted. This produced a listing of approximate blood lead as a function of air lead exposure for the Brunswick population. It should be noted that because of the use of respirators on the job, the concentration of lead in air that the workers breathed was actually considerably lower than that recorded by the personal samplers (which were placed approximately at neck level). A respirator efficiency of 90% has been assumed (Julie Walton, personal communication), meaning that an air lead concentration of 100 $\mu g/m^3$ would actually result in an inhaled concentration of 10 $\mu g/m^3$. As is evident from Figure 5.1, the relation between inhaled air lead concentration and blood lead is not easy to discern. Many complicating factors are likely: the time

Figure 5.1

Blood lead-air lead relationship, Brunswick workers:

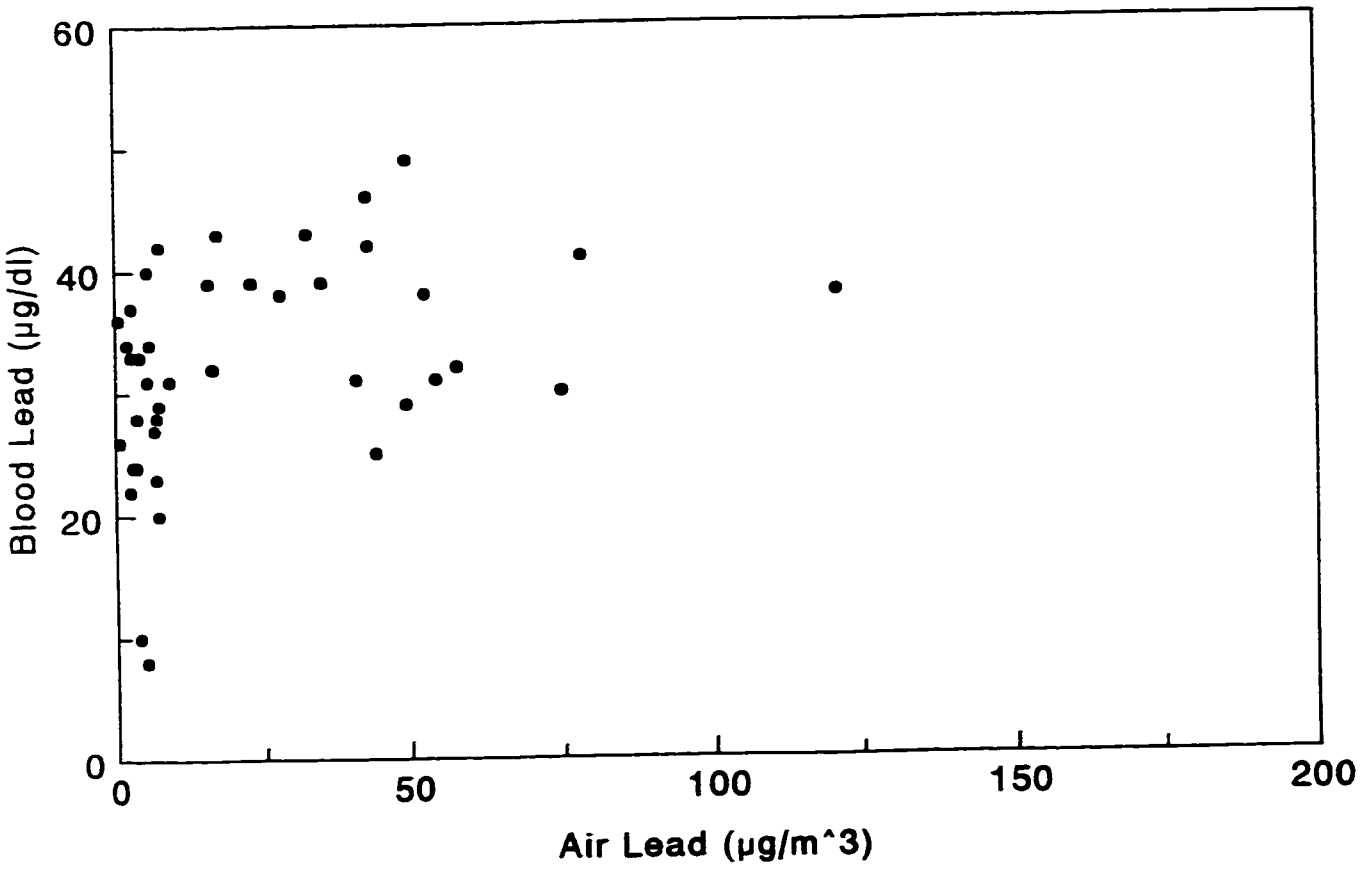

lapsed between air lead and blood lead measurements, variations between workers in endogenous contributions to total blood lead (resulting, in part, from previous exposure history), personal changes in working pattern and location, and differences in respirator efficiency. However, the curvilinear nature of the relation, which has been noted in the past (Snee, 1982), is quite apparent.

Rather than derive a new relation from the somewhat inconclusive Brunswick blood lead-air lead data, the suitability of previously published relations was examined. The results from personal air lead samplers in a study involving 29 workers from a lead-acid battery factory (Williams, 1969) are perhaps most relevant to the current analysis. The participating employees demonstrated personal air lead exposures of up to 300 $\mu g/m^3$ in the absence of respirator use. Samples were taken each day over two work-weeks, resulting in ten air lead estimates from each worker. These results were averaged to yield the mean air lead exposure during a typical eight-hour shift. Blood lead measurements were performed on six occasions during the second week of the survey. Benefits of this study were the simultaneous nature of the air lead and blood lead measurements, and the well-defined sequence of repetitive testing. Given these advantages, it is not surprising that the resulting blood lead-air lead plot (Figure 5.2)

Figure 5.2

Blood lead-air lead relationship, battery factory workers (data from Williams, 1969).

Lead exposure model is superimposed (Snee, 1982):

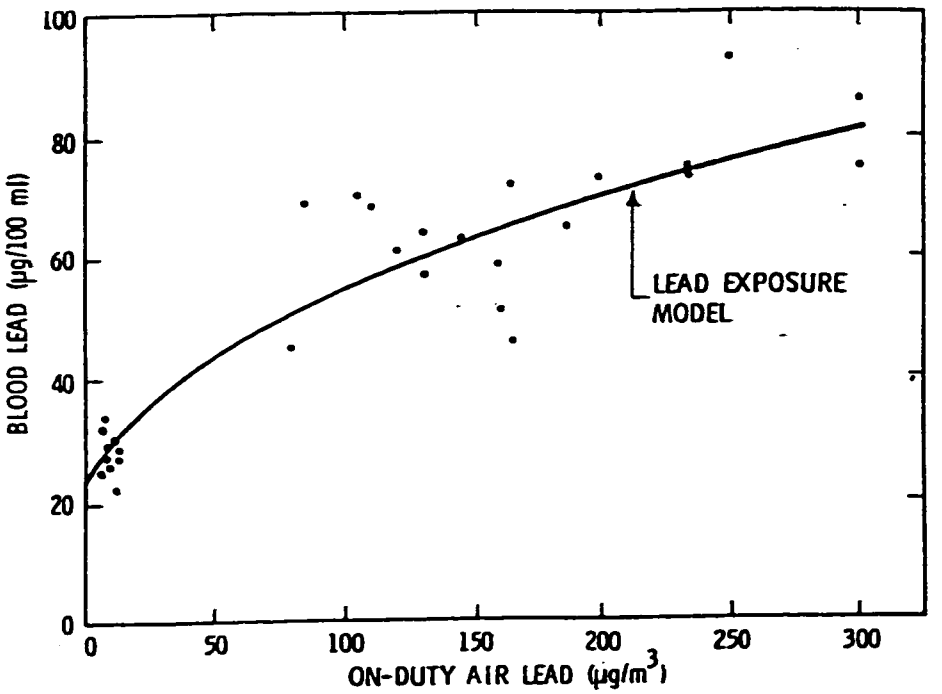

demonstrates a smaller degree of scatter than the Brunswick data.

The Williams data was originally modelled by a simple linear regression (Williams, 1969). As the curvilinear nature of the blood lead-air lead relation was recognized, log-log equations were introduced (Azar *et al.*, 1972) to describe such results. A disadvantage of this approach is its inconsistency with physical reality as air lead approaches zero. Specifically, a log-log relation predicts a negative blood lead as air lead approaches zero (or alternatively, a blood lead of zero if the equation is expressed in exponential form). In order to account for other sources of lead in the environment, the "lead exposure model" was introduced (Snee, 1982):

$$Blood\ Pb = A(Air\ Pb + B)^{K} \quad [5.1].$$

Nonlinear least squares regression was used to solve for the coefficients, producing an equation to describe the Williams data (Figure 5.2):

$$Blood\ Pb = 16.1((0.24 * Air\ Pb) + (0.76 * 0.5) + 1.65)^{.3779} \quad [5.2].$$

Off-work air lead exposure is assumed to be 0.5 $\mu g/m^3$ in this model. When this relation is superimposed on the Brunswick data, an overall consistency is observed (Figure 5.3). It is worth noting that by 1990, some Brunswick workers were using

improved respirators, operating at an efficiency >95%. If the more highly exposed individuals shown on the scatter plot had been using these respirators on the day of measurement, their effective air lead values would be reduced by a factor greater than two. If true, this scenario would work to bring some of the more extreme air lead values of Figure 5.3 into better agreement with the Snee relation. The lead exposure model, with coefficients from the Williams data, was retained as a first-order approximation of the Brunswick worker blood lead-air lead relation.

The procedure for estimating the air lead exposure of an individual Brunswick worker began by running his/her blood lead records through a computer program. For each year of employment, the worker's time weighted blood lead average was calculated. The time weighting was introduced so as to remove any possible bias which a straight averaging might produce (*eg.* if a worker demonstrating a high blood lead was more likely to be recalled for an additional measurement). The mean blood lead level was entered into Snee's lead exposure model to produce a mean air lead level at work for the employee. This level was then entered (to one significant figure) into the O'Flaherty model of lead kinetics, along with the background inputs from all other sources as described above. At this point, the year-by-year blood lead predictions from the O'Flaherty model were examined. If any yearly value

Figure 5.3

Blood lead-air lead relationship, Brunswick workers.

Lead exposure model is superimposed (Snee, 1982):

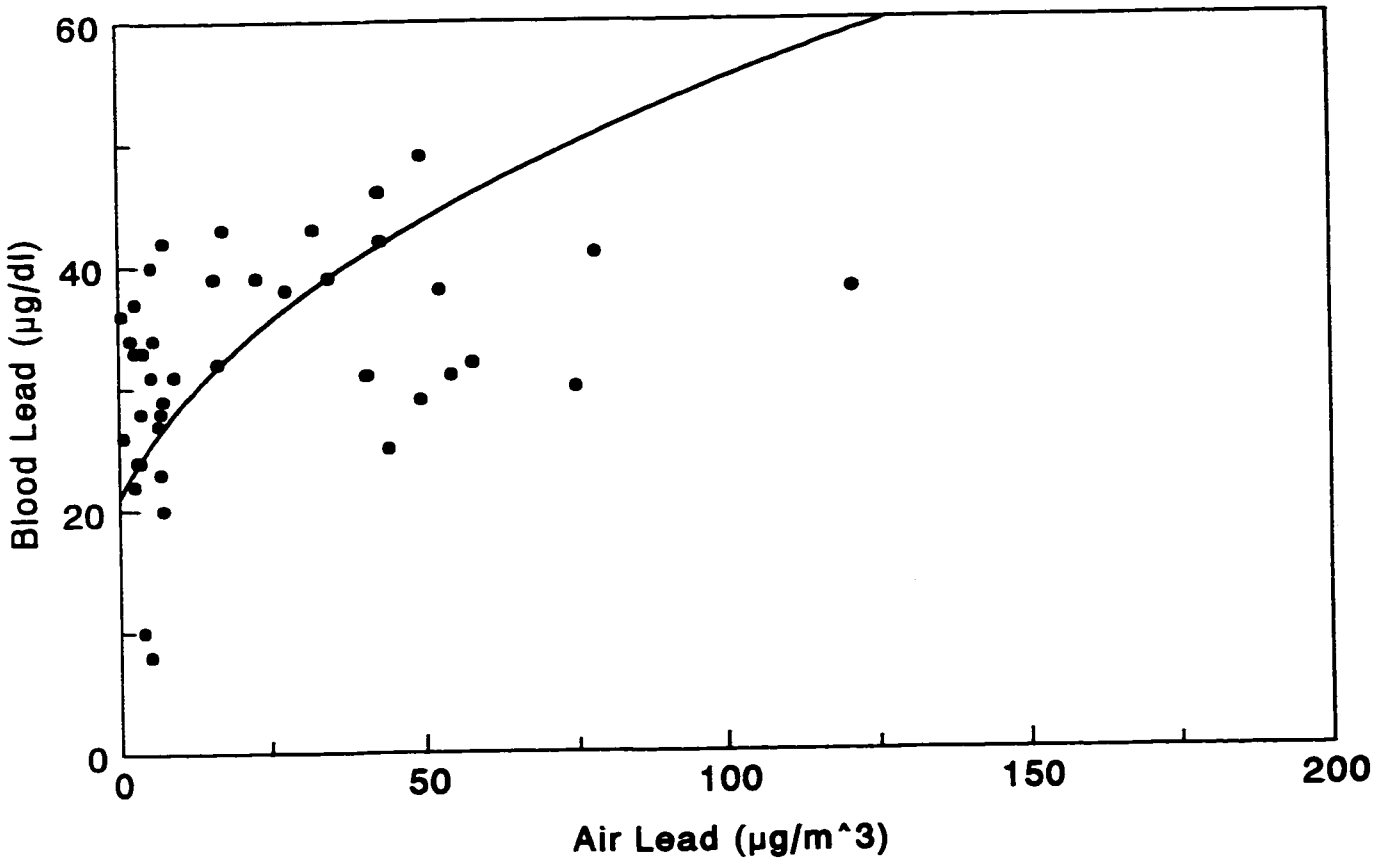

deviated from the observed mean by more than 10%, the assumed air lead input was adjusted accordingly. Often, the early air leads required an upward adjustment while some later entries needed to be scaled down. This observation was consistent with the physiological processes at work: recently hired workers have relatively little contribution to blood lead from bone stores and need additional external exposures to explain their blood levels.

5.3 Initial Results

In this manner, the employment history of lead exposure was modelled for the initial subset of 20 smelter workers. Cumulative blood lead indices were calculated by introducing an integration term to the model. The concentration of lead in cortical and trabecular bone was displayed continuously, and the levels were noted for times in 1994 (corresponding to the X-ray fluorescence measurements) and in 1991 (following the strike). The instantaneous blood lead was also recorded following the strike. This collection of modelled data allowed direct comparisons between the observed results from the Brunswick survey and the predictions of the O'Flaherty model (Tables 5.1-5.7).

On the whole, the results were encouraging, particulary for the revised model 96B and the tibia concentration data.

Table 5.1

Post-strike, blood lead vs. tibia lead concentration:

	all observations	subset of 20	model 96A	model 96B
slope	0.136±0.014	0.143±0.025	0.294±0.041	0.162±0.007
y-int.	13.6±0.8	13.8±1.2	14.1±1.7	9.1±0.8
N	204	20	20	20
r^2	0.31	0.43	0.55	0.93

Table 5.2

Post-strike, blood lead vs. calcaneus lead concentration:

	all observations	subset of 20	model 96A	model 96B
slope	0.078±0.007	0.083±0.013	0.421±0.029	0.542±0.023
y-int.	13.6±0.7	14.0±1.1	8.8±1.2	3.2±1.0
N	204	20	20	20
r^2	0.35	0.49	0.85	0.94

Table 5.3

Pre-1977 hire, tibia lead vs. RCBLI:

	all observations	subset of 20	model 96A	model 96B
slope	0.058±0.005	0.065±0.009	0.037±0.007	0.101±0.017
y-int.	-24±7	-33±14	-5±11	-18±25
N	209	10	10	10
r^2	0.42	0.75	0.58	0.67

Table 5.4

Pre-1977 hire, calcaneus lead vs. RCBLI:

	all observations	subset of 20	model 96A	model 96B
slope	0.127±0.008	0.123±0.020	0.022±0.010	0.023±0.008
y-int.	-76±11	-74±31	6±14	7±12
N	209	10	10	10
r^2	0.58	0.69	0.15	0.27

Table 5.5

More recent hire, tibia lead vs. RCBLI:

	all observations	subset of 20	model 96A	model 96B
slope	0.041±0.003	0.041±0.007	0.042±0.004	0.111±0.011
y-int.	-7±2	-9±5	-1±3	-6±6
N	158	10	10	10
r^2	0.56	0.64	0.85	0.87

Table 5.6

More recent hire, calcaneus lead vs. RCBLI:

	all observations	subset of 20	model 96A	model 96B
slope	0.084±0.005	0.087±0.016	0.038±0.008	0.035±0.007
y-int.	-26±4	-27±11	9±5	10±4
N	158	10	10	10
r^2	0.61	0.61	0.56	0.56

Table 5.7

Calcaneus lead vs. tibia lead:

	all observations	subset of 20	model 96A	model 96B
slope	1.70±0.04	1.73±0.12	0.50±0.08	0.21±0.02
y-int.	0.6±2.2	-1.3±6.2	16.0±3.3	16.0±2.3
N	367	20	20	20
r^2	0.81	0.85	0.47	0.70

Further refinements were nonetheless desirable. The following observations were made regarding the initial two versions of the model:

(1) The calcaneus, when modelled as a trabecular bone, is not consistent with observation (Tables 5.2, 5.4, and 5.6). This may in part be due to the nature of the calcaneus as a bone site. Substantial variability in bone turnover has been noted to exist amongst trabecular bones (for example, see the values for the spine and patella, Report of the Task Group on Reference Man (ICRP, 1975)). This effect could produce marked differences in lead concentration between different trabecular bones, especially in heavily exposed populations.

(2) The changes in diffusion constants D0 and R0 from model 96A to 96B had the effect of reducing the amount of lead leaving bone. As a consequence, the amount of lead in cortical bone forecast by the model became too large: the slopes of the bone lead to RCBLI relations are higher than observed (Tables 5.3 and 5.5). In response, the parameter governing transfer of lead from blood to bone, P0, could be scaled down.

(3) The distinction between the bone lead/RCBLI slopes observed between hiring groups is not evident in the modelled results. This suggests that the serum lead/blood lead relation contained in the model needs to be revised, or that the rate of bone turnover requires adjustment.

5.4 Sensitivity Analysis

In order to discover which model parameters would be most appropriate to revise (and the approximate magnitude of the necessary revisions), a sensitivity analysis was performed. This procedure consisted of isolating key model parameters and subjecting them to systematic variations. The analysis was performed on the same subset of 20 workers identified earlier. Given the rather severe disagreement between the modelled lead concentrations in trabecular bone and those observed in the calcaneus, cortical bone results were used to gauge the effectiveness of the model revisions. The original parameter values and eventual revisions are detailed in Appendix B. Effects of parameter variation on the slope relations are summarized in Tables 5.8-5.12. Differences in the y-intercepts were generally not significant.

5.5 Refinement of Model

These results suggested that the variation of certain parameter values would be more effective than others in reconciling model predictions with the *in vivo* lead concentration data. For example, it was noted above that the cortical lead/RCBLI slopes were too large under model 96B. The sensitivity analysis indicated that the most effective way to reduce these slopes would be to decrease the P0 parameter (which governs transfer of lead from plasma to bone).

Table 5.8

Variations in parameter D0 (diffusion between bone shells):

variation in D0	blood lead /cortical slope	cortical lead /RCBLI slope	cortical lead /RCBLI slope
		pre-1977	more recent
↑ x4	↓ 15%	↑ 27%	↑ 24%
↑ x2	↓ 9%	↑ 14%	↑ 12%
↓ x2	↑ 9%	↓ 11%	↓ 10%
↓ x4	↑ 15%	↓ 19%	↓ 18%

Table 5.9

Variations in parameter R0 (diffusion from bone to plasma):

variation in R0	blood lead /cortical slope	cortical lead /RCBLI slope	cortical lead /RCBLI slope
		pre-1977	more recent
↑ x4	↑ 17%	↓ 24%	↓ 23%
↑ x2	↑ 10%	↓ 15%	↓ 14%
↓ x2	↓ 11%	↑ 19%	↑ 17%
↓ x4	↓ 20%	↑ 38%	↑ 33%

Table 5.10

Variations in parameter P0 (diffusion from plasma to bone):

variation in P0	blood lead /cortical slope	cortical lead /RCBLI slope	cortical lead /RCBLI slope
		pre-1977	more recent
↑ x4	↓ 33%	↑ 99%	↑ 93%
↑ x2	↓ 15%	↑ 33%	↑ 32%
↓ x2	↑ 25%	↓ 32%	↓ 30%
↓ x4	↑ 46%	↓ 50%	↓ 46%

Table 5.11

Variations in parameters CMINFOR and TMINFOR

(rates of bone mineral formation):

variation in MINFOR	blood lead /cortical slope	cortical lead /RCBLI slope	cortical lead /RCBLI slope
		pre-1977	more recent
↑ x4	↑ 54%	↓ 28%	↑ 2%
↑ x2	↑ 25%	↓ 12%	↑ 4%
↓ x2	↓ 20%	↑ 4%	↓ 8%
↓ x4	↓ 37%	↑ 3%	↓ 16%

Table 5.12

Variations in parameters BIND and KBIND

(red blood cell lead-binding coefficients):

variations	blood lead /cortical slope	cortical lead /RCBLI slope	cortical lead /RCBLI slope
		pre-1977	more recent
BIND=2.9 and KBIND=0.0105	↓ 15%	↑ 13%	↑ 18%
BIND=2.8 and KBIND=0.0090	↓ 8%	↑ 7%	↑ 9%
BIND=2.6 and KBIND=0.0060	↑ 10%	↓ 8%	↓ 10%
BIND=2.5 and KBIND=0.0045	↑ 23%	↓ 17%	↓ 21%

As a preliminary step, the P0 parameter was reduced by a factor of two, and the effects were noted (Table 5.13, step 1). The down side of this action was that it served to elevate the predicted slope of the post-strike blood lead/bone lead relation. Nonetheless, in order to steer the model output closer to the overall observations, a reduction by a further factor of two was introduced to P0 (step 2).

At this point, the tibia lead/RCBLI slopes of the two hiring groups were subjected to closer scrutiny. While observations indicated that the population hired in recent years possessed a smaller tibia lead/RCBLI slope, the model produced contradicting results. Inspection of the sensitivity analysis revealed at least two potential parameter changes which consistently proved capable of rectifying this situation. A reduction in the red cell lead-binding coefficients, a reduction in the rates of bone mineral formation, or both, could serve to harmonize the model output with the experimental results.

Reducing the red cell coefficients has the net effect of making the serum lead/whole blood lead ratio relatively more extreme at high blood lead concentrations. This results in a proportionately higher uptake of lead to bone for workers exposed to the highest levels of lead intake, which would help to create the observed slope offset between the hiring groups.

Table 5.13

Changes introduced to model and associated effects:

model	blood lead /tibia lead slope	pre-1977, tibia lead /RCBLI slope	more recent, tibia lead /RCBLI slope
all observations	**0.136**	**0.058**	**0.041**
subset of 20	0.143	0.065	0.041
model 96B	0.162	0.101	0.111
step 1	0.202	0.069	0.078
step 2	0.237	0.050	0.060
step 3	0.302	0.043	0.050
step 4	0.243	0.045	0.045
step 5	0.191	0.045	0.042
step 6	0.185	0.058	0.054
step 7	0.153	0.060	0.054
model 97A	**0.160**	**0.058**	**0.045**

To illustrate with a numerical example, a highly exposed Brunswick worker employed in the early 1970's might have registered a blood lead of 100 μg/dl. With BIND=2.7 and KBIND=0.0075 (original values), this would imply a serum lead concentration of 2.68 μg/dl. A typical worker at Brunswick today would demonstrate a blood lead of 25 μg/dl, and an implied serum lead of 0.187 μg/dl. The difference in blood lead concentrations is a factor of 4; the difference in serum leads, a factor of 14. On the other hand, with BIND=2.5 and KBIND=0.0045, the worker with the blood lead of 100 μg/dl now has a suggested serum lead of 2.47 μg/dl. The modern worker with a blood lead of 25 μg/dl has an implied serum lead of 0.124 μg/dl. So, while the difference in blood lead concentrations is still a factor of 4, the difference in serum leads is a factor of 20. With a reduction in binding coefficients, then, the worker exposed to the more extreme conditions has an even greater bioavailability of lead relative to the more moderately exposed worker.

The results of a recent analysis of whole blood lead concentration and plasma lead concentration in a series of 43 lead smelter workers and seven controls (Schütz *et al.*, 1996) lends support to such a revision in red cell binding parameters. Figure 5.4 demonstrates the Schütz *et al.* data in comparison to that of deSilva (O'Flaherty, 1997). (It should be noted that blood serum is essentially plasma with the clotting agent fibrinogen removed. Therefore, in the context

Figure 5.4

Plasma lead as a function of blood lead concentration. Observations: deSilva (1981, circles); Schutz *et al.* (1996, sqaures). Theoretical relations: BIND=2.7 and KBIND=0.0075 (upper line); BIND=2.5 and KBIND=0.0045 (lower line); data points taken from O'Flaherty (1997):

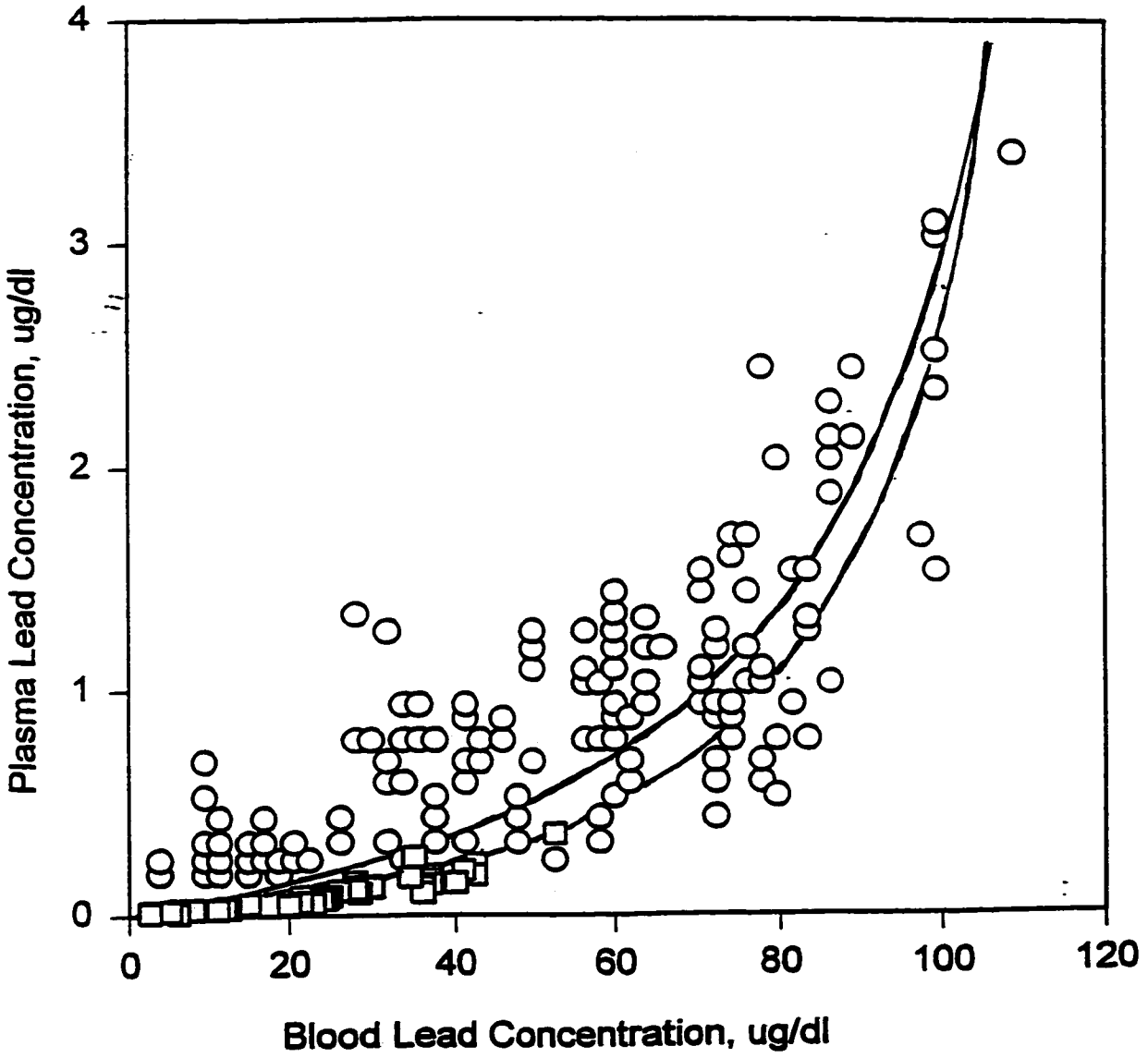

of lead concentration discussions, the two fluids may be considered equivalent.) Superimposed on Figure 5.4 are two curves: one generated with BIND=2.7 and KBIND=0.0075 (original values) and the other with BIND=2.5 and KBIND=0.0045. It is apparent that the revised binding figures are in better agreement with this data set. A somewhat more moderate revision of the binding parameters, with BIND=2.6 and KBIND=0.0060, was applied to the model (Table 5.13, step 3). Note that as a result, the offset in tibia lead/RCBLI slope between workers hired in the early years of smelter operation and those hired more recently has been closed to a small degree.

While the reduction of the binding parameters helped to some extent with the cumulative relations between tibia lead and blood lead, further refinement was necessary. As well, a lowering of the instantaneous (post-strike) blood lead/tibia lead slope was also required in order to bring the modelled results into closer agreement with observation. To demonstrate these two effects in tandem, one parameter emerged from the sensitivity analysis as a clear candidate for revision. If the rates of bone mineral formation were lowered, the two underlying inconsistencies between model and observation might be resolved.

With regard to the smelter population, a reduction in bone mineral formation rate has an unique effect on lead

metabolism model results. The associated reduction in bone turnover means that workers experiencing their highest exposures in the distant past (~20 years) retain *more* lead in bone when examined in the present. This is a logical outcome considering that the high amounts of lead taken up ~20 years ago would have had less opportunity to leave the bone tissue. Workers experiencing their most intense exposure more recently, however, retain *less* lead when monitored today. In this case, the reduction in bone turnover has resulted in a smaller replacement of old (relatively lead-free) bone mineral with new (lead-contaminated) mineral.

The original model input values for CMINFOR and TMINFOR (rates of bone mineral formation for cortical and trabecular bone) were 0.05 and 0.085 kg calcium/year. Using model expressions for the body weight of a typical, 40 year-old male (WBODY=74.9 kg), the amount of bone calcium is calculated to be CABONE=1.154 kg. Of this amount, 80% is cortical, so 0.923 kg of calcium may be found in cortical bone. By extension, 0.231 kg of calcium is in trabecular bone. The fractional cortical bone formation rate is then calculated by dividing the cortical bone formation rate (0.05 kg calcium/year) by the amount of cortical calcium (0.923 kg). The result, 0.054 /year, implies a turnover of cortical bone mineral of just over 5% /year for a typical male adult. The value for the fractional trabecular bone formation rate, calculated in the same manner, is 0.368 /year. These values of 5% and 37% for

the male are to be contrasted with results of 8% and 50% for the female. Weighted skeletal averages are therefore 12% and 16% for the male and female, respectively. Could a reduction in the modelled rate of bone mineral formation be justified?

Studies of tetracycline-labelled human bones have indicated that bone turnover in adult ribs is approximately 3.5% /year (Frost, 1969). The rib, however, is believed to turn over about 50% more rapidly than exclusively cortical bone sites (Kulp and Schulert, 1962). These results provide some potential justification for lowering the model parameters. The inward flux of calcium was identified by another study as being ~11% /year for the skeleton as a whole (Marshall *et al.*, 1973), consistent with the original model estimate for males. A point of debate, however, is to what extent this figure expresses bone formation as opposed to calcium ion exchange. The interpretation was that the true *turnover* rate in cortical bone was 2.5% /year (Marshall *et al.*, 1973), somewhat lower than the O'Flaherty model estimate for fractional cortical formation rate (5.4% /year). In reviewing data from these studies and others involving radium-labelling of bone and the number of osteons observed as a function of age, Parfitt estimates bone turnover rates of 2.5% and 10% /year for cortical and trabecular bone, implying a total skeletal rate of 4% /year (Parfitt, 1976).

Mean turnover rates quoted by the Report of the Task Group on Reference Man (ICRP, 1975) vary between bone site, with values ranging from 1.1-2.9% /year for cortical bones and 3.6-8.3% /year for trabecular bones. These results were adopted from surveys of strontium kinetics in the bones of eight adults (Bryant and Loutit, 1961, 1963). Interestingly, the turnover rate of 1.1% /year was derived from the tibia. The tibia was the cortical bone site selected for measurement in the Brunswick survey, and has been shown to be the site most representative of skeletal lead concentration in a study of five bone sites (Wittmers *et al.*, 1988). Annual turnover rate is estimated in the Report of the Task Group on Reference Man (ICRP, 1975) as 1% for adult cortical bone and 8% for adult vertebrae (from Loutit, 1962).

The difficult nature of estimating rates of bone turnover in humans is clear. Not only can problems arise in methodology, but the variations between bone sites and the difficulties in interpreting data complicate any assessment. The general indication appears to be that a downward revision of bone formation rates (in males) from the original values of 5.4% and 37% /year is justifiable, up to perhaps a factor of five.

The reduction of both CMINFOR and TMINFOR by a factor of two produced desired changes in the tibia lead/RCBLI and post-

strike blood lead/tibia lead relations (Table 5.13, step 4). For the first time, workers hired before 1977 demonstrated the greater tibia lead/RCBLI slope, although only by a small margin. The endogenous relation between instantaneous blood lead following the strike and tibia lead concentration moved from a slope of 0.30 to a slope of 0.24, closer to the desired value of 0.14. A further reduction in the bone mineral formation rates by an additional factor of two had similar effects (step 5). The distinction between the two hiring groups became more apparent: workers hired before 1977 demonstrated a tibia lead/RCBLI slope of 0.045, while those hired since that time produced a slope of 0.042. The relation between post-strike blood lead and tibia lead had a best fit slope of 0.19.

At this stage, some fine tuning of the parameters was considered necessary. In particular, the tibia lead/RCBLI relations were too shallow: the model was now predicting tibia lead concentrations which were too small considering the given exposure circumstance. To remedy this situation, the parameter dealing with diffusion of lead from plasma to bone, P0, was raised slightly (Table 5.13, step 6). This represented a small backtrack from the initial reductions in this parameter (steps 1 and 2). This variation in P0 had the additional benefits of providing a slight increase in the difference in slope between hiring groups, and a small

reduction in the slope of the endogenous relation. As a final revision, the bone mineral formation rates were rounded down such that CMINFOR=0.01 and TMINFOR=0.02. The fractional formation rates associated with these values are 1.1% and 8.7% /year for cortical and trabecular bone, respectively. This last revision (step 7) brought all three relations into closer agreement with observation.

Comparing the results of the "step 7" model to observation, one compelling difference remains. The slope of the tibia lead/RCBLI relation predicted by the model for workers hired recently is distinctly greater than that observed from the actual smelter workers. It was speculated that this difference was perhaps an artifact of the worker subset (N=20) selection process. As noted above, the subset was isolated so as to reflect the patterns observed in the population as a whole (N=381). Another selection criterion, however, was that the workers have well documented blood lead histories. This led to the exclusion of a sizable portion of the recently hired population that had been employed at the smelter for less than five years. It was postulated that this served to artificially inflate the tibia lead/RCBLI slope of the recently hired workers subset (N=10). As the "step 7" model was applied to more and more workers, the slope for the recently hired group was monitored closely to see if this was the case. With the inclusion of a greater cross-section of

workers, it became clear that the model slope was indeed reproducing the significantly lower observed result. The "step 7" model was therefore retained as the final revised product (model 97A), and applied to all of the smelter workers (Table 5.13). The final agreement with observation was excellent, and will be detailed more thoroughly below.

5.6 Model Results: Tibia Lead

The simulated results from the revised lead metabolism model may be compared directly with the observations obtained from the Brunswick smelter population. The experimental results are described in detail in Chapter 2. After introducing the revisions described above, the model values for cortical bone lead are in excellent agreement with observed tibia concentrations. Three crucial relations were reproduced to good approximation by the revised O'Flaherty model: one describing the endogenous release of lead from cortical bone, another the cumulative effect of lead exposure on cortical stores for workers hired before 1977, and a third the cumulative effect on stores for workers hired more recently. It is important to note that these lead concentration results were consistent with measures of cortical bone obtained at a site midway along the diaphysis of the tibia. Lead concentrations at other cortical sites could differ in magnitude, as could the associated rates of bone

turnover. The degree of variation between cortical sites is a matter of interest for future study.

The modelled post-strike blood lead levels (BPb, given in μg/dl) are shown as a function of tibia lead concentration (T, given in μg/g) in Figure 5.5. The best fit linear relation describing this data is the following:

$$BPb = (0.160 \pm 0.005)\,T + (11.3 \pm 0.3).$$

The coefficient of determination (r^2) is 0.74 from a sample size (N) of 204 simulated workers. This result compares with the same relation derived from observation:

$$BPb = (0.136 \pm 0.014)\,T + (13.6 \pm 0.8).$$

Considering only Brunswick workers hired before 1977, the tibia lead concentrations (μg/g bone mineral) were compared with revised CBLI values (year * μg/dl) for the modelled employees:

$$T = (0.0582 \pm 0.0014)\,CBLI - (17 \pm 2)\ [N=209; r^2=0.79].$$

These data are displayed together with those from workers hired more recently in Figure 5.6. The modelled results are in excellent agreement with the observed relation for workers hired in the early years of smelter operation:

$$T = (0.0584 \pm 0.0048)\,CBLI - (24 \pm 7).$$

Figure 5.5

Modelled blood lead levels as a function of tibia lead concentration following labour disruption:

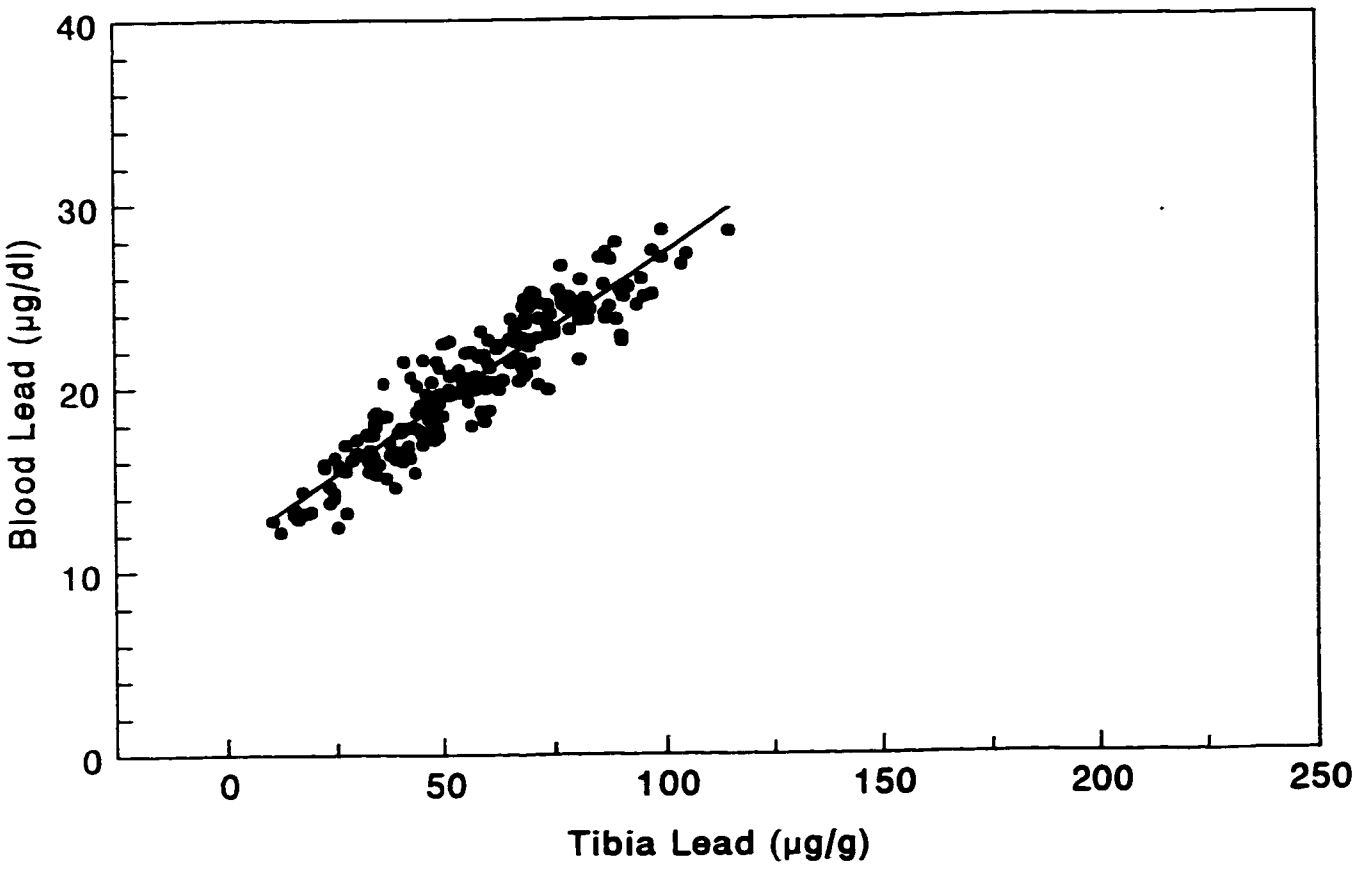

Figure 5.6

Modelled tibia lead concentration as a function of revised CBLI, with data divided by time of worker hire:

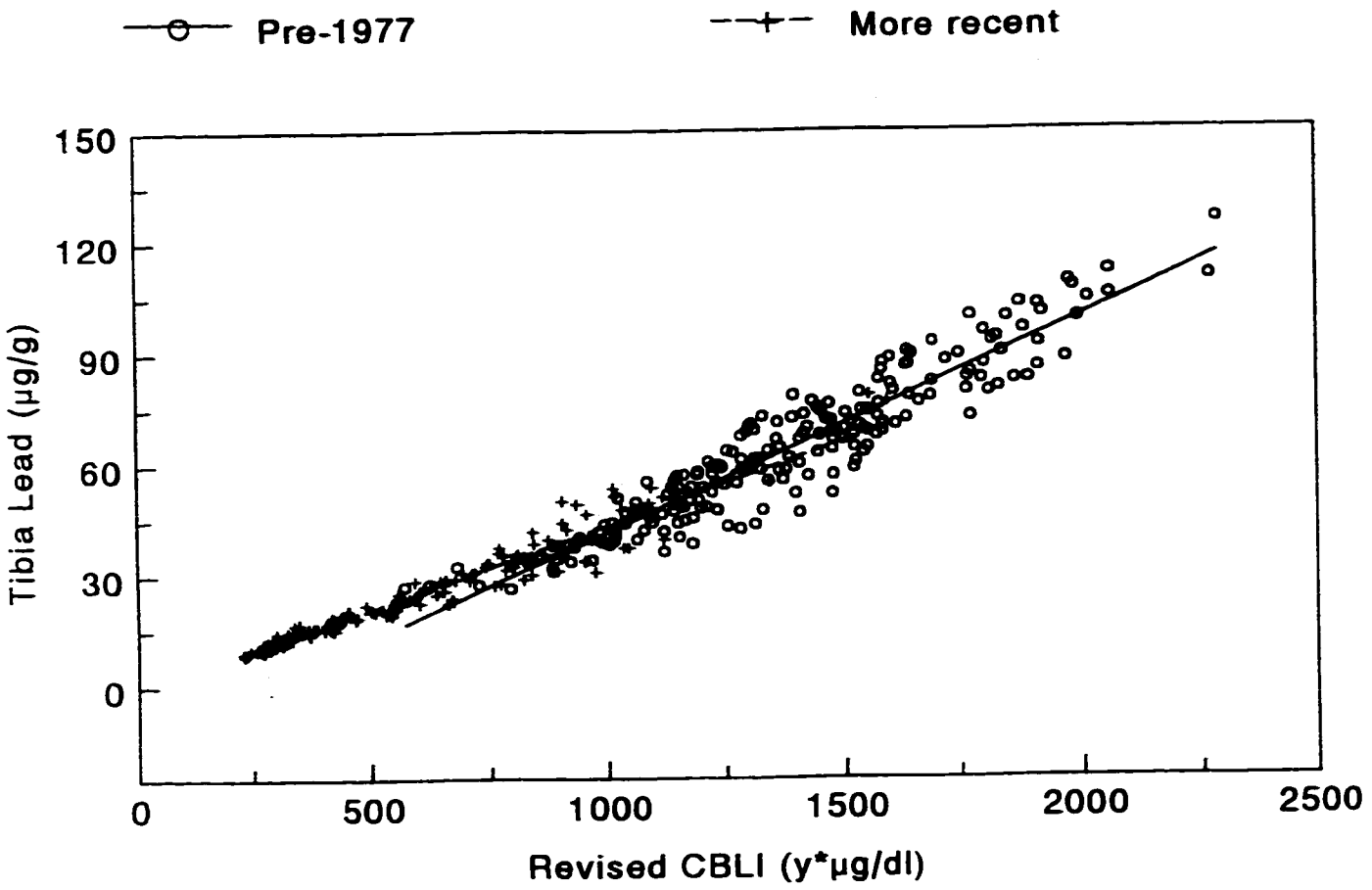

For workers hired more recently, the best fit linear equation relating the same model variables is

$$T=(0.0454\pm0.0009)CBLI-(2\pm1)\ [N=158;r^2=0.88].$$

This again compares favourably with observation:

$$T=(0.0406\pm0.0029)CBLI-(7\pm2).$$

Of particular interest here is the offset in tibia lead/RCBLI slope between the two hiring groups. While the difference predicted by the lead metabolism model is smaller in magnitude than that observed, its significance is no less remarkable. In fact, because of the very small degree of scatter in the simulated relations, the modelled offset is slightly *more* significant. The model suggests that the higher exposures characteristic of employment during the early Brunswick years translated to very much higher plasma lead concentrations, as represented by the non-linear relation of Figure 5.4. The elevated plamsa lead concentrations produced greater overall transfers to tissue in early workers, the effects of which are observable in bone to this day.

Substantial individual variation in lead metabolism was indicated by the scatter of observed results. It is clear that however well a model of lead metabolism may describe a population as a whole, it cannot be reliable on an individual basis without detailed knowledge of individual physiology. A

further contribution to the scatter in observed results is the uncertainty inherent in experimental measurement. The modelled results, by comparison, exhibit very little scatter. This is not surprising since individual variation in metabolism is not taken into account and measurement error is non-existent. The small degree of scatter which is present in the modelled relations is a product of the different exposure histories used as input.

An indication of the success of the O'Flaherty model on an individual basis may be provided by comparing predicted tibia lead concentration with the tibia measurement made in 1994. In the case of worker A, hired in 1979 at the age of 19, the model appears to have been particularly accurate. Figure 5.7 displays the modelled blood lead concentrations for this worker, together with his yearly mean observations. It is not surprising that agreement is excellent since model exposure conditions were derived directly from observed blood lead data (recall that model output was required to match observation within 10% in this respect). The model, however, also reproduces the observed tibia lead concentration very well, to within the uncertainty of the measurement (Figure 5.8). Notice also the very brief downturn in modelled tibia lead concentration during the strike, approximately at age 30 for this individual. A small extrapolation into the future has been provided, calculated with a workplace air lead exposure that approximates current Brunswick levels. In this

Figure 5.7

Modelled (continuous line) and observed (scatter points) blood lead concentrations as a function of time for Worker A:

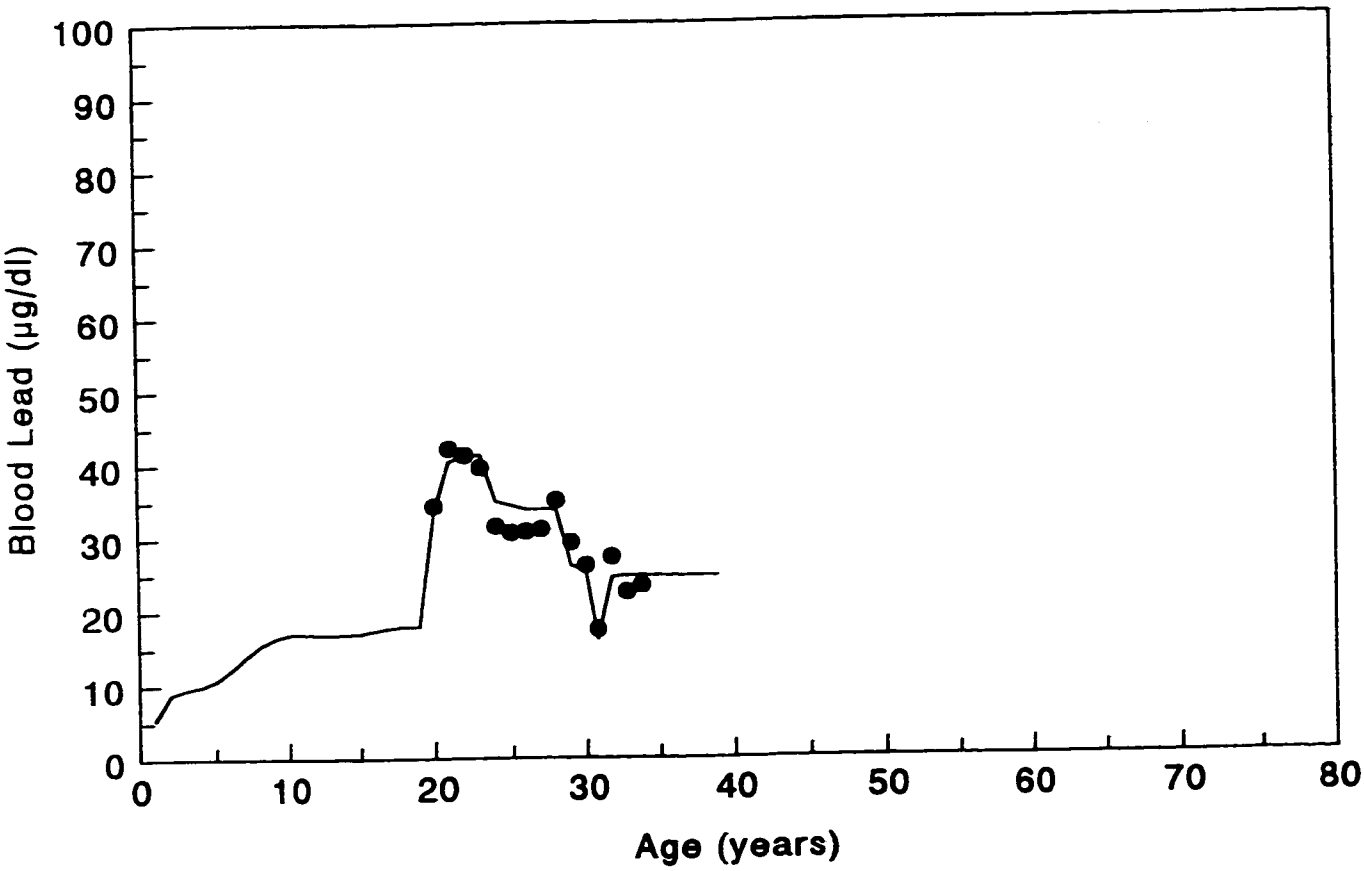

Figure 5.8

Modelled (continuous line) and observed (single point) tibia lead concentrations as a function of time for Worker A. Note the subtle decrease in tibia lead during the strike:

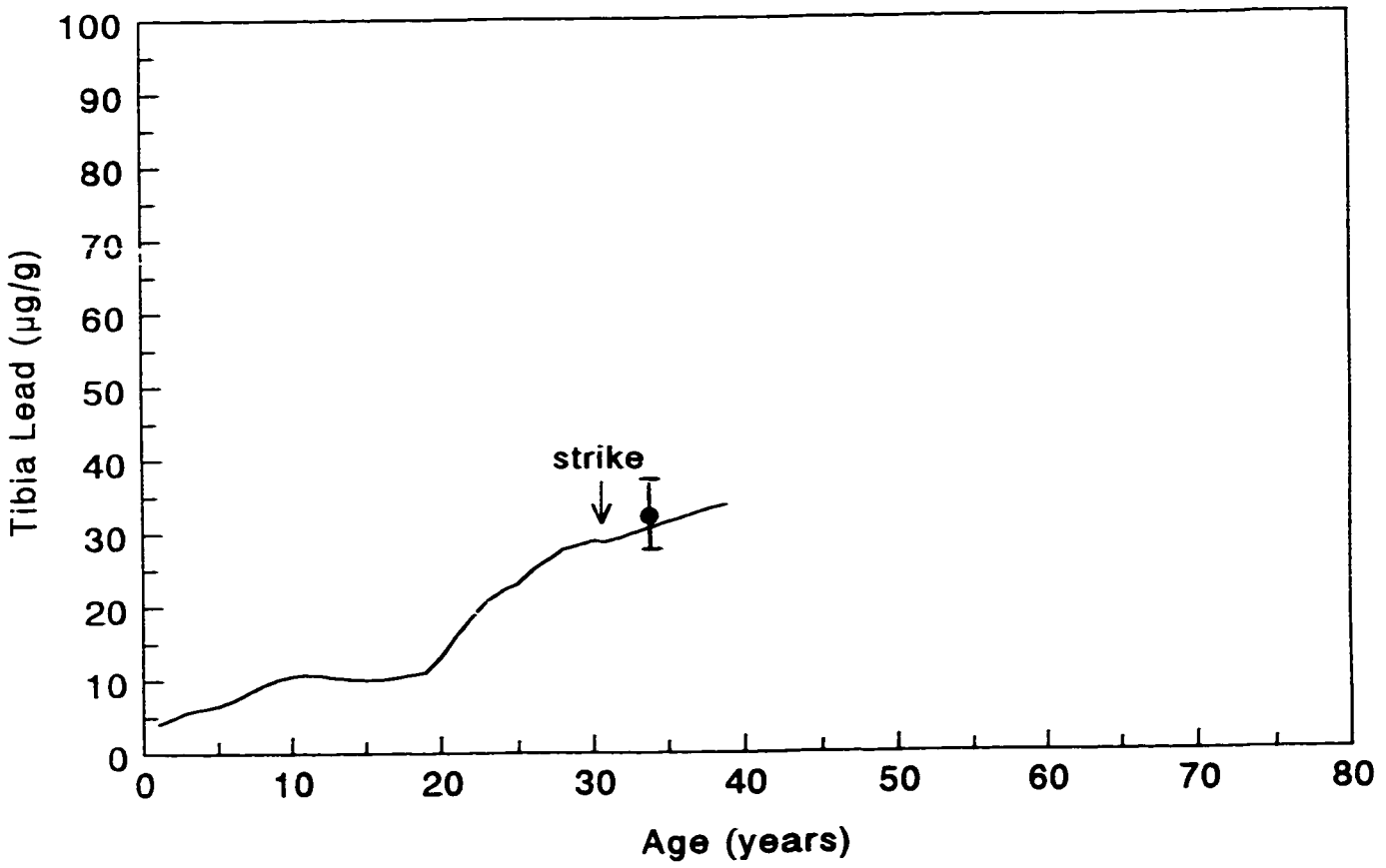

way, the possibility of repeat measurements may provide an independent verification of model validity.

Worker B was hired in 1966 at the age of 21, and was exposed to some fairly extreme conditions during his initial years. The simulated blood lead concentrations are again in very good agreement with observation (Figure 5.9). Since worker B is about 15 years older than worker A, his background exposure to lead during adolescence was assumed to be slightly greater; this is evidenced by the modelled blood lead concentrations. Figure 5.10 shows modelled tibia lead as a function of time. It is interesting to note the very rapid increase in bone lead resulting from the first decade of smelter exposure. The brief plateau at age 25 and sustained levelling beyond age 40 reflect blood lead reductions in the worker's recent past. Despite near-identical present day exposure patterns, worker B demonstrates a decline in tibia lead whereas the stores of worker A continue to increase. This is a clear indication of the difference in past exposure histories.

Worker C also joined the smelter workforce in 1966, at the age of 42. He retired from the job in 1985. Blood lead records were sparse for worker C over the last five years of his employment, so a gradual decline in exposure was

Figure 5.9

Modelled (continuous line) and observed (scatter points) blood lead concentrations as a function of time for Worker B:

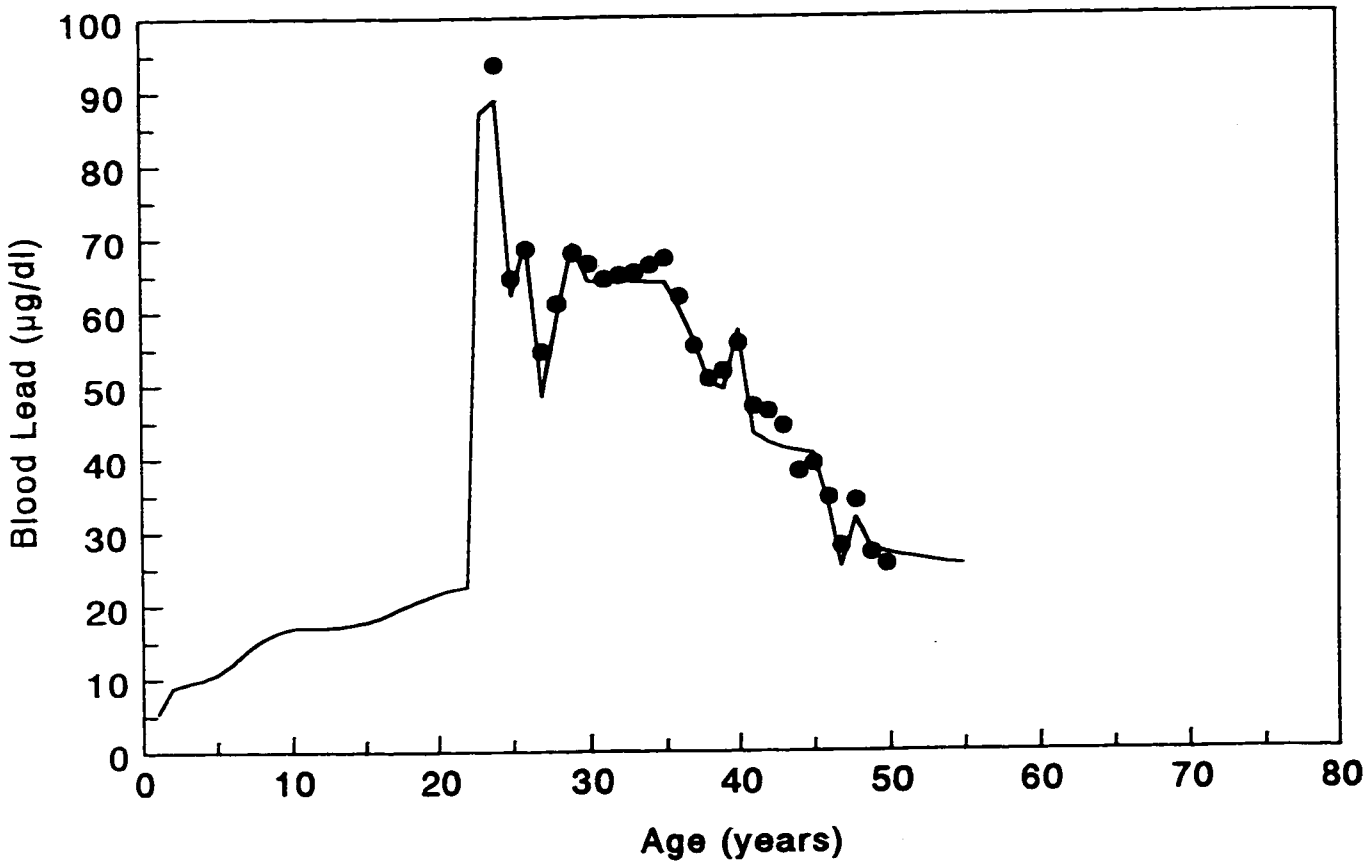

Figure 5.10

Modelled (continuous line) and observed (single point) tibia lead concentrations as a function of time for Worker B:

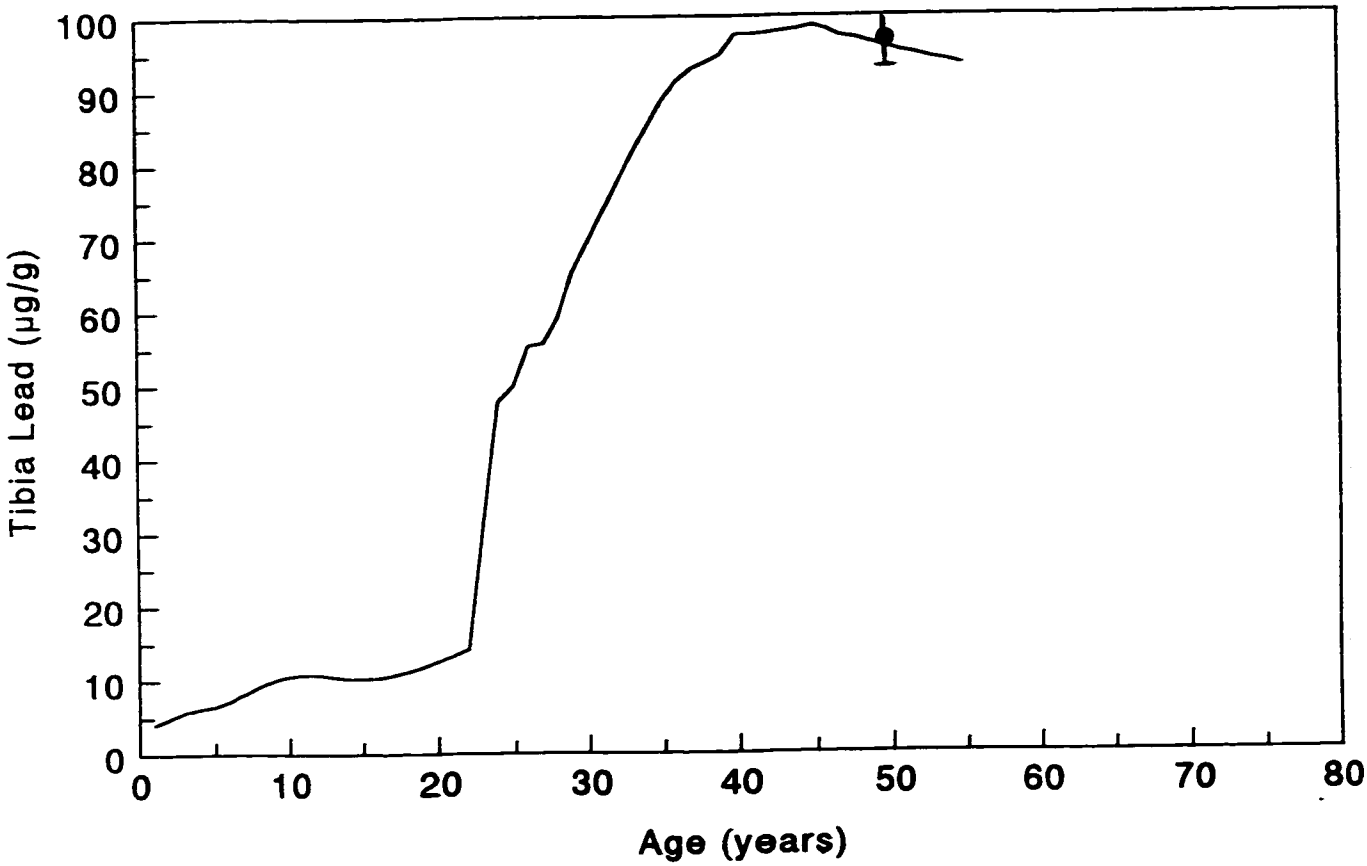

incorporated into the simulation (Figure 5.11). As a retired participant in the survey, the main contribution to present-day blood lead concentration for worker C is lead release from bone. This results in a decline in bone lead stores, as demonstrated in Figure 5.12. This gradual decline is expected to continue indefinitely, with blood lead levelling off to reflect endogenous and background exposures.

The agreement between theory and observation was not, of course, always as good as indicated by the preceding three examples. Workers D, E, and F (Figures 5.13-5.15) represent results for which the model predictions of tibia lead concentration do not neatly coincide with observation. Workers D and E were both born in 1952; Worker D started at the smelter at the age of 28, while Worker E began when 22 years old. Worker F was born in 1929, and was employed at the smelter from age 38 to 62. The model was especially unsuccessful in predicting the tibia lead concentration for Worker F. A variety of explanations are possible: perhaps this individual's rate of bone turnover is higher than expected, or maybe his red blood cells have an especially high affinity for lead. Bone lead measurement error is possible. The problem might partially originate with the simulated exposure conditions. Blood lead measurements were unavailable for this worker during his first year of employment, so exposure was inferred from his second year readings (which were extremely high, over 100 μg/dl on average).

Figure 5.11

Modelled (continuous line) and observed (scatter points) blood lead concentrations as a function of time for Worker C:

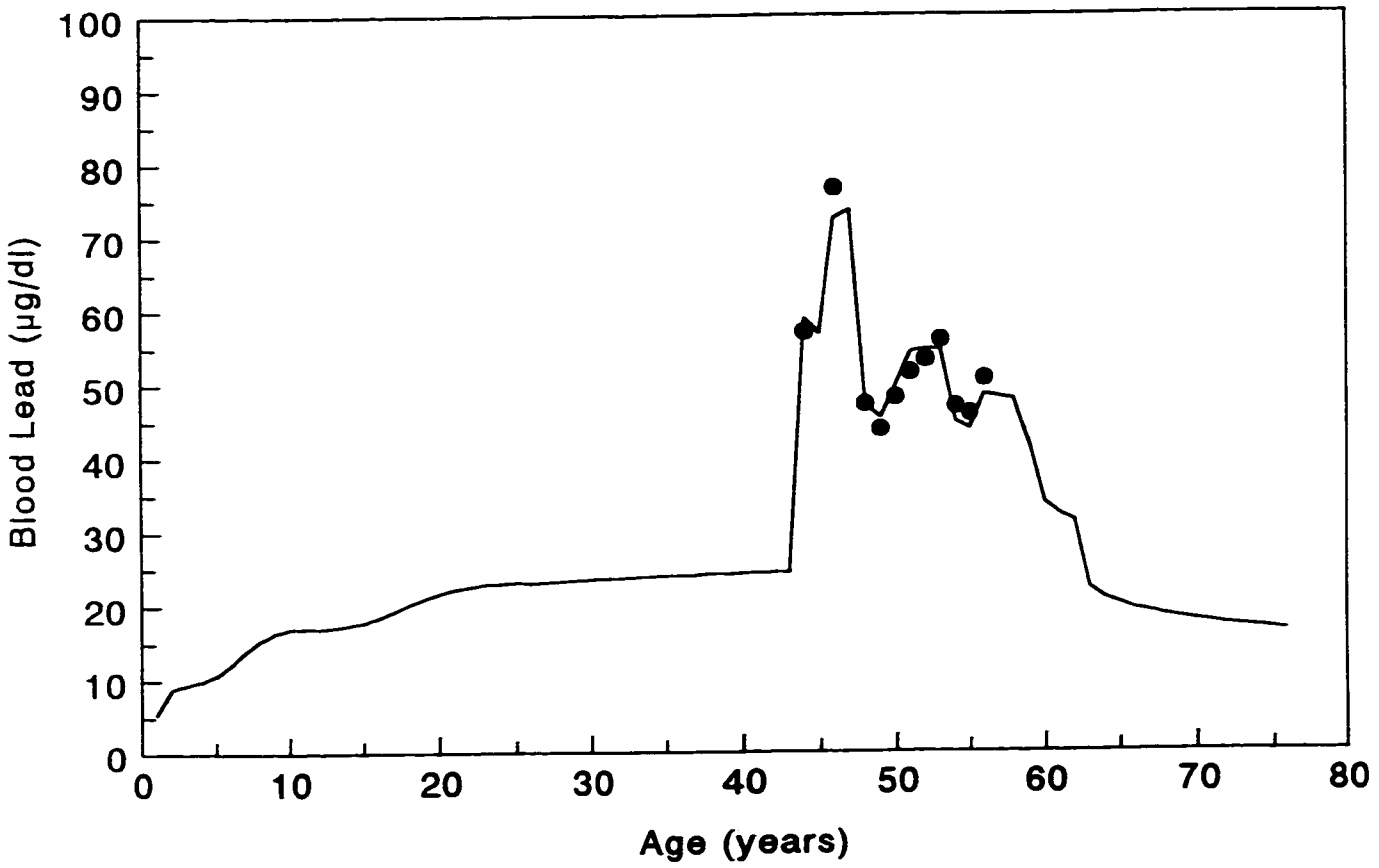

Figure 5.12

Modelled (continuous line) and observed (single point) tibia lead concentrations as a function of time for Worker C:

Figure 5.13

Modelled (continuous line) and observed (single point) tibia lead concentrations as a function of time for Worker D:

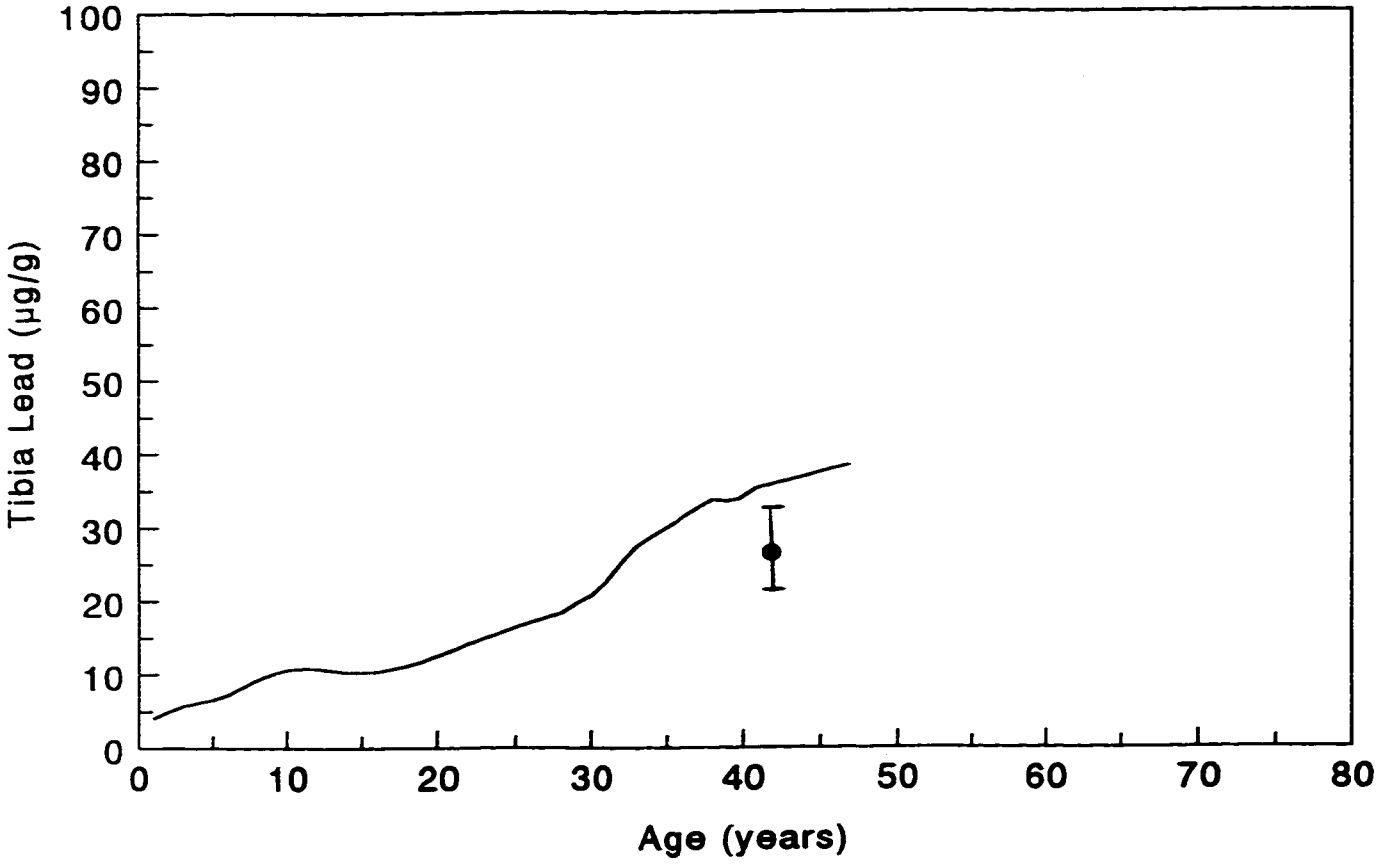

Figure 5.14

Modelled (continuous line) and observed (single point) tibia lead concentrations as a function of time for Worker E:

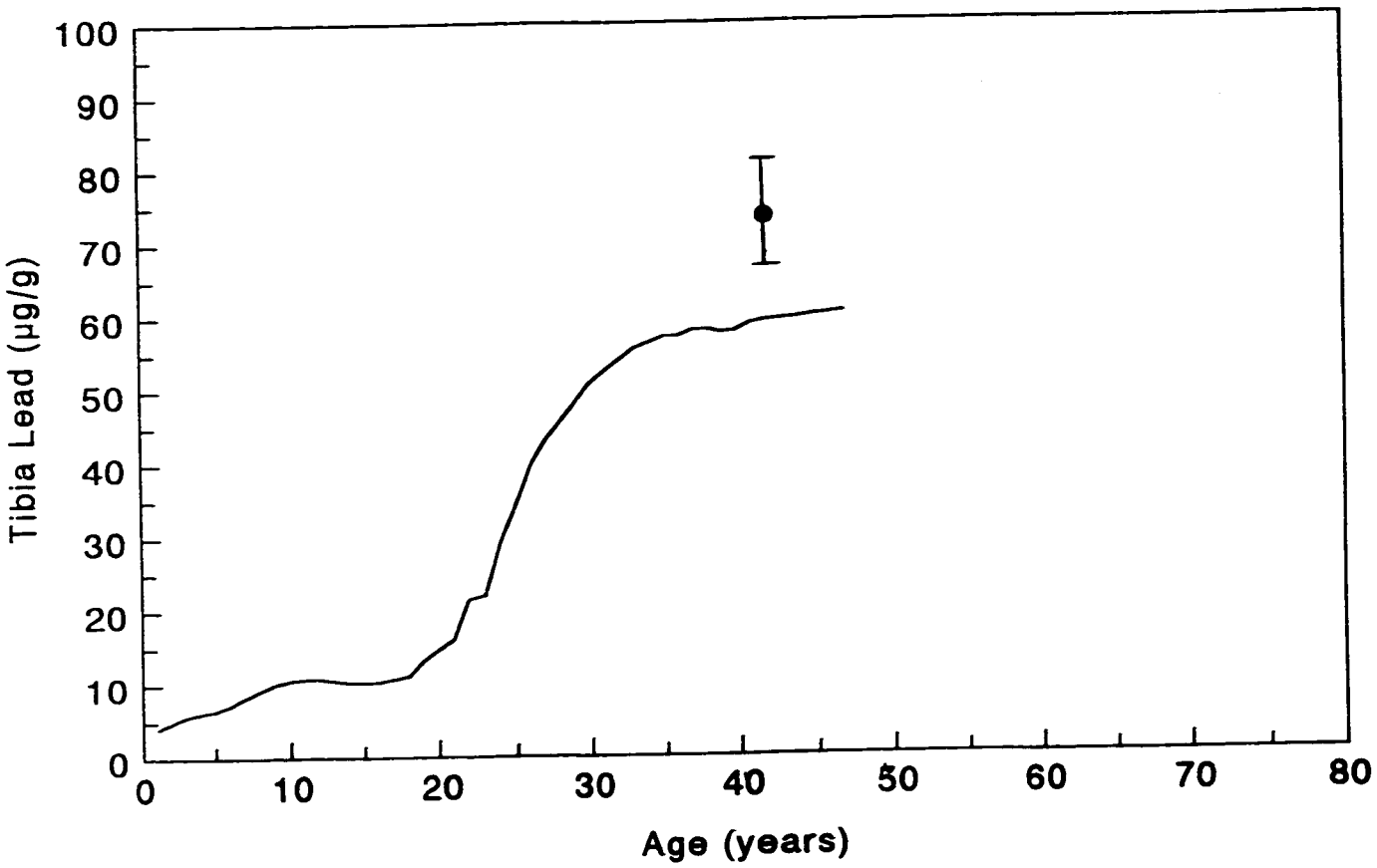

Figure 5.15

Modelled (continuous line) and observed (single point) tibia lead concentrations as a function of time for Worker F:

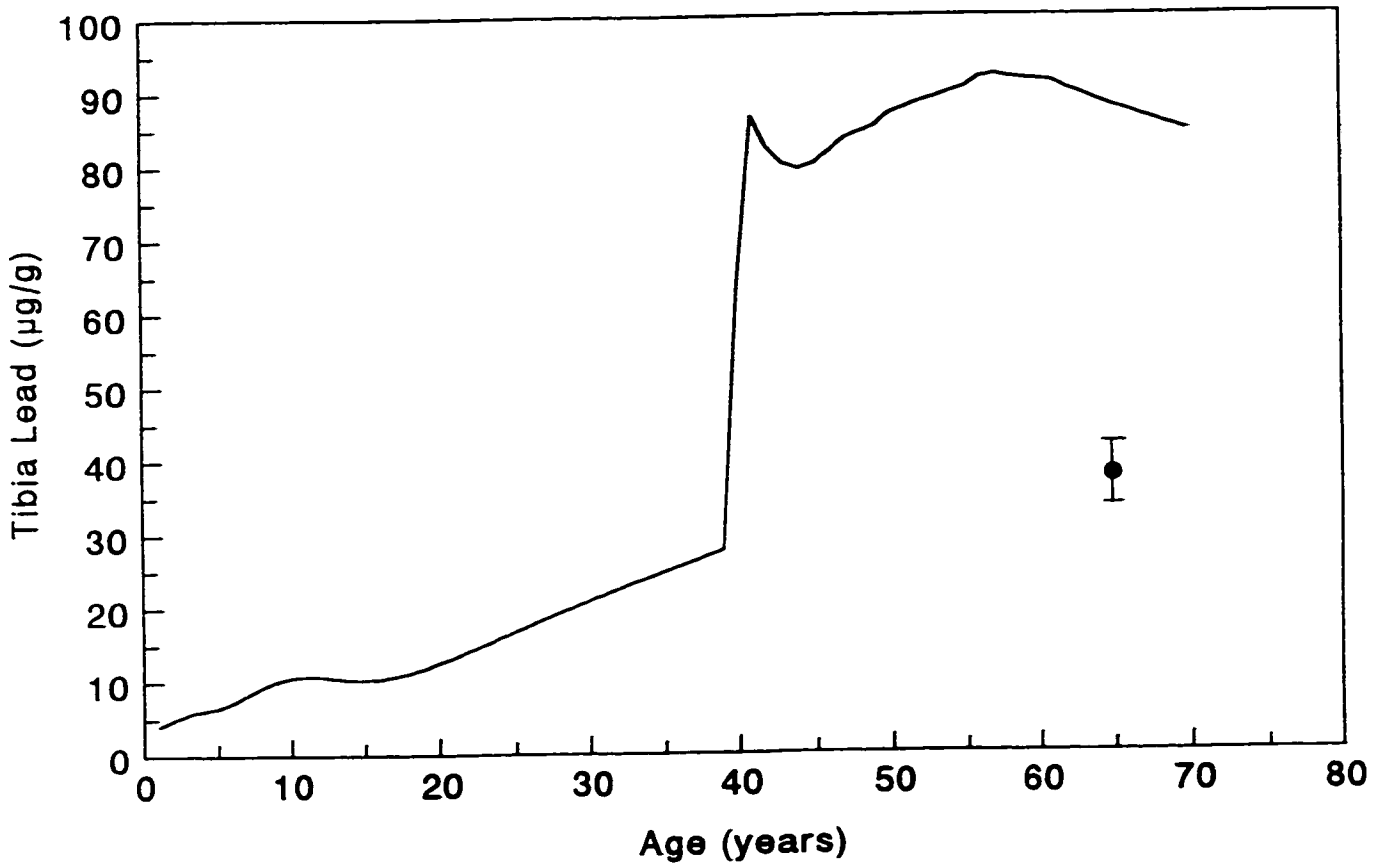

Overall, however, the individually modelled tibia lead concentrations were in good agreement with observation. Quantitatively, the reduced χ^2 between model output and observation was 6.0 μg/g. To place this in perspective, a comparison of concentrations derived from the best fit linear equations (relating tibia lead to CBLI for the appropriate hiring group) and observations produces a reduced χ^2 of 7.2 μg/g. The favourable χ^2 result comes in spite of the revised model's tendency to return tibia lead concentrations which are too high relative to observation. This drawback of the revised model is evident from a comparison of the y-intercepts between the modelled and observed tibia lead-CBLI relations. Further model refinements which could correct this feature, while maintaining population-wide trends, would allow improved predictive power on an individual-by-individual basis.

5.7 Model Results: Calcaneus Lead

The model output for trabecular bone lead was generally not in good agreement with observed calcaneus concentrations. For example, the linear equation best approximating the relation between post-strike blood lead (BPb, given in μg/dl) and calcaneus lead concentration (C, given in μg/g) is superimposed over the modelled data in Figure 5.16. The equation describing this relation is

$$BPb=(0.250\pm0.005)C+(9.2\pm0.2)\ [N=204; r^2=0.84].$$

In contrast, the observed relation between these variables was

$$BPb=(0.078\pm0.007)C+(13.6\pm0.7).$$

Modelled calcaneus lead concentrations (μg/g bone mineral) are plotted against revised CBLI (year * μg/dl) in Figure 5.17. For workers hired before 1977, the linear regression which best describes this relation is as follows:

$$C=(0.0271\pm0.0019)CBLI+(6\pm3)\ [N=209; r^2=0.25].$$

The observed relation, on the other hand, was of the form

$$C=(0.127\pm0.008)CBLI-(76\pm11).$$

Workers hired more recently displayed the following relation between model variables:

$$C=(0.0299\pm0.0016)CBLI+(5\pm1)\ [N=158; r^2=0.48].$$

Observation, however, once again revealed a substantially different relation:

$$C=(0.0842\pm0.0054)CBLI-(26\pm4).$$

On the whole, the trabecular lead concentrations output from the model were much lower than the calcaneus values measured during the smelter survey. This was particularly true for the workers who have spent the greatest number of

Figure 5.16

Modelled blood lead levels as a function of calcaneus lead concentration following labour disruption:

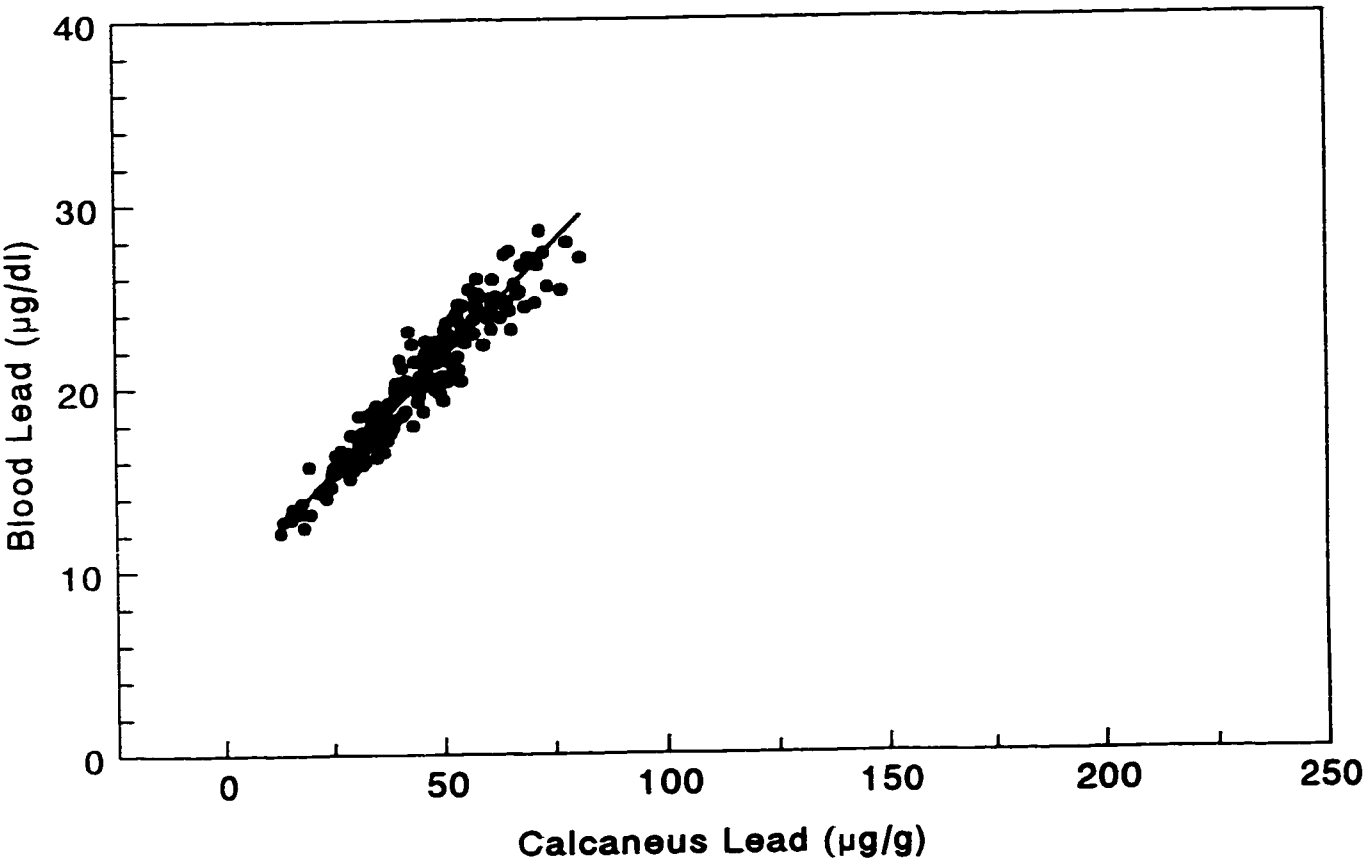

Figure 5.17

Modelled calcaneus lead concentration as a function of revised CBLI, with data divided by time of worker hire:

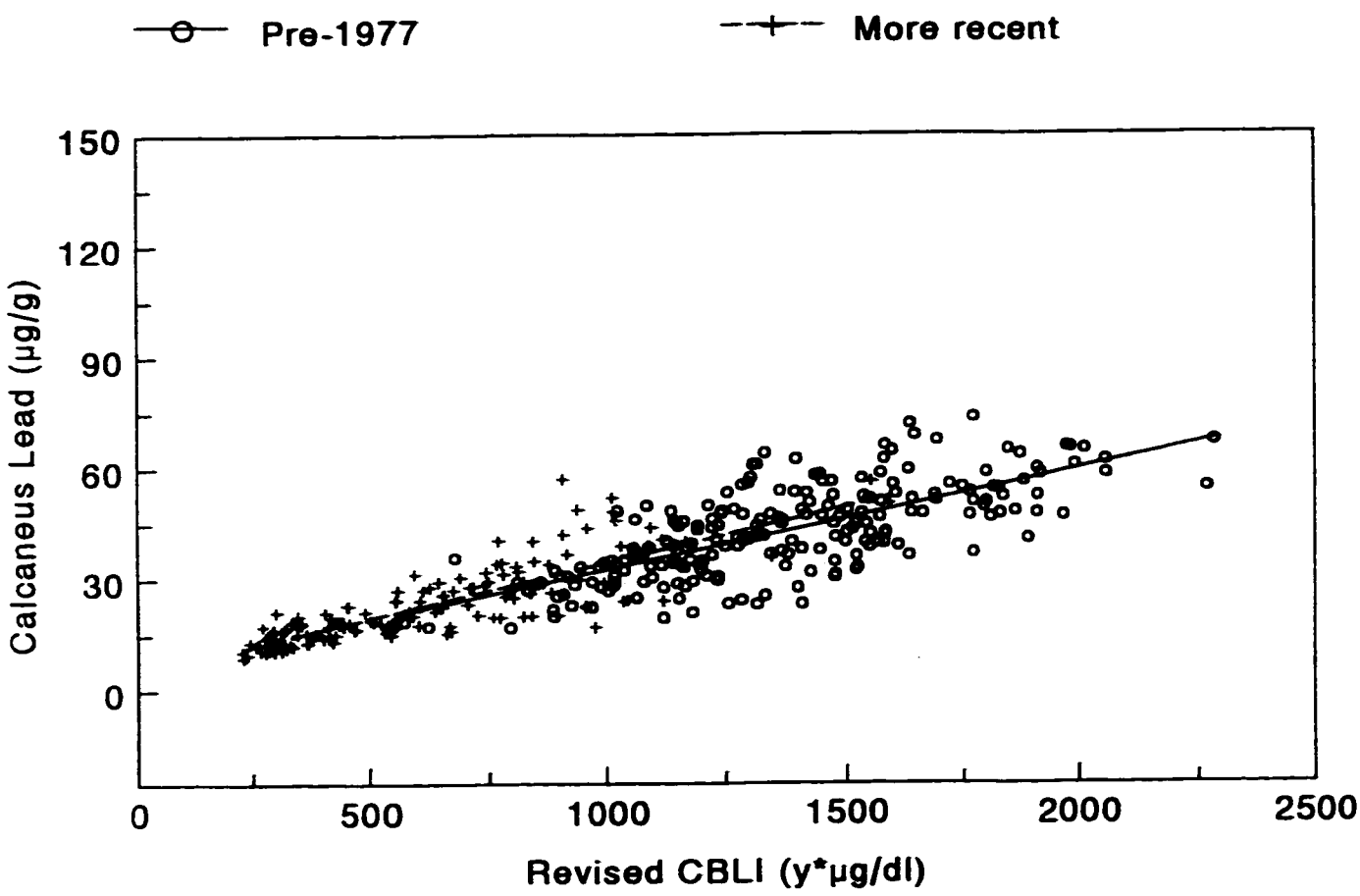

years on site. The model shows no significant difference in the bone lead/RCBLI relation between hiring groups, in strong contrast to the observed results. As well, the model indicates a positive y-intercept for this relation, as opposed to the clearly negative y-intercept which was observed. These discrepancies suggest that the calcaneus needs to be modelled in a fundamentally different way.

Surprisingly, the calcaneus/RCBLI relations for the Brunswick population were quite similar in appearance to the tibia/RCBLI relations. Lead appears to have been retained in the calcaneus over long periods of time, producing an offset in slope between hiring groups. Independent of exposure history, calcaneus lead concentrations were generally about 1.7 times those of the tibia (Chapter 2). These results argue against the suggestion of a short half-life for lead in the calcaneus (Erkkilä *et al.*, 1992). In fact, limited model trials imply that a lead turnover rate of approximately 1 % /year is required to best satisfy the current observations. The calcaneus appears to require a modelling approach similar to that for the tibia, but with a higher rate of lead uptake from blood to bone.

The problems encountered in modelling the calcaneus site as a trabecular bone do not, however, necessarily reflect upon the overall performance of the model. Model output was more consistent with the metabolism of lead at other trabecular

sites which display low lead retention or relatively high turnover. For example, Wittmers *et al.* (1988) found human lead concentrations at autopsy to be consistently *lower* in the vertebra, illium, and rib than in the tibia at ages greater than 35 years. In addition, biopsy results of vertebrae (Schütz *et al.*, 1987) and X-ray fluorescence measurements of the patella (Hu *et al.*, 1991) from lead industry workers are suggestive of relatively high rates of lead turnover in these trabecular sites. Substantial variation in lead uptake and retention is apparent between different trabecular sites (Wittmers *et al.*, 1988). Since trabecular bone comprises only about 20% of total bone composition, metabolic differences between individual trabecular sites should not introduce major errors to the current model.

The calcaneus results do, however, indicate that the trabecular component of bone may benefit from a further subdivision in subsequent modelling efforts. Human lead concentrations measured from several trabecular sites have suggested higher uptake and/or lower turnover of lead than demonstrated by the model. In a recent study of occupationally exposed subjects, sternum and calcaneus lead concentrations were well-correlated and higher in magnitude than tibia levels (Erkillä *et al.*, 1992). Likewise, X-ray fluorescence measurements in the patella have shown elevated concentrations of lead relative to the tibia in occupationally (Hu *et al.*, 1991) and environmentally (Hu *et al.*, 1996)

exposed groups. A relatively low rate of lead turnover in calcaneus was suggested by the strong correlation (r=0.89) observed between calcaneus lead concentration and a cumulative blood lead index from 90 Swedish lead workers (Somervaille *et al.*, 1989).

5.8 Model Results: Genetics

The comparison of bone lead/RCBLI slopes between Brunswick workers of ALAD type 1-1 and workers of type 1-2/2-2 was suggestive of a genetic difference in lead metabolism (Chapter 3). It is possible to make an independent test of the validity of this hypothesis by comparing modelled results from the identical genetic subgroups. Since the model contains no consideration of any genetic difference in lead kinetics, the model output should be essentially the same for both the 1-1 and 1-2/2-2 subgroups. On the other hand, if the metabolic difference inferred from the observations was an artifact of exposure condition or some other selection bias, the model should be able to reproduce the observed offset.

The complete set of modelled data, divided into genetic subgroups by ALAD type, is displayed in Figure 5.18. Isolating the 311 participating workers of ALAD type 1-1, a comparison of modelled tibia lead concentration (μg/g bone

Figure 5.18

Modelled tibia lead concentration as a function of revised CBLI, with data divided by ALAD type:

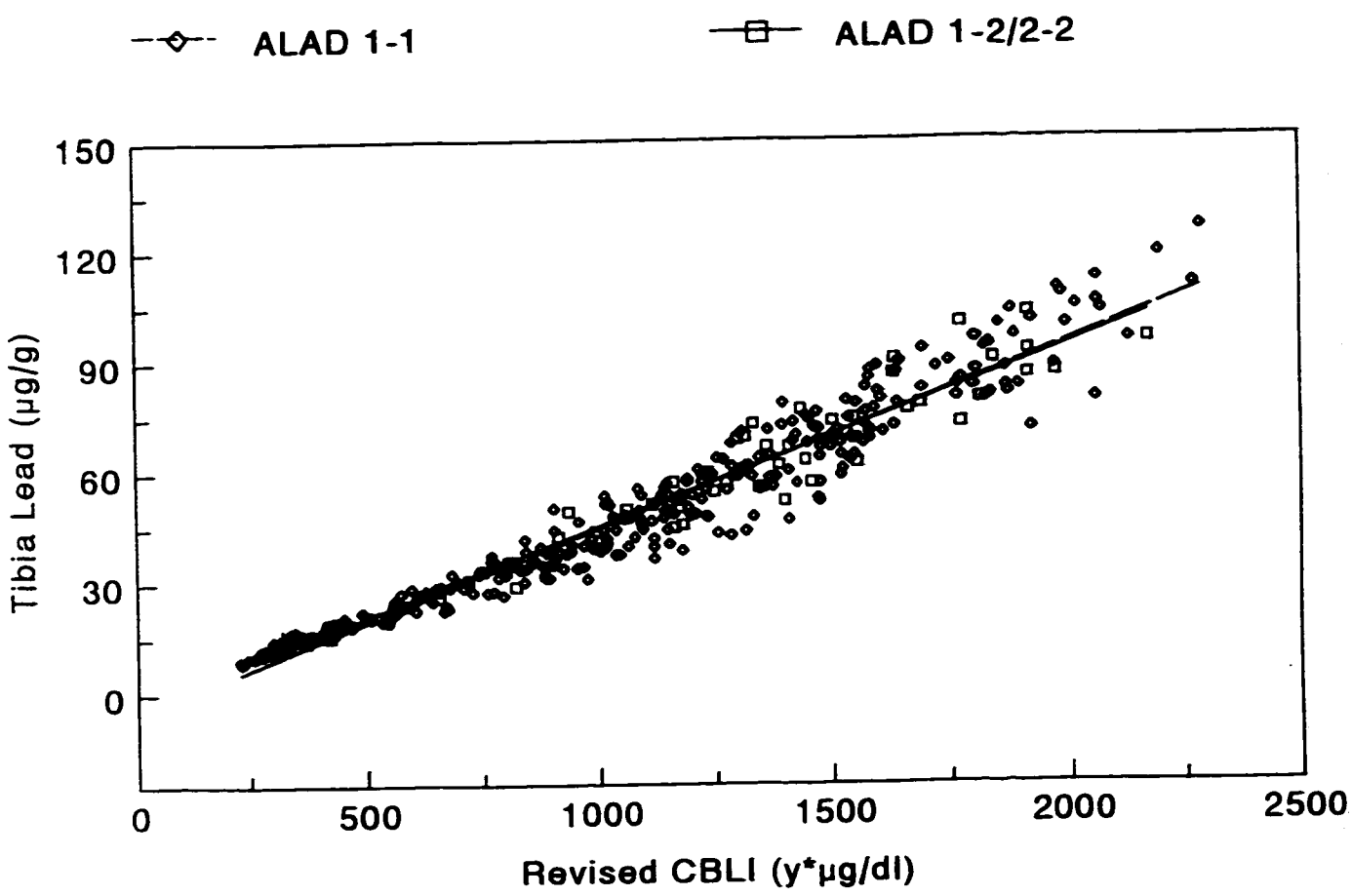

mineral) was made with revised CBLI (year * μg/dl). The following linear relation best describes the output:

$$T=(0.0503\pm0.0007)\,CBLI-(6\pm1)\;[N=311;r^2=0.88].$$

The observed relation from the ALAD 1-1 group of workers was

$$T=(0.0513\pm0.0020)\,CBLI-(14\pm2).$$

The model results for workers of type 1-2/2-2 was best fit by the linear relation

$$T=(0.0491\pm0.0014)\,CBLI-(4\pm2)\;[N=70;r^2=0.90].$$

This is to be compared with the equation relating the same variables observed in the Brunswick 1-2/2-2 population:

$$T=(0.0427\pm0.0045)\,CBLI-(7\pm6).$$

The difference in modelled tibia lead/RCBLI slope between the two genetic subgroups was 0.0012±0.0016. The simulated results therefore indicate that the slope for ALAD type 1-1 workers should be consistent with the slope from 1-2/2-2 workers. Observations, on the other hand, revealed a difference in slope of 0.0086±0.0049 between the genetic subgroups ($p<0.09$; borderline significance). The inability of the model to reproduce this particular result offers further evidence of the existence of an identifiable genetic factor which influences lead metabolism in humans. The exact nature

of the mechanism which exerts this effect remains open to speculation, as noted in Chapter 3. As investigation of the ALAD isozyme and lead kinetics progresses, it may become possible to incorporate a genetic feature within the O'Flaherty model.

Since there exists no reason to expect an offset in y-intercept between the genetic subgroups in regard to the tibia lead/RCBLI relations, this analysis may be repeated with a zero-intercept constraint (see Chapter 3). In this case, the linear relation best describing the ALAD 1-1 subgroup becomes

$$T=(0.0459\pm0.0003)\,CBLI[N=311;r^2=0.86];$$

while that for the 1-2/2-2 type workers is

$$T=(0.0461\pm0.0006)\,CBLI[N=70;r^2=0.88].$$

These results reinforce the conclusion that the differences observed in the Brunswick population have some basis in physiology, and are not mere artifacts of worker selection. As a final argument along this line, the modelled differences in slope for calcaneus lead/RCBLI were found to be 0.0001±0.0022 (with y-intercepts) and 0.0007±0.0009 (with zero-intercept constraint), again in stark contrast to observation.

Chapter 6

Digital Spectroscopy

6.1 Introduction

The X-ray fluorescence system is an application based on gamma-ray spectroscopy. Such a system has a number of components which are essential to its function. The experimental results described in previous chapters were obtained using state of the art equipment, and are by all indications highly accurate and precise. Nonetheless, as technological improvements continue unabated into the next century, opportunities for system upgrading will present themselves. One such opportunity was investigated in the form of a digital spectrometer, commercially referred to as DSPEC. This unit was produced and provided on a trial basis by EG&G Ortec (Oak Ridge, TN). In order to place the system revision in context, a brief overview of the current McMaster X-ray fluorescence system components will be provided. A description of the digital unit will follow, and the experimental trial results presented.

6.2 Conventional Gamma-Ray Spectroscopy

Gamma-ray spectroscopy is a means of quantitating

radiation of differing energies, and is a common application in the field of medical physics. Essential components of a spectroscopy system include a detector, preamplifier, amplifier, analog-to-digital converter (ADC), and multichannel analyzer (MCA). The digital gamma-ray spectrometer being investigated introduced new amplifier, ADC, and MCA components to the McMaster system.

6.2.1 Detector

The detector employed in the McMaster X-ray fluorescence system is a high-purity germanium (HPGe) device, a type of semiconductor or solid state detector. The chief advantage of a semiconductor detector which makes it essential for the present application is its outstanding energy resolution. Other positive aspects of semiconductor detectors include their excellent linearity of response, fast pulse timing characteristics, small size, and negligible entrance window absorption.

In brief, the detection of radiation with a solid state device relies on the electron energy band structure inherent to the semiconductor material. For semiconductors, the valence band of electrons is completely filled, but separated from the conduction band by only a small energy gap (about 0.7 eV for germanium). Incident radiation may cause the excitation of an electron into the conduction band, leaving a

positive "hole" in its wake. The production of these electron-hole pairs is the basis of solid state spectroscopy. The number of electron-hole pairs created is proportional to the energy deposited by the incident radiation. The collection of charge carriers is accomplished via the application of an intense electric field, the construction of which will be described below.

Within the germanium lattice, the presence of a pentavalent electron donor impurity (such as Phosphorus) results in an electron which is easily mobilized. Conversely, a trivalent electron acceptor produces an electron "hole" which may also migrate with relative ease. HPGe detectors may be classified as n-type or p-type, depending on whether an excess of donor or acceptor atoms remain after the germanium purification process.

The addition of an outer contact layer heavily doped with trivalent electron acceptor impurities results in a p+ region (the "+" indicates a very high conductivity). This is often accomplished by Boron-implantation. At the opposite end of the detecting volume is situated an n+ blocking contact (constructed via Lithium diffusion). A migration of electrons from the intrinsic material to the p+ contact results, creating a potential difference: the previously charge neutral p+ contact is presented with an influx of negative charges.

At equilibrium, the resulting electric field discourages any further electron diffusion. The small zone over which the charge imbalance exists is the "depletion region". The radiation sensitive depletion region can be increased to a more useful size by applying a reverse bias of several thousand volts. It is within this enlarged depletion region that radiation detection occurs in practical applications.

The McMaster X-ray fluorescence system employs the intrinsic germanium detector model GL2020R from Canberra Industries (Meriden, CT). The depletion region thickness on this detector is 20 mm, with a recommended applied bias voltage of -2500 V. The geometry of the detector is planar, and the active face area is 2000 mm^2. Energy resolution is excellent, with a factory quoted FWHM of less than 700 eV at 122 keV (amplifier time constant of 4 μs).

6.2.2 Preamplifier

For some types of radiation detectors (such as the Geiger-Mueller tube), the charge liberated in a single detected event is sufficient to immediately derive a fairly large voltage (Knoll, 1989). Solid state detectors, however, require an intermediate amplification between the detector and the shaping amplifier. The purpose of the preamplifier is to convert the relatively minute charge collected from detected

events to a more readily employed voltage output.

The preamplifier employed in the McMaster X-ray fluorescence system is a charge-sensitive, RC feedback model. Charge-sensitive preamplifiers produce a step-function voltage pulse with an amplitude proportional to the total integrated charge collected from the radiation detection (Knoll, 1989). The tail of the output pulse decays exponentially, with a time constant equal to the product of the feedback resistor and a capacitor. If detection occurs at a high rate, output pulses will ride upon the tails of previous pulses, and the voltage may approach a saturation threshold. This threshold is reached more quickly when larger energy detections are involved; preamps are therefore said to be energy rate limited. The preamplifier employed during these trials was the Model 2001CP from Canberra (Meriden, CT). This particular model has a time constant of 50 μs, and is limited to an energy rate of 200000 MeV/s, which is sufficient to ensure that saturation will not be a major consideration for the current application.

6.2.3 Amplifier

The amplifier shapes and enhances pulse information provided from the preamplifier. For a high count rate application, signal throughput can encounter serious

limitations at this stage of the processing chain. Generally, any enhancement of throughput will come only at the cost of degraded energy resolution.

The first task performed by the amplifier is to differentiate the preamp signal using a high-pass CR filter. This has two desirable effects: it provides a more rapid fall time for individual pulses than those supplied by the preamp, and it supplies a common signal baseline against which all pulses may be referenced. The amplifier integrates the resulting signals through a series of low-pass RC filters to produce near-Gaussian output pulses. The amplitudes of these pulses are proportional to the energies of the original detections.

The key parameter which influences the crucial tradeoff between throughput and resolution is the time constant. The time constant is normally the same for the differentiating and integrating circuits. Essentially, the time constant indicates the amount of time committed by the amplifier to characterizing an individual pulse. A short time constant allows the differentiator to pull the preamp pulses down to the baseline very quickly, and therefore results in a high throughput. The downside is that this "quick and dirty" approach allows more noise to pass through the amplifier, leading to a loss of energy resolution. Ballistic deficit,

another resolution-degrading effect, also becomes an influencing factor at short time constants. Ballistic deficit results when signal processing becomes such a rapid affair that the full amplitude of the most slowly rising preamp pulses is not properly evaluated. A long time constant produces better resolution, but reduced signal throughput: if a new pulse arrives before the previous pulse has been processed, the two events cannot be separated and the relevant information is lost.

For McMaster X-ray fluorescence applications to lead detection, a time constant of 1 μs is generally employed. This is a relatively short time constant, reflecting the very high rate of input involved, and the need to preserve high signal throughput. The current amplifier of choice for the McMaster X-ray fluorescence system is the Canberra Model 2024 Fast Spectroscopy Amplifier (Meriden, CT).

6.2.4 Analog-to-Digital Converter

The analog-to-digital converter (ADC) receives a voltage input from the amplifier, and changes this signal to a digital value which is appropriate for output to a multichannel analyzer. Input voltages normally range up to about 10 V. A 450 MHz Canberra Model 8077 Wilkinson-type ADC (Meriden, CT) is currently used in the McMaster X-ray fluorescence system.

The frequency of a Wilkinson ADC indicates the count rate of its internal clock, and dictates how quickly the ADC is able to process signals from the amplifier. The analog input voltage is initially used to charge a capacitor within the ADC. After the pulse signal from the amplifier has peaked, the capacitor is discharged linearly. An electronic time counter measures the interval between the beginning of the discharge and its completion. A 450 MHz ADC marks one count every 0.0022 μs; a 100 MHz ADC would mark one count every 0.01 μs. The number of timing counts logged for an individual signal is a reflection of the amplitude of its pulse, which in turn is proportional to the energy of the detected event. A higher energy event requires a longer timing interval, and results in a higher digital output. This digital output awaits processing by the multichannel analyzer, the final component of the signal processing chain.

6.2.5 Multichannel Analyzer

The digital value input to the multichannel analyzer (MCA) is the end result of a series of electronic procedures which began with the initial detection of a radiation event of a certain energy. Each digital value has a corresponding MCA energy channel, and a running record is kept of the number of detections per channel. For every new digital input, the appropriate energy channel is incremented by one count. The number of channels available is typically 2^{11}=2048 or 2^{12}=4096.

The MCA used in the X-ray fluorescence system is based within a standard IBM-compatible personal computer. A plug-in computer board and software interface provide a real-time display of the detected energy spectrum. The present MCA employed within the McMaster system is the Canberra Accuspec Multichannel Analyzer (Meriden, CT).

6.3 Digital Gamma-ray Spectroscopy

The DSPEC model, obtained on an experimental basis, represents the first commercially available digital signal processing based gamma-ray spectrometer. When incorporated into the X-ray fluorescence system, DSPEC took the physical place of the amplifier and analog-to-digital components. The detector and preamplifier configuration remained identical. High voltage supply was provided by DSPEC to the detector. The entire DSPEC unit was housed within a box structure measuring 31 x 35 x 14 cm. A multichannel analyzer computer card and associated software (MAESTRO for Windows) were supplied by EG&G Ortec (Oak Ridge, TN) to complete the revised system.

The main potential advantage of the DSPEC unit for the quantitation of lead levels *in vivo* derives from its pulse shaping properties and its enhanced throughput capabilities. As noted, the amplifier output from a conventional analog system is characterized by a Gaussian shaped pulse. The ideal

pulse shape, however, would have an exponential rising edge, a short duration peak, and an exponential falling edge (Knoll, 1989). This "cusp" shape is difficult to obtain with linear electronic components. The DSPEC unit uses digital integrated circuits to produce a "flat top cusp". The rapid rise and fall of such a signal can offer significant throughput advantages over conventional Gaussian shaping. At the same time, the finite top width ensures that the effects of ballistic deficit are not severe. The result is a tunable system which is capable of higher relative throughput, but without major concessions in resolution.

Following amplification of the preamp output, DSPEC samples the signal with a flash ADC. At this point, voltage amplification has occurred, but conventional pulse shaping has not been performed. The flash ADC operates by simultaneously presenting the voltage signal to a string of threshold comparators which are set to different voltage levels. The binary output from the comparators is then encoded to provide a digital readout of amplitude (Knoll, 1989). At this stage, digital signal processing is performed on the data via an internal algorithm. This "digital filtering" is the main difference between the DSPEC approach and conventional systems which use linear electronics to filter the signal.

There are many potential advantages to this type of digital approach to signal processing. The generation of the

flat top cusp is performed by entering values for a series of shaping parameters, which allows the system considerable flexibility to adapt for different types of detection applications. These parameters include "rise time", "flat top width", and "cusp shape-factor" (Figure 6.1). There are 32 rise and fall times, 5 widths, and 6 cusp factors available for selection from the MAESTRO computer interface, with no need for mechanical switch setting. In contrast, a typical analog amplifier may offer a half-dozen shaping times as the only selectable options for pulse shaping. The drifts in gain and baseline which occur over time and with variable temperature and count rate are said to be limited by DSPEC's digital components (The DSPEC User's Manual, EG&G Ortec), but this claim is beyond the scope of the current investigation. Finally, the high level of automation provided by DSPEC reduces user error in setting parameters such as the pole zero correction. Pole zero restoration is necessary to ensure that an amplified voltage pulse returns to a zero offset; the tendency to exhibit a non-zero offset results from the finite decay time associated with the preamp output (Knoll, 1989).

6.4 Trial Results

The McMaster X-ray fluorescence system was tested for performance with its conventional, analog components, and then with the DSPEC configuration in their place. The quantitation of performance was accomplished through spectral analysis.

Figure 6.1

Digital Shaping Parameters:

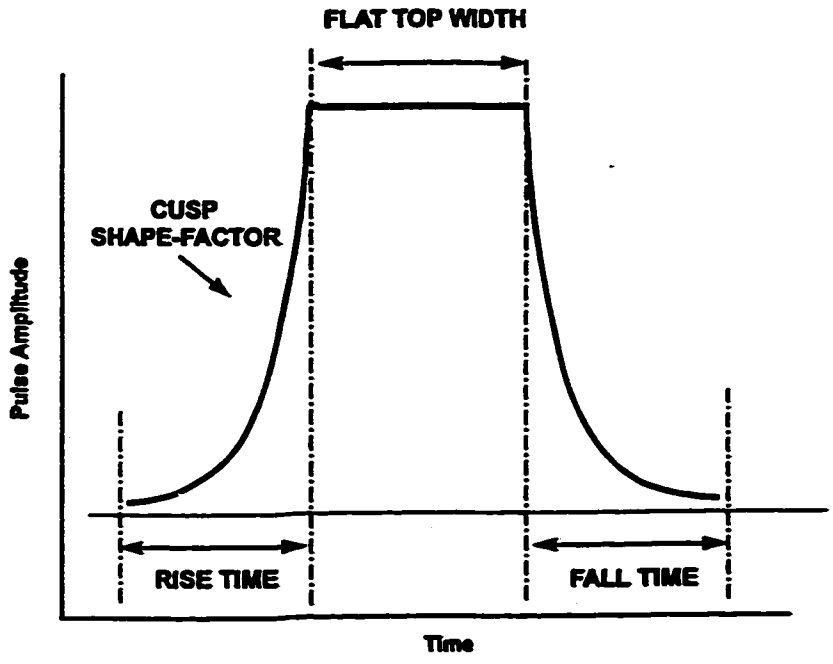

Digital Filter Response

Specifically, phantoms were used to make 30 minute real time measurements (the same time was employed for the Brunswick workers) with the two different equipment configurations, and using a variety of different DSPEC shaping parameters.

One phantom was constructed of plaster of Paris, and contained a lead concentration of ~0 μg/g. The relatively narrow diameter of this cylindrical phantom provided a very "clean", precise spectrum, characteristic of that expected from a bare bone. This type of phantom is used to generate calibration curves for the X-ray fluorescence lead detection system. The spectra resulting from a series of such phantoms (each doped with a different, known concentration of lead) are analyzed to determine the ratio of fluorescent X-ray peaks to coherent peak. The ratio of peaks increases with increasing lead concentration. For a narrow-diameter plaster of Paris phantom, the coherent peak at 88.034 keV demonstrates a large amplitude and is obvious.

The second phantom used was constructed of resin, contained a lead concentration of ~0 μg/g, and presented a considerably larger physical sample. The size of this phantom was more consistent with that presented by a human subject with tissue overlying the bone site of interest. As such, the results obtained from this sample were likely more indicative of those expected during clinical application. System dead time is higher, and the amplitude of the coherent peak is

slightly less remarkable.

The spectral analysis routine used to derive the results is based on a Marquardt nonlinear least squares fit (Marquardt, 1963). To review, a function of Gaussian form is introduced to represent the coherent scatter peak (at E_γ=88.034 keV):

$$y=Ae^{-(\frac{X-X_0}{W})^2} \quad [6.1].$$

Here, A is the amplitude for a peak, X is the channel number, X_0 is the channel number for the centre of the Gaussian, and W is the width of the function. This width, W, is also applied to the Gaussian peaks resulting from lead K X-ray detections: $K_{\alpha 2}$ (72.8 keV), $K_{\alpha 1}$ (75.0 keV), $K_{\beta 3}$ (84.5 keV), $K_{\beta 1}$ (85.0 keV), and $K_{\beta 2}$ (87.3 keV). The Compton background, which falls off rapidly over the 70-80 keV range, is best represented by a double exponential function in the K_α region. At higher energies, the Compton background levels off to some degree, and is more readily approximated by a single exponential (Somervaille *et al.*, 1985).

The fits resulting from the various trials were used to rate the performance of the system. The chief quantities of interest were the following: resolution, coherent peak count and associated uncertainty, and background under the coherent peak function. Resolution was defined as the full width half maximum (FWHM) of the coherent scatter peak. The

concentration of lead in a sample is derived from the ratios of characteristic lead X-rays to the coherent peak; the number of counts for the coherent peak is therefore crucial. The relative uncertainty of this peak propagates through to the final uncertainty in lead concentration. The background underneath the peak function provides an indication of noise level. A superior system would be characterized by high resolution (a low FWHM), a small relative uncertainty in the coherent peak, and a small background contribution.

The DSPEC parameter of rise time corresponds to roughly twice the traditional analog time constant (The DSPEC User's Manual, EG&G Ortec). A time constant of 1 μs is normally employed during lead measurements, and the optimal DSPEC rise time was therefore expected to be about 2 μs in duration. Rise times of 0.8, 1.6, and 2.4 μs were used during the experimental trials. The flat top width preset value was 1.2 μs; higher values would be expected to improve resolution, lower values should increase throughput. Experimental settings of 0.8, 1.2, 1.6, and 2.4 μs were introduced for the flat top width. The cusp shape-factor may range from 0.5 to 1.0, with larger values tending toward a straight-line rise and fall. Under most conditions, the optimal cusp value will lie in the upper half of this range (The DSPEC User's Manual, EG&G Ortec). Cusp shape-factors of 0.6, 0.8, and 1.0 were investigated.

As a first approach, the default flat top width of 1.2 μs was retained, a shape-factor of 1.0 was entered, and rise times of 1.6 and 2.4 μs were introduced in turn. These settings represented a starting point for comparison with analog results derived for an amplifier time constant of 1 μs. In all cases, two separate trials were performed for both the plaster-of-Paris phantom (PP) and the resin phantom (R). These results are presented in Table 6.1.

Tests were also performed with the same shape-factor (1.0) and flat top width (1.2 μs) values, but with very rapid rise and fall times (0.8 μs). The expectation in this case was for considerably higher throughput results at the expense of energy resolution. The observations for these trials aresummarized in Table 6.2.

DSPEC trials were then carried out with a slightly longer flat top width of 1.6 μs. The goal of extending flat top width is to improve resolution. The tradeoff comes in the form of a reduction in the number of detections. Simply put, since more time is devoted to processing each pulse, fewer pulses are able to be processed. Table 6.3 displays the results recorded for two sets of parameters which exploit a longer flat top width.

The third shaping parameter varied during these trials

Table 6.1

Trial Results: Initial Settings

	FWHM	Peak Counts	% error	Bkgd	Total Counts
Plaster-of-Paris					
Analog #1	753 eV	8582±35	0.41	2077	3.06×10^7
Analog #2	751 eV	8458±35	0.42	2211	3.01×10^7
1.6-1.0-1.2 #1	716 eV	9637±37	0.38	2197	3.17×10^7
1.6-1.0-1.2 #2	716 eV	9623±37	0.38	2100	3.16×10^7
2.4-1.0-1.2 #1	675 eV	8920±36	0.40	1915	2.85×10^7
2.4-1.0-1.2 #2	671 eV	9035±36	0.40	1858	2.85×10^7
Resin					
Analog #1	760 eV	1291±17	1.29	4195	6.27×10^7
Analog #2	797 eV	1261±17	1.33	4662	6.25×10^7
1.6-1.0-1.2 #1	727 eV	1616±18	1.11	7449	7.18×10^7
1.6-1.0-1.2 #2	728 eV	1604±18	1.12	7569	7.17×10^7
2.4-1.0-1.2 #1	678 eV	1412±17	1.20	5031	5.89×10^7
2.4-1.0-1.2 #2	683 eV	1417±17	1.19	4967	5.89×10^7

was the cusp shape-factor. The majority of tests were performed with the shape-factor equal to 1.0, corresponding to a straight line rise and fall. Two trials, however, were performed to examine the effect of changing the shape-factor. Rise time and flat top width were held fixed at 1.6 μs in both cases, as indicated in Table 6.4.

A final test of the DSPEC shaping parameters was performed with extended rise time *and* flat top width settings. The energy resolution for this particular trial was anticipated to be superior to any of the previous attempts. The throughput reduction, however, was likely to be severe. The results of this test are presented in Table 6.5.

6.5 Discussion

In comparing results between the original analog system and the revised DSPEC setup, the DSPEC settings of 1.6 μs-1.0-1.2 μs and 2.4 μs-1.0-1.2 μs (rise time, shape-factor, flat top width) were used as an initial guide to the relative performance of the two configurations (Table 6.1). On this basis, for the plaster-of-Paris phantom, the two configurations yielded comparable results. Total counts were greatest for the DSPEC 1.6 μs-1.0-1.2 μs settings, least for the DSPEC 2.4 μs-1.0-1.2 μs settings, and intermediate for the analog system. Employing a paired sample t-test, the two DSPEC trials showed a significant offset in total count

Table 6.4

Trial Results: Shape-factor Variation

	FWHM	Peak Counts	% error	Bkgd	Total Counts
Plaster-of-Paris					
1.6-0.8-1.6 #1	714 eV	8701±35	0.40	2261	2.87×10^7
1.6-0.8-1.6 #2	706 eV	8885±36	0.40	2067	2.91×10^7
1.6-0.6-1.6 #1	717 eV	8708±35	0.40	2269	2.94×10^7
1.6-0.6-1.6 #2	711 eV	8730±35	0.40	2273	2.94×10^7
Resin					
1.6-0.8-1.6 #1	717 eV	1490±17	1.15	6047	6.57×10^7
1.6-0.8-1.6 #2	694 eV	1516±18	1.15	5684	6.58×10^7
1.6-0.6-1.6 #1	720 eV	1546±18	1.13	6372	6.79×10^7
1.6-0.6-1.6 #2	713 eV	1578±18	1.11	6274	6.75×10^7

Table 6.5

Trial Results: Rise Time and Flat Top Width Extension

	FWHM	Peak Counts	% error	Bkgd	Total Counts
Plaster-of-Paris					
2.4-1.0-2.4 #1	667 eV	7928±34	0.43	1778	2.64×10^7
2.4-1.0-2.4 #2	668 eV	7878±34	0.43	1891	2.64×10^7
Resin					
2.4-1.0-2.4 #1	675 eV	1219±16	1.30	4560	5.28×10^7
2.4-1.0-2.4 #2	660 eV	1251±16	1.29	4434	5.28×10^7

(significance defined as $p<0.05$ for a two-tailed test). A significant difference in background counts was also apparent between the two DSPEC settings. Peak counts were lower for the analog system, perhaps as a result of peak broadening associated with the poorer resolution. The relative uncertainties in coherent peak were remarkably similar in all three cases. The main difference in performance was the significantly superior resolution achieved by the DSPEC apparatus.

For the resin phantom, the DSPEC results were more notable. The number of coherent peak counts recorded were higher for the DSPEC configuration, significantly so for the high throughput 1.6 μs-1.0-1.2 μs setting. Likewise, the relative uncertainty in peak counts was superior, reaching a low of 1.11% for the first trial with the 1.6 μs-1.0-1.2 μs combination. At the same time, very good resolution was maintained by the DSPEC system. The best resolution was found for the 2.4 μs-1.0-1.2 μs setting, although this was accompanied by a significant reduction in throughput relative to the 1.6 μs-1.0-1.2 μs shaping approach ($p<0.01$). These results, together with those from the plaster-of-Paris phantom, suggest a potential for more precise *in vivo* lead concentration measurements using digital spectroscopy.

It is worth noting that a previous analysis employing the same analog system (GL2020R detector, 2001CP preamplifier,

2024 amplifier, 8077 ADC, Accuspec MCA) determined values for energy resolution similar to those reported here (Cake, 1994). During these trials, mean resolutions of 724 eV and 776 eV were derived for plaster-of-Paris and resin phantoms, respectively. The substitution of the Canberra S100 MCA for the Accuspec MCA was found to provide improved resolution (mean values of 716 eV and 718 eV). As well, for a resin phantom, the relative uncertainty in coherent peak area was improved by just over 10% with this MCA substitution (Cake, 1994). In light of these considerations, some caution should be exercised in drawing conclusions on the relative merits of DSPEC and analog systems in general based on the present trials alone. Nonetheless, substantial differences were observed between the two systems which were employed, and revisions to the DSPEC shaping parameters may be attempted to further improve fitting results.

One such revision came in the form of reduced rise and fall times (0.8 μs; Table 6.2). Compared with the original DSPEC settings, these trials displayed higher count throughput, particularly for the resin phantom ($p<0.01$). The higher peak count results for the resin phantom produced lower relative uncertainties (1.09 and 1.08%) than had been observed with the rise/fall time of 1.6 μs (1.11 and 1.12%). This slight improvement was not significant, but was accompanied by a significant degradation in energy resolution. A mean FWHM of 790 eV was observed with the reduced rise time, compared

with an original mean of 728 eV. Since lead concentration is derived from closely-spaced X-ray peaks, this loss in resolution is a definite drawback.

Table 6.3 presents results from an attempt to improve fitting with an extended flat top width of 1.6 μs. The number of counts processed showed a small but significant decline with the longer shaping width. This was evident for rise times of either 0.8 or 1.6 μs, and applied to total counts ($p<0.01$ for resin phantom), peak counts ($p<0.05$), and background counts ($p<0.05$). As a consequence, count statistics were mildly limited in these trials. The mean relative uncertainties in peak count for the resin phantom increased from 1.08% to 1.10% (rise time of 0.8 μs) and from 1.12% to 1.14% (rise time of 1.6 μs). The improvements in resolution were also slight, and not significant. With the rise time of 0.8 μs, the extended flat top width took the mean resolution for the resin phantom from 790 eV to 778 eV. At a rise time of 1.6 μs, the mean resolution improved from 728 eV to 716 eV. Overall, the extension of the flat top width appeared to have very limited effect.

Rise time and flat top width were held constant at 1.6 μs in order to investigate the effect of varying the pulse shape-factor. The results observed for shape-factors of 0.6 and 0.8 are recorded in Table 6.4; these are to be compared against

those found for a shape-factor of 1.0. The differences between trial results in this case were minuscule. In terms of throughput, the shape-factor of 0.6 appeared to introduce a slight advantage with the resin phantom, but the difference was not significant. A similar improvement was observed in the relative uncertainty of the resin coherent peak (mean uncertainty of 1.12% compared to 1.15% for factor of 0.8 and 1.14% for factor of 1.0). Even with such little difference between trials, a tradeoff between resolution and throughput appeared evident. Mildly better energy resolution and inferior throughput was associated with a shape-factor of 0.8. Mean resolution with the resin phantom was 706 eV for a shape-factor of 0.8, compared with means of 716 eV for shape-factors of 0.6 or 1.0. In general, variation of shape-factor appeared to have no pertinent effect on overall system performance.

Trials were performed with extended rise times and flat top widths of 2.4 μs to test the resolution capabilities of the DSPEC system. These parameters yielded the best resolution of any attempted (Table 6.5). Mean resolution with the resin phantom was 668 eV, compared to the 716 eV recorded with the rise times and flat top widths equal to 1.6 μs. Not surprisingly, however, the number of counts available with the extended pulse processing were significantly reduced. By way of illustration, the mean number of coherent peak counts was reduced from 1526±17 (1.6 μs rise time and flat top width) to

1235±16 (2.4 μs). Relative uncertainty in peak counts increased significantly from 1.14% to an unacceptably high 1.30%. Extending the rise time and flat top width to this degree is therefore not recommended for applications to lead measurement.

The DSPEC apparatus, with the proper shaping parameters, appears superior to the present X-ray fluorescence spectroscopy configuration. Based on spectral analysis of phantom results, the optimal DSPEC rise and fall time is 1.6 μs. Longer rise/fall times introduce serious deficits in throughput, while shorter times hurt energy resolution. Flat top widths of either 1.2 or 1.6 μs appear acceptable, as do shape-factors ranging from 0.6 to 1.0. Any changes made to flat top width or shape-factor within these specifications should have no major influence on overall system performance. The DSPEC digital spectroscopy system represents an opportunity for improved precision in the non-invasive bone lead measurement technique of X-ray fluorescence.

Chapter 7

Conclusion

The measurement of bone lead by *in vivo* X-ray fluorescence is an invaluable procedure in the assessment of chronic lead exposure. Bone lead concentrations were analyzed at the tibia and calcaneus bone sites for 367 active and 14 retired workers from the Brunswick lead smelter. Blood lead records from individual smelter workers were used to gauge the extent of the endogenous contribution to lead exposure, and to construct personal exposure histories. When used as input to a computer model of lead metabolism, it was possible with these histories to project the distribution of lead to tissue as a function of time. The modelled influx to and efflux from bone tissue was compared with observed results from the Brunswick population. Approximately 95% of the workers' lead body burdens may be expected to reside in bone.

The relation between blood lead (in μg/dl) and tibia lead (in μg/g) was characterized by a slope of 0.136±0.014 in a subset of workers returning from a 10-month strike. After appropriate refinements, the O'Flaherty model of lead metabolism predicted this relation would display a slope of 0.160±0.005. In the model, the return of lead from bone stores to the bloodstream is a consequence of bone turnover

and lead ion exchange. In practical terms, it may be concluded that a lead smelter worker possessing a tibia lead concentration of 100 μg/g can expect a continual endogenous contribution to blood lead of perhaps 15 μg/dl. A pregnant woman with a tibia lead store of 50 μg/g is presented with an internal contribution to blood lead of 7 μg/dl, before taking into account the increased rates of bone turnover associated with later stages of pregnancy and lactation. These figures are baseline results for blood lead which do not include ongoing external exposures at work or from the general environment.

Despite the significant and continuous return of lead from bone stores to the bloodstream, bone tissue does maintain a relatively secure hold on lead in the human body. In the past, this fact has been demonstrated by postmortem examinations and by observed correlations between bone lead concentrations and cumulative measures of blood lead. The Brunswick smelter results showed that the proportion of lead in blood transferred to bone tissue varied as a function of exposure history. Workers hired in the early years of smelter operation, when levels of exposure were higher, demonstrated a relatively greater transfer of lead to bone. This effect may be a consequence of a differential partitioning of lead between plasma and whole blood, depending upon whether the source of exposure in endogenous or exogenous. Alternatively, the result may be attributed to a non-linear relation between

lead in plasma and lead in whole blood, caused by saturation of lead binding sites in red blood cells. Employing a relation based on a saturation hypothesis, modelled results for lead uptake to cortical bone were in excellent agreement with observation. The implication for lead transfer to other tissues and target organs is clear: relatively greater proportions of lead are transferred at progressively higher blood lead concentrations.

The modelled distribution of lead to and from trabecular bone was not in agreement with observed lead concentrations in the calcaneus. Lead in the calcaneus was well correlated with cumulative blood lead, and with the same bone lead to cumulative blood lead pattern seen from the tibia. Calcaneus results were therefore indicative of a bone metabolism similar to the tibia. This was an unexpected result from a trabecular bone, but provided confirmation from a second tissue site of the variable lead transfer hypothesis. Future work should investigate variations in lead metabolism between different trabecular bone sites.

A common polymorphism in the δ-aminolevulinate dehydratase (ALAD) enzyme influences the distribution of lead in humans. Blood lead levels were confirmed to be higher for smelter workers expressing the more rare $ALAD^2$ allele. The magnitude of the blood lead elevation was 10-20% at the time of the Brunswick survey. Serum lead concentrations and

historical blood lead records also displayed an offset. The concentration of lead in bone, however, was not associated with ALAD genotype. This was at least in part a consequence of a reduced uptake of lead by bone tissue in $ALAD^2$ workers. The reduction in transfer efficiency was significant for the more moderately exposed employees of recent hire. The lead metabolic model did not incorporate a genetic component, and did not reproduce the observed differences in this context. This result lends further support to the theory that the ALAD polymorphism influences lead kinetics. As more is learned of the role of the ALAD polymorphism in human lead metabolism, it may become possible to incorporate its effects into future modelling efforts.

The revised version of the O'Flaherty model is capable of reproducing in detail lead kinetics in humans, as inferred from observations of lead concentration in a cortical bone site. Since approximately 75% of the body's lead burden resides in cortical bone, a considerable degree of confidence may be placed in model output. Model predictions may be compared with X-ray fluorescence bone lead results from other industrial surveys, including an anticipated 1999 follow-up with Brunswick workers. As the biological effects of low to moderate lead exposure are clarified, future applications of the model should include consideration of a number of pressing questions in lead toxicology. Is the amount of lead mobilized

from bone a danger to pregnant women or their babies? Does an increase in endogenous lead exposure post-menopause present significant health risk? Is kidney failure or neurological impairment in lead industry workers associated with a cumulative dose to target organs? Does the risk of bioeffect arise only beyond a certain threshold dose? What threat does lead represent over the range of doses expected from environmental exposure?

Experimental X-ray fluorescence trials incorporating a digital spectrometer revealed superior energy resolution capabilities and improved throughput relative to a conventional system. In phantom testing, the associated reduction in elastic peak count uncertainty was approximately 15%. If a similar benefit is derived in clinical application, the median tibia lead precision in a nonoccupationally exposed group of males would be improved by approximately 0.5 μg/g. By the definition established at a 1992 X-ray fluorescence workshop organized by the National Institute of Environmental Health Sciences, the minimum detectable level of lead in bone for *in vivo* analysis is twice the median standard error for a given population. Therefore, in the hypothetical male population, the detection limit would be lowered by about 1 μg/g. This improvement, while modest in scale, would contribute to making X-ray fluorescence measurements of lead concentration more applicable to the general population

exposed to chronic, low levels of lead. An improved precision would be an obvious benefit to future industrial surveys, contributing to both the reliability of X-ray fluorescence measurement and its further application in modelling human lead metabolism.

References

Abdelnour J, Wheeler GL, Forbes RM. A compartment model of lead uptake in mature and young adult male rats. In: Trace substances in environmental health, VIII. Columbia, Missouri: University of Missouri Press, 1974; 411-416.

Ahlgren L, Liden K, Mattson S, Tejning S. X-ray fluorescence analysis of lead in human skeleton *in vivo*. Scand J Work Environ Health, 1976; 2:82-86.

Annest JL, Pirkle JL, Makuc D, Neese JW, Bayse DD, Kovar MG. Chronological trend in blood lead levels between 1976 and 1980. N Engl J Med, 1983; 308:1373-1377.

Armstrong R, Chettle DR, Scott MC, Somervaille LJ, Pendlington M. Repeated measurements of tibia lead concentrations by *in vivo* x ray fluorescence in occupational exposure. Br J Ind Med, 1992; 49:14-16.

Assennato G, Paci C, Molinini R, Candela RG, Baser ME, Altamura BM, Giorgino R. Sperm count suppression without endocrine dysfunction in lead-exposed men. Arch Environ Health, 1986; 41:387-390.

Azar A, Snee RD, Habibi K. Relationship of community levels of air lead and indices of lead absorption. In: Environmental Health Aspects of Lead, Proceedings of an International Symposium held in Amsterdam, 1972; 581-594.

Baker EL, Landrigan PJ, Barbour AG, Cox DH, Folland DS, Ligo RN, Throckmorton J. Occupational lead poisoning in the United States: clinical and biochemical findings related to blood lead levels. Br J Ind Med, 1979; 36:314-322.

Barry PSI. Comparison of concentrations of lead in human tissues. Br J Ind Med, 1975; 32:119-139.

Batschelet E, Brand L, Steiner A. On the kinetics of lead in the human body. J Math Biol, 1979; 8:15-23.

Battistuzzi G, Petrucci R, Silvagni L, Urbani FR, Caiola S. δ-aminolevulinate dehydratase: a new genetic polymorphism in man. Ann Hum Genet, 1981; 45:223-229.

Bellinger D, Hu H, Titlebaum L, Needleman HL. Attentional correlates of dentin and bone lead levels in adolescents. Arch Environ Health, 1994; 49:98-105.

Bellinger D, Leviton A, Rabinowitz M, Allred E, Needleman H, Schoenbaum S. Weight gain and maturity in fetuses exposed to low levels of lead. Environ Res, 1991; 54:151-158.

Bellinger D, Leviton A, Waternaux C, Needleman H, Rabinowitz M. Longitudinal analyses of prenatal and postnatal lead

exposure and early cognitive development. N Engl J Med, 1987; 316:1037-1042.

Benkmann HG, Bogdanski P, Goedde HW. Polymorphism of delta-aminolevulinic acid dehydratase in various populations. Hum Hered, 1983; 33:62-64.

Bleecker ML, McNeill FE, Lindgren KN, Masten VL, Ford DP. Relationship between bone lead and other indices of lead exposure in smelter workers. Toxicol Lett, 1995; 77:241-248.

Bowins RJ and McNutt RH. Electrothermal isotope diluton inductively coupled plasma mass spectrometry method for the determination of sub-ng ml^{-1} levels of lead in human plasma. J Anal At Spectrom, 1994; 9:1233-1236.

Bryant FJ and Loutit JF. Human bone metabolism deduced from strontium assays. AERE-R, 1961; 3718.

Bryant FJ and Loutit JF. The entry of strontium-90 into human bone. Proc Roy Soc, 1963; 159B:449-465.

Cake KM. *In vivo* x-ray fluorescence of bone lead in the study of human lead metabolism. Hamilton, Ontario: McMaster University, 1994.

Cake KM, Bowins RJ, Vaillancourt C, Gordon CL, McNutt RH, Laporte R, Webber CE, Chettle DR. Partition of circulating lead between serum and red cells is different for internal and external sources of lead. Am J Ind Med, 1996; 29:440-445.

Cantor KP, Sontag JM, Heid MF. Patterns of mortality among plumbers and pipefitters. Am J Ind Med, 1986; 10:73-89.

Chettle DR, Scott MC, Somervaille LJ. Lead in bone: sampling and quantitation using K x-rays excited by ^{109}Cd. Environ Health Perspect, 1991; 91:49-55.

Chisolm JJ, Mellits ED, Quaskey SA. The relationship between the level of lead absorption in children and the age, type, and condition of housing. Environ Res, 1985; 38:31-45.

Christoffersson JO, Schütz A, Ahlgren L, Haeger-Aronsen S, Mattsson S, Skerfving S. Lead in finger-bone analysed *in vivo* in active and retired lead workers. Am J Ind Med, 1984; 6:447-457.

Cooper WC, Wong O, Kheifets L. Mortality among employees of lead battery plants and lead-producing plants, 1947-1980. Scand J Work Environ Health, 1985; 11:331-345.

Cutler MG, McLaughlin M, McNeil E, Moore MR. Effects of delta-aminolaevulinic acid on contractile activity in the isolated small intestine of the rabbit. Neuropharmacology, 1985; 24:1005-1009.

deSilva PE. Determination of lead in plasma and studies on its relationship to lead in erythrocytes. Br J Ind Med, 1981; 38:209-217.

EG&G Ortec. The DSPEC digital gamma-ray spectrometer and its use with MAESTRO for Windows and GammaVision user's manual. Oak Ridge: EG&G Ortec, 1997.

Ericson JE, Smith DR, Flegal AR. Skeletal concentrations of lead, cadmium, zinc, and silver in ancient North American Pecos Indians. Environ Health Perspect, 1991; 93:217-223.

Erkkilä J, Armstrong R, Riihimäki V, Chettle DR, Paakkari A, Scott M, Somervaille L, Starck J, Kock B, Aitio A. *In vivo* measurements of lead in bone at four anatomical sites: long term occupational and consequent endogenous exposure. Br J Ind Med, 1992; 49:631-644.

Factor-Litvak P, Graziano JH, Kline JK, Popovac D, Mehmeti A, Ahmedi G, Shrout P, Murphy MJ, Gashi E, Haxhiu R, Rajovic L, Nenezic DU, Stein ZA. A prospective study of birthweight and length of gestation in a population surrounding a lead smelter in Kosovo, Yugoslavia. Int J Epidemiol, 1991; 20:722-728.

Firestone RB. Table of Isotopes. New York: John Wiley & Sons, Inc., 1996.

Flegal AR, Nriagu JO, Niemeyer S, Coale KH. Isotopic tracers of lead contamination in the Great Lakes. Nature, 1989; 339:455-458.

Forbes RM, Cooper AR, Mitchell HH. The composition of the adult human body as determined by chemical analysis. J Biol Chem, 1953; 203:359-366.

Frost HM. The bone dynamics in osteoporosis and osteomalacia. Springfield, Illinois: Charles C. Thomas, Publisher, 1966.

Frost HM. Tetracycline-based histological analysis of bone remodelling. Calc Tiss Res, 1969; 3:211-217.

Gerhardsson L, Attewell R, Chettle DR, Englyst V, Lundström N-G, Nordberg GF, Nyhlin H, Scott MC, Todd AC. *In vivo* measurements of lead in bone in long-term exposed lead smelter workers. Arch Environ Health, 1993; 48:147-156.

The Globe & Mail. Blinds could pose lead hazard, 1996; June 26:A8.

The Globe & Mail. Ottawa to study plastic products after blinds scare, 1996; June 27:A9.

The Globe & Mail. Pregnant women warned, 1996; June 28:A1.

Gordon CL, Chettle DR, Webber CE. An improved instrument for the *in vivo* detection of bone lead. Br J Ind Med, 1993;

50:637-641.

Gordon CL, Webber CE, Chettle DR. The reproducibility of ^{109}Cd-based X-ray fluorescence measurements of bone lead. Environ Health Perspect, 1994; 102:690-694.

Graziano JH, Blum CB, Lolacono NJ, Slavkovich V, Manton WI, Pond S, Moore MR. A human *in vivo* model for the determination of lead bioavailability using stable isotope dilution. Environ Health Perspect, 1996; 104:176-179.

Griffin RM and Matson WR. The assessment of individual variability to trace metal insult: low-molecular-weight metal complexing agents as indicators of trace metal insult. Am Ind Hyg Assoc J, 1972; 33:373-377.

Gross SB, Pfitzer EA, Yeager DW, Kehoe RA. Lead in human tissues. Toxicol Appl Pharmacol, 1975; 32:638-651.

Hall EJ. Radiobiology for the radiologist. Philadelphia: J.B. Lippincott Company, 1994.

Harding G. Comments on the article 'photoelectron bremsstrahlung- analytical possibilities?'. Phys Med Biol, 1995; 40:471-476.

Hernberg S and Nikkanen J. Enzyme inhibition by lead under normal urban conditions. Lancet, 1970; 7637: 63-64.

Hertzman C, Ward H, Ames N, Kelly S, Yates C. Childhood lead exposure in Trail revisited. Can J Pub Health, 1991; 82:385-391.

Hu H, Payton M, Korrick S, Aro A, Sparrow D, Weiss ST, Rotnitzky A. Determinants of bone and blood lead levels among community-exposed middle-aged to elderly men. Am J Epidemiol, 1996; 144:749-759.

Hu H, Pepper L, Goldman R. Effect of repeated occupational exposure to lead, cessation of exposure, and chelation on levels of lead in bone. Am J Ind Med, 1991; 20:723-735.

Hubbell JH and Øverbø I. Relativistic form factors and photon coherent scattering cross sections. J Phys Chem Ref Data, 1979; 8:69-105.

International Commission on Radiological Protection Publication 20. Alkaline earth metabolism in adult man. Oxford: Pergamon Press, 1973.

International Commission on Radiological Protection Publication 23. Report of the task group on reference man. Oxford: Pergamon Press, 1975.

Jaffe EK, Bagla S, Michini PA. Reevaluation of a sensitive indicator of early lead exposure. Measurement of

porphobilinogen synthase in blood. Biol Trace Element Res, 1991; 28:223-231.

Jeyaratnam J, Devathasan G, Ong CN, Phoon WO, Wong PK. Neurophysiological studies on workers exposed to lead. Br J Ind Med, 1985; 42:173-177.

Keenleyside A, Song X, Chettle DR, Webber CE. The lead content of human bones from the 1845 Franklin expedition. J Archaeol Sci, 1996; 23:461-465.

Knoll GF. Radiation detection and measurement. Toronto: John Wiley & Sons, 1989.

Koren G, Chang N, Gonen R, Klein J, Weiner L, Demshar H, Pizzolato S, Radde I, Shime J. Lead exposure among mothers and their newborns in Toronto. Can Med Assoc J, 1990; 142:1241-1244.

Kosnett MJ, Becker CE, Osterloh JD, Kelly TJ, Pasta DJ. Factors influencing bone lead concentration in a suburban community assessed by noninvasive k X-ray fluorescence. JAMA, 1994; 271:197-203.

Kulp JL and Schulert AR. Strontium-90 in man. Science, 1962; 136:619-632.

Langlois P, Smith L, Fleming S, Gould R, Goel V, Gibson B. Blood lead levels in Toronto children and abatement of lead-contaminated soil and house dust. Arch Environ Health, 1996; 51:59-67.

Leggett RW. An age-specific kinetic model of lead metabolism in humans. Environ Health Perspect, 1993; 101:598-616.

Lolin Y and O'Gorman P. An intra-erythrocytic low molecular weight lead binding protein in acute and chronic lead exposure and its possible protective role in lead toxicity. Ann Clin Biochem, 1988; 25:688-697.

Loutit JF. The metabolism of strontium-90 in bone. Chem Industry, 1962; 1228-1229.

Mahaffey KR, Rosen JF, Chesney RW, Peeler JT, Smith CM, DeLuca HF. Association between age, blood lead concentration, and serum 1,25-dihydroxycholecalciferol levels in children. Am J Clin Nutr, 1982; 35:1327-1331.

Manton WI. Total contribution of airborne lead to blood lead. Br J Ind Med, 1985; 42:168-172.

Manton WI and Cook JD. High accuracy (stable isotope dilution) measurements of lead in serum and cerebrospinal fluid. Br J Ind Med, 1984; 41:313-319.

Manton WI and Malloy CR. Distribution of lead in body fluids

after ingestion of soft solder. Br J Ind Med, 1983; 40:51-57.

Marcus AH. Multicompartment kinetic model for lead I. Bone diffusion models for long-term retention. Environ Res, 1985a; 36:441-458.

Marcus AH. Multicompartment kinetic model for lead II. Linear kinetics and variable absorption in humans without excessive lead exposures. Environ Res, 1985b; 36:459-472.

Marcus AH. Multicompartment kinetic model for lead III. Lead in blood plasma and erythrocytes. Environ Res, 1985c; 36:473-489.

Marquardt DW. An algorithm for least-squares estimation of nonlinear parameters. J Soc Indust Appl Math, 1963; 11:431-441.

Marshall JH, Lloyd EL, Rundo J, Liniecki J, Marotti G, Mays CW, Sissons HA, Snyder WS. Alkaline earth metabolism in adult man. Health Physics, 1973; 24:125-221.

Marshall JH and Onckelinx C. Radial diffusion and power function retention of alkaline earth radioisotopes in adult bone. Nature, 1968; 217:742-743.

Mason HJ, Somervaille LJ, Wright AL, Chettle DR, Scott MC. Effect of occupational lead exposure on serum 1,25-dihydroxyvitamin D levels. Hum Exp Toxicol, 1990; 9:29-34.

Méranger JC, Subramanian KS, Chalifoux C. Survey for Cd, Co, Cr, Cu, Ni, Pb, Zn, Ca and Mg in Canadian drinking water supplies. J Assoc Off Anal Chem, 1981; 64:44.

Mitchell and Gauthier Associates Inc. Advanced Continuous Simulation Language Reference Manual. Concord, Massachusetts: Mitchell and Gauthier Associates Inc., 1992.

Mitchell HH, Hamilton TS, Steggerda FR, Bean HW. The chemical composition of the adult human body and its bearing on the biochemistry of growth. J Biol Chem, 1945; 158:625-637.

Morgan WD, Ryde SJS, Jones SJ, Wyatt RM, Hainsworth IR, Cobbold SS, Evans CJ, Braithwaite RA. *In vivo* measurements of cadmium and lead in occupationally-exposed workers and an urban population. Biol Trace Elem Res, 1990; 26:407-414.

Nakhoul F, Kayne LH, Brautbar N, Hu M-S, McDonough A, Eggena P, Golub MS, Berger M, Chang C-T, Jamgotchian N, Lee DBN. Rapid hypertensinogenic effect of lead: studies in the spontaneously hypertensive rat. Toxicol Ind Health, 1992; 8:89-102.

National Research Council. Measuring lead exposure in infants, children, and other sensitive populations. Washington: National Academy Press, 1993.

Nriagu JO. Saturnine gout among Roman aristocrats. New Engl J Med, 1983; 308:660-663.

O'Flaherty EJ. Physiologically based models for bone-seeking elements I. Rat skeletal and bone growth. Toxicol Appl Pharmacol, 1991a; 111:299-312.

O'Flaherty EJ. Physiologically based models for bone-seeking elements II. Kinetics of lead disposition in rats. Toxicol Appl Pharmacol, 1991b; 111:313-331.

O'Flaherty EJ. Physiologically based models for bone-seeking elements III. Human skeletal and bone growth. Toxicol Appl Pharmacol, 1991c; 111:332-341.

O'Flaherty EJ. Physiologically based models for bone-seeking elements IV. Kinetics of lead disposition in humans. Toxicol Appl Pharmacol, 1993; 118:16-29.

O'Flaherty EJ. Physiologically based lead kinetic model manual. Cincinnati: University of Cincinnati, 1997.

Ontario Ministry of Environment and Energy. Air Quality in Ontario 1993. Toronto: Queen's Printer for Ontario, 1994.

Parfitt AM. The actions of parathroid hormone on bone: relation to bone remodeling and turnover, calcium homeostasis, and metabolic bone disease. Metabolism, 1976; 25:809-844.

Petrucci R, Leonardi A, Battistuzzi G. The genetic polymorphism of δ-aminolevulinate dehydrase in Italy. Hum Genet, 1982; 60:289-290.

Pirkle JL, Brody DJ, Gunter EW, Kramer RA, Paschal DC, Flegal KM, Matte TD. The decline in blood lead levels in the United States. JAMA, 1994; 272:284-291.

Quenouille, MH. Associated Measurements. New York: Academic Press, 1952.

Rabinowitz MB. Toxicokinetics of bone lead. Environ Health Perspect, 1991; 91:33-37.

Rabinowitz MB, Wetherill GW, Kopple JD. Kinetic analysis of lead metabolism in healthy humans. J Clinical Invest, 1976; 58:260-270.

Raghavan SRV, Culver BD, Gonick HC. Erythrocyte lead-binding protein after occupational exposure I. Relationship to lead toxicity. Environ Res, 1980; 22:264-270.

Rodamilans M, Osaba MJM, To-Figueras J, Fillat FR, Marques JM, Perez P, Corbella J. Lead toxicity on endocrine testicular function in an occupationally exposed population. Human Toxicol, 1988; 7:125-128.

Roels HA, Konings J, Green S, Bradley D, Chettle DR, Lauwerys RR. Time-integrated blood lead concentration is a valid surrogate for estimating the cumulative lead dose assessed by tibial lead measurement. Environ Res, 1995; 69:75-82.

Rosen JF, Chesney RW, Hamstra A, DeLuca HF, Mahaffey KR. Reduction in 1,25-dihydroxyvitamin D in children with increased lead absorption. N Engl J Med, 1980; 302:1128-1131.

Roy MM, Gordon CL, Beaumont LF, Chettle DR, Webber CE. Further experience with bone lead content measurements in residents of southern Ontario. Appl Rad Isotop, 1997; 48:391-396.

The Royal Society of Canada. Lead in the Canadian environment: science and regulation. Toronto: The Royal Society of Canada, 1986.

Schütz A, Skerfving S, Mattson S, Christoffersson J-O, Ahlgren L. Lead in vetebral bone biopsies from active and retired lead workers. Arch Environ Health, 1987; 42:340-346.

Schütz A, Bergdahl IA, Ekholm A, Skerfving S. Measurement by ICP-MS of lead in plasma and whole blood of lead workers and controls. Occup Environ Med, 1996; 53:736-740.

Schwartz BS, Lee B-K, Stewart W, Ahn K-D, Springer K, Kelsey K. Associations of δ-aminolevulinic acid dehydratase genotype with plant, exposure duration, and blood lead and zinc protoporphyrin levels in Korean workers. Am J Epidemiol, 1995; 142:738-745.

Schwartz J. The relationship between blood lead and blood pressure in the NHANES II survey. Environ Health Perspect, 1988; 78:15-22.

Schwartz J, Landrigan PJ, Baker EL, Orenstein WA, von Lindern IH. Lead induced anemia: dose-response relationships and evidence for a threshold. Am J Public Health, 1990; 80:165-168.

Shirai T, Ohshima M, Masuda A, Tamano S, Ito N. Promotion of 2-(ethylnitrosamino)ethanol-induced renal carcinogenesis in rats by nephrotoxic compounds: positive responses with folic acid, basic lead acetate, and N-(3,5-dichlorophenyl) succinimide but not with 2,3-dibromo-1-propanol phosphate. J Natl Cancer Inst, 1984; 72:477-482.

Silbergeld EK, Schwartz J, Mahaffey K. Lead and osteoporosis: mobilization of lead from bone in postmenopausal women. Environ Res, 1988; 47:79-94.

Simons TJB. Passive transport and binding of lead by human red blood cells. J Physiol, 1986; 378:267-286.

Smith CM, Wang X, Hu H, Kelsey KT. A polymorphism in the δ-aminolevulinic acid dehydratase gene may modify the

pharmacokinetics and toxicity of lead. Environ Health Perspect, 1995; 103:248-253.

Snee RD. Models for the relationship between blood lead and air lead. Int Arch Occup Environ Health, 1982; 50:303-319.

Solliway BM, Schaffer A, Pratt H, Yannai S. A multidisciplinary study of lead-exposed subjects I. Delayed target detection P-300 latency, an electrophysiological paramter, correlates with urinary delta-ALA. Environ Res, 1994; 67:168-182.

Somervaille LJ, Chettle DR, Scott MC. *In vivo* measurement of lead in bone using x-ray fluorescence. Phys Med Biol, 1985; 30:929-943.

Somervaille LJ, Chettle DR, Scott MC, Aufderheide AC, Wallgren JE, Wittmers LE, Rapp GR. Comparison of two *in vitro* methods of bone lead analysis and the implications for *in vivo* measurements. Phys Med Biol, 1986; 31:1267-1274.

Somervaille LJ, Chettle DR, Scott MC, Tennant DR, McKiernan MJ, Skilbeck A, Trethowan WN. *In vivo* tibia lead measurements as an index of cumulative exposure in occupationally exposed subjects. Br J Ind Med, 1988; 45:174-181.

Somervaille LJ, Nilsson U, Chettle DR, Tell I, Scott MC, Schütz A, Mattsson S, Skerfving S. *In vivo* measurements of bone lead - a comparison of two x-ray fluorescence techniques used at three different bone sites. Phys Med Biol, 1989; 34:1833-1845.

Staessen JA, Lauwerys RR, Buchet J-P, Bulpitt CJ, Rondia D, Vanrenterghem Y, Amery A, the Cadmibel Study Group. Impairment of renal function with increasing blood lead concentrations in the general population. N Engl J Med, 1992; 327:151-156.

Tanner DC and Lipsky MM. Effect of lead acetate on N-(4'-fluoro-4-biphenyl)acetamide-induced renal carcinogenesis in the rat. Carcinogenesis, 1984; 5:1109-1113.

Todd AC and Chettle DR. *In vivo* x-ray fluorescence of lead in bone: review and current issues. Environ Health Perspect, 1994; 102:172-177.

Todd AC and Landrigan PJ. X-ray fluorescence analysis of lead in bone. Environ Health Perspect, 1993; 101:494-495.

Todd AC, McNeill FE, Palethorpe JE, Peach DE, Chettle DR, Tobin MJ, Strosko SJ, Rosen JC. *In vivo* XRF of lead in bone using K x-ray excitation with ^{109}Cd sources: radiation dosimetry studies. Environ Res, 1992; 57:117-132.

Wallace DM, Kalman DA, Bird TD. Hazardous lead release from glazed dinnerware: a cautionary note. Sci Tot Environ, 1985; 44:289-292.

Webber CE, Chettle DR, Bowins RJ, Beaumont LF, Gordon CL, Song X, Blake JM, McNutt RH. Hormone replacement therapy may reduce the return of endogenous lead from bone to the circulation. Environ Health Perspect, 1995; 103:1150-1153.

Wedeen RP, Maesaka JK, Weiner B, Lipat GA, Lyons MM, Vitale LF, Joselow MM. Occupational lead nephropathy. Am J Med, 1975; 59:630-641.

Wetmur JG. Influence of the common human δ-aminolevulinate dehydratase polymorphism on lead body burden. Environ Health Perspect, 1994; 102(Suppl 3):215-219.

Wetmur JG, Kaya AH, Plewinska M, Desnick RJ. Molecular characterization of the human δ-aminolevulinate dehydratase 2 ($ALAD^2$) allele: implications for molecular screening of individuals for genetic susceptibility to lead poisoning. Am J Hum Genet, 1991a; 49:757-763.

Wetmur JG, Lehnert G, Desnick RJ. The δ-aminolevulinate dehydratase polymorphism: higher blood lead levels in lead workers and environmentally exposed children with the 1-2 and 2-2 isozymes. Environ Res, 1991b; 56:109-119.

Wielopolski L, Rosen JF, Slatkin DN, Zhang R, Kalef-Ezra JA, Rothman JC, Maryanski M, Jenks ST. *In vivo* measurement of cortical bone lead using polarised X-rays. Med Phys, 1989; 16:521-528.

Wielopolski L, Slatkin DN, Vartsky D, Ellis KJ, Cohn SH. Feasibility study for the *in vivo* measurement of lead in bone using 1-X-ray fluorescence. IEEE Trans Nucl Sci, 1981; 28:114-116.

Williams MK, King E, Walford J. An investigation of lead absorption in an electric accumulator factory with the use of personal samplers. Br J Ind Med, 1969; 26:202-216.

Williamson JH. Least-sqaures fitting of a straight line. Can J Phys, 1968; 46:1845-1847.

Wittmers LE, Wallgren J, Alich A, Aufderheide AC, Rapp G. Lead in bone. IV. Distribution of lead in the human skeleton. Arch Environ Health, 1988; 43:381-391.

Woodard HQ and White DR. The composition of body tissues. Br J Radiol, 1986; 59:1209-1219.

Ziemsen B, Angerer J, Lehnert G, Benkmann H-G, Goedde HW. Polymorphism of delta-aminolevulinic acid dehydratase in lead-exposed workers. Int Arch Occup Environ Health, 1986; 58:245-247.

Appendix A

```
PROGRAM: Physiologically-based Toxicokinetic Model: Lead in Humans
!-------------------------------------------------------------
!NOW.CSL
!July, 1996
!Ellen J. O'Flaherty
!This version of the physiologically-based human lead kinetic
!model is written for ACSL Level 10, and corresponds to the
!cynomolgus monkey model with trabecular and cortical bone. It
!has the bone same parameter values as the cynomolgus monkey
!model except for cortical bone remodelinng, which is
!set higher in the human.  Mass balance is achieved.


INITIAL

!**Miscellaneous**
ALGORITHM IALG=2        !Gear integration algorithm for stiff
                        !systems


!**Timing Commands**
CONSTANT TSTOP=0.       !Length of simulation (yr)
CONSTANT AGE0=0.        !Age at which simulation begins (yr)
CONSTANT AGEA=25.       !Age at which bone growth ceases and
                        !remodeling becomes the sole bone formation
                        !process (yr)
CONSTANT CINT=1.        !Communication interval (yr)


!**General Physiologic Parameters**
CONSTANT YOB=0.         !Year of birth
CONSTANT WBIRTH=3.5     !Weight at birth (kg)
CONSTANT WCHILD=0.      !Maximum weight for early hyperbolic
                        !section of growth curve (kg)
CONSTANT HALF=0.        !Age at which weight is half WCHILD (yr)
CONSTANT WADULT=0.      !Maximum weight for later logistic section
                        !of growth curve (kg)
CONSTANT KAPPA=0.       !Logistic constant kappa
CONSTANT LAMBDA=0.      !Logistic constant lambda (1/(kg-yr))

WBODY0=WBIRTH+WCHILD*AGE0/(HALF+AGE0)+WADULT/(1.+KAPPA*EXP&
     (-LAMBDA*WADULT*AGE0))
                        !Body weight at start of simulation (kg)
WBODYW=WBIRTH+WCHILD*.3/(HALF+.3)+WADULT/(1.+KAPPA*EXP(-LAMBDA*&
     WADULT*.3))        !Body weight at start of weaning, set at
                        !age 0.3 year (kg)
WBODY1=WBIRTH+WCHILD*1./(HALF+1.)+WADULT/(1.+KAPPA*EXP(-LAMBDA*&
     WADULT*1.))        !Body weight at age 1 year (kg)
WBODYA=WBIRTH+WCHILD*AGEA/(HALF+AGEA)+WADULT/(1.+KAPPA*EXP&
     (-LAMBDA*WADULT*AGEA))
```

```
                        !Body weight at age AGEA (kg)

QCC=340.*365.           !Cardiac output in the adult (L/yr/kg)
QC=QCC*((WBIRTH+WADULT+WCHILD)**.74)
                        !Cardiac output in the adult (L/yr)

CONSTANT QLC=.25        !Fraction cardiac output going to liver
CONSTANT QKC=.17        !Fraction cardiac output going to kidney
CONSTANT QWC=.44        !Fraction cardiac output going to other
                        !well-perfused tissues
CONSTANT QBONEC=.05     !Fraction cardiac output going to bone
QPC=1.-(QLC+QKC+QWC+QBONEC)
                        !Fraction cardiac output going to other
                        !poorly-perfused tissues

CONSTANT VBLC=.067      !Total blood volume (L/kg BW)
CONSTANT VLC=.04        !Liver volume in the adult (L/kg BW)
CONSTANT VKC=.0085      !Kidney volume in the adult (L/kg BW)
CONSTANT VBLWPC=.0576 !Volume of blood in well-perfused tissues
                        !(L/kg BW)
CONSTANT VWC=.16        !Volume of well-perfused tissues, including
                        !blood, liver and kidney, in the adult
                        !(L/kg BW)
VPC=1.-VWC              !Volume of poorly-perfused tissues,
                        !including bone, in the adult (L/kg BW)

CONSTANT HCTA=0.        !Hematocrit in the adult


!**Bone Parameters**
CONSTANT DO=1.E-7       !Diffusion constant (cm/da/.5E-4 cm)
CONSTANT RO=1.E-7       !Permeability constant (cm/da/.5E-4 cm)
CONSTANT PO=.04         !Permeability constant (cm/da/.5E-4 cm)
CONSTANT H=3.54E7       !Total haversian canal length per liter
                        !of bone (cm/L)
CONSTANT PI=3.141592    !Value of pi
L=1000./(PI*(RAD8**2.))
                        !Total canalicule length per liter of
                        !bone ((no. canalicules/cm3)*(1-cm length
                        !/canalicule/cm3)*(1000 cm3/L bone))
                        !(cm/L)

CONSTANT S=.000314      !Surface area of canalicule (cm2/cm
                        !canalicule length)

CONSTANT RAD1=.00005    !Radii of
CONSTANT RAD2=.00010    !the eight
CONSTANT RAD3=.00015    !shells of bone
CONSTANT RAD4=.00020    !in the canalicular
CONSTANT RAD5=.00025    !(diffusion)
CONSTANT RAD6=.00030    !region of
CONSTANT RAD7=.00035    !deeper bone
CONSTANT RAD8=.00040    !(cm)
```

```
S1=2.*PI*RAD1          !Surface areas of
S2=2.*PI*RAD2          !the eight shells
S3=2.*PI*RAD3          !of bone in the
S4=2.*PI*RAD4          !canalicular
S5=2.*PI*RAD5          !(diffusion)
S6=2.*PI*RAD6          !region of
S7=2.*PI*RAD7          !deeper bone
S8=2.*PI*RAD8          !(cm2/cm canalicule length)

V1=PI*(RAD1**2.)       !Volumes of
V2=PI*(RAD2**2.)-V1    !the eight shells
V3=PI*(RAD3**2.)-(V1+V2)
                       !of bone in the
V4=PI*(RAD4**2.)-(V1+V2+V3)
                       !canalicular
V5=PI*(RAD5**2.)-(V1+V2+V3+V4)
                       !(diffusion)
V6=PI*(RAD6**2.)-(V1+V2+V3+V4+V5)
                       !region of
V7=PI*(RAD7**2.)-(V1+V2+V3+V4+V5+V6)
                       !deeper bone
V8=PI*(RAD8**2.)-(V1+V2+V3+V4+V5+V6+V7)
                       !(cm3/cm canalicule length)


!**Lead Parameters**
CONSTANT PL=50.        !Liver/plasma partition coefficient
CONSTANT PK=50.        !Kidney/plasma partition coefficient
CONSTANT PW=50.        !Well-perfused tissue/plasma partition
                       !coefficient
CONSTANT PP=2.         !Poorly-perfused tissue/plasma partition
                       !coefficient
CONSTANT LEAD=15000.   !Fractional clearance of lead from plasma
                       !into forming bone (L plasma cleared/L bone
                       !formed)
CONSTANT BIND=2.7      !Maximum capacity of sites in red cells to
                       !bind lead (mg/L of red cell volume)
CONSTANT KBIND=.0075   !Half-saturation concentration of lead for
                       !binding by sites in red cells (mg/L of
                       !red cell volume)
CONSTANT G=1.2         !Linear parameter for unbound lead in red
                       !cells


END                    !Of Initial Section


DYNAMIC


DERIVATIVE
```

```
AGE=AGE0+T              !Age (yr)
YEAR=YOB+AGE            !Calendar year


!**Scaled and Other Derived Parameters**
WBODY=WBIRTH+WCHILD*AGE/(HALF+AGE)+WADULT/(1.+KAPPA*EXP&
     (-LAMBDA*WADULT*AGE))
                        !Body weight as a function of age (kg)
WSKEL=.058*WBODY**1.21
                        !Skeletal weight (kg)
VBONE=.0168*WBODY**1.188
                        !Bone volume (L)
CVBONE=.8*VBONE         !Cortical bone volume (L)
TVBONE=VBONE-CVBONE     !Trabecular bone volume (L)
WBONE=.0290*WBODY**1.21
                        !Bone weight (kg)
DBONE=WBONE/VBONE       !Bone density (g/cm3)
WMARR=.00702*WBODY**1.46
                        !Marrow weight (kg)
WMFDB=.0226*WBODY**1.23
                        !Marrow-free dry bone weight (kg)
WASH=.0138*WBODY**1.25
                        !Ash weight (kg)
CABONE=.005236*WBODY**1.25
                        !Bone calcium (kg)
CAAGEA=.005236*WBODYA**1.25
                        !Bone calcium at age AGEA (kg)

P=365.*P0/DBONE         !Permeability constant for diffusion across
                        !the canalicule-bone interface from
                        !canalicule to bone (cm/yr/.5E-4cm)
R=365.*R0/DBONE         !Permeability constant for diffusion across
                        !the canalicule-bone interface from bone to
                        !canalicule (cm/yr/.5E-4cm)
D=365.*D0/DBONE         !Permeability constant for diffusion within
                        !bone (cm/yr/.5E-4cm)

QCG=QC*((WBODY/(WBIRTH+WADULT+WCHILD))**.67)
                        !Cardiac blood output (L/yr)

QL=QLC*QCG              !Blood flow to liver (L/yr)
QK=QKC*QCG              !Blood flow to kidney (L/yr)
QW=QWC*QCG              !Blood flow to other well-perfused
                        !tissues (L/yr)

QB=QBONEC*QCG           !Blood flow to bone (L/yr)
CQB=.5*QB               !Blood flow to cortical bone (L/yr)
CQBC=CQB*CBFRC/CBFR     !Blood flow to cortical bone engaged in
                        !active modeling during growth (L/yr)
CQBA=CQB-CQBC           !Blood flow to cortical bone engaged in
                        !adult-type remodeling (L/yr)
TQB=QB-CQB              !Blood flow to trabecular bone (L/yr)
TQBC=TQB*TBFRC/TBFR     !Blood flow to trabecular bone engaged in
```

```
                        !active modeling during growth (L/yr)
TQBA=TQB-TQBC           !Blood flow to trabecular bone engaged in
                        !adult-type remodeling (L/yr)
BBFR=QB/WBONE           !Specific bone blood flow rate (L/yr/kg
                        !bone)
QP=QCG-(QL+QK+QW+QB)    !Blood flow to other poorly-perfused
                        !tissues (L/yr)

VBL=VBLC*WBODY          !Total blood volume (L)
VBLWP=VBLWPC*WBODY      !Blood volume in well-perfused tissues (L)
VBLPP=VBL-VBLWP         !Blood volume in poorly-perfused tissues
                        !(L)

VL=VLC*(WBIRTH+WADULT+WCHILD)*((WBODY/(WBIRTH+WADULT&
     +WCHILD))**.85)    !Liver volume (L)
VK=VKC*(WBIRTH+WADULT+WCHILD)*((WBODY/(WBIRTH+WADULT&
     +WCHILD))**.84)    !Kidney volume (L)
VWT=VWC*(WBIRTH+WADULT+WCHILD)*((WBODY/(WBIRTH+WADULT&
     +WCHILD))**.85)    !Total volume of well-perfused tissues (L)
VW=VWT-(VL+VK+VBLWP)    !Volume of other well-perfused tissues (L)
VP=WBODY-(VWT+VBONE+VBLPP)
                        !Volume of other poorly-perfused tissues
                        !(L)


!**Condition for Termination of Run**
TERMT(T.GE.TSTOP)


!**KINETICS**


!**Body and Bone Growth**
RWBODY=HALF*WCHILD/((HALF+AGE)**2.)+KAPPA*LAMBDA*(WADULT**2.)*&
      EXP(-LAMBDA*WADULT*AGE)/((1.+KAPPA*EXP(-LAMBDA*WADULT*&
      AGE))**2.)        !Rate of change of body weight (kg/yr)
RWBONE=1.21*.0290*(WBODY**.21)*RWBODY
                        !Rate of change of bone weight (kg/yr)
RVBONE=1.188*.0168*(WBODY**.188)*RWBODY
                        !Rate of change of bone volume (L/yr)
RCBONE=1.25*.005236*(WBODY**.25)*RWBODY
                        !Rate of change of calcium content of bone
                        !(kg/yr)
FCBONE=RCBONE/CABONE    !Fractional rate of change of either
                        !calcium content of bone or of bone weight
                      !(1/yr)

CONSTANT TMINFOR=.085 !Trabecular bone formation rate in the
                        !adult (by calcium) (kg/yr)
TBFRCA=RSW(AGE.LE.12.,.017+0.8*EXP(.5*AGE)/(EXP(2.)+EXP(.5*AGE))&
     ,TMINFOR+1.015*0.8*EXP(-.4*(AGE-12.)))
                        !Trabecular bone formation rate (by
                        !calcium) (kg/yr)
```

```
TFBAGEA=TMINFOR+1.015*0.8*EXP(-.4*(AGEA-12.))
                        !Trabecular bone formation rate at age AGEA
                        !(by calcium) (kg/yr)

CONSTANT CMINFOR=.05    !Cortical bone formation rate in the adult
                        !(by calcium) (kg/yr)
CBFRCA=RSW(AGE.LE.12.,.08+0.2*EXP(.5*AGE)/(EXP(2.)+EXP(.5*AGE)),&
     CMINFOR+1.058*0.2*EXP(-.4*(AGE-12.)))
                        !Cortical bone formation rate (by calcium)
                        !(kg/yr)
CFBAGEA=CMINFOR+1.058*0.2*EXP(-.4*(AGEA-12.))
                        !Cortical bone formation rate at age AGEA
                        !(by calcium) (kg/yr)

!These bone formation rates give a fractional trabecular bone
!formation rate (TFBFR) of 0.5/yr and a fractional cortical bone
!formation rate (CFBFR) of .08/yr in the adult, for a weighted
!average fractional bone formation rate (FBFR) of .16/yr.

BFRCA=TBFRCA+CBFRCA     !Total bone formation rate (by calcium)
                        !(kg/yr)
FBAGEA=TFBAGEA+CFBAGEA
                        !Total bone formation rate at age AGEA (by
                        !calcium) (kg/yr)

FBFR=BFRCA/CABONE       !Fractional bone formation rate (1/yr)
TFBFR=TBFRCA/(0.2*CABONE)
                        !Fractional trabecular bone formation rate
                        !(1/yr)
CFBFR=CBFRCA/(0.8*CABONE)
                        !Fractional cortical bone formation rate
                        !(1/yr)

BFR=FBFR*VBONE          !Total bone formation rate (by volume)
                        !(L/yr)
TBFR=TFBFR*TVBONE       !Trabecular bone formation rate (by volume)
                        !(L/yr)
CBFR=CFBFR*CVBONE       !Cortical bone formation rate (by volume)
                        !(L/yr)

CRVAF=LEAD*CBFR         !Clearance of lead from blood during
                        !mineralization of newly-apposed cortical
                        !bone (L/yr)
TRVAF=LEAD*TBFR         !Clearance of lead from blood during
                        !mineralization of newly-apposed trabecular
                        !bone (L/yr)

BRR=BFR-RVBONE          !Total bone resorption rate (L/yr)
TBRR=BRR*TBFR/BFR       !Trabecular bone resorption rate (L/yr)
CBRR=BRR-TBRR           !Cortical bone resorption rate (L/yr)

FBRR=BRR/VBONE          !Fractional total bone resorption rate
                        !(1/yr)
```

```
TFBRR=TBRR/TVBONE       !Fractional trabecular bone resorption rate
                        !(1/yr)
CFBRR=CBRR/CVBONE       !Fractional cortical bone resorption rate
                        !(1/yr)

VBAGEA=.0168*WBODYA**1.188
                        !Total bone volume at age AGEA (L)
CVBAGEA=0.8*VBAGEA      !Cortical bone volume at age AGEA (L)
TVBAGEA=VBAGEA-CVBAGEA
                        !Trabecular bone volume at age AGEA (L)

BFAGEA=VBAGEA*FBAGEA/CAAGEA
                        !Total bone formation rate (by volume) at
                        !age AGEA (L/yr)
TBFAGEA=TVBAGEA*TFBAGEA/(0.2*CAAGEA)
                        !Trabecular bone formation rate (by volume)
                        !at age AGEA (L/yr)
CBFAGEA=BFAGEA-TBFAGEA
                        !Cortical bone formation rate (by volume)
                        !at age AGEA (L/yr)


PROCEDURAL (CVBONEA,TVBONEA,CVBONEC,TVBONEC,CBFRC,TBFRC,CBFRA,&
TBFRA,CRFBON,TRFBON,CBRRA,TBRRA,CBRRC,TBRRC=1,1,1,1,1,1,1,1,1,1,1
,1,1,1)
IF (AGE.EQ.0.) GOTO BIRTH
GOTO LATER
LATER..CONTINUE
IF(AGE.LT.AGEA) GOTO YOUNG
GOTO ADULT
YOUNG..CONTINUE
      CONSTANT EXPO=.6
      CVBONEA=CVBONE*(AGE/AGEA)**EXPO
                        !Cortical bone volume participating in
                        !adult-type bone remodeling (L)
      TVBONEA=TVBONE*(AGE/AGEA)**EXPO
                        !Trabecular bone volume participating in
                        !adult-type bone remodeling (L)
      CVBONEC=CVBONE-CVBONEA
                        !Cortical bone volume participating in
                        !active bone modeling during growth (L)
      TVBONEC=TVBONE-TVBONEA
                        !Trabecular bone volume participating in
                        !active bone modeling during growth (L)
      CRFBON=(.6/AGEA)*(((1.E-33+AGE/AGEA)**(-.4))-1.)
      TRFBON=(.6/AGEA)*(((1.E-33+AGE/AGEA)**(-.4))-1.)
                        !Fractional rate of transformation of BONEC
                        !to BONEA, or of transfer of lead from
                        !BONEC to BONEA (1/yr)
      CBFRA=CBFR*CVBONEA/CVBAGEA
                        !Formation rate of cortical bone
                        !participating in adult-type bone
                        !remodeling (by volume of bone) (L/yr)
```

```
      TBFRA=TBFR*TVBONEA/TVBAGEA
                        !Formation rate of trabecular bone
                        !participating in adult-type bone
                        !remodeling (by volume of bone) (L/yr)
      CBFRC=RSW(CBFRA.LE.CBFR,CBFR-CBFRA,0.)
                        !Formation rate of cortical bone
                        !participating in active modeling during
                        !growth (by volume of bone) (L/yr)
      TBFRC=RSW(TBFRA.LE.TBFR,TBFR-TBFRA,0.)
                        !Formation rate of trabecular bone
                        !participating in active modeling during
                        !growth (by volume of bone) (L/yr)
      CBRRC=CBRR*CBFRC/CBFR
                        !Resorption rate of cortical bone
                        !participating in active modeling during
                        !growth (by volume of bone) (L/yr)
      TBRRC=TBRR*TBFRC/TBFR
                        !Resorption rate of trabecular bone
                        !participating in active modeling during
                        !growth (by volume of bone) (L/yr)
      CBRRA=CBRR-CBRRC
                        !Resorption rate of cortical bone
                        !participating in adult-type remodeling (by
                        !volume of bone) (L/yr)
      TBRRA=TBRR-TBRRC
                        !Resorption rate of trabecular bone
                        !participating in adult-type remodeling (by
                        !volume of bone) (L/yr)
GOTO TERM
ADULT..CONTINUE
      CVBONEC=0.
      CVBONEA=CVBONE
      CRFBON=0.
      CBFRA=CBFR
      CBFRC=CBFR-CBFRA
      CBRRC=CBRR*CBFRC/CBFR
      CBRRA=CBRR
      TVBONEC=0.
      TVBONEA=TVBONE
      TRFBON=0.
      TBFRA=TBFR
      TBFRC=TBFR-TBFRA
      TBRRC=TBRR*TBFRC/TBFR
      TBRRA=TBRR
GOTO TERM
BIRTH..CONTINUE
      CVBONEC=CVBONE
      CVBONEA=0.
      CRFBON=0.
      CBFRA=CBFAGEA*CVBONEA/CVBONE
      CBFRC=CBFR-CBFRA
      CBRRC=CBRR*CBFRC/CBFR
      CBRRA=CBRR-CBRRC
```

```
      TVBONEC=TVBONE
      TVBONEA=0.
      TRFBON=0.
      TBFRA=TBFAGEA*TVBONEA/TVBONE
      TBFRC=TBFR-TBFRA
      TBRRC=TBRR*TBFRC/TBFR
      TBRRA=TBRR-TBRRC
GOTO TERM
TERM..CONTINUE
END


!**Absorption of Lead**
CONSTANT RFOOD1=200.   !Average rate of ingestion of lead in food
                       !by adult pre-1970 (ug/da)
AMT1=RFOOD1*365./1000.
                       !Average rate of ingestion of lead in food
                       !by adult pre-1970 (mg/yr)
CONSTANT RFOOD2=30.    !Contemporary average rate of ingestion of
                       !lead in food by adult (ug/da)
AMT2=RFOOD2*365./1000.
                       !Contemporary average rate of ingestion of
                       !lead in food by adult (mg/yr)
FOOD=RSW(YEAR.LE.1970.,AMT1,AMT1-(AMT1-AMT2)*EXP(.4*(YEAR-1970.)&
     )/(EXP(4.)+EXP(.4*(YEAR-1970.))))
                       !Rate of ingestion of lead in food by
                       !generic adult (mg/yr)

CONSTANT ROTHER=0.     !Rate of ingestion of lead from other,
                       !unspecified oral sources by generic adult
                       !(ug/da)
OTHER=ROTHER*365./1000.
                       !Rate of ingestion of lead from unspecified
                       !oral sources by generic adult (mg/yr)

CONSTANT CWATER=0.     !Concentration of lead in drinking water
                       !(mg/L)
CONSTANT DWATER=2.     !Rate of drinking water consumption by
                       !generic adult (L/da)
WATER=365.*CWATER*DWATER
                       !Rate of ingestion of lead in drinking
                       !water by generic adult (mg/yr)

RWATER=365.*DWATER*((WBODY/(WCHILD+WADULT))**.67)
                       !Rate of drinking water consumption at any
                       !age (L/yr)

RFOODA=FOOD+WATER+OTHER
                       !Rate of ingestion of lead from food,
                       !drinking water, and other oral sources by
                       !generic adult (mg/yr)

CONSTANT CFMLA=.020    !Concentration of lead in infant formula or
```

```
                        !milk (mg/L, or ppm)
DFMLAI=365.*((WBODY-WBIRTH)**.2)/1.15
                        !Rate of consumption of formula or milk by
                        !infant (L/yr) (this is 0.67 L/da, or 22.6
                        !oz/day, at age 10.5 da (WBODY=3.78), and
                        !.98 L/da, or 33.1 oz/da, at age 97.5 da
                        !(WBODY=5.36); the formula consumption data
                        !are from Ryu et al., 1983)
RFMLAI=RSW(AGE.LE.0.3,CFMLA*DFMLAI,0.)
                        !Rate of ingestion of lead in formula or !
                        !milk by infant up to age 0.3 year (mg/yr)

DFMLAW=365.*((WBODYW-WBIRTH)**.2)/1.15
                        !Rate of consumption of formula or milk by
                        !infant at start of weaning, or 0.3 year
                        !(L/yr)
RFMLAW=CFMLA*DFMLAW     !Rate of ingestion of lead in formula or
                        !milk by infant at start of weaning, or 0.3
                        !year (mg/yr)
RFMLAB=RSW(AGE.GT..3.AND.AGE.LE.1.,RFMLAW-(RFMLAW/.7)*(AGE-.3),&
     0.)
                        !Rate of ingestion of lead in formula or
                        !milk by baby from start of weaning to age
                        !1 year, when consumption of formula has
                        !become zero (mg/yr)

CONSTANT RFOOD3=0.      !Rate of ingestion of lead by baby in foods
                        !including liquids other than milk or
                        !infant formula at age 1 year (ug/da)
RFOOD4=.7*365.*RFOOD3/700.
                        !Rate of total lead ingestion by baby from
                        !food and milk or infant formula at age 1
                        !year (mg/yr)
RSOLID=RSW(AGE.GE..3.AND.AGE.LE.1.,(AGE-.3)*365.*RFOOD3/700.,0.)
                        !Rate of ingestion of lead by baby in foods
                        !including liquids other than milk or
                        !infant formula (mg/yr)
RFOODB=RFMLAI+RFMLAB+RSOLID
                        !Rate of total lead ingestion by baby from
                        !food and milk or infant formula up to age
                        !1 year (mg/yr)


PROCEDURAL (RFOOD=1,1)
IF (WBODY.LE.WBODY1) GOTO LESS
GOTO MORE
LESS..CONTINUE
     RFOOD=RFOODB       !Rate of ingestion of lead from solid foods
                        !and liquids including infant milk or
                        !formula by baby up to age 1 year (mg/yr)
GOTO OVER
MORE..CONTINUE
     RFOOD=RSW(AGE.GT.1.,RFOOD4+(((WBODY-WBODY1)/WADULT)**.67)&
```

```
     *(RFOODA-RFOOD4),0.)
                          !Rate of ingestion of lead from food,
                          !drinking water, and other oral sources by
                          !individual more than 1 year old (mg/yr)
GOTO OVER
OVER..CONTINUE
END


CONSTANT CDUST=0.         !Concentration of lead in dust (ug/g or
                          !mg/kg)
CONSTANT MDUST2=.028      !Rate of ingestion of dust by a
                          !two-year-old; maximum intake during
                          !childhood (kg/yr; equivalent to .074 g/da)
RD=RDUST*1000./(CDUST*365.)
                          !Rate of ingestion of dust at any age
                          !during childhood (g/da)

DFACT1=RSW(AGE.GT..3.AND.AGE.LE.2.,1.111758*(EXP(AGE-.3)-1.)/&
     (.5+(EXP(AGE-.3)-1.)),0.)
DFACT2=RSW(AGE.LE.2.,0.,1.-(EXP(AGE-2.)-1.)/(.5+(EXP(AGE-2.)-1.)&
     ))

RDUST=RSW(AGE.LE.2.,MDUST2*CDUST*DFACT1,MDUST2*CDUST*DFACT2)
                          !Rate of ingestion of lead in dust at any
                          !age during childhood (mg/yr)

CONSTANT CSOIL=0.         !Concentration of lead in soil (ug/g or
                          !mg/kg)
CONSTANT MSOIL3=.022      !Rate of ingestion of soil by a
                          !three-year-old; maximum intake during
                          !childhood (kg/yr; equivalent to .061 g/da)
RS=RSOIL*1000./(CSOIL*365.)
                          !Rate of ingestion of soil at any age
                          !during childhood (g/da)

SFACT1=RSW(AGE.GT..5.AND.AGE.LE.3.,1.089425*(EXP(AGE-.5)-1.)/&
     (1.+(EXP(AGE-.5)-1.)),0.)
SFACT2=RSW(AGE.LE.3.,0.,1.-(EXP(AGE-3.)-1.)/(10.+(EXP(AGE-3.)-1.&
     )))

RSOIL=RSW(AGE.LE.3.,MSOIL3*CSOIL*SFACT1,MSOIL3*CSOIL*SFACT2)
                          !Rate of ingestion of lead in soil at any
                          !age during childhood (mg/yr)

RMOUT=RSOIL+RDUST         !Rate of ingestion of lead in soil and dust
                          !at any age during childhood, assuming
                          !complete bioavailability (mg/yr)
CONSTANT DBIOAV=1.        !Fractional bioaccessability of lead from
                          !dust
CONSTANT SBIOAV=1.        !Fractional bioaccessability of lead from
                          !soil
```

```
CONSTANT RPAINT=0.      !Rate of ingestion of lead in paint at any
                        !age during childhood (ug/da)
PAINT=RPAINT*365./1000.
                        !Rate of ingestion of lead in paint at any
                        !age during childhood (mg/yr)

RMOUTH=DBIOAV*RDUST+SBIOAV*RSOIL+PAINT
                        !Rate of ingestion of lead in soil, dust,
                        !and paint at any age during childhood,
                        !with adjustment for bioavailability of
                        !lead from soil and dust (mg/yr)

INGEST=RFOOD+RMOUTH     !Rate of total lead ingestion from food,
                        !water, and other oral sources by
                        !individual of any age (mg/yr)

FRABS=.60-.52/(1.+30.*EXP(-AGE))
                        !Fractional absorption of lead from mixed
                        !sources in the gastrointestinal tract
RAGI=FRABS*INGEST       !Rate of absorption of lead from the
                        !gastrointestinal tract (mg/yr)
A=INTEG(RAGI,0.)        !Cumulative amount of lead absorbed from
                        !the gastrointestinal tract (mg)

RESP=RSW(WBODY.GE.15.,-15.+6.88*ALOG(WBODY),.44+1.17*ALOG(WBODY))
                        !Respiration rate (m3/da)

CONSTANT CAIR1=.002     !Background concentration of lead in air
                        !pre-1975 (mg/m3)
CONSTANT CAIR2=.00015   !Current background concentration of lead
                        !in air (mg/m3)
TIMES=EXP(YEAR-1975.)/(EXP(7.)+EXP(YEAR-1975.))
AIR=RSW(YEAR.LE.1975.,CAIR1,CAIR1-(CAIR1-CAIR2)*TIMES)
                        !Background concentration of lead in air
                        !(mg/m3)
RAIR=AIR*RESP*365.      !Rate of inhalation of background lead from
                        !ambient air (mg/yr)

CONSTANT CWKPL=0.       !Concentration of lead in workplace air
                        !(mg/m3)
CIND=CWKPL*40./168.     !Time-weighted average concentration of
                        !lead in workplace air (mg/m3)
RIND=CIND*RESP*365.     !Time-weighted average rate of inhalation
                        !of lead from workplace air (mg/yr)

CONSTANT CAMB=0.        !Concentration of lead in ambient air from
                        !specified sources other than background
                        !(mg/m3)
RADD=RIND+CAMB*RESP*365.
                        !Rate of inhalation of lead from air !
                        !sources other than background (mg/yr)
INHALE=RAIR+RADD        !Total rate of inhalation of lead from all
                        !air sources, background and specific
```

```
                        !(mg/yr)

CONSTANT FRLUNG=.50     !Fractional absorption from the lung
RALUNG=FRLUNG*INHALE    !Rate of absorption from the lung (mg/yr)
ALUNG=RSW(INHALE.EQ.0.,0.,INTEG(RALUNG,0.))
                        !Cumulative amount of lead absorbed from
                        !the lung (mg)


!**Lead in Blood**
HCT=RSW(AGE.LE..01,.52+AGE*14,HCTA*(1.+(.66-HCTA)*EXP(-(AGE-.01)&
     *13.9)))
                        !Hematocrit
PLASMA=1.-HCT           !Plasma fraction of blood volume

RABL=QL*CBL+QK*CBK+QW*CBW+QP*CBP+CQBC*CCBHC+CQBA*CBDA&
     +TQBC*TCBHC+TQBA*TCBHA+RALUNG-QCG*CB
                        !Rate of change of amount of lead in blood
                        !(mg/yr)
ABL=INTEG(RABL,0.)      !Amount of lead in blood (mg)
CB=ABL/VBL              !Concentration of lead in blood (mg/L)
PbB=CB*100.             !Concentration of lead in blood (ug/dL)

CPLASMA=((CB-HCT*BIND-G*HCT*KBIND-PLASMA*KBIND)/(2.*(PLASMA+HCT*&
     G)))+(((((HCT*BIND+G*HCT*KBIND+PLASMA*KBIND-CB)**2.)&
      +4.*KBIND*CB*(PLASMA+HCT*G))**.5)/(2.*(PLASMA+HCT*G)))
                        !Concentration of lead in plasma (mg/L)
PbP=CPLASMA*100.        !Concentration of lead in plasma (ug/dL)


!**Excretion of Lead**
GFR=RSW(WBODY.LE.11.7,708.5*(WBODY**1.3774),4391.9*(WBODY**.636))
                        !Glomerular filtration rate (L plasma/yr)
QEG=(1.-.92/(1.+50.*EXP(-AGE)))*GFR
                        !Total elimination clearance of lead from
                        !plasma (L/yr)
CLK=.7*QEG              !Renal clearance of lead from plasma (L/yr)
RAKX=CLK*CBPK           !Rate of renal excretion (mg/yr)
AKX=INTEG(RAKX,0.)      !Amount of lead excreted by the kidney (mg)

CLL=QEG-CLK             !Hepatic clearance from plasma (in bile)
                        !(L/yr)
RALX=CLL*CBPL           !Rate of hepatic excretion (mg/yr)
ALX=INTEG(RALX,0.)      !Amount of lead excreted by the liver (mg)

RAX=RALX+RAKX           !Total rate of lead excretion (mg/yr)
AX=ALX+AKX              !Total amount of lead excreted (mg)

RFEC=INGEST-RAGI+RALX !Rate of fecal excretion of lead (mg/yr)


!**Lead in Liver**
RAL=QL*(CB-CBL)+RAGI-RALX
```

```
                        !Rate of change of amount (mg/yr)
AL=INTEG(RAL,0.)        !Amount (mg)
CL=AL/VL                !Concentration (mg/L)
CBPL=AL/(VL*PL)         !Concentration of lead in venous plasma
                        !leaving liver (mg/L)
CBL=PLASMA*CBPL+HCT*CBPL*(G+BIND/(KBIND+CBPL))
                        !Concentration of lead in venous blood
                        !leaving liver (mg/L)


!**Lead in Kidney**
RAK=QK*(CB-CBK)-RAKX    !Rate of change of amount (mg/yr)
AK=INTEG(RAK,0.)        !Amount (mg)
CK=AK/VK                !Concentration (mg/L)
CBPK=AK/(VK*PK)         !Concentration of lead in venous plasma
                        !leaving kidney (mg/L)
CBK=PLASMA*CBPK+HCT*CBPK*(G+BIND/(KBIND+CBPK))
                        !Concentration of lead in venous blood
                        !leaving kidney (mg/L)


!**Lead in Other Well-Perfused Tissues**
RAW=QW*(CB-CBW)         !Rate of change of amount (mg/yr)
AW=INTEG(RAW,0.)        !Amount (mg)
CW=AW/VW                !Concentration (mg/L)
CBPW=AW/(VW*PW)         !Concentration of lead in venous plasma
                        !leaving other well-perfused tissues (mg/L)
CBW=PLASMA*CBPW+HCT*CBPW*(G+BIND/(KBIND+CBPW))
                        !Concentration of lead in venous blood
                        !leaving other well-perfused tissues (mg/L)


!**Lead in Poorly-Perfused Tissues**
RAP=QP*(CB-CBP)         !Rate of change of amount (mg/yr)
AP=INTEG(RAP,0.)        !Amount (mg)
CP=AP/VP                !Concentration (mg/L)
CBPP=AP/(VP*PP)         !Concentration of lead in venous plasma
                        !leaving poorly-perfused tissues (mg/L)
CBP=PLASMA*CBPP+HCT*CBPP*(G+BIND/(KBIND+CBPP))
                        !Concentration of lead in venous blood
                        !leaving poorly-perfused tissues (mg/L)


!**Lead in Metabolically Active Region of Cortical Bone**
CRVAFC=LEAD*CBFRC       !Clearance of lead from blood during
                        !mineralization of newly-apposed cortical
                        !bone engaged in active modeling during
                        !growth (L/yr)
CRAFBC=CRVAFC*CPLASMA   !Rate of deposition of lead in cortical
                        !bone engaged in active modeling during
                        !growth (mg/yr)
CRARBC=CBRRC*CCMC       !Rate of return of lead to blood with
                        !resorption of cortical bone engaged in
```

```
                        !active modeling during growth (mg/yr)
CAMC=INTEG(CRAFBC-CRARBC-CRFBON*CAMC,0.)
                        !Amount of lead incorporated into cortical
                        !bone engaged in active modeling during
                        !growth (mg)
CCMC=RSW(AGE.LT.AGEA,CAMC/(CVBONEC+1.E-33),0.)
                        !Concentration of lead in cortical bone
                        !engaged in active modeling during growth
                        !(mg/L)
CRAMBC=CRARBC-CRAFBC    !Net rate of change of amount of lead in
                        !blood perfusing cortical bone engaged in
                        !active modeling during growth (mg/yr)
CCBHC=RSW(CBFRA.LT.CBFR,CB+CRAMBC/(CQBC+1.E-33),0.)
                        !Concentration of lead in blood leaving
                        !cortical bone engaged in active modeling
                        !during growth (mg/L)

CRVAFA=LEAD*CBFRA       !Clearance of lead from blood during
                        !mineralization of newly-apposed mature
                        !cortical bone engaged in remodeling (L/yr)
CRAFBA=CRVAFA*CPLASMA   !Rate of deposition of lead in the
                        !metabolically active region of mature
                        !cortical bone engaged in remodeling
                        !(mg/yr)
CRARBA=CBRRA*CCB        !Rate of return of lead to blood with
                        !resorption of mature cortical bone engaged
                        !in remodeling (mg/yr)
CRAMBA=CRARBA-CRAFBA    !Net rate of change of amount of lead in
                        !blood perfusing the metabolically active
                        !region of mature cortical bone engaged in
                        !remodeling (mg/yr)
CCBHA=CB+CRAMBA/(CQBA+1.E-33)
                        !Concentration of lead in blood leaving the
                        !metabolically active region of mature
                        !cortical bone engaged in remodeling (mg/L)
CCBPHA=((CCBHA-HCT*BIND-G*HCT*KBIND-PLASMA*KBIND)/&
     (2.*(PLASMA+HCT*G)))+((((HCT*BIND+G*HCT*KBIND+PLASMA&
     *KBIND-CCBHA)**2.)+4.*KBIND*CCBHA*(PLASMA+HCT*G))&
     **.5)/(2.*(PLASMA+HCT*G)))
                        !Concentration of lead in plasma leaving
                        !the metabolically active region of mature
                        !cortical bone engaged in remodeling


!**Lead in Trabecular Bone**
TRVAFC=LEAD*TBFRC       !Clearance of lead from blood during
                        !mineralization of newly-apposed trabecular
                        !bone engaged in active modeling during
                        !growth (L/yr)
TRAFBC=TRVAFC*CPLASMA   !Rate of deposition of lead in trabecular
                        !bone engaged in active modeling during
                        !growth (mg/yr)
TRARBC=TBRRC*TCMC       !Rate of return of lead to plasma with
```

```
                        !resorption of trabecular bone engaged in
                        !active modeling during growth (mg/yr)
TAMC=INTEG(TRAFBC-TRARBC-TRFBON*TAMC,0.)
                        !Amount of lead incorporated into
                        !trabecular bone engaged in active modeling
                        !during growth (mg)
TCMC=RSW(AGE.LT.AGEA,TAMC/(TVBONEC+1.E-33),0.)
                        !Concentration of lead in trabecular bone
                        !engaged in active modeling during growth
                        !(mg/L)
TRAMBC=TRARBC-TRAFBC    !Net rate of change of amount of lead in
                        !blood perfusing trabecular bone engaged in
                        !active modeling during growth (mg/yr)
TCBHC=RSW(TBFRA.LT.TBFR,CB+TRAMBC/(TQBC+1.E-33),0.)
                        !Concentration of lead in blood leaving
                        !trabecular bone engaged in active modeling
                        !during growth (mg/L)

TRVAFA=LEAD*TBFRA       !Clearance of lead from blood during
                        !mineralization of newly-apposed mature
                        !trabecular bone engaged in remodeling
                        !(L/yr)
TRAFBA=TRVAFA*CPLASMA   !Rate of deposition of lead in mature
                        !trabecular bone engaged in remodeling
                        !(mg/yr)
TRARBA=TBRRA*TCMA       !Rate of return of lead to blood with
                        !resorption of mature trabecular bone
                        !engaged in remodeling (mg/yr)
TAMA=INTEG(TRAFBA-TRARBA+TRFBON*TAMC,0.)
                        !Amount of lead incorporated into mature
                        !trabecular bone engaged in remodeling (mg)
TCMA=RSW(AGE.LT.AGEA,TAMA/(TVBONEA+1.E-33),TAMA/TVBONE)
                        !Concentration of lead in mature trabecular
                        !bone engaged in remodeling (mg/L)
TRAMBA=TRARBA-TRAFBA    !Net rate of change of amount of lead in
                        !blood perfusing mature trabecular bone
                        !engaged in remodeling (mg/yr)
TCBHA=CB+TRAMBA/(TQBA+1.E-33)
                        !Concentration of lead in blood leaving
                        !mature trabecular bone engaged in
                        !remodeling (mg/L)


!**Lead in Diffusion Region of Mature Cortical Bone**
VTOTAL=PI*(RAD8**2.)    !Total diffusion region bone volume
                        !(cm3 per cm canalicule length)
F1=V1/VTOTAL            !Fraction of diffusion region bone volume
                        !in the first shell
F2=V2/VTOTAL            !Fraction of diffusion region bone volume
                        !in the second shell
F3=V3/VTOTAL            !Fraction of diffusion region bone volume
                        !in the third shell
F4=V4/VTOTAL            !Fraction of diffusion region bone volume
```

```
                        !in the fourth shell
F5=V5/VTOTAL            !Fraction of diffusion region bone volume
                        !in the fifth shell
F6=V6/VTOTAL            !Fraction of diffusion region bone volume
                        !in the sixth shell
F7=V7/VTOTAL            !Fraction of diffusion region bone volume
                        !in the seventh shell
F8=V8/VTOTAL            !Fraction of diffusion region bone volume
                        !in the eighth shell

RDBIN=(S*L*CVBONEA/1000.)*(P*CCBPHA)
                        !Rate of loss of lead from blood into
                        !mature cortical bone by diffusion (mg/yr)
RDBEX=(S*L*CVBONEA/1000.)*(R*CB1)
                        !Rate of return of lead to blood from
                        !mature cortical bone by diffusion (mg/yr)
RDB=RDBEX-RDBIN         !Net rate of change of amount of lead in
                        !blood perfusing the diffusion region of
                        !mature cortical bone (mg/yr)
CBDA=RSW((T.EQ.0.),0.,CCBHA+RDB/(CQBA+1.E-33))
                        !Concentration of lead in blood leaving the
                        !diffusion region of mature cortical bone
                        !(mg/L)
CBPDA=((CBDA-HCT*BIND-G*HCT*KBIND-PLASMA*KBIND)/(2.*(PLASMA+HCT*&
     G)))+(((((HCT*BIND+G*HCT*KBIND+PLASMA*KBIND-CBDA)**2.)&
      +4.*KBIND*CBDA*(PLASMA+HCT*G))**.5)/(2.*(PLASMA+HCT*G)))
                        !Concentration of lead in plasma leaving
                        !the diffusion region of mature cortical
                        !bone

RAFB=CRAFBC+CRAFBA      !Total rate of deposition of lead with
                        !newly-apposed cortical bone (mg/yr)
RBIN=RDBIN+RAFB         !Total rate of entry of lead into cortical
                        !bone, formation and diffusion together
                        !(mg/yr)
RARB=CRARBC+CRARBA      !Total rate of return of lead to plasma
                        !with resorption of cortical bone (mg/yr)
RBEX=RDBEX+RARB         !Total rate of return of lead from cortical
                        !bone, resorption and diffusion together
                        !(mg/yr)
PCENT=100.*RBEX/(RALUNG+RAGI+RBEX+1.E-33)
!Note that these calculations are for cortical bone alone.  It is
!assumed that trabecular bone lead is in sufficiently rapid
!equilibrium with plasma lead that it does not represent
!"historical" bone stores.  This is an assumption only.

RAB1=(S*L*CVBONEA/1000.)*(P*CCBPHA-R*CB1)-(D*CVBONEA*S1*L/1000.)&
     *(CB1-CB2)+F1*(CRAFBA-CRARBA+CRFBON*CAMC)
                        !Rate of change of amount of lead in shell
                        !1 of cortical bone (mg/yr)
AB1=INTEG(RAB1,0.)      !Amount of lead in shell 1 of cortical bone
                        !(mg)
CB1=AB1/(1.E-33+CVBONEA*F1)
```

```
                        !Concentration of lead in shell 1 of
                        !cortical bone (mg/L)

RAB2=(D*CVBONEA*L/1000.)*(CB1*S1+CB3*S2-CB2*(S1+S2))+F2*(CRAFBA&
      -CRARBA+CRFBON*CAMC)
                        !Rate of change of amount of lead in shell
                        !2 of cortical bone (mg/yr)
AB2=INTEG(RAB2,0.)      !Amount of lead in shell 2 of cortical bone
                        !(mg)
CB2=AB2/(1.E-33+CVBONEA*F2)
                        !Concentration of lead in shell 2 of
                        !cortical bone (mg/L)

RAB3=(D*CVBONEA*L/1000.)*(CB2*S2+CB4*S3-CB3*(S2+S3))+F3*(CRAFBA&
      -CRARBA+CRFBON*CAMC)
                        !Rate of change of amount of lead in shell
                        !3 of cortical bone (mg/yr)
AB3=INTEG(RAB3,0.)      !Amount of lead in shell 3 of cortical bone
                        !(mg)
CB3=AB3/(1.E-33+CVBONEA*F3)
                        !Concentration of lead in shell 3 of
                        !cortical bone (mg/L)

RAB4=(D*CVBONEA*L/1000.)*(CB3*S3+CB5*S4-CB4*(S3+S4))+F4*(CRAFBA&
      -CRARBA+CRFBON*CAMC)
                        !Rate of change of amount of lead in shell
                        !4 of cortical bone (mg/yr)
AB4=INTEG(RAB4,0.)      !Amount of lead in shell 4 of cortical bone
                        !(mg)
CB4=AB4/(1.E-33+CVBONEA*F4)
                        !Concentration of lead in shell 4 of
                        !cortical bone (mg/L)

RAB5=(D*CVBONEA*L/1000.)*(CB4*S4+CB6*S5-CB5*(S4+S5))+F5*(CRAFBA&
      -CRARBA+CRFBON*CAMC)
                        !Rate of change of amount of lead in shell
                        !5 of cortical bone (mg/yr)
AB5=INTEG(RAB5,0.)      !Amount of lead in shell 5 of cortical bone
                        !(mg)
CB5=AB5/(1.E-33+CVBONEA*F5)
                        !Concentration of lead in shell 5 of
                        !cortical bone (mg/L)

RAB6=(D*CVBONEA*L/1000.)*(CB5*S5+CB7*S6-CB6*(S5+S6))+F6*(CRAFBA&
      -CRARBA+CRFBON*CAMC)
                        !Rate of change of amount of lead in shell
                        !6 of cortical bone (mg/yr)
AB6=INTEG(RAB6,0.)      !Amount of lead in shell 6 of cortical bone
                        !(mg)
CB6=AB6/(1.E-33+CVBONEA*F6)
                        !Concentration of lead in shell 6 of
                        !cortical bone (mg/L)
```

```
RAB7=(D*CVBONEA*L/1000.)*(CB6*S6+CB8*S7-CB7*(S6+S7))+F7*(CRAFBA&
      -CRARBA+CRFBON*CAMC)
                          !Rate of change of amount of lead in shell
                          !7 of cortical bone (mg/yr)
AB7=INTEG(RAB7,0.)        !Amount of lead in shell 7 of cortical bone
                          !(mg)
CB7=AB7/(1.E-33+CVBONEA*F7)
                          !Concentration of lead in shell 7 of
                          !cortical bone (mg/L)

RAB8=(D*CVBONEA*L/1000.)*(CB7*S7-CB8*S7)+F8*(CRAFBA-CRARBA&
     +CRFBON*CAMC)        !Rate of change of amount of lead in shell
                          !8 of cortical bone (mg/yr)
AB8=INTEG(RAB8,0.)        !Amount of lead in shell 8 of cortical bone
                          !(mg)
CB8=AB8/(1.E-33+CVBONEA*F8)
                          !Concentration of lead in shell 8 of
                          !cortical bone (mg/L)

CAB=AB1+AB2+AB3+AB4+AB5+AB6+AB7+AB8+CAMC
                          !Total amount of lead in cortical bone (mg)
CCB=CAB/CVBONE            !Concentration of lead in cortical bone
                          !(mg/L)
CCMFDB=CAB/(.8*WMFDB)     !Concentration of lead in marrow-free dry
                          !cortical bone (mg/L)

RTAB=TRAFBA+TRAFBC-TRARBA-TRARBC
                          !Rate of change of amount of lead in
                          !trabecular bone (mg/yr)
TAB=INTEG(RTAB,0.)        !Total amount of lead in trabecular bone
                          !(mg)
TCB=TAB/TVBONE            !Concentration of lead in trabecular bone
                          !(mg/L)
TCMFDB=TAB/(.2*WMFDB)     !Concentration of lead in marrow-free dry
                          !trabecular bone (mg/L)

AB=CAB+TAB                !Total amount of lead in bone (mg)
CBONE=AB/VBONE            !Average concentration of lead in bone
                          !(mg/L)
CSKEL=AB/WSKEL            !Average skeletal lead concentration (ug/g)
CBONEppm=AB/WBONE         !Average bone lead concentration (ug/g, or
                          !ppm)
CMFDBppm=AB/WMFDB         !Average lead concentration per unit weight
                          !of marrow-free dry bone (ug/g, or ppm)


!**Balances**
FLOW=QCG-(QL+QK+QW+QP+QB)
VOLUME=WBODY-(VL+VK+VW+VP+VBL+VBONE)
BURDEN=AL+AK+AP+AW+ABL+AB
MASS=A+ALUNG-(AX+BURDEN)
```

```
END                    !Of Derivative Section

END                    !Of Dynamic Section

END
```

Appendix B

Model parameters:

	96A	96B	97A
D0	1×10^{-8}	1×10^{-7}	1×10^{-7}
R0	3×10^{-7}	1×10^{-7}	1×10^{-7}
P0	0.04	0.04	0.015
CMINFOR	0.05	0.05	0.01
TMINFOR	0.085	0.085	0.02
BIND	2.7	2.7	2.6
KBIND	0.0075	0.0075	0.006

Appendix C

Journal Publications:

1. Fleming DEB, Boulay D, Richard NS, Robin J-P, Gordon CL, Webber CE, Chettle DR. Accumulated body burden and endogenous release of lead in employees of a lead smelter. Environ Health Perspect, 1997; 105:224-233.

2. Chettle DR, Fleming DEB, McNeill FE, Webber CE. Serum (plasma) lead, blood lead, and bone lead [Letter to the Editor]. Am J Ind Med, 1997; 32:319-320.

3. Fleming DEB, Wetmur JG, Desnick RJ, Robin J-P, Boulay D, Richard NS, Gordon CL, Chettle DR, Webber CE. Effect of the δ-aminolevulinate dehydratase polymorphism on the accumulation of lead in bone and blood in lead smelter workers. Accepted for publication. Environ Res.

Abstracts and Presentations:

1. Fleming D. X-ray fluorescence and bone lead measurement. Mount Allison University Department of Physics, Engineering, & Geoscience Seminar Series. Sackville, New Brunswick. October 18, 1995.

2. Fleming D. X-ray fluorescence and bone lead measurement of smelter workers. Radiology Research Day: McMaster University Medical Centre. Hamilton, Ontario. May 23, 1996.

3. Wetmur JG, Desnick RJ, Robin J-P, Boulay D, Richard NS, Gordon CL, Webber CE, Fleming DEB, Chettle DR. The influence of the common human ALAD polymorphism on accumulation of lead in bones.
   (a) Presented (by JG Wetmur) at the Conference of the American Society of Human Genetics. San Francisco, California. October 29, 1996.
   (b) Abstract appeared in Am J Hum Gen, 1996; 59:A294.

4. Fleming D. Bone lead and the Brunswick smelter workers. Interviewed on *Information Morning* with Joanne Roberts, CBC Radio, Moncton, New Brunswick. Aired on March 18, 1997.

5. Fleming DEB, Chettle DR, Webber CE, Richard NS, Boulay D, Robin J-P, O'Flaherty EJ. Human lead metabolism: investigations with *in vivo* X-ray fluorescence.
   (a) Presented at Radiology 1997: Imaging, Science & Oncology. Birmingham, UK. May 19-21, 1997.
   (b) Abstract appeared in Br J Radiol, 1997; 70 Suppl:103.

6. Fleming DEB, Chettle DR, Wetmur JG, Desnick RJ, Robin J-P,

Boulay D, Richard NS, Gordon CL, Webber CE. ALAD Study. Lead Occupational Health Conference. Bloomingdale, Illinois. October 21-24, 1997.

7. Fleming D. Human lead metabolism. Radiology Research Day: McMaster University Medical Centre. Hamilton, Ontario. November 12, 1997 (awarded second prize in basic sciences division).